Structure Activity Relationship Studies of Inhibitors of Industrially and Medicinally Important Enzymes

A thesis submitted in partial fulfilment of the
requirements for the degree of

Doctor of Philosophy in Chemistry

at the
University of Canterbury

by

Maureen J. Prince

University of Canterbury
1999

In Loving Memory of Tania and Pa

TABLE OF CONTENTS

TABLE OF FIGURES

TABLE OF TABLES

ACKNOWLEDGEMENTS

I would firstly like to thank my supervisor Dr Andrew Abell for his encouragement and guidance throughout this work.

My thanks also go to my associate supervisor Dr Juliet Gerrard, who has been ever generous with her time in explaining the intricacies of enzymes and the measurement of their kinetics.

I would also like to acknowledge the many staff members of the Chemistry Department whom have been so very helpful over the years. Special thanks goes to Bruce Clark for collecting all my mass spectra, to Rewi Thompson for help with the NMR spectrometer, to Rob McGregor and Dave MacDonald for all my glassblowing requirements and to Prof. Ward Robinson and Dr Jan Wikiara for their help in determining crystal structures.

I Thank the Marsden fund for providing financial support.

Special thanks to Eli Lilly, especially Ann McNulty for the assay analysis of my steroid 5-α reductase compounds.

To my fellow 655 lab dudes who have made the last few years all the more interesting: your singing, dancing and general lack of taste and ability in all things musical has been strangely appreciated. To the fellow members of the Abell group: thanks for all the helpful discussion, gossip sessions and for all the dry solvents.

To my family and friends: thanks for being there for me. Your love and support over the years has been greatly appreciated.

Finally, to my hubby, Bazzarazzamatazza, your endless love, support, expertise in all things mechanical and computer orientated, and sense of humour have made it all bearable.

ABSTRACT

This thesis presents the results of structure-activity relationship (SAR) studies on inhibitors of two important enzymes: *alpha*-amylase and steroid 5α-reductase.

Ascorbic acid, a reported inhibitor of *alpha*-amylase, has been investigated to determine which of its structural features are necessary for its inhibitory action. These studies have involved the synthesis of thirteen derivatives of L-ascorbic acid and three derivatives of D-isoascorbic acid, incorporating systematic modifications of the functional groups present in both molecules. We have found that the ene-diol moiety in ascorbic acid is crucial for its inhibitory action. Modification of this functionality significantly reduces inhibitory activity.

Ascorbic acid, and some of its derivatives, are shown to be potent inhibitors of barley-malt, porcine-pancreas, human-saliva, bacterial- and fungal *alpha*-amylases.

Kinetic studies to determine the mode of inhibition of ascorbic acid demonstrate that it has characteristics of a competitive inhibitor of *alpha*-amylase.

SAR studies on inhibitors of steroid 5α-reductase were focused on three main areas; modification of known inhibitors to improve potency and isozyme selectivity, synthesis and investigation of a potential new class of inhibitor and investigation into the utility of a novel pharmacophore.

A 4-methyl-octahydrobenzoquinolinone derivative, incorporating a photoisomerisable phenylazo group at the C9 position was synthesised, as was a dihydrophenanthrene-2-carboxylic acid derivative containing a styryl substituent at C7.

A series of piperidone derivatives was synthesised to investigate their potential as steroid 5α-reductase inhibitors.

Four lactam-based inhibitors of steroid 5α-reductase were modified to incorporate a thiolactam, a previously uninvestigated pharmacophore.

Glossary of Acronyms

Arg	Arginine
Asn	Asparagine
Asp	Aspartic acid
β-PGM	β-Phosphoglucomutase
BPNPG7	Blocked p-nitrophenol maltoheptaoside
BPH	Benign prostatic hyperplasia
bs	Broad singlet (NMR)
CI-MS	Chemical-ionisation mass spectrometry
C#	Refers to a specific carbon atom numbered by #
d	Doublet (NMR)
dd	Doublet of doublets (NMR)
dt	Doublet of triplets (NMR)
DHA	Dehydroascorbic acid
DHFA	Dihydroxyfumaric acid
DHT	Dihydrotestosterone
E	Enzyme
EI	Enzyme-inhibitor complex
EI-MS	Electron-ionisation mass spectrometry
ES	Enzyme-substrate complex
ESI	Inhibitor-enzyme-substrate complex
ES-MS	Electrospray mass spectrometry
FAB-MS	Fast atom bombardment mass spectrometry
Fmoc	9-fluoromethylchlorocarbamate
FTIR	Fourier transform infrared
Glu	Glutamic acid
G6P-DH	Glucose-6-phosphate dehydrogenase
His	Histidine
HMBC	Heteronuclear multibond coupling spectroscopy
HMQC	Heteronuclear single quantum coherence spectroscopy
I	Inhibitor
Kat	Katal, unit of enzyme activity

k_{cat}	Catalytic constant
kD	Kilo Dalton, units of protein mass
K_I	Enzyme-inhibitor dissociation constant
K_{Iapp}	Apparent K_I
K_m	Michaelis-Menten constant
m	Multiplet (NMR)
M-M	Michaelis-Menten
MP	Maltose phosphorylase
NAD	Nicotinamide adenine dinucleotide
NADH	Reduced NAD
NADP	Nicotinamide adenine dinucleotide phosphate
NADPH	Reduced NADP
o-tol	Ortho toluene
P	Product
Pi	Phosphate
plc	Preparative thin layer chromatography
PPA	Porcine-pancreatic *alpha*-amylase
*p*TSA	*p*-Toluenesulfonic acid
q	Quartet (NMR)
QSAR	Quantitative structure-activity relationship
s	Singlet (NMR)
S	Substrate
SAR	Structure-Activity Relationship
SE	Standard error
SR	Steroid 5α-Reductase
T	Testosterone
TFA	Trifluoroacetic acid
TMS	Trimethyl silane
U	Enzyme unit
V_{max}	Maximal limiting rate
υ	Rate
$\Delta^{\#,\#}$	The position of unsaturation in a ring system where # refer to the appropriate carbon atoms

1 Introduction

1.1 Structure-Activity Relationship Studies

Structure-activity relationship (SAR) studies are a powerful tool for investigating chemical properties that influence interactions and reactions between molecules. These studies determine the change in activity, reactivity or binding of a molecule, due to the systematic introduction of chemically induced structural modifications.[1-3] Examples include simple alterations such as the lengthening, shortening or branching of chains, the introduction of new substituents or altering the position of attachment of existing substituents, and the introduction of chemical isosteres. As well as providing information regarding optimal structural properties, such as size and shape, SAR studies enable the determination of electronic and lipophilic properties that are important for the biological activity of the molecule.

SAR studies are generally utilised in two ways. Firstly, they give insight into the specific functionality of a molecule that is essential to its activity. This 'pharmacophore' encompasses properties such as structure (geometry, conformation, size), electronic properties and the lipophilic nature of the group under consideration. Once a pharmacophore has been identified, further development may include the preparation of structural analogues of a 'lead'* molecule in an attempt to improve its properties.[1,2] Secondly, SAR studies are used to develop highly active compounds for the elucidation of information about the molecule with which the lead compound binds and interacts. An example of an area in which both of these aspects of SAR studies are very applicable is that of medicinal chemistry; in particular drug design.

The development of a new medicine is often based around the discovery of novel active compounds by general screening procedures.[1,2] Natural products isolated from various plant, marine, and microbial origins, are a rich source of

---

* A 'lead' molecule is an initial active compound on which the SAR studies are undertaken.

undiscovered, structurally-diverse and potentially-active molecules. As these compounds often have complex structures, SAR studies are useful for identifying the active pharmacophore, which can then be isolated and developed further.

An example of this was the discovery of the natural product asperlicin, which is an antagonist of cholecystokinin. Determination of the core pharmacophore present in asperlicin lead to the development of a highly potent and specific, orally-active compound L-364,718 (Figure 1.1).[4]

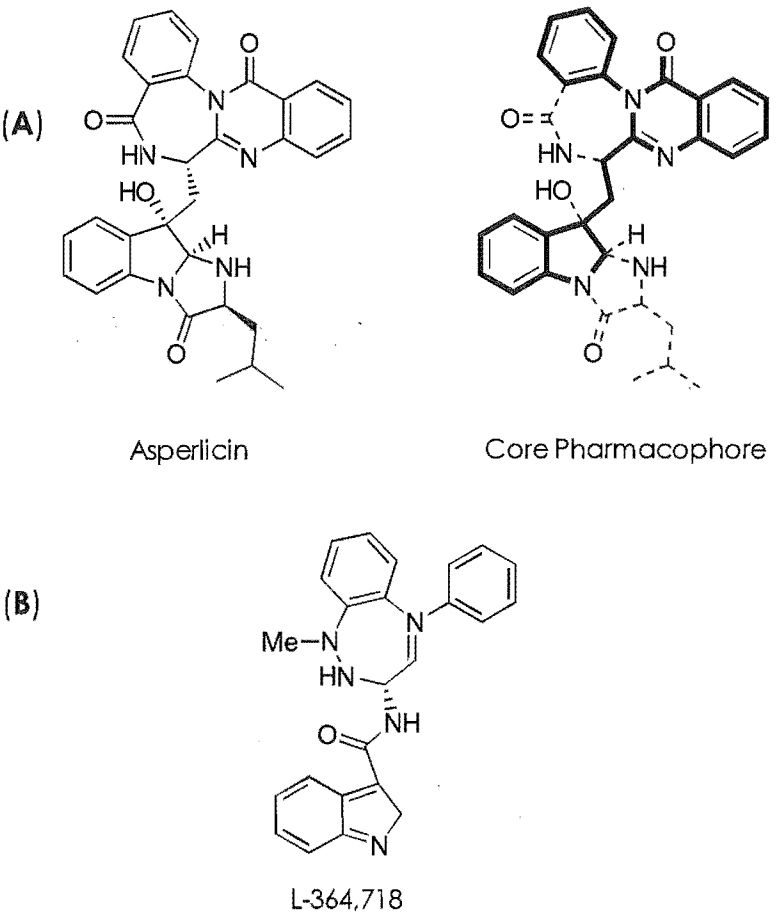

Figure 1.1: (**A**) The structure of asperlicin and its core pharmacophore (shown in bold). (**B**) The structure of L-364,718.

Common targets for drug design are enzymes. The biological pathways responsible for many disease states often involve enzyme-catalysed reactions. An obvious medical intervention is to block these pathways by inhibition of the appropriate enzyme.[3] This can result in a decrease in the amount of the reaction product formed, or an accumulation of the enzyme substrate, either (or both) of which may be desirable in treating an ailment.

1.1.1 Synthetic Techniques

Once an enzyme has been targeted for inhibition, initial drug development begins with the identification of a lead compound. Often this compound will resemble the structure of the natural substrate of the enzyme; however, lead compounds may also be obtained by screening procedures in which numerous libraries of known compounds are evaluated for the desired activity.

A recent advance in the synthesis of structurally diverse libraries of compounds is combinatorial chemistry. This technique relies on the availability of synthetic 'building blocks' with which all possible permutations of the desired molecules are constructed.[5-7] Until recently, this technology has been mostly utilised in the synthesis of diverse peptide libraries using amino acids as the 'building blocks'; however, this technique has now found application in the area of general organic synthesis. Combinatorial synthesis can also be used for optimising the properties of a lead molecule.

1.1.2 Computer-Aided Techniques

If the target enzyme has been isolated and characterised, a computer-generated selection of possible inhibitors can be investigated. There are many computer programs available that can be employed to generate and visualise the three-dimensional structure of an enzyme.[1,2,8] These programs use information gained from techniques such as X-ray crystallography, NMR spectroscopy, molecular modelling and computational chemistry. The affinity and specificity of a potential inhibitor for an enzyme may then be determined using a combination of complementary surface topographies, electronic properties, and hydrophobic sites, in both molecules.[8]

Computer programs employed to find pharmacophore properties of a potential inhibitor (complementary to the enzyme) look for properties such as hydrogen bonding, charged groups, and hydrophobic areas of the inhibitor. They can also relate minimum energy conformations of possible inhibitors to the known characteristics of the enzyme active site.

If the target enzyme is uncharacterised, computer-based analysis of chemically and structurally distinct inhibitors for similar properties can provide information about the spatial arrangement of the enzyme's active site and

electronic and hydrophobic binding properties of the enzyme. This information can then be used in the design of more potent and selective drugs.

Further development of novel medicines usually includes quantitative structure-activity relationship studies (QSAR).[8] These provide models in which the biological activity of a compound is related to its physicochemical properties in a numerical fashion. Particular focus is given to the structural features of a compound that influence *in vivo* transportation and distribution to the target site. Measurable biological data (such as K_I and IC_{50} values – section 4.2) that indicate the activity of a molecule, are related to pharmacokinetic parameters such as lipophilicity, polarisability, electronic parameters, steric parameters and molecular weight.

QSAR results are mostly used in conjunction with SAR studies, to find the optimum compromise between drug activity and *in vivo* delivery to the target site.

1.2 Work Presented in this Thesis

The work presented in this thesis involves SAR studies of inhibitors of two enzyme systems.

1. *alpha*-amylase
2. steroid 5α-reductase

Alpha-amylases are a well-studied class of enzymes in which the amino-acid sequences have been determined and, more recently, crystal structures of various species of enzyme have been solved.[9-14] X-ray-crystallographic analysis has also been carried out on various *alpha*-amylase enzymes with inhibitors bound in the active site. These studies have provided insight into the enzyme-ligand interactions that occur during binding and have allowed a mechanism by which these enzymes function to be postulated.

Given that inhibition of *alpha*-amylase is beneficial in various medical and industrial circumstances (section 2.3) we have investigated ascorbic acid - a reported inhibitor of *alpha*-amylase. Our SAR studies have been aimed at determining the pharmacophore of this molecule using systematic chemical modifications of the structure. We have also used kinetic studies to investigate the mode of inhibition for ascorbic acid and one of its derivatives.

The inhibition of steroid 5α-reductase (SR) has been postulated to be of importance in treating various urological and skin ailments.[15-17] Unlike *alpha*-amylase, the structure of SR has yet to be well characterised, so the design of inhibitors of this enzyme has involved numerous SAR studies to develop potent inhibitors and provide information about the structure of SR and its mechanisms of action.

Our SAR studies, with respect to SR, have involved three separate areas of investigation.

1. The chemical modification of two known SR inhibitors to improve their potency and selectivity;
2. The synthesis and investigation of a new class of inhibitor that is structurally analogous to known potent inhibitors;
3. The chemical modification of various known inhibitors to incorporate a novel pharmacophore mimic.

The activity of the prepared compounds has been measured against human type 1 SR.

1.3 References

(1) Wermuth, C. G., Ed. *The Practice of Medicinal Chemistry*; Academic Press: San Diego, 1996.

(2) Wolff, M. E., Ed. *Burger's Medicinal Chemistry and Drug Discovery*, 5th ed.; John Wiley and Sons Inc: New York, 1995; Vol. 1.

(3) Hansch, C.; Sammes, P. G.; Taylor, J. B., Eds. *Comprehensive Medicinal Chemistry. The Rational Design, Mechanistic Study and Therapeutic Application of Chemical Compounds*; Pergamon Press: Oxford, 1990; Vol. 2 Enzymes and Other Molecular Targets.

(4) Abell, A. D., Ed. *Advances in Amino Acid Mimetics and Peptidomimetics*; JAI Press Inc.: Greenwich, 1997; Vol. 1.

(5) Jung, G., Ed. *Combinatorial Peptide and Nonpeptide Libraries*; VCH: Weinheim, 1996.

(6) Wilson, S. R.; Czarnik, A. W., Eds. *Combinatorial Chemistry. Synthesis and Application*; John Wiley and Sons: New York, 1997.

(7) Terrett, N. K. *Combinatorial Chemistry*; Oxford University Press: New York, 1998.

(8) Hansch, C.; Sammes, P. G.; Taylor, J. B., Eds. *Comprehensive Medicinal Chemistry. The Rational Design, Mechanistic Study and Therapeutic Application of Chemical Compounds*; Pergamon Press: Oxford, 1990; Vol. 4 Quantitative Drug Design.

(9) Qian, M.; Haser, R.; Buisson, G.; Duée, E.; Payan, F. *Biochemistry* **1994**, *33*, 6284-6294.

(10) Qian, M.; Haser, R.; Payan, F. *J. Mol. Biol.* **1993**, *231*, 785-799.

(11) Wong, D. W. S. *Food Enzymes. Structure and Mechanism*; Chapman and Hall: New York, 1995.

(12) Kadziola, A.; Søgaard, M.; Svensson, B.; Haser, R. *J. Mol. Biol.* **1998**, *278*, 205-217.

(13) Machius, M.; Vértesy, L.; Huber, R.; Weigand, G. *J. Mol. Biol.* **1996**, *260*, 409-421.

(14) Brzozowski, A. M.; Davies, G. J. *Biochemistry* **1997**, *36*, 10837-10845.

(15) Abell, A. D.; Henderson, B. R. *Current Medicinal Chemistry* **1995**, *2*, 583-597.

(16) Kenny, B.; Ballard, S.; Blagg, J.; Fox, D. *J. Med. Chem.* **1997**, *40*, 1293-1315.

(17) Andersson, S.; Berman, D. M.; Jenkins, E. P.; Russell, D. W. *Nature* **1991**, *354*, 159-161.

2 *ALPHA*-AMYLASES

One of the beneficial aspects of eating copious amounts of cakes, biscuits and pastries is the plentiful supply of carbohydrates that they provide to one's body. The process of digestion, to enable utilisation of this energy source, involves many biological processes and the action of many enzymes. One of the most important is the hydrolytic enzyme *alpha*-amylase.

Alpha-amylases (1,4-α-D-glucanohydrolases, EC 3.2.1.1*) are members of a class of enzymes called glucosidases, which catalyse the breakdown of carbohydrates.[1-5] Their main function is to catalyse the hydrolysis of α-1,4-glucosidic linkages in various oligo or polysaccharides, to produce maltose units, with retention of the α configuration at the C1 anomeric carbon (Figure 2.1).

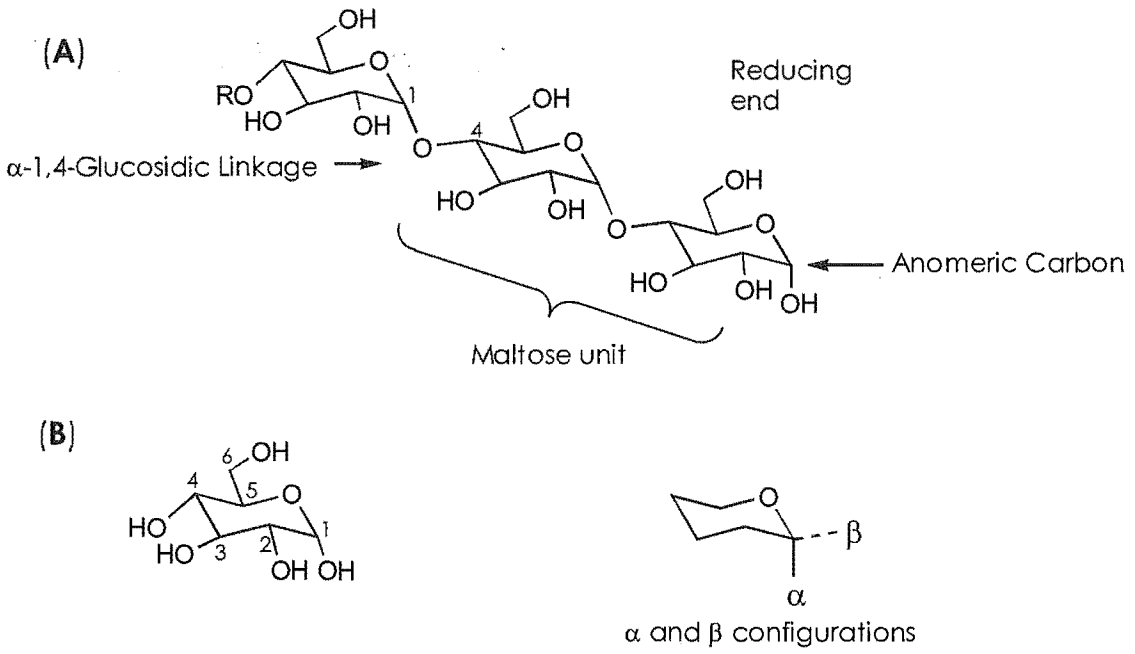

Figure 2.1: (**A**) *Alpha*-amylase hydrolyses the glucosidic linkage between C1 and C4 of two adjacent glucose molecules. (**B**) The terms α and β refer to the stereochemical configuration of the hydroxyl group at the anomeric carbon C1.

Alpha-amylases are found in most organisms that require the conversion of stored or ingested carbohydrate to energy. They are, therefore, readily found in bacteria, fungi, plants and animals.[1] In animals, the main sources of the enzyme

---

* This number is the classification number for alpha-amylases assigned by the Enzyme Commision.

are from the salivary glands and the pancreas, whereas in plants, *alpha*-amylase production is most often associated with seed germination.[6] The enzymes from these varying sources have different pH and temperature requirements for optimal activity (Table 2.1).[7]

Table 2.1: Optimal pH and temperature requirements for various *alpha*-amylases.

Enzyme	Source	pH range	Optimal pH	Optimal temp	Inactivation temp
Pancreatic	Porcine pancreas	5.5 – 8.5	6.0 – 7.0	40 - 45	75
Bacterial	*Bacillus subtilis*	4.5 – 9.0	6.5 – 7.5	70 - 85	95
Thermostable bacterial	*Bacillus licheniformis*	5.8 – 8.0	7.0	90 - 105	120
Fungal	*Aspergillus oryzae*	4.0 – 7.0	5.0 – 6.0	55 - 60	80
Malt	Barley	3.5 – 7.5	4.5 – 7.0	60 - 70	85

2.1 The Utility of *Alpha*-Amylase

Alpha-amylase is an important enzyme due to its necessity in the metabolism of carbohydrates, but is also an industrially- and medicinally-useful enzyme.

2.1.1 Industrial Applications of *Alpha*-Amylase

The main industries to utilise *alpha*-amylases are those in which the manufacturing processes involve the use of starch – the natural substrate of the enzyme.[6-8] For example, in the baking industry, the level of *alpha*-amylase activity in flour can affect the quality of baked goods. For breads, *alpha*-amylase activity is directly related to the taste, crust colour, toasting qualities, and volume of the loaf. Thus, the ability to determine and control the amount of enzyme activity in this process is important. The same is true for the brewing industry where *alpha*-amylases contribute to the breakdown and fermentation processes of grain mashes.[8]

The differences in *alpha*-amylase enzymes from different species have been utilised by industry to great advantage for their specific starch-processing requirements. In the modified-starch industry, the high-temperature stability of certain bacterial *alpha*-amylases has made their use popular for the conversion of starches into syrups for use in confectionery and fruit processing. Previous methods of saccharification involved the use of acid to hydrolyse the starches,

which lead to many by-products. The use of enzymes for this process has provided greater control and specificity over end products.[7]

2.1.2 Medicinal Applications of *Alpha*-Amylase

The medical interest in *alpha*-amylase stems from its involvement in the metabolism of carbohydrates. *Alpha*-amylase is secreted from the pancreas and salivary glands into the digestive tract where it acts on ingested carbohydrates.[3,9] From there, it is transferred into the blood stream before eventually being excreted in the urine. In most animals, the serum (blood or urine) levels of *alpha*-amylase are quite low. However, in disease states such as acute pancreatitis or salivary lesions, these levels can increase. Therefore, diagnosis of these conditions, routinely includes analysis of a serum sample to determine the levels of *alpha*-amylase activity in the patient.[3,9-13]

The *inhibition* of *alpha*-amylase activity also has many medicinal applications. The breakdown of carbohydrates ultimately leads to the formation of glucose, the main energy source in the body. The level of glucose circulating in the blood is regulated by the release of insulin and is maintained at approximately 100 mg/dl.[3] In disease states such as non-insulin-dependent diabetes mellitus, hyperglycaemia, and hyperinsulinaemia, glucose and insulin levels are unregulated and can lead to further disease such as cataracts.[14] The use of *alpha*-amylase inhibitors to slow the breakdown of carbohydrates is currently being investigated as a possible aid in the treatment of these ailments.[3]

The importance of *alpha*-amylase in these areas of industry and medicine has lead to much research on how *alpha*-amylases function and how their activity can be controlled to improve their usefulness. The following section outlines the current knowledge of the general structure and mechanisms of action of *alpha*-amylases. In section 2.3 the use of inhibitors as tools for learning more about the structure and function of *alpha*-amylases, and for controlling their activity, is discussed.

2.2 Structure and Mechanisms of Action of *Alpha*-Amylase

2.2.1 Substrate

Alpha-amylases are classified as endo enzymes. As such, they hydrolyse their substrate at random sites within the molecule rather than from the ends.[1-3]

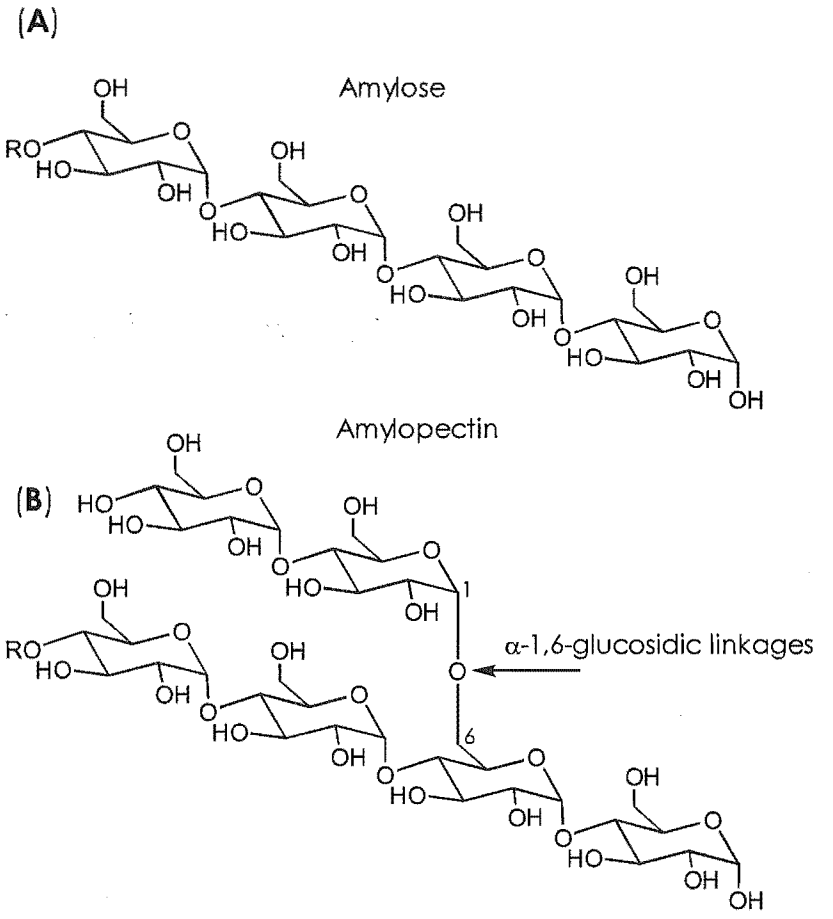

Figure 2.2: (**A**) Amylose. (**B**) Amylopectin. The α-1,6 linkages in this molecule are resistant to hydrolysis by *alpha*-amylase.

The natural substrates of *alpha*-amylase are oligosaccharides and polysaccharides.[1-3,5,7,8] These carbohydrates are mainly sourced from plants in the form of starch, a major source of dietary carbon for animals. Starch is made up of two main polysaccharides: amylose (15 – 25%) and amylopectin (75 – 85%) (Figure 2.2).

Amylose is a mostly unbranched, chain-like molecule consisting of up to 1000 glucose residues connected *via* α-1,4-glucosidic linkages. These chains twist

and coil to give helical three-dimensional structures, which help hold the molecules of the starch grains together.[8] Upon hydrolysis by *alpha*-amylase, amylose is converted, almost completely, into maltose.[3]

Amylopectin is a highly-branched polysaccharide with an average molecular weight of 10^7 g/mol. The longest chain lengths in the molecule contain approximately 25 glucose units. These chains are connected to each other *via* α-1,6-glucosidic linkages. *Alpha*-amylase is unable to hydrolyse α-1,4 linkages adjacent to these branch points, so the products of the enzyme action on amylopectin are maltose (90%) and small α-dextrins containing the 1,6-bonds.[3] The branching in amylopectin molecules also prevents them from folding into helical-type structures.

2.2.2 STRUCTURE

The average molecular weight of *alpha*-amylases is approximately 50 kD,[1,2] thus the enzyme is small relative to its natural substrate. It is a metalloenzyme; binding a calcium ion and also a chloride ion, which are both necessary for the structural integrity and activity of the enzyme.

The amino-acid sequence for several different *alpha*-amylases, including plant, animal and bacterial species has been established.[2,15-19] All exhibit a high degree of homology showing three well-conserved regions. The tertiary structures of porcine-pancreatic, *aspergillus oryzae* and barley-*alpha*-amylase have been determined by X-ray crystallography,[2,15-19] All show similar structural motifs that relate to the homologous regions of amino-acid sequence and their active site, calcium binding site and chloride binding site are in similar locations (Table 2.2).

The most prominent feature of the *alpha*-amylase tertiary structures is an $(\alpha/\beta)_8$ barrel which forms domain A in all three enzymes (Figure 2.3).[1,2] Another common feature is an extended loop which joins the α-helix 3 and β-strand 3 in the $(\alpha/\beta)_8$ barrel. This structure forms domain B in porcine pancreas and barley *alpha*-amylases, and is also present in the *aspergillus oryzae* enzyme (although it doesn't constitute a separate domain). A third structural feature is a section of anti-parallel β-sheet of between five and ten β-strands located at the C-terminal end of the enzyme. This structure makes up domain B in *aspergillus oryzae* and domain C in porcine pancreas and barley *alpha*-amylase.

Table 2.2: A comparison of the structural features of porcine pancreatic, *aspergillus oryzae* and barley *alpha*-amylases.

	PORCINE PANCREAS (PPA)	***ASPERGILLUS ORYZAE***	**BARLEY**
COMPOSITION	496 amino-acid residues, 1x Ca^{2+}, 1x Cl^-	478 amino-acid residues, 2x Ca^{2+}, 1x Cl^-	403 amino-acid residues, 3x Ca^{2+}, 1x Cl^-
DOMAIN A	Comprised of residues 1-99 and 170-404. Folds as an $(\alpha/\beta)_8$ barrel.	Comprised of residues 1-380. Folds as an $(\alpha/\beta)_8$ barrel. Loop between $A\alpha_3$ and $A\beta_3$ is extended chain containing 3 β-strands.	Comprised of residues 1-88 and 153-350. Folds as an $(\alpha/\beta)_8$ barrel.
DOMAIN B	Comprised of residues 100-169. Located between $A\alpha_3$ and $A\beta_3$ of domain A. Folds as 2 antiparallel β-sheets (3 & 4 strands) plus 1 parallel β-sheet of 2 strands.	Comprised of residues 381-478. Folds as 1, 8 stranded antiparallel β-sheet. Is linked to domain A *via* a single poly-peptide chain.	Comprised of residues 89-152. Located between $A\alpha_3$ and $A\beta_3$ of domain A. Has an irregular folding pattern stabilised by Ca^{2+} ions.
DOMAIN C	Comprised of residues 405-496. Folds as 2 facing antiparallel β-sheets (4 strands each), plus 1 antiparallel β-sheet of 2 strands.	NA	Comprised of residues 305-403. Folds as a 5 stranded antiparallel β-sheet.
ACTIVE SITE	Located between the C-terminal end of the β-barrel and domain B. Proposed catalytic residues are Asp300, Asp197 and Glu 233.	Located between the C-terminal end of the β-barrel and domain B. Proposed catalytic residues are Asp297 and Glu 230.	Located between the C-terminal end of the β-barrel and domain B.
CALCIUM BINDING SITE	Located between domains A and B. Coordinated by 8 ligands. Asn100, Arg158, Asp167(bidentate), His 201 plus 3 H_2O. Geometry is that of a distorted pentagonal bipyramid.	Maps exactly onto the Ca^{2+} binding site in PPA. The coordinating residues are Asn121, Glu162, Asp175 and His 210. They are located on the extended loop in domain A.	Similar location to PPA. The calcium near the active site is coordinated by 7 ligands in a distorted pentagonal bipyramid geometry.
CHLORIDE BINDING SITE	Located close to the active site Cl^- is coordinated by 5 ligands. Arg195, Asn298, Arg337(bidentate) and 1 H_2O.		
SUBSTRATE BINDING SITE	Is comprised of 5 subsites. The active site is between sites 3 and 4.	Is comprised of 7 subsites. The active site is between site 4 and 5.	Is comprised of 10 subsites. The active site is between site 6 and 7.

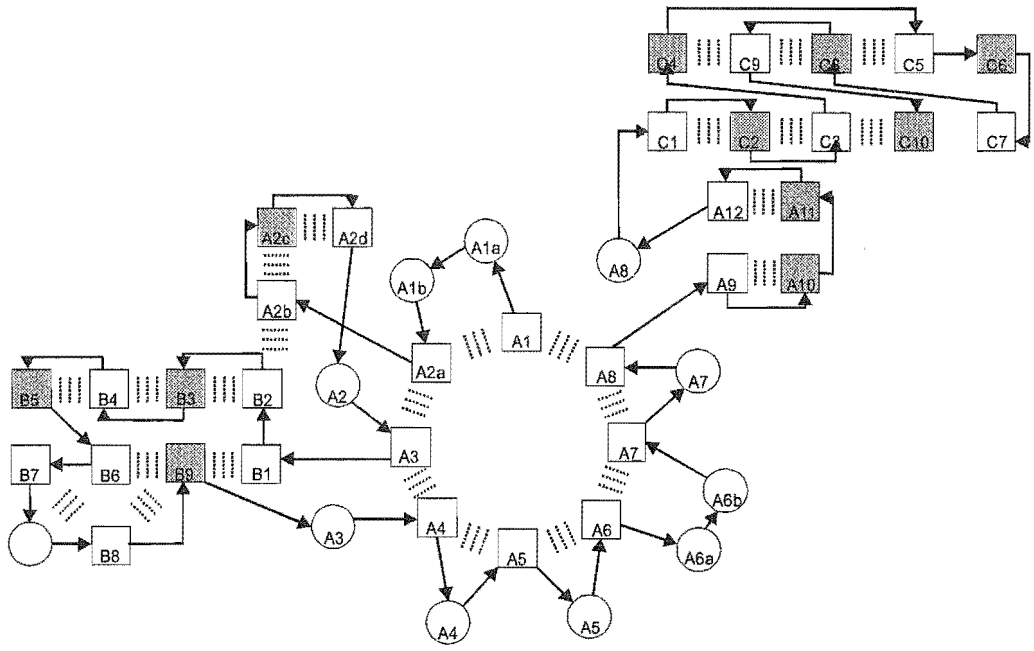

Figure 2.3: A schematic diagram of porcine pancreatic *alpha*-amylase. The circles represent α-helices and the squares represent β-strands. The colourless squares are directed into the page, and the shaded squares, out of the page. The hashed lines show hydrogen bonding. The labels indicate to which domain the structure belongs.

2.2.2.1 Active Site

The active site of the enzyme is located in a V-shaped cleft at the C-terminal end of the β-barrel in domain A. Amino-acid residues involved in the activity of the enzyme are located either on the loops of the barrel at the C-terminal ends, or on β-strands adjacent to the loops. The location of the active residues in these regions is thought to allow flexibility in the amino-acid sequence of different *alpha*-amylases without disrupting the $(\alpha/\beta)_8$ barrel structure.

2.2.2.2 Ion Binding Sites

The presence of a calcium ion is important for the tertiary structure of the enzyme as well as its activity.[1,2] In porcine-pancreas *alpha*-amylase, the calcium ion, located between domains A and B, is coordinated by eight ligands to form a distorted pentagonal bipyramid. The ion is thought to stabilise and maintain the activity in the active site by the correct positioning of catalytic residues. The relative position of the calcium ion in *aspergillus oryzae* and barley *alpha*-amylases has been shown to overlap with that of the porcine pancreatic enzyme.

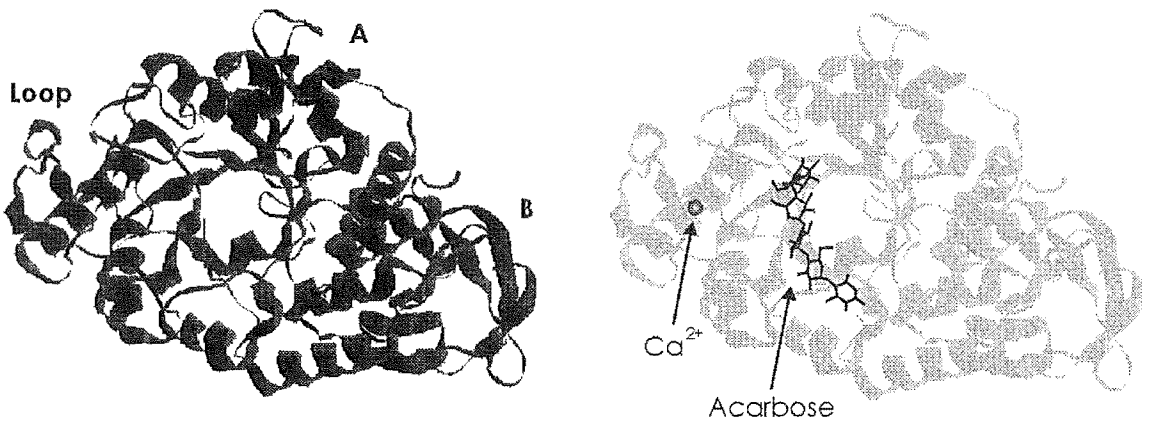

Figure 2.4: Ribbon cartoon of aspergillus oryzae *alpha*-amylase. The left figure shows the domains of the enzyme. The right figure shows the inhibitor acarbose bound in the active site and the binding site of the primary calcium ion.

However, *aspergillus oryzae* has an additional calcium binding site that may be involved in the catalytic step of the enzyme, and barley *alpha*-amylase has a total of three calcium binding sites, which are thought to be involved in stabilising the folding of domain B in this enzyme.

The chloride ion is also located close to the active site and is coordinated by five ligands. The binding of this ion in mammalian *alpha*-amylases, has been shown to shift the pH of optimum activity to neutrality and to increase their activity.[2,18]

2.2.3 Mechanism of Action

The hydrolysis of α-1,4-glucosidic bonds catalysed by *alpha*-amylase, in most instances, involves the transfer of a glucosyl residue (donor) to a water molecule (acceptor). This reaction is achieved with retention of configuration at C1, suggesting that solvolysis occurs before the product is released from the enzyme. Two mechanisms for the hydrolysis reaction have been postulated.[1,2] One involves a double nucleophilic displacement while the other proposes the presence of an oxocarbonium ion intermediate.

2.2.3.1 The Nucleophilic Displacement Mechanism

A nucleophilic-displacement mechanism for the hydrolysis reaction catalysed by amylolytic enzymes was first proposed by Koshland.[1,2] For the reaction due to *alpha*-amylase where there is retention of configuration at C1, a double displacement is envisioned (Figure 2.5). A concerted protonation of the

glucosidic oxygen by an acidic residue, and the attack of the anomeric carbon by a carboxyl anion, gives a covalently-bound glucosyl–enzyme intermediate with a β configuration. A second displacement catalysed by a basic residue, hydrolyses the covalent glucosyl–enzyme bond, to yield the product with an α configuration.

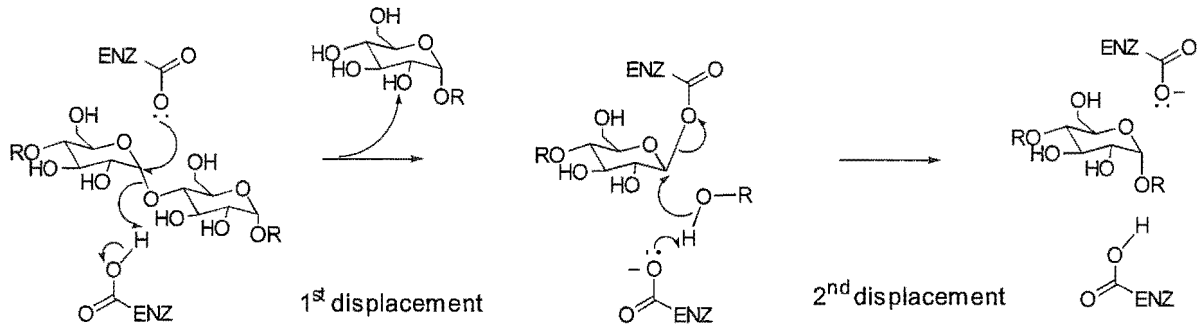

Figure 2.5: Nucleophilic double displacement mechanism.

2.2.3.2 The Oxocarbonium Ion Mechanism

In this mechanism, protonation of the glucosidic oxygen by an acidic residue, together with an enzyme-induced ring distortion to a half-chair configuration, leads to an enzyme-stabilised glycosyl oxocarbonium-ion intermediate. The half-chair configuration is assumed to relieve steric strain at the anomeric carbon and allow front-side attack by water to give an α product (Figure 2.6).

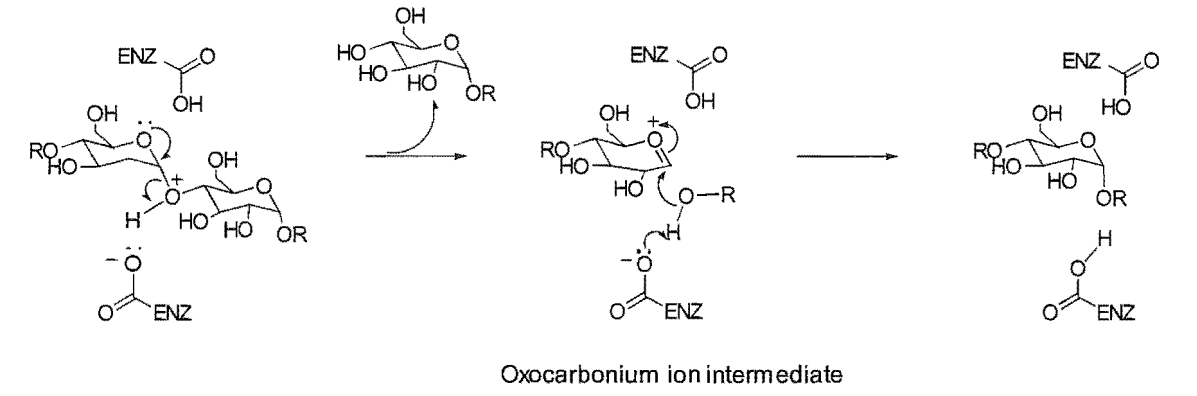

Figure 2.6: Oxocarbonium ion mechanism.

If complete formation of the oxocarbonium ion is achieved, *i.e.* bond breaking occurs before nucleophilic attack by the acceptor molecule, then an

S_N1 type mechanism is envisioned. However, if the nucleophile reacts before complete ion formation, then an S_N2 type displacement mechanism with an oxocarbonium-ion-like transition state would probably occur.

2.2.3.3 The Catalytic Residues

The catalytic residues in the active site are thought to be glutamic acid (Glu) and aspartic acid (Asp), which both contain carboxylate moieties.[15-20] These residues act as both acid and base in the proposed hydrolysis mechanisms. The tertiary structures of porcine pancreatic-, *aspergillus oryzae*- and barley *alpha*-amylase show that both residues lie within close proximity of each other in the active site and are suitably located for protonation of the glucosidic oxygen in the substrate.

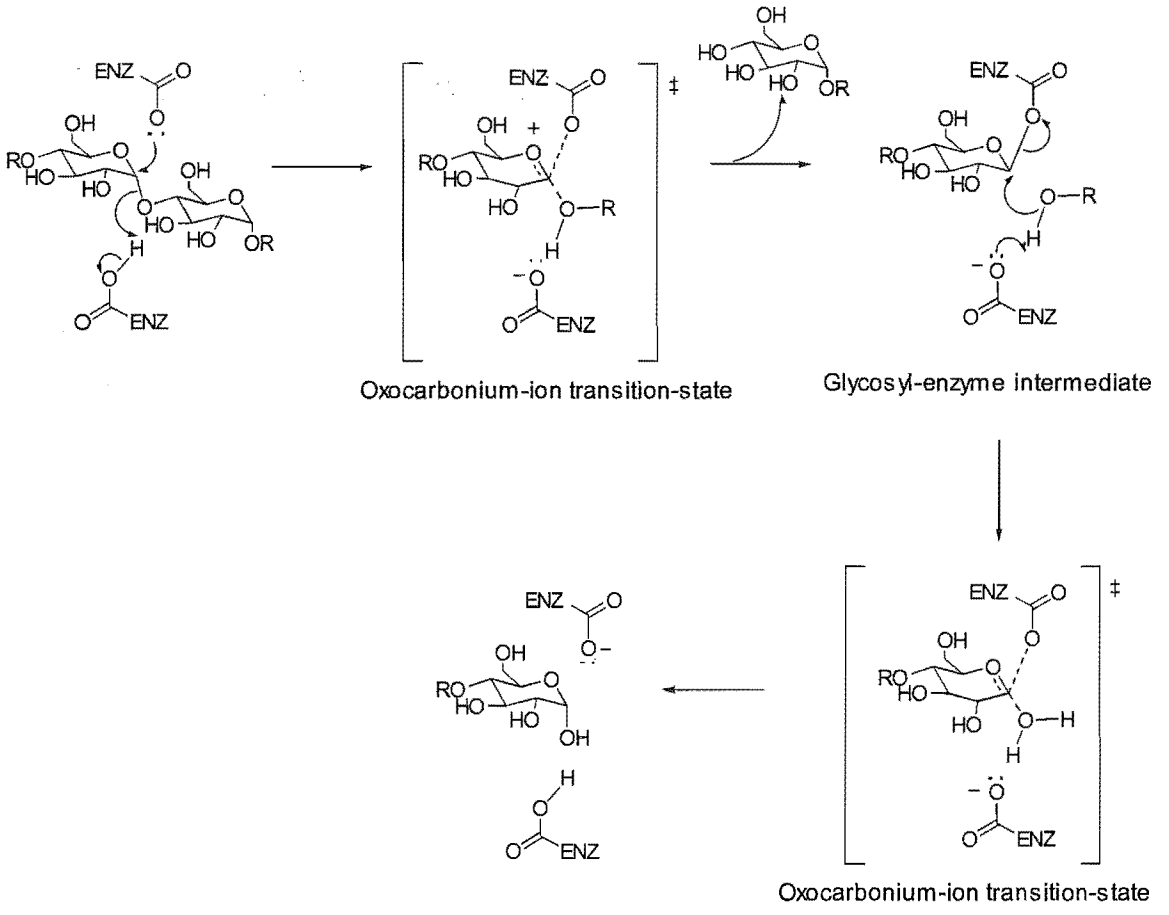

Figure 2.7: Current proposed mechanism of hydrolysis by *alpha*-amylases.

Tao *et al.*[2,18,19] detected the formation of a glycosyl-enzyme intermediate in porcine-pancreatic *alpha*-amylase in cryogenic experiments with ^{13}C-labelled C1 maltotetraose as substrate. However, a crystal structure by Qian *et al.*[18,19] of the

same enzyme soaked with acarbose – a transition-state-analogue inhibitor – suggested that the Glu233 and Asp300 catalytic residues were positioned too far from the glucosidic linkage to allow formation of a covalent bond. Their study proposed that the substrate-enzyme intermediate is unlikely and hydrolysis is more likely by general acid catalysis.

Recently, McCarter and Whithers reported the isolation and identification of a covalently-bound inhibitor-enzyme intermediate.[21] Their study involved the use of a mechanism-based inhibitor, 2-deoxy-2,2-difluoroglycoside, which has been shown to bind irreversibly in the active site of porcine-pancreatic *alpha*-amylase. Based on this evidence, the mechanism of hydrolysis is currently proposed to proceed *via* the original double-displacement mechanism proposed by Koshland. The enzyme-glycoside intermediate is formed and subsequently hydrolysed *via* transition states with substantial oxocarbonium ion character as shown in Figure 2.7.

2.2.4 Action Patter n

The action pattern of an enzyme is a description of the way in which an enzyme interacts with its substrate.[1,2] *Alpha*-amylase, as a polymer-degrading enzyme, has a variety of oligosaccharide and polysaccharide substrates and each interacts with the enzyme in a specific fashion. For example, different substrates may exhibit different modes of binding that influence the way in which the enzyme hydrolyses them to products; however, the mechanism by which the enzyme works can also be influenced by environmental factors such as pH, temperature, or substrate concentrations. The combination of all these environmental factors, and any other influences on how the enzyme functions, are characteristics of the action pattern of the enzyme.

2.2.4.1 Subsite Model

A proposed model that accounts for the different actions of different *alpha*-amylase enzymes is the subsite model.[1,2] This model assumes that the active site is comprised of separate subsites which each bind a glucose residue of the substrate. The subsite in which the hydrolysis reaction occurs is the catalytic site. As the residues in the substrate are essentially identical, they have equal probability of binding in any site and, therefore, can form a variety of complexes

with the enzyme (Figure 2.8). Each subsite has a certain substrate affinity or binding energy, which influences the binding mode of the polymer. According to Thoma *et al.*[1] the concentrations of each complex will be proportional to the sum of the binding energies for each occupied subsite. Thus the substrate-enzyme complex can be either productive or non-productive, depending on the binding energies and whether the catalytic subsite is bound in the complex.

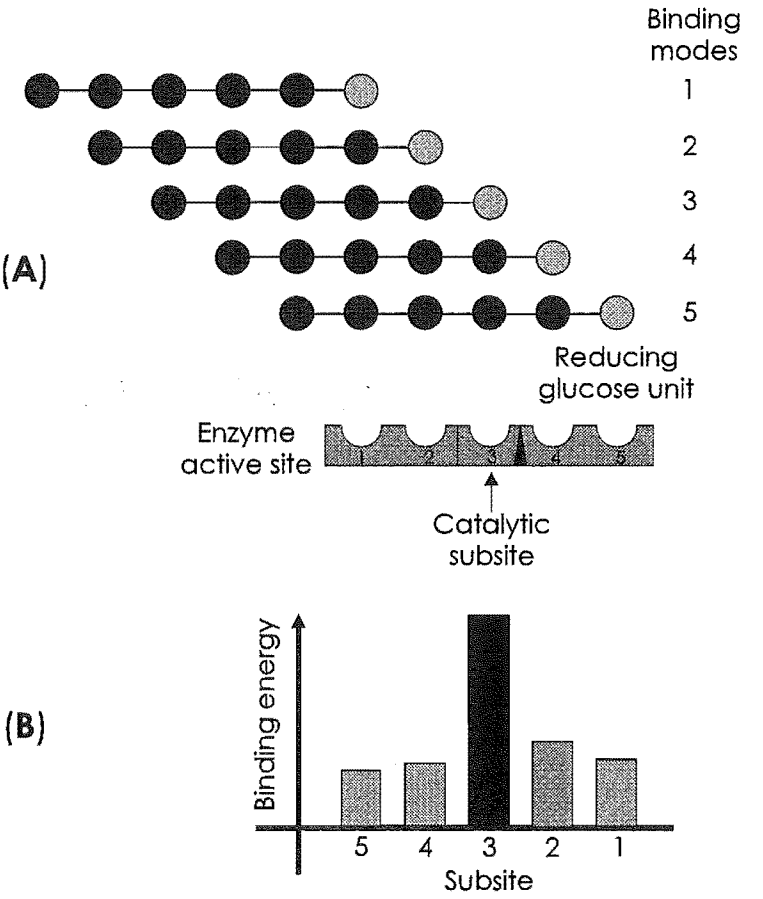

Figure 2.8: (**A**) A schematic representation of the different binding modes of a substrate molecule in the subsites of an enzyme. The circles represent glucose residues the pale coloured circles indicate the reducing end of the molecule. (**B**) Different binding energies of each subsite will influence the binding modes of the substrate.

Use of the subsite model requires knowledge of the approximate number of subsites, the location of the catalytic subsite, the substrate affinity for a particular subsite and the rate of hydrolysis. Many workers have established the subsite model for various *alpha*-amylases[1,2] using a variety of techniques including product analysis, labelling experiments and kinetic studies.

Porcine-pancreatic, *aspergillus oryzae* and barley *alpha*-amylases contain 5, 7 and 10 subsites respectively. In the former two, the catalytic site is between subsites 3 and 4, whereas for the latter, it is between sites 6 and 7.

2.2.5 Multimolecular Reactions

Although hydrolysis is the main reaction catalysed by *alpha*-amylase, it is not the only one. Since the hydrolysis reaction is reversible, *alpha*-amylase must also catalyse stereospecific substrate synthesis. Hehre *et al.*[1] have demonstrated this point by showing that *alpha*-amylases only have specificity for glycosyl *donors* in the catalysed reaction, not *acceptors*. Thus the assumed acceptor, water, can in fact be replaced by another substrate molecule. Under certain reaction conditions the action pattern of *alpha*-amylase is known to include catalysis of reactions such as transglycosylation, condensation, or shift-binding (Figure 2.9).[2]

Transglycosylation occurs when a glycosyl group from another substrate molecule acts as the acceptor instead of a water molecule. Condensation, the reverse of hydrolysis, is where two small substrates are polymerised to form a new glucosidic bond. The enzyme then rapidly cleaves the newly formed substrate molecule. Shift-binding is thought to occur when there is a high concentration of small substrate molecules and two molecules each bind half of the same active site. The binding affinities of one molecule pushes the other into a new binding position, allowing cleavage of a new bond.

The catalysis of these multimolecular-type reactions is mostly dependent on the substrate concentration and chain length. The smaller the chain length, the less likely the substrate is to bind to all the enzyme's subsites, and the smaller the chance of productive binding with the enzyme. When the concentration of these small substrates is high, the probability of multimolecular reactions occurring is increased.

Porcine-pancreatic *alpha*-amylase catalyses condensation reactions in the presence of high concentrations of maltotriose, and performs condensation and transglycosylation reactions with high concentrations of maltotetraose.[1,2] For substrates containing five or more glucose residues the catalysed reaction involves unimolecular hydrolysis.

For *aspergillus oryzae alpha*-amylase the main multimolecular reaction is transglycosylation.[2]

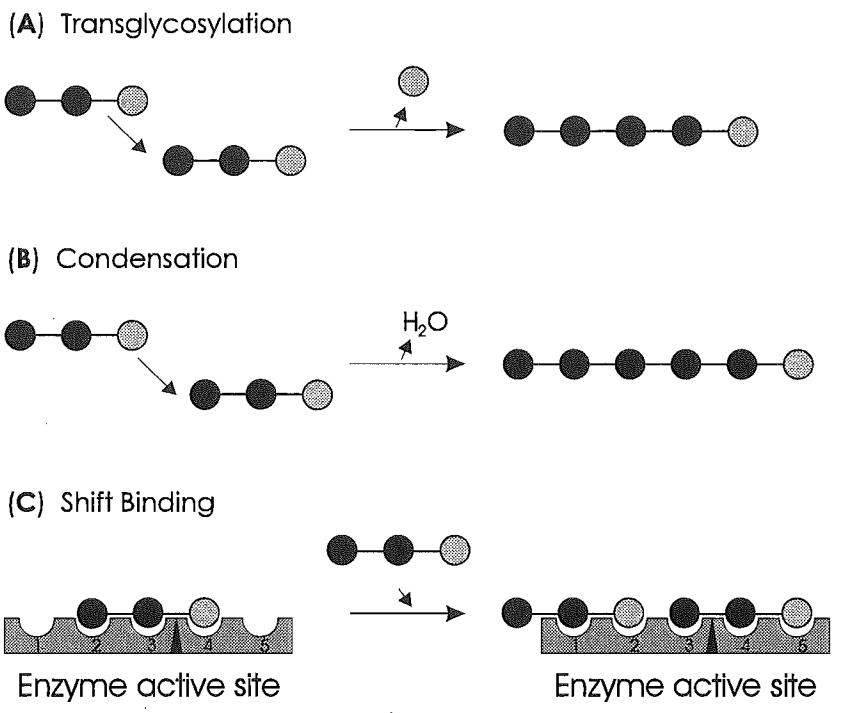

Figure 2.9: Alternative reactions catalysed by *alpha*-amylase. (**A**) transglycosylation, (**B**) condensation, (**C**) shift-binding. Dark circles are glucose units, pale circles are the reducing end of the molecule, the block is the active site of the enzyme.

2.3 Inhibitors of *Alpha*-Amylase

Although the action of *alpha*-amylase is important for the breakdown and metabolism of carbohydrates for the majority of species, there is also a demand in certain circumstances for inhibition of the enzyme's activity. An inhibitor is defined as any substance that reduces the rate of an enzyme-catalysed reaction when present in the reaction mixture. The inhibition is generally due to an interaction between either the enzyme or substrate and inhibitor, that slows or prevents the productive binding of the enzyme and substrate.[22,23]

The study of enzyme inhibitors provides useful information about how an enzyme works. Structural, chemical, and electronic properties of an inhibitor can provide insight into how a substrate binds, how the catalysed reaction proceeds, or what functionalities present in the enzyme govern and maintain the optimal activity of the enzyme. This information, in turn, can be used to develop enzymes with more desirable properties or better enzyme inhibitors.

Inhibition studies of *alpha*-amylase have been used to ascertain the number of binding sites in the active sites of different enzymes and the relative

affinity of each site for the substrate.[2] Studies have also provided much of the information that is known about the action pattern of *alpha*-amylases.[1]

Inhibitors of *alpha*-amylase are also applicable in the areas of medicine and agriculture.

2.3.1 Medicinal Uses of *Alpha*-Amylase Inhibitors

The control of disease states related to carbohydrate metabolism, such as diabetes, hyperglycaemia, or hyperinsulinaemia, is usually achieved through control of diet. This involves a reduction in carbohydrate intake and the regular intake of small meals.[3] Reducing the rate at which carbohydrates are metabolised through the inhibition of *alpha*-amylase has an application in the treatment of such medical conditions. Reducing the production of secondary metabolites, thus, ultimately reducing the amount of glucose produced, may allow for more control of blood sugar levels.

2.3.2 Agricultural Uses of *Alpha*-Amylase Inhibitors

Alpha-amylases present in stored wheat have very low activities in the absence of moisture. In the presence of moisture, however, germination occurs and the activity of the *alpha*-amylase increases to facilitate plant growth. This sprouting leads to the breakdown of stored starch and proteins in the wheat grains, making any flour produced unsuitable for baking and therefore of little value.[6] The development of an *alpha*-amylase inhibitor for use on wheat harvested in wet conditions would provide commercial benefit for both the agricultural sector and industries reliant on quality wheat products.

2.3.3 Substrate Analogue Inhibitors

There are many naturally occurring inhibitors of *alpha*-amylases, from various plant, bacterial, and microbial sources, described in the literature.[3,5,16,17,24,25] They are usually proteins, or oligosaccharide and polysaccharide compounds with structures similar to that of the natural substrate of the enzyme. Examples include compounds like nojirimycin and lucomycin A,

(Figure 2.10) and the end products of *alpha*-amylase action on starch, e.g. maltose, maltotriose and maltotetraose .

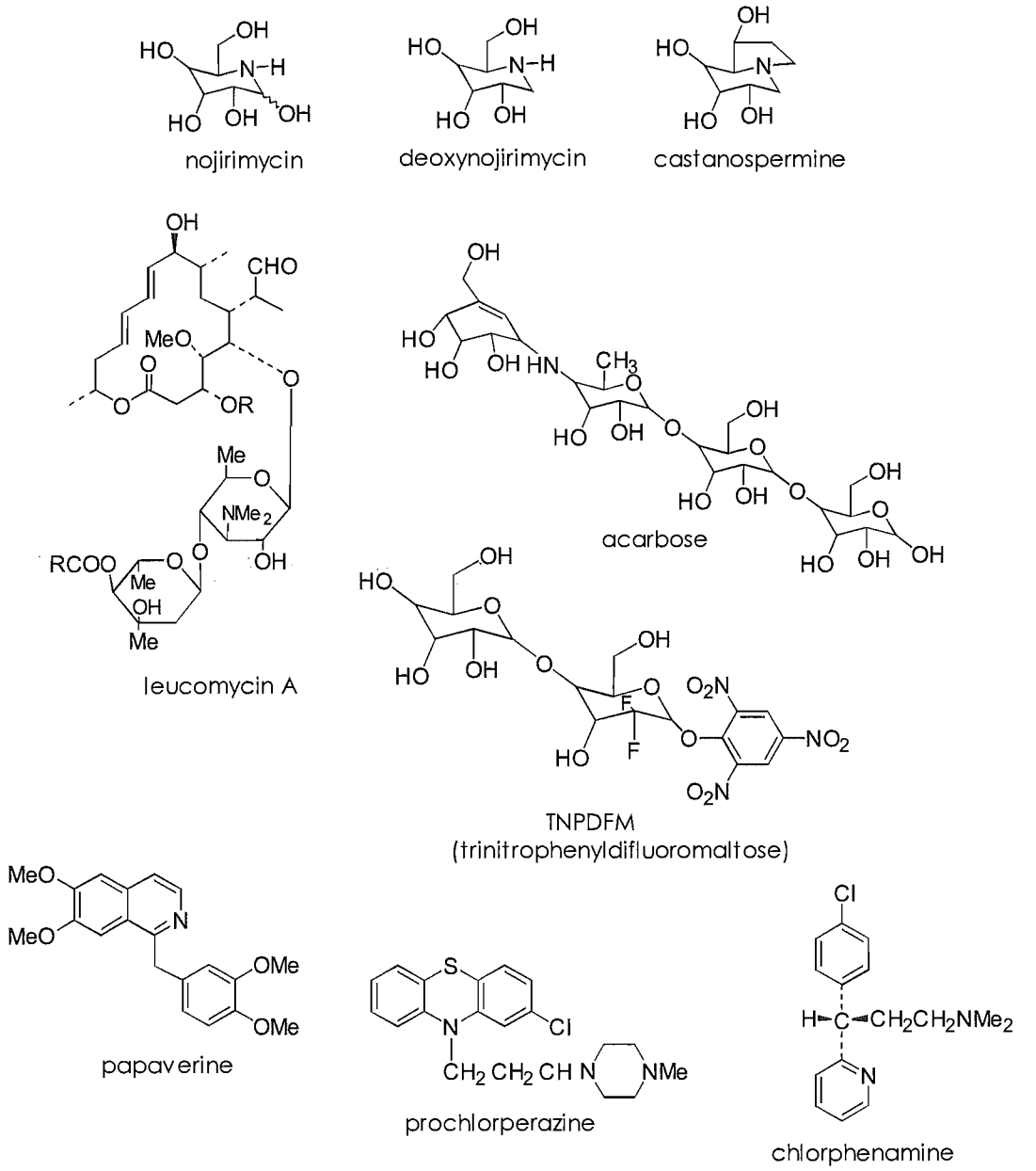

Figure 2.10: Inhibitors of *alpha*-amylases.

Many inhibitors have also been synthesised based on the structure of the natural substrate (section 2.2.1). The similarities between the structure of the natural substrate and the inhibitors effectively 'trick' the enzyme into binding the inhibitor.

The most effective of these inhibitors are often more structurally similar to a transition-state intermediate in the catalysed reaction (section 2.2.3) than either

the enzyme substrate or products. This is due to the fact that the enzyme binds the transition state more tightly than the substrate as a method of reducing the activation energy for the reaction.[26]

2.3.3.1 Transition–State Mimic

An example of an inhibitor that binds *alpha*-amylase as a transition state mimic is a compound given the generic name acarbose. Acarbose is a pseudo-oligosaccharide inhibitor that was first isolated from culture broths of *Actinoplanes* strain SE 50.[3] It belongs to a family of pseudo-oligosaccharide inhibitors all containing a characteristic core unit (acarvosine) essential for their inhibitory action. Acarvosine consists of a cyclitol unit (hydroxymethylconduritol residue) and an amino sugar (4-amino-4,6-dideoxy-D-glucopyranose), which is linked to a variable number of glucose residues *via* α-1,4-glucosidic linkages. In the case of acarbose, the number of attached sugars is two (Figure 2.11). It has been shown that the double bond in the cyclitol unit is important for the inhibitory activity, and that neither the cyclitol unit nor the amino sugar alone is capable of inhibiting *alpha*-amylase.

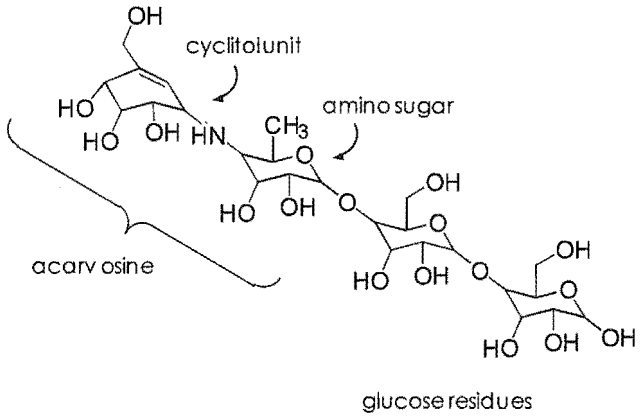

Figure 2.11: Acarbose.

The crystal structures of porcine-pancreas, *aspergillus oryzae* and barley-malt *alpha*-amylases, containing acarbose bound in the active site of the enzyme, have been solved by various workers.[15,17-19] These structures have provided information regarding the probable binding of substrate molecules in the active site, and the identification of catalytic residues through their location and binding of acarbose. As discussed in section 2.2.3 these findings have given insight into the possible hydrolysis mechanism of the enzymes. In each crystal

structure, the bound inhibitor contains additional glucose residues that extend from the original four-unit acarbose filling all the available subsites. Given that *alpha*-amylase is able to cleave only the reducing end glucose residue from acarbose,[15,17,18] it has been postulated that the altered molecules found occupying the active site in these studies were due to transglycosylation reactions catalysed by the enzyme (section 2.2.5).

Acarbose is thought to be a transition-state analogue of the natural substrate; the half-chair conformation of the cyclitol unit resembles that of the proposed oxocarbonium-ion transition-state intermediate in the hydrolysis reaction (section 2.2.3). This cyclitol unit has been located in all instances in the catalytic subsite of the enzymes.

Acarbose is currently being prescribed for the treatment of diabetes,[14] however, antisocial side effects (e.g. flatulence) associated with this treatment have piqued medical interest in the development of alternative inhibitors.

The majority of substrate-analogue inhibitors bind their target enzyme reversibly, effectively hindering the catalysed reaction rather than preventing it. However, some inhibitors are irreversible and their binding can result in covalent linkages that prevent the enzyme catalysed reaction occurring. One type of inhibitor that produces these covalent linkages is a mechanism-based inhibitor.

2.3.3.2 Mechanism-Based Inhibitors

Mechanism-based inhibitors are initially bound by the enzyme as a substrate analogue; however, subsequent enzyme action results in an activated molecule that inhibits the enzyme. The first reported mechanism-based irreversible inhibitor of *alpha*-amylase was a 2-deoxy-2,2-difluoroglycoside (McCarter and Withers),[21] which forms a stable enzyme-glycosyl intermediate that hydrolyses to product only very slowly (Figure 2.12). The presence of fluorine atoms at the C2 position of the glucose analogue destabilises the oxocarbonium-ion transition-state and prevents crucial hydrogen bonding to the enzyme, which results in a slowing down of the catalysed reaction. Incorporation of a reactive leaving group helps accelerate the formation of the enzyme-glycosyl intermediate, but the rate of the subsequent reaction is reduced, effectively inactivating the enzyme.

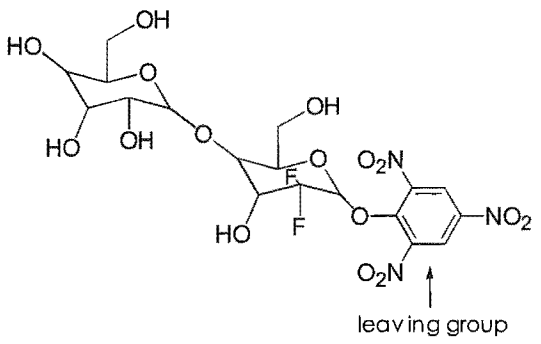

Figure 2.12: The mechanism-based inhibitor trinitrophenyl-2-deoxy-2,2-difluoroglycoside.

The development of this inhibitor has provided valuable insight into the mechanism of hydrolysis by *alpha*-amylases (Section 2.2.3).

2.3.4 Protein-Based Inhibitors

There have been many proteinaceous inhibitors discovered from plants and microbial origins and their activity against varieties of *alpha*-amylases from exogenous and endogenous sources investigated.[24]

Protein inhibitors of *alpha*-amylase generally exhibit time-dependent reversible inhibition of their target enzyme, in most cases by a non-competitive mechanism (section 4.3.2.1). A crystal structure of the inhibitor Tendamistat complexed with porcine-pancreatic *alpha*-amylase,[16] has revealed that this inhibitor binds the enzyme such that the active site of the enzyme is blocked, preventing substrate binding. Some protein inhibitors, however, have been postulated to bind the enzyme's natural substrate as a method of reaction inhibition.

Optimal pH is also important for protein inhibitory activity. In general the greatest activity is observed when the protein is operating at its isoelectric point or at a pH where the net electric charge on the protein inhibitor is opposite to that of the *alpha*-amylase.

2.3.5 Other Inhibitors

Some reported inhibitors of *alpha*-amylase are not of the typical oligosaccharide structure. Examples include papaverine, chlorpromazine and prochlorperazine (Figure 2.10). These molecules are reasonably large with a lot of

functionality. However, simple compounds have also been reported to inhibit *alpha*-amylase. One such molecule is ascorbic acid.[27]

2.3.5.1 Ascorbic Acid

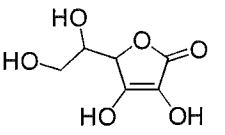

Figure 2.13: Ascorbic acid.

Ascorbic acid, or vitamin C (Figure 2.13), is a simple, water-soluble molecule that is probably most well known for its antiscorbutic effects and thus its necessity in the human diet.[28,29] The main biological function of ascorbic acid is as an anti-oxidant or reducing agent and during reaction is converted to dehydroascorbic acid (DHA) (Figure 2.14). This oxidation is thought to occur by two, one-electron steps *via* an ascorbyl free radical. DHA is a potentially toxic and unstable compound, which is normally rapidly converted back to ascorbic acid by enzyme catalysed processes. Thus ascorbic acid and DHA are two halves of a redox couple which functions by cycling between their reduced and oxidised states.

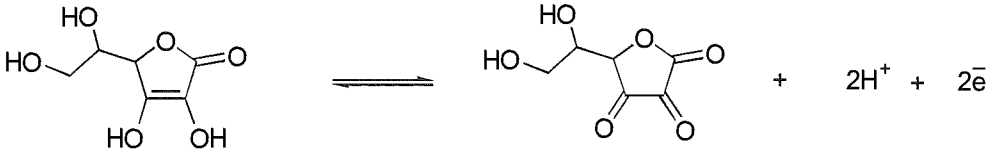

Figure 2.14: The redox couple of ascorbic acid and dehydroascorbic acid.

Our attention was drawn to an obscure report by Palla and Verrier,[27] suggesting that ascorbic acid is a powerful inhibitor of *alpha*-amylase. This report appears to have been overlooked, as no references to this work could be found in subsequent literature. Because of its ready availability, low cost, and relatively uncomplicated structure, ascorbic acid is an ideal compound to study with respect to its inhibitory actions. We decided, therefore, to thoroughly investigate the inhibitory action of ascorbic acid with regard to *alpha*-amylases. We chose to focus our studies on determining the structural features of ascorbic acid that were necessary for its action and to undertake kinetic studies to elucidate its mode of

inhibition. With this information, the development of potent ascorbic-acid-based *alpha*-amylase inhibitors may be possible.

The following part of this thesis presents the results of our structure-activity investigations into ascorbic acid as an inhibitor of *alpha*-amylases.

2.4 REFERENCES

(1) Boyer, P. D., Ed. *The Enzymes*, 3rd ed.; Academic Press: New York, 1971; Vol. 5.

(2) Wong, D. W. S. *Food Enzymes. Structure and Mechanism*; Chapman and Hall: New York, 1995.

(3) Truschelt, E.; Frommer, W.; Junge, B.; Müller, L.; Schmidt, D. D.; Wingender, W. *Angew. Chem. Int. Ed. Engl.* **1981**, *20*, 744-761.

(4) Schomburg, D.; Salzmann, M., Eds. *Enzyme Handbook*; Springer-Verlag: Berlin, 1990.

(5) Søgaard, M.; Abe, J.-ichi; Martin-Eauclaire, M. F.; Svensson, B. *Carbohydrate Polymers* **1993**, *21*, 137-146.

(6) Hill, R. D.; MacGregor, A. W. In *Advances in Cereal Science and Technology*; 1988; Vol. IX.

(7) Gerhartz, W., Ed. *Enzymes in Industry. Production and Applications*; VCH: Weinheim, 1990.

(8) Reed, G., Ed. *Enzymes in Food Processing*, 2nd ed.; Academic Press: New York, 1975.

(9) Pierre, K. J.; Ker-Kong, T.; Rauscher, E.; Wahlefeld, A. W.; Foo, Y.; Rosalki, S. B. In *Methods of Enzymatic Analysis*, 3rd ed.; Bergmeyer, H. U.; Bergmeyer, J.; Graßl, M., Eds.; Verlag Chemie: Weinheim, 1984; Vol. IV, pp. 145-177.

(10) Ceska, M.; Birath, K.; Brown, B. *Clin. Chim. Acta* **1969**, 26, 437-444.

(11) Klein, B.; Foreman, J. A.; Searcy, R. L. *Clinical Chemistry* **1970**, *16*, 32-38.

(12) Searcy, R. L.; Wilding, P.; Berk, J. E. *Clin. Chim. Acta* **1967**, *15*, 189-197.

(13) McCleary, B. V.; Sheehan, H. *Journal of Cereal Science* **1987**, 6, 237-251.

(14) Uchida, R.; Nasu, A.; Tokutake, S.; Kasai, K.; Tobe, K.; Yamaji, N. *Chem. Pharm. Bull.* **1999**, *47*, 187-193.

(15) Brzozowski, A. M.; Davies, G. J. *Biochemistry* **1997**, *36*, 10837-10845.

(16) Machius, M.; Vértesy, L.; Huber, R.; Weigand, G. *J. Mol. Biol.* **1996**, *260*, 409-421.

(17) Kadziola, A.; Sϕgaard, M.; Svensson, B.; Haser, R. *J. Mol. Biol.* **1998**, *278*, 205-217.

(18) Qian, M.; Haser, R.; Buisson, G.; Duée, E.; Payan, F. *Biochemistry* **1994**, *33*, 6284-6294.

(19) Qian, M.; Haser, R.; Payan, F. *J. Mol. Biol.* **1993**, *231*, 785-799.

(20) Heightman, T. D.; Vasella, A. T. *Angew. Chem. Int. Ed.* **1999**, *38*, 750-770.

(21) Braun, C.; Brayer, G. D.; Withers, S. G. *J. Biol. Chem.* **1995**, *270*, 26778-26781.

(22) Voet, D.; Voet, J. G. *Biochemistry*; John Wiley and Sons: New York, 1990.

(23) Cornish-Bowden, A.; Wharton, C. W. *Enzyme Kinetics*; IRL Press: Oxford, 1988.

(24) Silano, V. In *Enzymes and Their Role in Cereal Technology*; Kruger, J. E.; Lineback, D.; Staffer, C. E., Eds.; 1987.

(25) Ogawa, S.; Ikeda, N. *Carbohydrate Research* **1988**, *175*, 294-301.

(26) Bugg, T. *An Introduction to Enzyme and Coenzyme Chemistry*; Blackwell Science: Oxford, 1997.

(27) Palla, J. C.; Verrier, J. *Ann. Technol. Agric.* **1974**, *23*, 151-159.

(28) Sies, H.; Stahl, W. *Vitamin C The state of the art in disease prevention sixty years after the Nobel Prize*; Springer-Verlag: Milano, 1998.

(29) Davies, M. B.; Austin, J.; Partridge, D. A. *Vitamin C. Its Chemistry and Biochemistry*; The Royal Society of Chemistry: Letchworth, 1995.

3 Ascorbic-Acid Inhibitors

SAR studies on ascorbic acid required the preparation of derivatives incorporating systematic changes in its structure, to enable the determination of those features that were necessary for its inhibitory action against *alpha*-amylase. Although ascorbic acid is a simple molecule, it is highly functionalised. It contains four hydroxyl groups, and a double bond, organised into an ene-diol moiety and a diol chain (Figure 3.1). The ene-diol forms part of a five-membered lactone ring with the diol chain attached at C4.

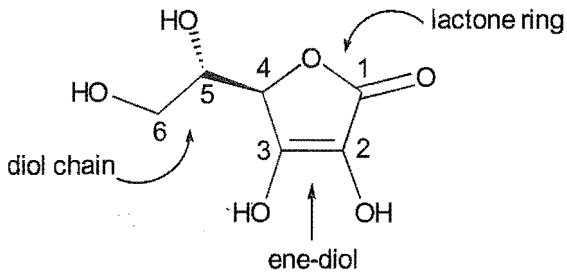

Figure 3.1: The structure of L-Ascorbic acid.

The natural form of ascorbic acid has an L configuration at C5.[1] However, the epimer D-isoascorbic acid is also commercially available, so we were able to investigate the importance of this stereochemistry on its inhibitory action.

3.1 Derivatives of Ascorbic Acid

Most of the ascorbic-acid derivatives investigated were known compounds, prepared using literature methods. Chemical modification centred mainly on the hydroxyl groups and included protection with acetal, acyl or alkyl groups. The effect of reducing the C2 – C3 double bond was also investigated. Table 3.1 gives a complete list of the derivatives prepared.

Characterisation of the synthesised products utilised proton and ^{13}C NMR spectroscopy, mass spectrometry, and IR spectroscopy. These data were compared to literature values where appropriate. In some instances the observed proton-NMR data is described relative to the resonances observed for ascorbic acid. These are as follows: ^{1}H NMR (D_2O) δ 4.88 (1H, H4), 3.98 (1H, H5), 3.67 (2H, H6).

NMR studies have shown that the preferred conformations about the C4-C5 and C5 – C6 bonds of ascorbic acid in solution are the same as those observed in the crystal lattice.[1] Thus, we were interested in analysing the crystal structures of the prepared ascorbic-acid derivatives for the purpose of modelling optimal structural conformations. However, suitable crystals were only obtained for two of the prepared derivatives.

Table 3.1: L-ascorbic acid and D-isoascorbic-acid derivatives prepared.

No.	Name	Structure
3.1	5,6-isopropylidene-L-ascorbic acid	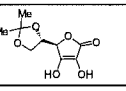
3.2	3-O-methyl-5,6-isopropylidene-L-ascorbic acid	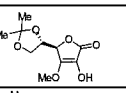
3.3	2-acetyl-3-O-methyl-5,6-isopropylidene-L-ascorbic acid	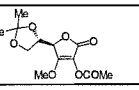
3.4	3-O-methyl-L-ascorbic acid	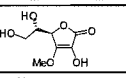
3.5	2,3-di-O-methyl-5,6-isopropylidene-L-ascorbic acid	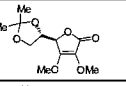
3.6	2,3-di-O-methyl-L-ascorbic acid	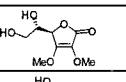
3.7	2,3-di-O-methyl-6-acetyl-L-ascorbic acid	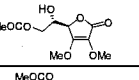
3.8	2,3-di-O-methyl-5,6-diacetyl-L-ascorbic acid	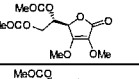
3.9	5,6-di-acetyl-L-ascorbic acid	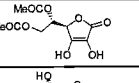
3.10	2,3-di-O-methyl-6-propionyl-L-ascorbic acid	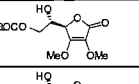
3.11	2,3-di-O-methyl-6-butyryl-L-ascorbic acid	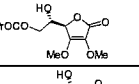
3.12	6-palmitate-L-ascorbic acid	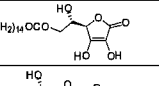
3.13	L-gulono-1,4-lactone	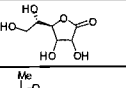
3.14	5,6-isopropylidene-D-isoascorbic acid	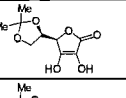
3.15	2,3-di-O-methyl-5,6-isopropylidene-D-isoascorbic acid	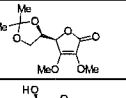
3.16	2,3-di-O-methyl-D-isoascorbic acid	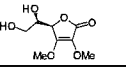

Synthesis of 5,6-Isopropylidene-L-Ascorbic Acid (3.1)

Compound **3.1** was prepared using the method of Jung *et al.*[2] A solution of L-ascorbic acid, acetone, and acetyl chloride was stirred together at room

temperature for three hours and then refrigerated. Product **3.1** precipitated out of solution and was recrystallised from acetone/petroleum ether in a 84% yield. Analysis by proton-NMR spectroscopy revealed an additional six-proton singlet resonance, relative to ascorbic acid, at δ 1.30, corresponding to the methyl groups of the isopropylidene moiety.

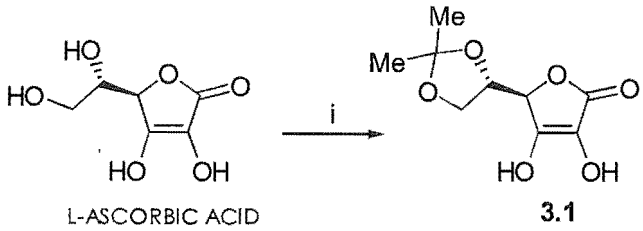

L-ASCORBIC ACID **3.1**

Scheme 3.1: (i) acetone, acetyl chloride, stirred 3 hours.

3.1.1 Protection of the C2 or C3 Hydroxyl Groups

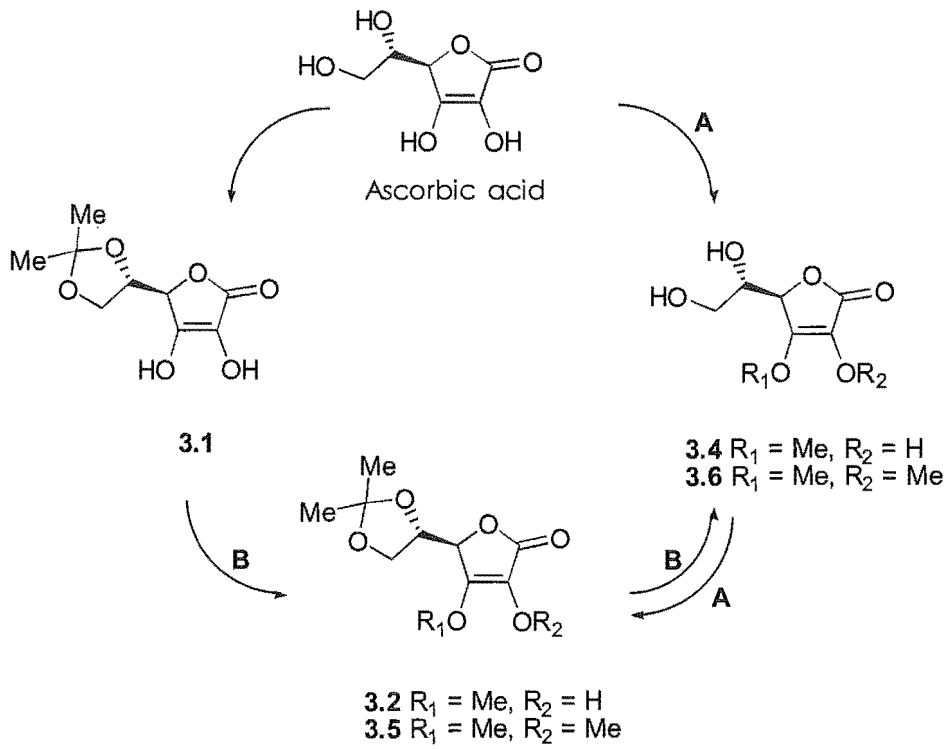

Figure 3.2: Potential routes to methylated derivatives of ascorbic acid and compound **3.1**.

The available literature[2,6] suggests that derivatives of ascorbic acid and compound **3.1** in which the C2 and/or C3 hydroxyl groups are protected by

methylation, can be prepared by either of two routes as shown in Figure 3.2. Route **A** involves the methylation of ascorbic acid followed by protection of the diol chain with an acetonide group, while route **B** involves methylation of compound **3.1** followed by hydrolysis of the acetonide group.

Given the reported success of direct methylation of ascorbic acid, preparation of these compounds was initially attempted by route **A** using a procedure reported by Jung *et al.*[2] However, this procedure, and subsequent alternative protocols utilising diazomethane as the methylating agent,[3-6] resulted in either unreacted starting material or complex mixtures of products (as determined by proton-NMR spectroscopy). We therefore prepared the target derivatives using route **B**.

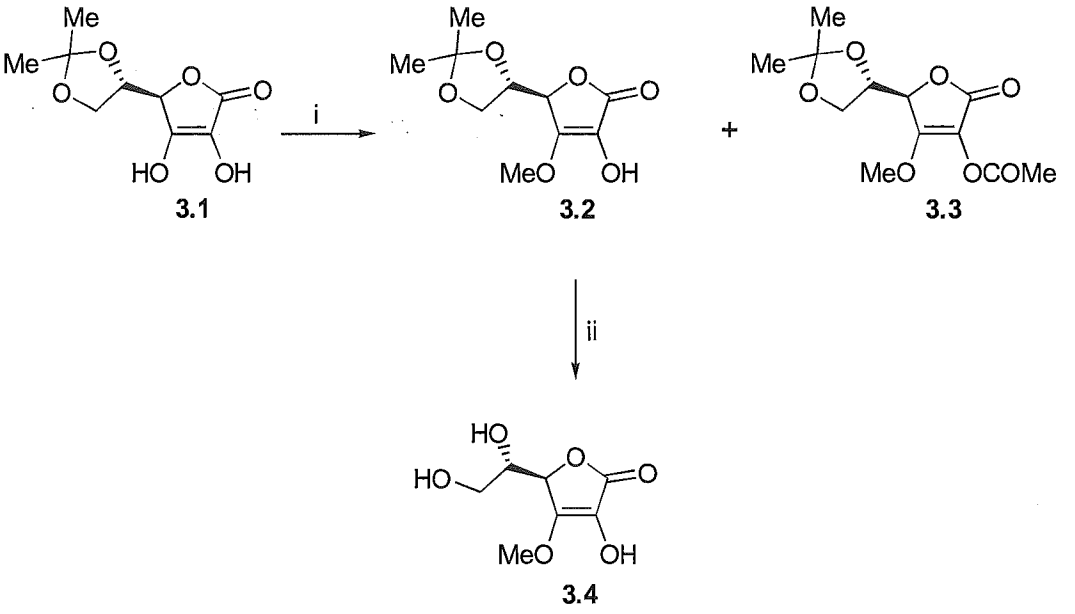

Scheme 3.2: (i) $NaHCO_3$, DMSO, MeI, stirred at 50°C overnight; (ii) methanol, 2M HCl, stirred overnight.

Three compounds synthesised in this way are shown in Scheme 3.2. Preparation of the singly protected C3 methoxy derivative **3.4** allowed us to establish the necessity of this functional group for inhibitory activity (see Chapter 4). Preparation of compound **3.2** incorporating protection of the C3, C5 and C6 hydroxyl groups allowed a comparison to be made between the activity of compounds **3.1** and **3.4** and thus the importance of these functional groups could also be ascertained.

Synthesis of 3-O-Methyl-5,6 Isopropylidene-L-Ascorbic Acid (3.2) and 2-Acetyl-3-O-Methyl-5,6-Isopropylidene-L-Ascorbic Acid (3.3)

3-O-Methyl-5,6-isopropylidene-L-ascorbic acid (**3.2**) was prepared using the procedure of Nihro *et al.*[7] as shown in Scheme 3.2. Compound **3.1**, $NaHCO_3$ and DMSO were stirred together, followed by addition of iodomethane. Reaction overnight followed by work-up and purification gave **3.2** in a 19% yield. Analysis by proton-NMR spectroscopy revealed an additional three-proton singlet resonance at δ 4.18 corresponding to the methoxy group.

Compound **3.3** was isolated in a 8% yield during the purification of product **3.2** (Scheme 3.2). The proton-NMR spectrum for **3.3** included an additional three-proton singlet resonance at δ 2.29 relative to compound **3.2**, which was assigned to the acetate group. Proton resonances at δ 1.40 and 1.36 indicated that the acetonide group was still intact, thus acylation had not occurred at C5 or C6 in product **3.3.** Additional NMR experiments revealed a nOe between the C4 proton at δ 4.67 and the methoxy group at δ 4.08, indicating that methylation had probably occurred on the C3 hydroxyl group. Thus the acetate was assigned as being attached at the C2 position.

Synthesis of 3-O-Methyl-L-Ascorbic Acid (3.4)

The singly protected compound **3.4** was synthesised by hydrolysis of the acetonide of compound **3.2** (Scheme 3.2). Removal of the solvent and purification gave **3.4** as an oil in a 56% yield. Characterisation by proton-NMR spectroscopy revealed an absence of the singlet resonances of the acetonide group, previously present in compound **3.2.**

Attempted Synthesis of 2-O-methyl-L-Ascorbic Acid

Attempts were made to prepare 2-O-methyl-5,6-isopropylidene-L-ascorbic acid using a procedure described by Seib *et al.*[3] To a stirred solution of **3.1** in an aqueous NaOH solution (pH >10, determined using pH paper) at 60°C, was added dimethyl sulfate, and the mixture was reacted for 1 hour. Analysis of the products by proton-NMR spectroscopy revealed a mixture of compounds that were not characterised. Alternative methods described by Nihro *et al.*[7] and Kato *et al.*[8] gave similar results.

3.1.2 Protection of C2 and C3 Hydroxyl Groups

Modification at all four hydroxyl groups, and subsequent hydrolysis to give the C2-C3 protected derivative allowed the significance of the C2 hydroxyl group for inhibitory activity to be investigated and the importance of the C5 and C6 groups relative to the C2 and C3 groups to be established.

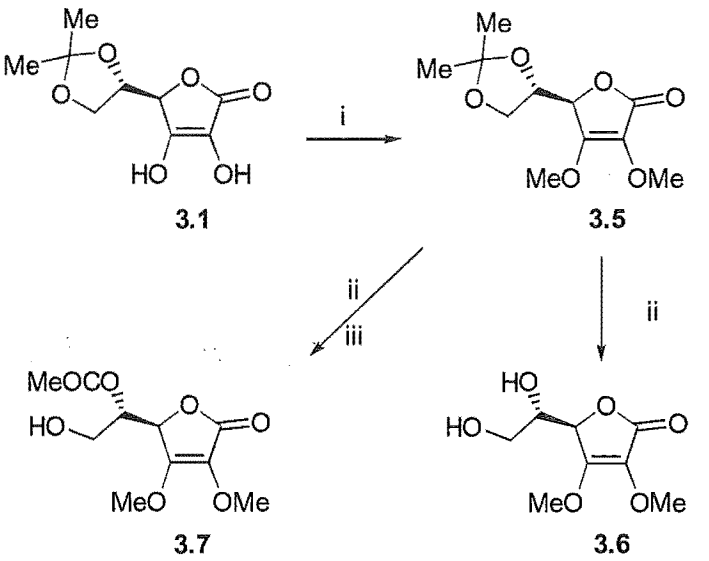

Scheme 3.3: (i) dimethyl sulfate, K_2CO_3, acetone, refluxed overnight; (ii) methanol, 2M HCl, 50°C 4 hours; (iii) H^+, ethyl acetate.

Synthesis of 2,3-Di-O-Methyl-5,6-Isopropylidene-L-Ascorbic Acid (3.5)

Compound **3.5** was prepared using a general procedure reported by Le Merrer *et al.*[9] (Scheme 3.3). Compound **3.1** was refluxed overnight in a mixture containing K_2CO_3, acetone, and dimethyl sulfate to give **3.5** in a 29% yield after crystallisation. The proton-NMR spectrum showed two three-proton singlets at δ 4.15 and 3.86, due to the methoxy groups on C3 and C2 respectively.

Synthesis of 2,3-Di-O-Methyl-L-Ascorbic Acid (3.6)

Compound **3.6** was prepared by the hydrolysis of the acetonide of compound **3.5** as shown in Scheme 3.3. Evaporation of the solvent gave **3.6** in a 70% yield after recrystallisation. A proton-NMR spectrum of **3.6** revealed the absence of the methyl resonances at δ 1.39 and 1.36 associated with the isopropylidene group in **3.5**.

3.1.3 Protection of C5 and C6 Hydroxyl Groups

Synthesis of 2,3-Di-O-Methyl-6-Acetyl-L-Ascorbic Acid (3.7)

Compound **3.7** was fortuitously obtained when attempting to workup the hydrolysed product **3.6** by extraction with ethyl acetate.

Compound **3.5** was stirred in a mixture of methanol and aqueous HCl at 50°C for 4 hours. Extraction of the mixture with ethyl acetate followed by removal of the solvent gave a solid residue, which was recrystallised from ether to give **3.7** as colourless prisms in a 74% yield (Scheme 3.3). Proton-NMR spectroscopy revealed a three-proton singlet at δ 2.11. The C6 protons of **3.7** were also shifted downfield relative to compound **3.6**, from δ 3.80 to 4.34 and 4.22.

The ^{13}C-NMR spectrum of **3.7** contained additional resonances, relative to **3.6**, at δ 20.81 and 171.01, due to the presence of the acetyl group. Given that ethyl acetate was the only source of acylating agent in the reaction, we propose that residual acid present in the reaction mixture, after evaporation of the solvent, catalysed a transesterification reaction between the free primary alcohol of **3.6** and ethyl acetate to give compound **3.7**. Due to the quality of the crystals prepared, an X-ray crystal structure analysis was performed to confirm the structure of compound **3.7*** (Figure 3.3). A search of the Cambridge Crystallographic Database revealed no previous reports of this compound.

In the crystalline state **3.7** has two main intermolecular hydrogen-bonding interactions (Figure 3.4). The first is between the carbonyl oxygen of the acetyl moiety and the C4 hydrogen of the lactone ring of an adjacent molecule, and the second is between the C1 carbonyl oxygen and the C5 hydroxyl group of another adjacent molecule. The second interaction is easily seen in the lower part of Figure 3.4, labelled D. This figure also shows the screw axis of the P(2)1 space group in which this molecule crystallises, seen by inspection of the molecules labelled A, B and C.

* For complete crystallographic data the reader is referred to appendix C.

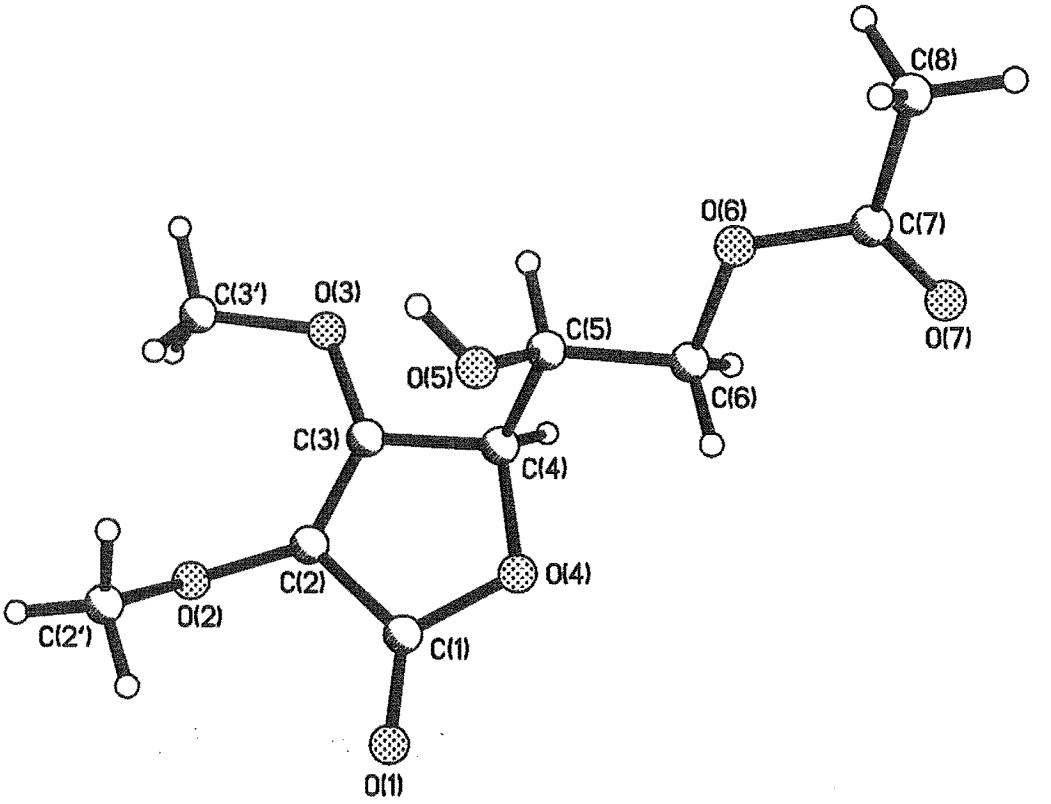

Figure 3.3: The crystal structure of 2,3-di-O-methyl-6-acetyl-L-ascorbic acid.

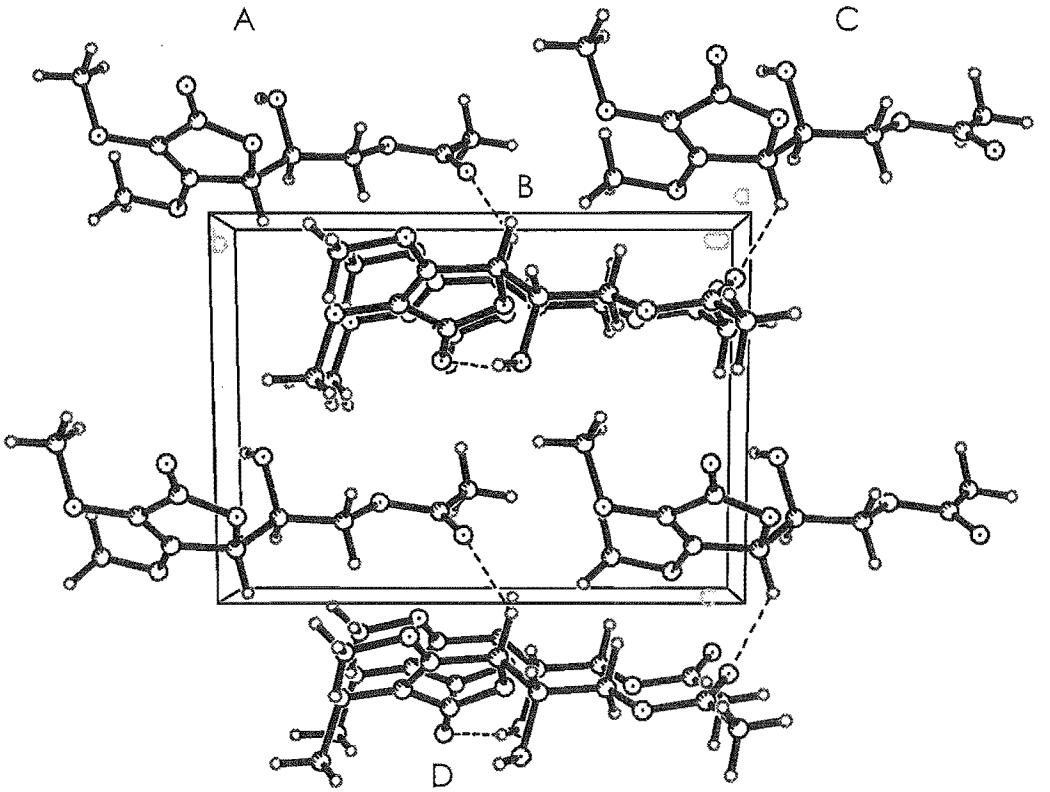

Figure 3.4: Packing arrangement of compound **3.7** looking down the a axis.

Synthesis of 2,3-Di-O-Methyl-5,6-Diacetyl-L-Ascorbic Acid (3.8)

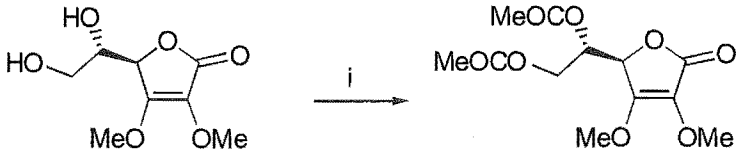

3.6 **3.8**

Scheme 3.4: (i) acetic anhydride, pyridine, stirred two hours.

Attempts to optimise the synthesis of compound **3.7** lead to the diacetyl compound **3.8**. This derivative was expected to have similar activity to compound **3.5** as all four hydroxyl groups are protected in both compounds. Preparation of **3.8** also enabled the effect of different choices of C5 and C6 protection on inhibitory activity to be investigated.

Compound **3.6** was dissolved in pyridine and stirred with acetic anhydride at room temperature for 2 hours. The solvent was removed and the resulting solid recrystallised from ether to give crystals of **3.8** as transparent plates in a 24% yield. proton-NMR spectroscopy ($CDCl_3$) revealed a six-proton singlet at δ 2.07 corresponding to acetate groups at C5 and C6. As expected, the resonances for the C6 and C5 protons were significantly downfield (at δ 4.36, 4.26 and 5.35 respectively) relative to the chemical shifts of the same protons in **3.6** (Figure 3.5). The ^{13}C-NMR spectrum contained additional resonances relative to **3.6** (at δ 20.36, 20.55, 169.38 and 170.22), corresponding to the two acetyl moieties.

Synthesis of 5,6-Di-Acetyl-L-Ascorbic Acid (3.9)

To ensure that the activity observed for compound **3.1** was not as a result of hydrolysis under the assay conditions, and therefore due to ascorbic acid, a derivative containing acetyl protecting groups at C5 and C6 was prepared. Synthesis of this compound (**3.9**) also enabled comparison with the activity of **3.8.**

The 5,6-diacetyl ascorbic-acid derivative **3.9**, was prepared based on a procedure by Creighton *et al.*[10] (Scheme 3.5).

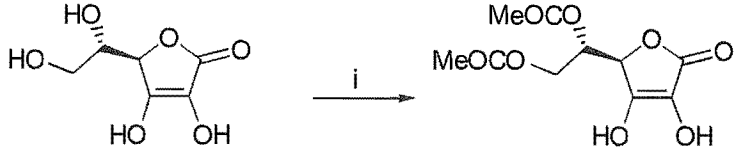

L-ASCORBIC ACID **3.9**

Scheme 3.5: (i) acetic anhydride, H_2SO_4, stirred 40°C 2 hours.

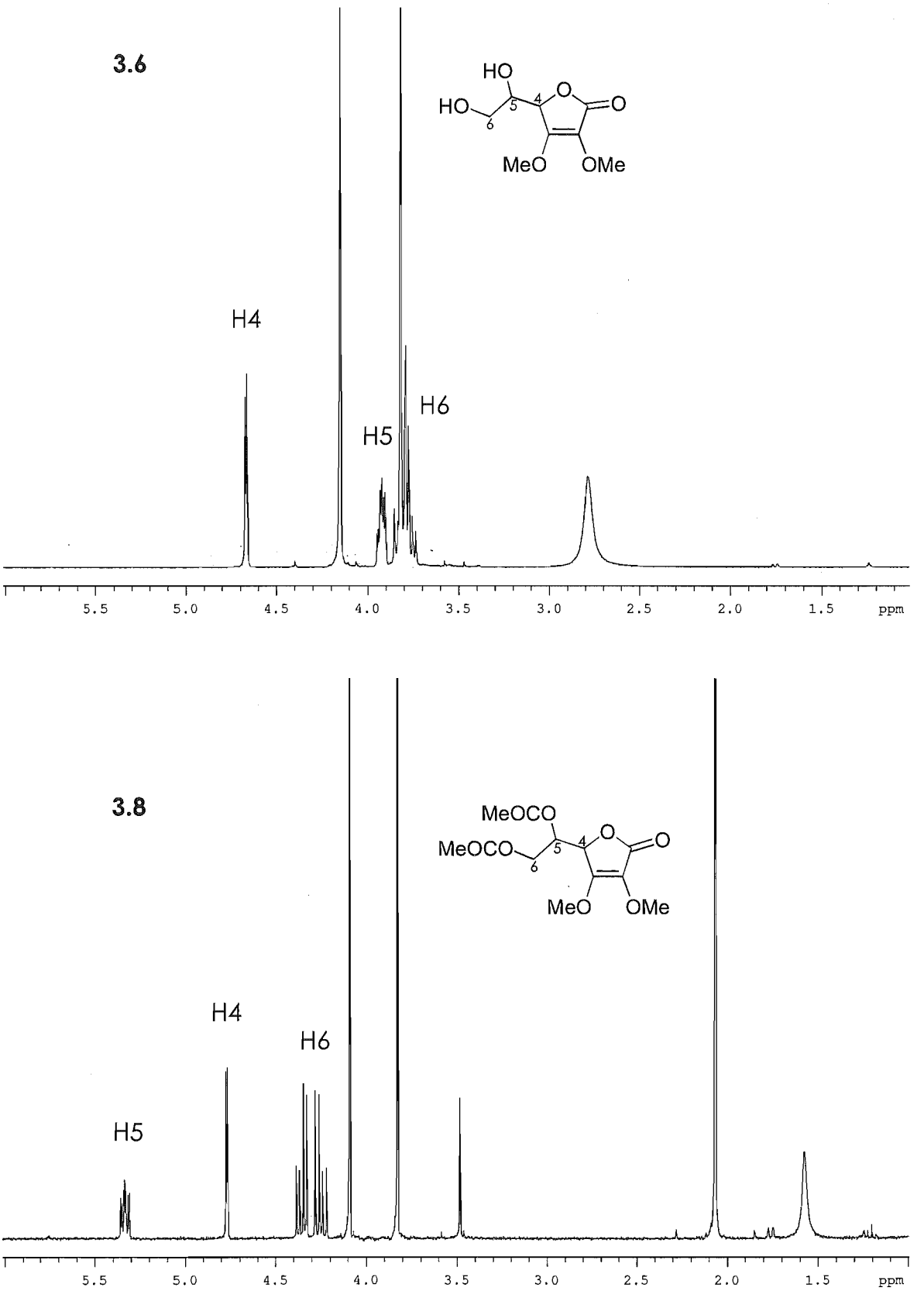

Figure 3.5: proton NMR spectra of compounds **3.6** and **3.8**.

A drop of concentrated aqueous H_2SO_4 was added to a mixture of ascorbic acid and acetic anhydride and the mixture was stirred with gentle heating for 2 hours. Evaporation of the solvent, and seeding of the resultant syrup, produced **3.9** as crystalline needles. A proton-NMR spectrum revealed the expected downfield shift, relative to ascorbic acid, of the resonances corresponding to the C5 and C6 protons of **3.9** (δ 5.43, 4.37 and 4.23 respectively). The acetyl methyl groups appeared as two three-proton singlets at δ 2.00 and 1.97.

3.1.4 Extended-Acyl-Group Protection of the C6 Hydroxyl Group

The reactivity of the C6 primary alcohol of ascorbic acid in the presence of the C2- and C3-protected ene-diol of compound **3.6**, is demonstrated by the simplicity with which **3.7** was prepared (Scheme 3.3). Due to the ease with which this reaction occurred, it was decided to investigate the possible synthesis of similar derivatives, containing extended carbon chains at C6, using a similar methodology (Figure 3.6). Compounds were prepared incorporating a propionyl and a butyryl group: compounds **3.10** and **3.11** respectively (Figure 3.6). As part of this series, we attempted to prepare a compound containing a benzoate moiety. However, reaction of compound **3.6**, *p*-TSA and ethyl benzoate at 50°C overnight and subsequent workup, returned only starting material as determined by proton-NMR analysis.

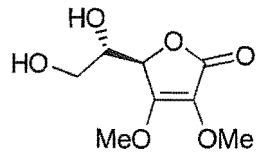

3.6

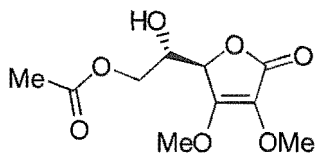

3.7

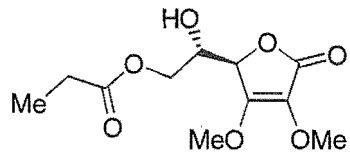

3.10

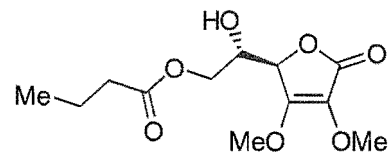

3.11

Figure 3.6: Derivatives **3.6**, **3.7**, **3.10** and **3.11**.

This series of syntheses gave lower yields for the longer acyl-group substitutions, (**3.7** = 74%, **3.10** = 12%, **3.11** = 7%, see Figure 3.6 for structures). These results led us to conclude that the success of transesterification reactions at C6 of compound **3.6**, using these simple procedures, had some dependency on the size of the introduced ester group.

Synthesis of 2,3-Di-O-Methyl-6-Propionyl-L-Ascorbic Acid (3.10)

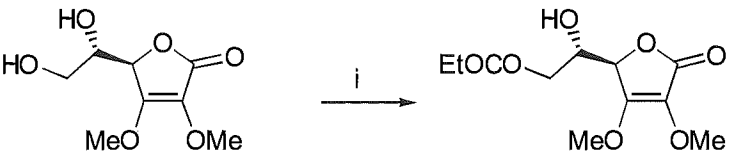

3.6 **3.10**

Scheme 3.6: (i) ethyl propionate, *p*TSA, 70°C overnight.

Compound **3.6**, *p*TSA and ethyl propionate were stirred at 70°C overnight (Scheme 3.6). Workup and purification by radial chromatography gave **3.10** in a 12% yield. The proton-NMR spectrum was consistent with acylation at C6, as characterised by a downfield shift of the C6-proton resonances relative to those seen in the spectrum of compound **3.6**. The presence of a two-proton quartet at δ 2.38 and a three-proton triplet at δ 1.15 was consistent with a propionyl group. The ^{13}C-NMR spectrum of **3.10** showed additional resonances at δ 8.97, 27.38 and 174.45, relative to the starting material **3.6**, consistent with the presence of a propionyl group.

The appearance of a molecular ion with a mass of 260 in the mass spectrum of this compound confirmed the incorporation of the propionyl group.

Synthesis of 2,3-Di-O-Methyl-6-Butyryl-L-Ascorbic Acid (3.11)

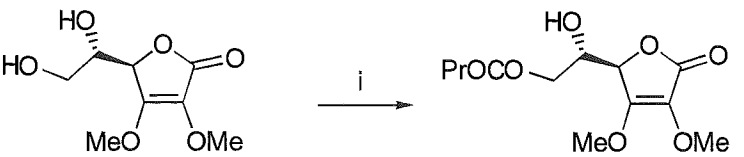

3.6 **3.11**

Scheme 3.7: (i) ethyl butyrate, *p*TSA, 70°C overnight.

Compound **3.6** was stirred with ethyl butyrate in the presence of *p*TSA. Workup and purification by radial chromatography gave **3.11** as a yellow oil in a 7% yield. Analysis by proton-NMR spectroscopy revealed a downfield shift of the C6 proton resonances to δ 4.35 and 4.23, relative to **3.6**, characteristic of C6 acylation. The appearance of an additional two-proton triplet at δ 2.34, a two-proton quartet at δ 1.67, and a three-proton triplet at δ 0.96 was consistent with acylation by a butyryl moiety. The ^{13}C-NMR spectrum contained the appropriate additional resonances for a butyryl group: δ 13.61, 18.32, 35.93 and 173.64.

The appearance of a molecular ion with a mass of 274 in the mass spectrum of **3.11** confirmed the incorporation of a butyryl group.

Synthesis of 6-Palmitate-L-Ascorbic Acid (3.12)

This compound was synthesised to establish if a large steric group attached to ascorbic acid affected its inhibitory properties (Scheme 3.8). It also provided a means of determining whether the inhibitory activity of compounds **3.9** and **3.10** were dominated by (a) the length of the chain at C6, or (b) the protection of the secondary alcohols at C2 and C3. Preparation of **3.12** further tested the necessity of the C6 hydroxyl group for activity.

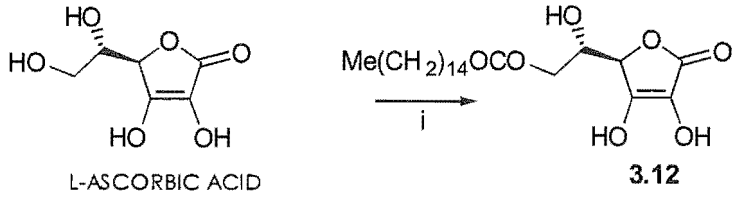

Scheme 3.8: (i) palmitic acid, H_2SO_4.

Compound **3.12** was prepared as described by Seib *et al.*[11] Ascorbic acid and palmitic acid were stirred together in concentrated aqueous H_2SO_4. Workup gave **3.12** as a white solid in a 42% yield. proton-NMR data on this compound ($CDCl_3$/DMSO) was in agreement with the literature. As expected for acylation, the chemical shifts of the C6 protons of **3.12** were downfield, relative to ascorbic acid, at δ 4.28 and 4.20. The following resonances defined the palmitate chain: a two-proton triplet at δ 2.33; a two-proton multiplet at 1.61; a 26-proton multiplet at 1.25 and a three-proton triplet at 0.87 for the terminal methyl group.

3.1.5 Reduction of the Double Bond

Synthesis of L-Gulono-1,4-Lactone (3.13)

This compound tested the necessity of the double bond for the inhibitory action of ascorbic acid. It was prepared using literature methods[12,13] (Scheme 3.9). An aqueous solution of ascorbic acid was hydrogenated over Pd/C for three days. Workup gave **3.13** as colourless prisms, which were suitable for X-ray crystallographic analysis (Figure 3.7). proton-NMR showed the expected appearance of an additional two-proton resonance at δ 4.43 due to reduction of the double bond.

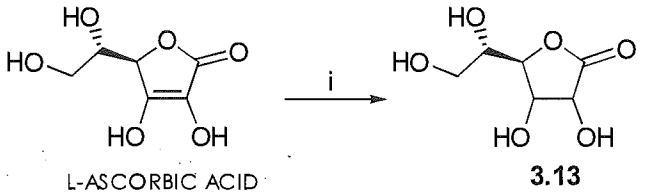

L-ASCORBIC ACID **3.13**

Scheme 3.9: (i) 10% Pd/C, water, H_2, 40 psi, 3 days.

The crystal structure of **3.13** shows that hydrogenation of the ascorbic-acid ene-diol moiety has occurred from the less-hindered face of the lactone ring resulting in two new stereocentres in which the hydroxyl groups extend out from the plane of the ring (Figure 3.7).

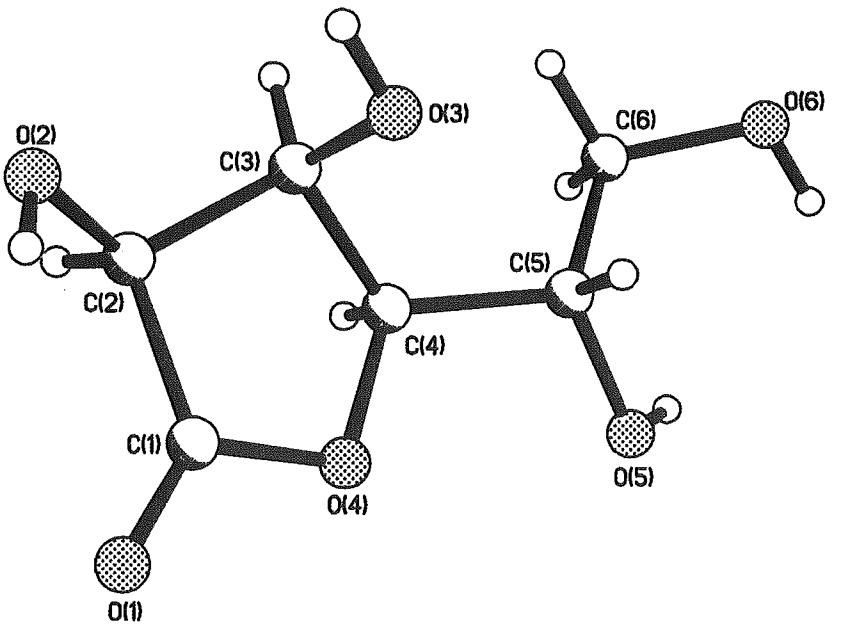

Figure 3.7: Crystal structure of **3.13**.

Unlike compound **3.7**, compound **3.13** crystallised in an orthorhombic crystal system with the space group P(2)1(2)1(2)1. It can be seen from Figure 3.8, that compound **3.13** has two major intermolecular hydrogen bonding interactions to two separate, adjacent molecules: one between O4 and the C3 hydrogen, and another between the carbonyl oxygen atom and the C2 hydrogen.

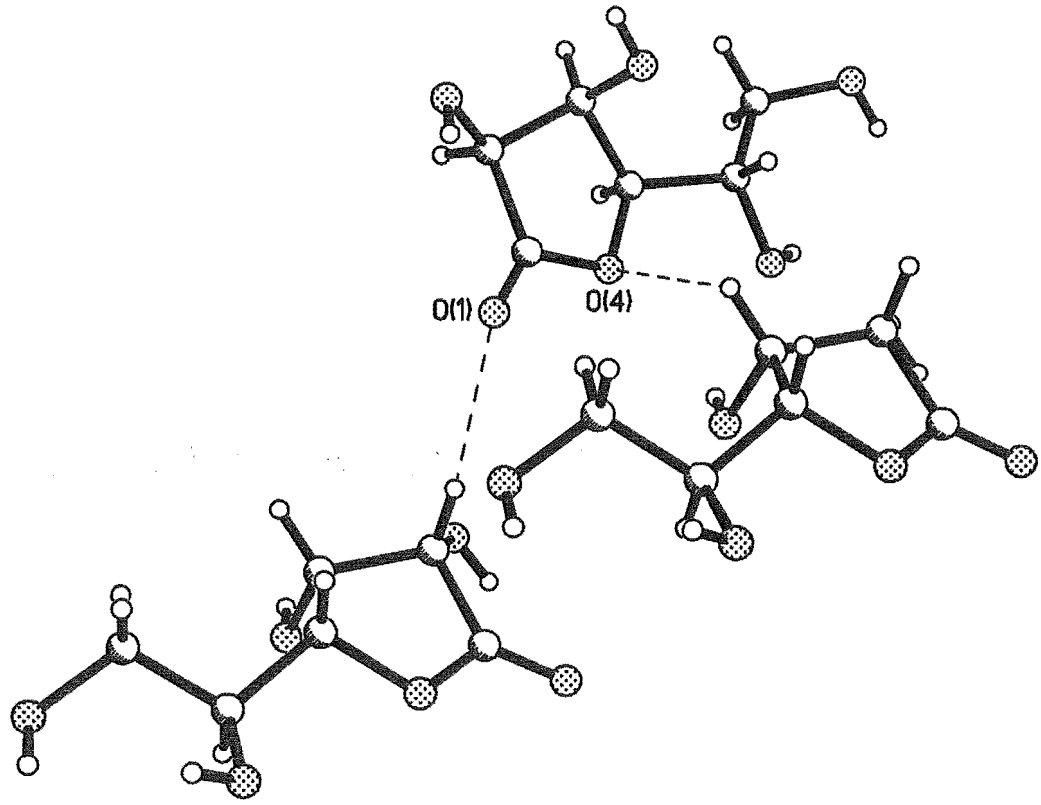

Figure 3.8: Hydrogen bonding between molecules of **3.13**.

3.1.6 D-Isoascorbic-Acid Derivatives

The synthesis of D-isoascorbic acid derivatives allowed the effects on the inhibitory activity of ascorbic acid due to epimerisation at C5 to be evaluated.

Synthesis of 5,6-Isopropylidene-D-Isoascorbic Acid (3.14)

Initial attempts to prepare **3.14** using the method of Jung,[2] returned only starting material. Therefore, it was prepared by a method described by Godefroi *et al.*[13] (Scheme 3.10). D-Isoascorbic acid and dimethoxypropane were stirred in boiling acetone with $SnCl_3$ for 15 minutes at which time the reaction was quenched by the addition of pyridine. Workup gave compound **3.14** as white

solid in a 64% yield. Characterisation by proton-NMR revealed two three-proton resonances at δ 1.34 and 1.27 corresponding to the acetonide group.

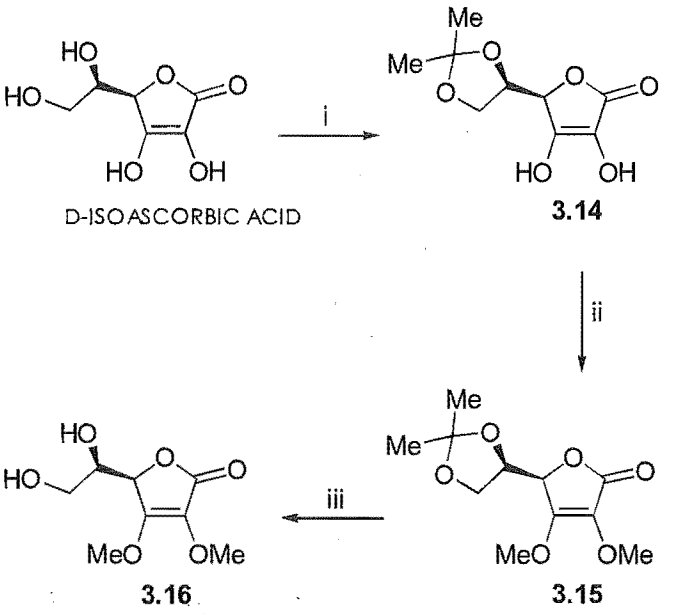

Scheme 3.10: (i) acetone, $SnCl_2$, dimethoxypropane, pyridine; (ii) acetone, K_2CO_3, dimethyl sulfate; (iii) slow hydrolysis.

Synthesis of 2,3-Di-O-Methyl-5,6-Isopropylidene-D-Iso-Ascorbic Acid (3.15) and 2,3-Di-O-Methyl-D-Iso-Ascorbic Acid (3.16)

Preparation of **3.15** was achieved using the same method previously described to prepare derivative **3.5**. Workup and purification by radial chromatography gave **3.15** as an oil in a 68% yield. A proton-NMR spectrum of this product contained two additional three-proton resonances, relative to compound **3.14**, at δ 4.15 and 3.85, due to the methoxy groups on C3 and C2 respectively.

A forgotten sample of **3.15**, left to stand open to the atmosphere for a few weeks and subsequently analysed by proton-NMR spectroscopy, revealed loss of the acetonide resonances at δ 1.45 and 1.37 to give compound **3.16**.

3.1.7 Additional Compounds Tested

Along with the ascorbic-acid derivatives prepared, we were interested to test compounds that structurally resembled possible reaction products of ascorbic acid, in particular a ring opened analogue and the oxidised dehydroascorbic acid.

3.1.7.1 Dihydroxyfumaric Acid

Dihydroxyfumaric acid (DHFA) was purchased to determine if it was necessary to have the ring system for inhibitory action. As can be seen in Figure 3.9, dihydroxyfumaric acid is a straight-chain molecule containing an ene-diol and carboxylate functionalities. As the ene-diol predominantly exists as the thermodynamically-stable trans isomer (95%),[14] the requirement for a cis ene-diol conformation could also be tested.

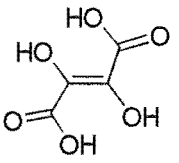

Figure 3.9: Dihydroxyfumaric acid.

3.1.7.2 Dehydroascorbic Acid

Since ascorbic acid is readily oxidised, (section 2.3.5.1), the possibility exists that inhibition of *alpha*-amylase by ascorbic acid is due to the first stable oxidation product: dehydroascorbic acid (Figure 3.10). To test this possibility, dehydroascorbic acid (kindly supplied by Sian Fayle) was also tested for inhibitory activity against *alpha*-amylase.

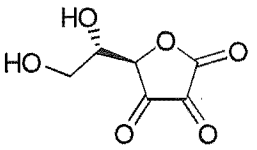

Figure 3.10: Dehydroascorbic acid.

3.2 Summary

Sixteen ascorbic-acid derivatives were prepared, incorporating a range of functional-group modifications. In most instances the modification was achieved by protection of the hydroxyl groups with methyl, acyl, or acetyl groups. D-isoascorbic-acid derivatives were also prepared, as was a reduced compound.

Two unexpected acylated molecules were isolated: **3.3** and **3.7**. A crystal structure analysis of compound **3.7** confirmed its structure.

A simple procedure for the acylation of the C6 hydroxyl group in a C2 and C3 hydroxyl-protected derivative was also investigated.

The inhibition activity of these derivatives, which has lead to the identification of the pharmacophore of this molecule, and the possible mode of inhibition of ascorbic acid is discussed in the following chapter.

3.3 References

(1) Davies, M. B.; Austin, J.; Partridge, D. A. *Vitamin C. Its Chemistry and Biochemistry*; The Royal Society of Chemistry: Letchworth, 1995.

(2) Jung, M. E.; Shaw, T. J. *J. Am. Chem. Soc.* **1980**, *102*, 6304-6311.

(3) Lu, P.-W.; Lillard, D. W.; Seib, P. A.; Kramer, K. J.; Liang, Y.-T. *J. Agric. Food Chem.* **1984**, *32*, 21-28.

(4) Haworth, W. N.; Hirst, E. L.; Smith, F. *J. Org. Chem.* **1934**, 1556-1560.

(5) Szarek, W. A.; Kim, K. S. *Carbohydrate Research* **1978**, *67*, C13-C16.

(6) Shrihatti, V. R.; Nair, P. M. *Indian J. Chem.* **1997**, *15B*, 861-863.

(7) Nihro, Y.; Miyataka, H.; Sudo, T.; Matsumoto, H.; Satoh, T. *J. Med. Chem.* **1991**, *34*, 2152-2157.

(8) Kato, K.; Terao, S.; Shimamoto, N.; Hirata, M. *J. Med. Chem.* **1988**, *31*, 793-798.

(9) Le Merrer, Y.; Gravier-Pelletier, C.; Dumas, J.; Depezay, J. C. *Tetrahedron Letters* **1990**, *31*, 1003-1006.

(10) Creighton, M.; Wenner, W.; Wuest, H. M. *J. Org. Chem.* **1948**, *13*, 613-615.

(11) Cousins, R. C.; Seib, P. A.; Hoseney, R. C.; Deyoe, C. W.; Liang, Y. T.; Lillard, D. W., Jr. *Journal of the American Oil Chemists' Society* **1977**, *54*, 308-312.

(12) Andrews, G. C.; Crawford, T. C.; Bacon, B. E. *J. Org. Chem.* **1981**, *46*, 2976-2977.

(13) Vekemans, J. A. J. M.; Boerekamp, J.; Godefroi, E. F.; Chittenden, G. J. F. *Recl. Trav. Chim. Pays-Bas* **1985**, *104*, 266-272.

(14) Aldrich, Catalogue Handbook of Fine Chemicals.

4 Inhibitory Activity of Ascorbic Acid and Derivatives

The effects that structural modification of ascorbic acid has on its inhibitory action against *alpha*-amylase, were determined by measuring the uninhibited activity of the enzyme and comparing this to its activity in the presence of each ascorbic-acid derivative prepared.

The activity of an enzyme is a measure of the rate of the reaction that it catalyses; the higher the activity, the faster the initial rate of the reaction. (For *alpha*-amylases, this reaction is the hydrolysis of α-1,4-glucosidic linkages.) The international standard for expressing enzyme activity is in katal (kat), one unit of which is equal to *the enzyme activity sufficient to catalyse the transformation of one mole of substrate in one second under standard conditions*.[1] However, these units are excessively large; for example, normal cellular enzyme activity is typically 20 μkat/L.[1] Therefore, the more traditional units of *the amount of enzyme that can catalyse the transformation of one micromole of substrate in one minute* are commonly employed. One unit (U) of *alpha*-amylase is often defined as the amount of protein that produces 1.0 μmole of maltose in 1 minute at pH 6.9 and 20°C.[2]

The activity of an enzyme is determined with an enzyme assay, which is an experimental method for quantifying the conversion of substrates into products. This is most easily achieved by directly monitoring either a loss in enzyme substrate or a gain in products. However, this is not always possible, and indirect methods must then be employed.

Apart from the determination of an enzyme's activity, appropriate assays also provide information about mechanistic processes and the optimal catalytic environment for the enzyme. This information has many practical applications. For *alpha*-amylase, which catalyses the hydrolysis of many different oligosaccharides and polysaccharides, the activity of the enzyme is highly dependent on the substrate.

4.1 *Alpha*-Amylase Assays

The action of *alpha*-amylase produces a variety of characteristic changes to its substrate.[3] These include a decrease in substrate viscosity and turbidity, an increase in the number of molecules bearing reducing ends,* a reduction in the degree of iodine staining of the substrate, and changes in the optical rotation of the substrate. These characteristics can be easily monitored, and most have been used to develop assays for the determination of *alpha*-amylase activity. For well-defined substrates the amount of a defined product can also be measured.

In order to accurately measure the inhibitory effectiveness of the ascorbic-acid derivatives against *alpha*-amylase, we required an assay that was simple to set up and use, was reliable, and *specifically* measured the activity of *alpha*-amylase. The following section provides a brief overview of the different types of *alpha*-amylase assays available. Due to the enzyme selectivity, improved kinetics and ease of use reported for the Megazyme assay, it was selected for the analysis of the inhibitory activity of the ascorbic-acid derivatives studied in this work.

4.1.1 Saccharogenic and Amyloclastic Assays

Early *alpha*-amylase assays were based on an increase in the number of reducing ends (saccharogenic), and/or changes in the turbidity, viscosity and iodine-staining ability (amyloclastic) of the substrate following hydrolysis.

4.1.1.1 Saccharogenic Assays

If it is assumed that every action-event of *alpha*-amylase on its substrate will produce a molecule with a reducing end, then the number of reducing ends present after hydrolysis gives an estimate of the enzyme's activity. Assays based on this principle utilise the redox chemistry of sugars and were developed from techniques used to determine blood glucose levels. Typical assay procedures include the reduction of copper, ferricyanide, picric acid or 3,5-dinitrosalicylic acid.[4] The methods of Nelson and Somogyi[5] are well-known examples; a sample containing reducing ends is reacted with an alkaline cuprous-oxide reagent and

* The reducing end of a carbohydrate molecule is the terminal in which the C1 anomeric carbon is not bonded to another molecule. Each hydrolysis event produces a new reducing end such that the resulting two fragments each have one.

then visualised by the addition of a chromogenic compound such as arsenophosphate. The colour intensity of the solution is related to its concentration (*via* the Beer-Lambert law), and is compared to a series of known-concentration standards.

If precautions are taken to ensure purity of reagents and care in experimental techniques, this type of assay can give reliable, reproducible results. However, there are many disadvantages to this assay. It is quite laborious and time consuming, and it requires the daily preparation of standard solutions, making it inconvenient for rapid screening. The assays are based on the presence of reducing compounds but do not distinguish between different types; therefore, the presence of glucose or other reducing agents can cause false positive results. Finally, as any glucosidase enzyme is able to produce reducing ends, saccharogenic type assays are not specific for *alpha*-amylase.

4.1.1.2 Amyloclastic Assays

Whereas the saccharogenic assays described above are based on the accumulation of product, amyloclastic assays monitor the destruction of substrate. The turbidity and viscosity of starch solutions are related to the swelling of the starch granules (when introduced into the solution) and subsequent interaction between these swollen grains. Hydrolysis results in a loss of turbidity due to a reduction in grain size, and a decrease in viscosity due to disruptions in the intermolecular interactions and structure of the starch.[4] The activity of *alpha*-amylase is related to the amount of enzyme required to reduce viscosity by 20%; however, the results are dependent on the type and purity of the substrate. These assays are useful for rapid screening of activity, but are severely limited in regard to the kinetic information they provide. They are most useful when used in conjunction with another assay.

The most useful amyloclastic assay is based on the starch-iodine test.[4,6,7] The intensity of the characteristic blue-coloured complex formed when iodine is added to starch is reduced upon hydrolysis of the starch.[3] The colour of iodine in starch is due to the helical arrangement of the amylose chain in the starch grains. Each helical turn consists of six glucose residues that surround a single iodine atom. Longer helices, therefore, result in the formation of linear chains of iodine atoms. The colour is dependent on the length of the iodine chain, and is therefore, a

function of the number of helical turns; a blue complex is only observed in chains of more than 45 glucose units. Hydrolysis results in a change in colour until the achromatic point is reached (*i.e.* the point at which all colour is dispersed - Table 4.1).[4]

The change in 'staining ability' of carbohydrate chains less than 25 units in length is not notable, so although this assay is able to measure the initial attack of the enzyme on starch substrates, it is insensitive to multiple attacks.[3] The degree of enzyme activity is estimated by colour comparisons with standard solutions.

Table 4.1: Colour of the amylose-iodine complex as a function of the number of helical turns in amylose.

NO. OF HELICAL TURNS	COLOUR
< 2	None
2	Brown
3 – 5	Red
6 – 8	Purple
> 9	Blue

Because this assay measures the hydrolysis of the substrate, when the achromatic point is reached the enzyme is no longer operating under substrate saturation conditions. Consequently, this type of assay doesn't provide an accurate estimate of the enzyme's activity. Interference by proteins in the starch–iodine assay can also give false positive results. Iodine-based assays are unable to measure abnormally high or low amylase levels, they require a set of standard solutions and, as with the saccharogenic assays they are not specific for *alpha*-amylases.

A review of up to 50 different saccharogenic and amyloclastic type assays by Searcy *et al.*[4] concluded that the saccharogenic methods are superior to amyloclastic assays due to the increased information they provided. However, routine use of either of these types of assay has diminished due to the development of highly defined enzyme substrates.

4.1.2 Chromogenic-Substrate Assays

An improvement in *alpha*-amylase assays came with the introduction of chromogenic substrates. The idea was based on the use of certain dyes to colour

cellulose-type fabrics.[8] These water-soluble dyes are covalently bound to the starch polymer *via* ether or ester linkages to give an insoluble, coloured product.

The first reported use of a dyed substrate was by Rinderknecht and Wilding who described the preparation of insoluble, dyed starch grains using Remazol brilliant-blue dye under alkaline conditions.[9] Hydrolysis of the starch leads to soluble, coloured fragments, which can be separated from the unreacted, insoluble material and measured photometrically.

The development of these substrates has included a variety of different dyes and starches from various sources (Table 4.2),[10] the most effective being those prepared from well-defined starches, which give meaningful results over a wide range of amylase activities.

Table 4.2: Comparison of different dyed substrates for amylase assays

SUBSTRATE	DYE
Amylopectin	Reactone red 2B
Amylopectin	Procion brilliant red M-2 BS
Dyed starch	Cibachron blue F 3 GA
Dyed starch	Remazol brilliant blue R
Dyed amylose	Cibachron blue F 3 GA

The use of dyed substrates allows quantitation of hydrolysis events provided the ratio of dye to substrate molecules is known. However, care must be taken not to incubate the reactions for too long. This causes the apparent reaction rate to increase as smaller chains formed during hydrolysis are cleaved more rapidly than longer chains.[3] Careful removal of the unreacted substrate is also important for an accurate measurement of the activity.

Advantages of this type of assay include its ease of use, and the accuracy of the information obtained regarding the enzyme's activity. However, this method once again requires a set of standard solutions against which the activity is measured, and a 'blank' for each set of measurements.

Assays using dyed substrates are also non-specific for *alpha*-amylases.

4.1.3 Defined-Substrate Assays

The most recent advance in assays for *alpha*-amylase has been the use of highly-defined simple substrates. These allow for high purity of the substrate as well as the monitoring of specific hydrolysis products. Often the substrate will contain a chromophore that is released in the assay and detected photometrically.

Alternatively, the assay can incorporate a coupled reaction, where the hydrolysis products of *alpha*-amylase action are substrates for a second reaction, the products of which can be monitored. In many cases, the assay also includes coupling enzymes that either assist in the substrate cleavage to release the chromophore, or are necessary for the coupled reaction.

Examples of assays using the defined substrates maltotetraose and 4-nitrophenyl maltoheptaoside are described below,[10] along with the Megazyme assay used in this work.

4.1.3.1 MALTOTETRAOSE

This assay involves four coupled reactions (Figure 4.1). Maltotetraose is cleaved by *alpha*-amylase to give two maltose molecules. Maltose and phosphate (Pi) react in the presence of maltose phosphorylase (MP) to produce glucose and β-glucose-1-phosphate. The β-glucose-phosphate, in the presence of β-phosphoglucomutase (β-PGM), is converted to glucose-6-phosphate, which, in the presence of glucose-6-phosphate dehydrogenase (G6P-DH), is oxidised to gluconate-6-phosphate by NAD^+, producing NADH.

The assay is followed photometrically by measuring the increase in NADH production *via* its absorption at 339 nm. In this way a direct measure of the *alpha*-amylase activity is obtained.

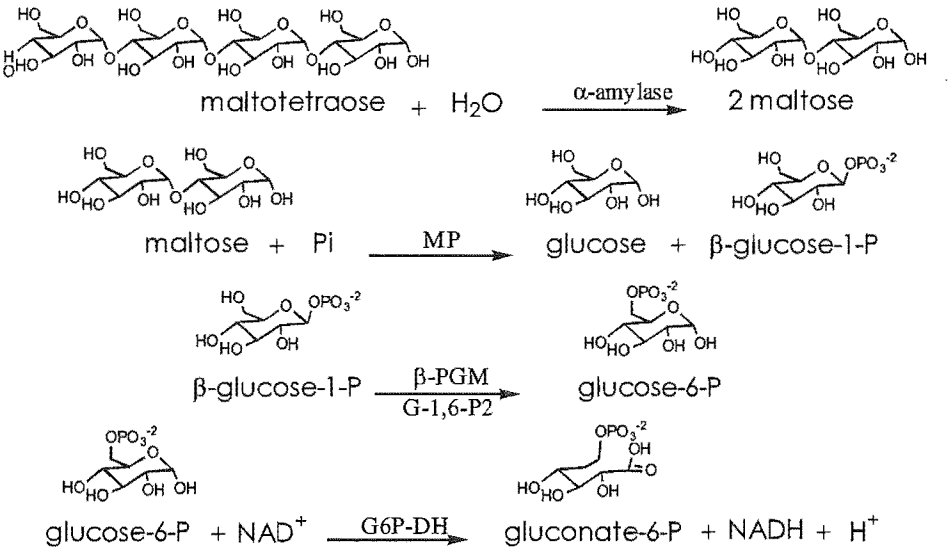

Figure 4.1: Maltotetraose coupled assay.

Errors mainly occur in this assay when analysing samples with high levels of maltose. However, the assay of samples from cereal, food, or fermentation industries is complicated by the presence of interfering enzymes such as β-amylase, amyloglucosidase, α-glucosidase, and various debranching enzymes, all of which are capable of cleaving the substrate.

4.1.3.2 4-NITROPHENYL-MALTOHEPTAOSIDE

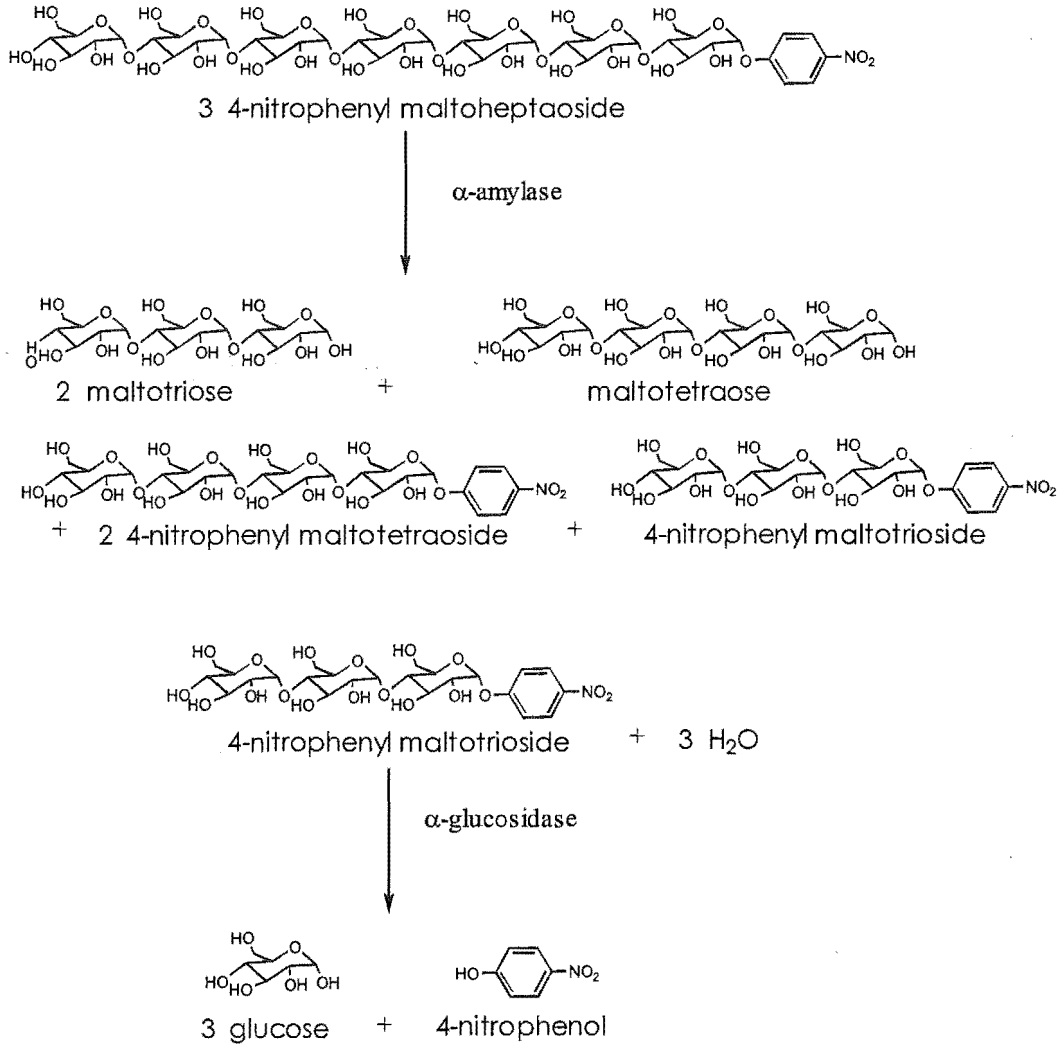

Figure 4.2: 4-nitrophenylheptaoside colorimetric assay.

This assay involves a co-enzyme α-glucosidase that has high specificity for small substrates (2-3 residues). It is monitored by the release of a coloured chromophore. 4-Nitrophenyl maltoheptaoside is hydrolysed by *alpha*-amylase into mostly maltotriose, maltotetraose, 4-nitrophenyl maltotetraoside and 4-nitrophenyl-maltotrioside. The 4-nitrophenyl maltotrioside is then cleaved by α-

glucosidase to give glucose and 4-nitrophenol (Figure 4.2). The enzyme activity is directly related to the release of 4-nitrophenol, which is measured photometrically *via* its absorbance at 405 nm.

This assay is specific for *alpha*-amylase and gives generally reliable measures of activity. However, it is possible that the substrate is hydrolysed by *alpha*-amylase to give 4-nitrophenyl maltopentaoside, which may be further cleaved by the enzyme. This creates the potential for inaccuracy in the measurement of activity. In addition, the use of this type of assay is limited for samples containing interfering enzymes.

One assay utilising a defined substrate, which has overcome the problem of interfering enzymes is the 'Megazyme' Assay.

4.1.3.3 Megazyme Assay

The Megazyme assay by McCleary and Sheehan[11] uses a non-reducing-end-blocked *p*-nitrophenyl maltoheptaoside (BPNPG7) previously developed by Blair[12] (Figure 4.3). The presence of the blocking group, in addition to the *p*-nitrophenol chromophore, provides the substrate with resistance to attack by β-amylase, α-glucosidase and glucoamylase, all of which function as exo enzymes; hydrolysing their substrates from the ends. Only *alpha*-amylase, an endo enzyme, which cleaves its substrate at internal linkages, is able to hydrolyse the substrate.

The assay includes α-glucosidase and glucoamylase, in excess levels, as coupling enzymes. Unlike *alpha*-amylase, these glucosidases are specific for small substrates (2-3 units) and act rapidly on the *alpha*-amylase-hydrolysed substrate to release the nitrophenol molecule. This improves the kinetics of the assay, as each molecule of the chromophore released corresponds to a single action-event by *alpha*-amylase. The production of nitrophenol is measured photometrically *via* the absorption of the phenolate ion at 410 nm.

The Megazyme assay is specific for *alpha*-amylase, and, as well as its ease of use, it is reported to provide accurate and reliable kinetic data on the activity of the enzyme, providing the necessary precautions, (with regard to experimental technique and purity of reagents), are taken.

In spite of investigations to ascertain the suitability of the Megazyme assay for analysis of our compounds, we did experience some difficulties obtaining

reproducible results for our inhibition and kinetic analyses. This is reflected in the errors associated with our reported values in sections 4.2 and 4.3. Whilst the Megazyme assay gives excellent results when used as a fixed-time assay, there remains scope for further development to produce an assay that reliably gives initial rate data for *alpha*-amylase activity.

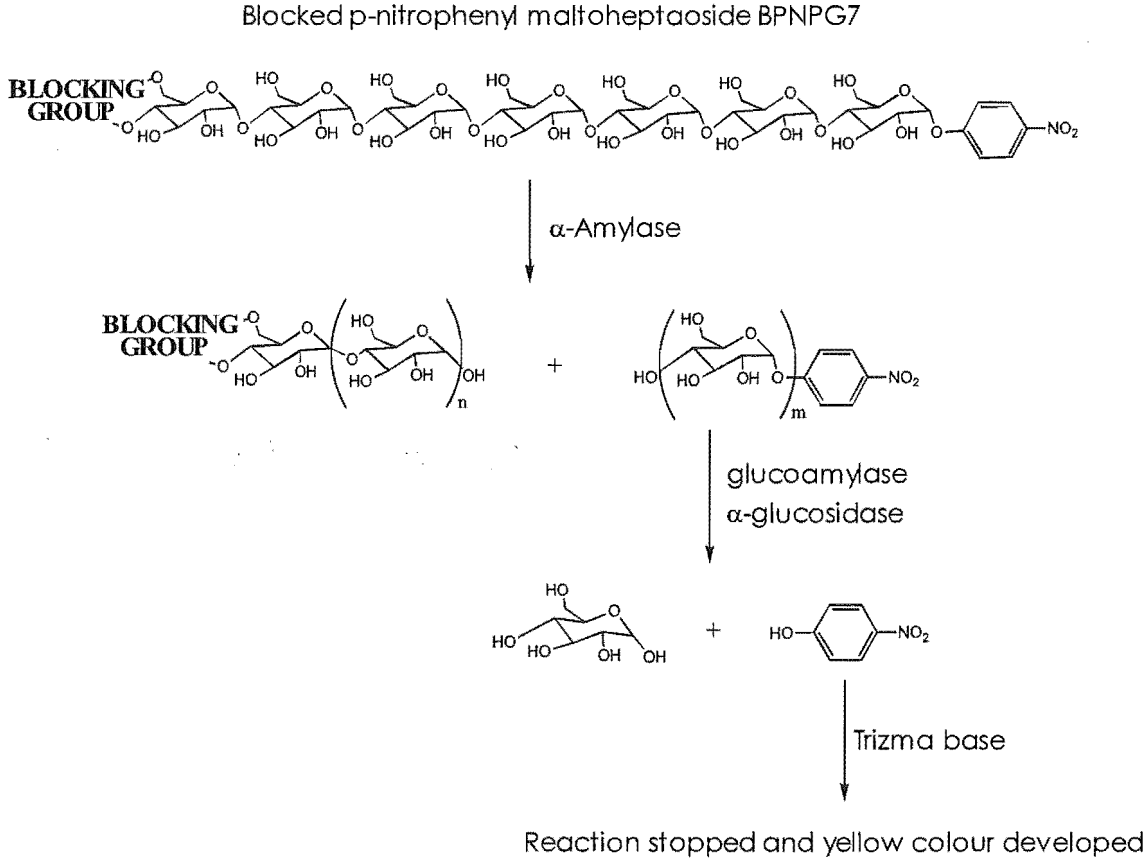

Figure 4.3: Megazyme Assay: *alpha*-amylase hydrolyses the substrate to remove the blocking group. This allows rapid attack by α-glucosidase and glucoamylase, which releases the p-nitrophenol molecule. The addition of Trizma base inactivates the enzymes and deprotonates the phenol to give the more highly-coloured phenolate ion, which is detected photometrically.

4.2 Inhibitory Analysis of Ascorbic-acid Derivatives

The inhibitory effectiveness of the ascorbic-acid derivatives was analysed by comparing the activity of the enzyme in the presence of each inhibitor, with

the activity of the uninhibited enzyme. The activity in all instances was determined using the Megazyme *alpha*-amylase assay* (section 4.1.3.3).

The assay protocol involved mixing the inhibitor and enzyme together, then initiating the reaction by the addition of substrate.† The reaction was terminated after 10 minutes by the addition of excess base, which inactivates the enzymes and deprotonates the released nitrophenol chromophore.

The initial rate of the *alpha*-amylase action on the substrate was determined by measuring the absorbance of *p*-nitrophenolate at 410 nm after a set time. The absorbance of the chromophore reflects its concentration in solution and may be directly related to the number of action events due to *alpha*-amylase. A high level of absorbance is indicative of a high initial-rate of enzyme activity, a low absorbance indicating a low initial-rate.

The initial rates in this study are calculated in terms of 'Megazyme' units as defined by McCleary *et al.*[11] One unit is equal to *the amount of enzyme required to produce one micromole of p-nitrophenol in one minute*. These units are simply converted to other standards units.

The reduction in *alpha*-amylase activity due to inhibition was calculated as a percentage of the uninhibited activity. For example, a value of 25% indicates the normal enzyme activity was reduced by one quarter in the presence of the inhibitor. Initial assays were performed using barley-malt *alpha*-amylase, as this enzyme is inexpensive, readily available and stable at 4°C. However, derivatives that showed good inhibitory action, were further assayed against fungal, bacterial, pancreas, and saliva *alpha*-amylases. The results of these assays are shown in Table 4.3

---

* The assumption was made that the reduced activity of the enzyme in the presence of the inhibitor was due to inhibition of *alpha-amylase*, and that the coupling enzymes were unaffected. This is reasonable, given that the coupling enzymes are in large excess.

† This method was chosen for experimental convenience. No significant differences were observed in the results when pre-incubating the inhibitors with *alpha-amylase*, relative to pre-incubating the inhibitors with the *substrate* (see chapter 7).

Table 4.3: The percentage inhibition of *alpha*-amylases by 5 mM of inhibitor

Derivative	*Alpha*-amylases				
	Malt	fungal	bacterial	pancreas	saliva
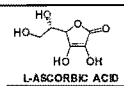 L-ASCORBIC ACID	95%	-	-	-	-
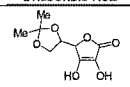 **3.1**	90%	94%	98%	99%	88%
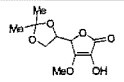 **3.2**	29%	17%	8%	-	0%
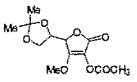 **3.3**	9%	"	"	"	"
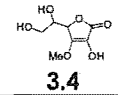 **3.4**	9%	"	"	"	"
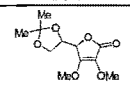 **3.5**	2%	"	"	"	"
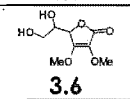 **3.6**	4%	"	"	"	"
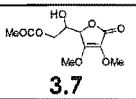 **3.7**	3%	"	"	"	"
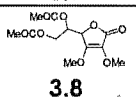 **3.8**	7%	"	"	"	"
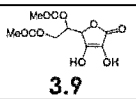 **3.9**	89%	91%	92%	99%	-
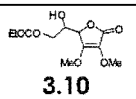 **3.10**	10%	-	-	-	-
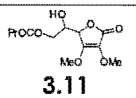 **3.11**	0%				-
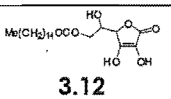 **3.12**	90%	70%	84%	88%	69%
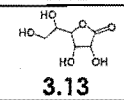 **3.13**	4%	-	-	-	-
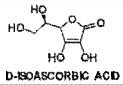 D-ISOASCORBIC ACID	96%	98%	99%	100%	100%
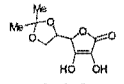 **3.14**	90%	91%	93%	99%	98%
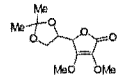 **3.15**	0%	"	"	"	"

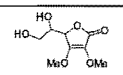 **3.16**	11%	-	-	-	-
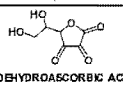 DEHYDROASCORBIC ACID	53%	-	-	-	-
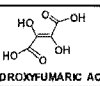 DIHYDROXYFUMARIC ACID	92%	-	-	-	-

A summary of the results from these studies is presented in Figure 4.4. The most obvious result from this SAR study, as seen in Table 4.3, is that all the potent inhibitors of barley-malt-*alpha*-amylase show similar activity against fungal, bacterial, pancreas, and saliva *alpha*-amylases. This result is not unexpected given the high structural and functional homology of *alpha*-amylases (Section 2.2.2).

The poor activity displayed by dehydroascorbic acid, relative to ascorbic acid, suggests that this form of ascorbate is unlikely to be largely involved in *alpha*-amylase inhibition. However, the ring-open analogue of ascorbic acid – dihydroxyfumaric acid – shows significant inhibitory activity, suggesting that the ring structure of ascorbic acid is not important.

Further inspection of Table 4.3 reveals more interesting trends: All of the most potent inhibitors, **3.1**, **3.11**, **3.12**, and **3.14** possess unprotected hydroxyl groups at the C2 and C3 positions of ascorbic acid (Figure 3.1). Protection of the C5 and C6 hydroxyl moieties by acetal and acyl groups in these derivatives appears to be well tolerated, including the presence of an extended carbon chain on C6 as found in derivative **3.12**.

The stereochemistry at C5 appears to be unimportant for inhibitory activity as displayed by the results for L-ascorbic acid, D-isoascorbic acid and their acetonide protected derivatives **3.1** and **3.14**. This is in keeping with the original results of Palla *et al.* who reported powerful inhibition of wheat *alpha*-amylase by ascorbic acid and its D isomer.[13]

In contrast, all derivatives with protecting groups on both the C2 and C3 hydroxyl groups results in a marked decrease in activity. The same is true for derivatives **3.3** and **3.4** where only the C3 hydroxyl group is methylated. Reduction of the double bond between C2 and C3 also results in a marked reduction in inhibitory activity.

These combined results strongly suggest that the ene-diol moiety in ascorbic acid is essential for the inhibition of *alpha*-amylase (Figure 4.4).

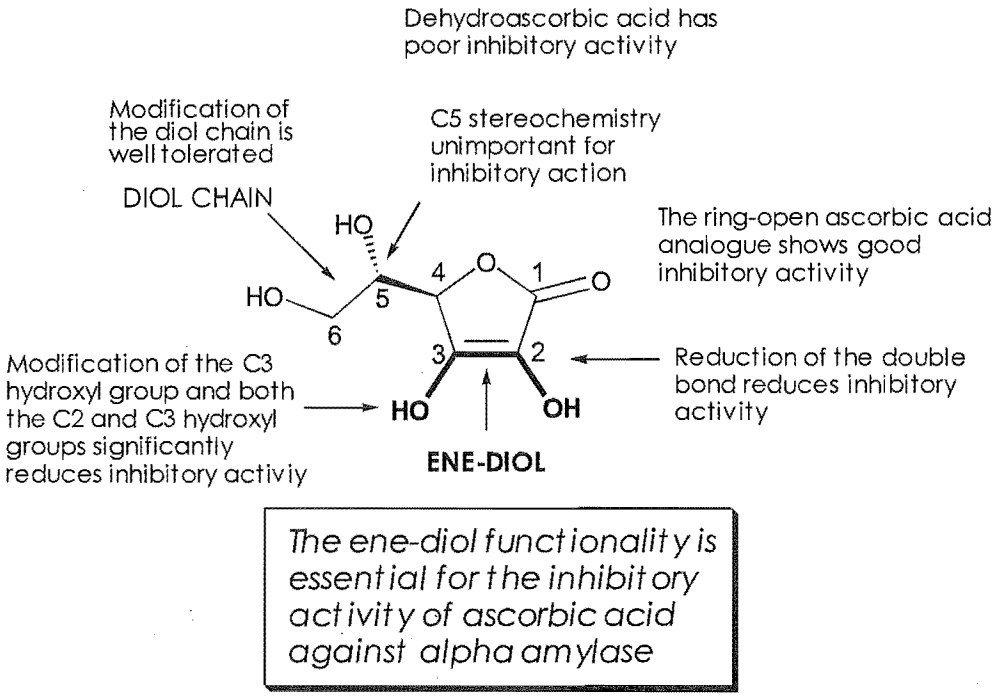

Figure 4.4: The core ene-diol pharmacophore of ascorbic acid.

Two possible reasons for the enhanced activity of the ene-diol-containing inhibitors, revealed by this study, are steric and electronic interactions, between the inhibitor and *alpha*-amylase.

The two main structural features of ascorbic acid are the lactone ring and the diol chain that extends out of the plane of the ring from the C4 position. In ascorbic acid, O2 and O3 lie in the plane of the lactone ring; however, upon reduction of the C2-C3 double bond, the hybridisation at these centres becomes sp^3 and the hydroxyl groups subsequently protrude out of the plane of the ring. This is clearly seen in the crystal structure of the reduced ascorbic acid derivative **3.13** (Figure 3.7). Given that inhibitory action is significantly reduced after reduction of the double bond, maintenance of planarity across the ene-diol system may be important for the binding interactions of ascorbic acid with *alpha*-amylase.

A modification of ascorbic acid's shape may also explain the reduced activity of the derivatives containing methoxy groups at C2 and C3. The increased size of the introduced methyl groups, relative to the original hydrogen

atoms, may provide enough steric interference to prevent successful binding interactions.

Alternatively, the presence of the methoxy group may interfere with important electronic properties of the molecule. The C3 hydroxyl group is the most acidic in ascorbic acid with $pk_a = 4.2$.[14] Deprotonation to give the ascorbate anion results in a delocalisation of the charge over the π system to the C1 carbonyl group. The ability of ascorbic acid to form this resonance structure may be important for binding interactions to the enzyme since methylation at the C3 hydroxyl group prevents this resonance structure from forming.

The interference role of the methyl group – be it structural or electronic – might be determined by analysis of the singly-protected C2 hydroxyl group. If the electronic properties of ascorbic acid are important for its inhibitory action, protection at C2 should have no deleterious effect on inhibitory activity. However, if the methyl group interferes sterically, or by hindering hydrogen bonding, the C2-protected derivative may result in a similar loss of activity.

4.2.1 Stability of Protecting Groups

Given the similarity of inhibition activity between ascorbic acid and the potent derivatives protected only at C5 and C6 (**3.1**, **3.11**, **3.12** and **3.14**), it was postulated that the protecting functionality might be hydrolysed under the conditions of the assay, and results for these compounds in fact represented inhibition by underivatised ascorbic acid. To investigate this possibility, NMR spectra were collected for the acyl and acetyl protected derivatives **3.1** and **3.12** both before and after subjecting them to similar temperature conditions, and for the same time, as occurs in the assay. Neither sample displayed resonances corresponding to ascorbic acid. Based on these observations we have assumed that under the reaction conditions of the assay no solvent mediated hydrolysis occurred.

4.2.2 Inhibitor Potency

On average, the derivatives **3.1**, **3.11**, **3.12**, **3.14**, both epimers of ascorbic acid, and DHFA showed greater than 90% inhibition of *alpha*-amylase activity at 5-mM concentrations of inhibitor. We were interested in determining the potency of

The results clearly show that the production of *p*-nitrophenol is linear over the time frame of the assay; therefore, the absorbances recorded ten minutes after the initiation of the reaction are proportional to the initial rate of reaction. This result is consistent with data reported by McCleary *et al.*[11]

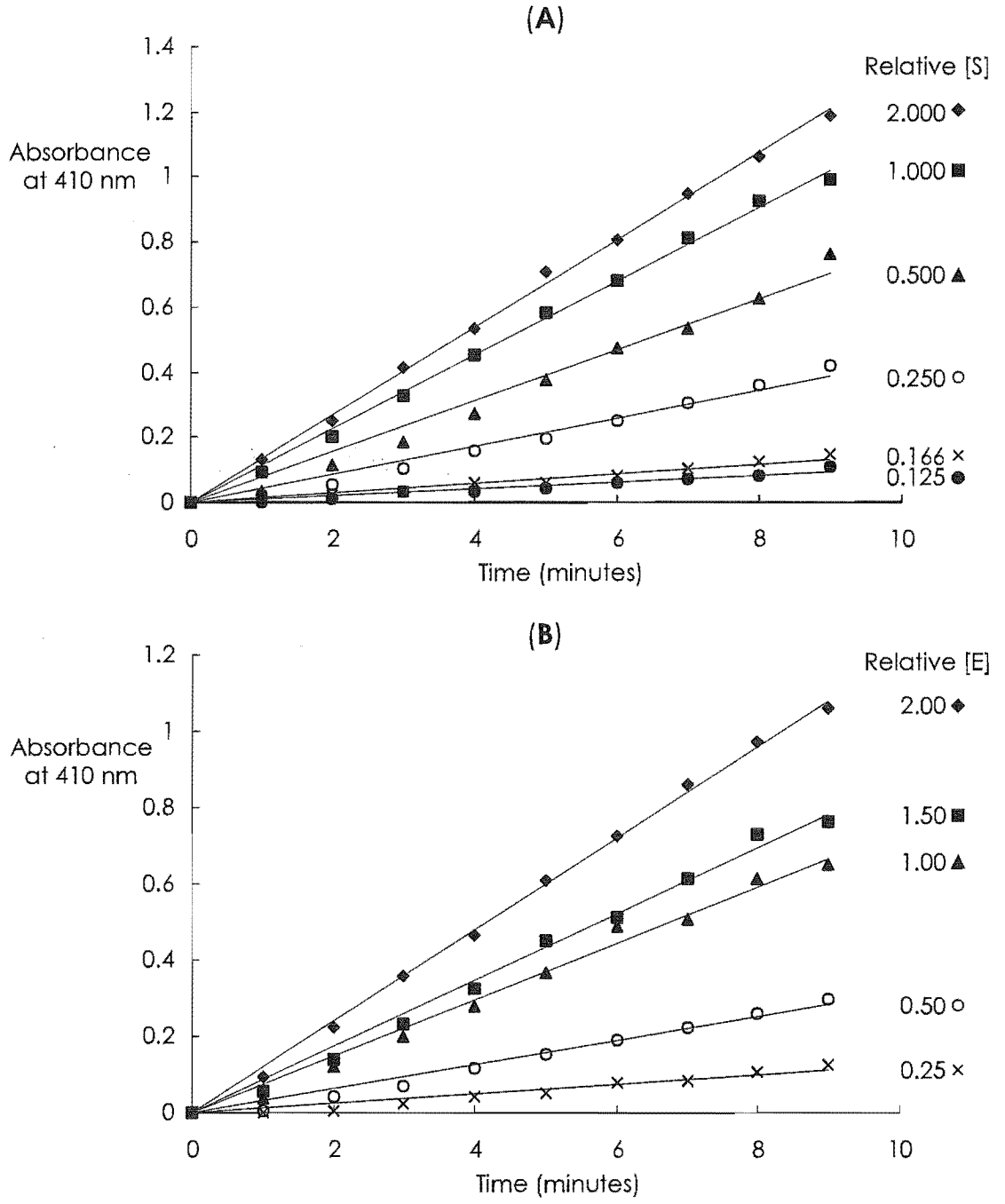

Figure 4.6: Graphs showing the linearity of the Megazyme assay over a 10 minute period.

Similar experiments were carried out with inhibitors in the assay to ensure that it remained linear over a 10-minute period in their presence. Figure 4.7 shows

the results for the inhibitors ascorbic acid and compound **3.1.** As with the uninhibited case, the results of the assay vary linearly over a 10-minute period.

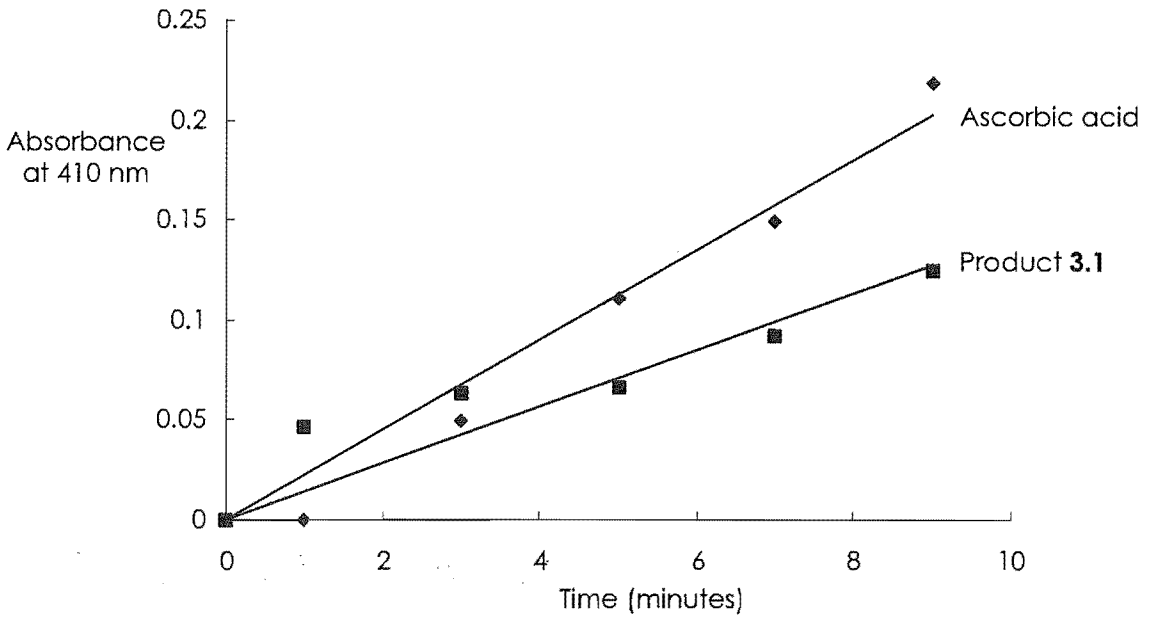

Figure 4.7: Linearity of the Megazyme assay in the presence of inhibitors.

4.3.1.2 The Michaelis-Menten Model

The most widely-used model for assessing the kinetic parameters of an enzyme system is the Michaelis-Menten (M-M) model. This model is based on the following reaction scheme and has been shown to be useful for the analysis of a wide range of enzyme systems.[16,17]

$$E + S \underset{k_{-1}}{\overset{k_1}{\rightleftharpoons}} ES \xrightarrow{k_2} E + P \qquad (4.1)$$

The enzyme (E) and substrate (S) reversibly form an enzyme-substrate complex (ES) which reacts to give product (P) whilst regenerating E. The rate equation derived from the M-M model (derived in appendix A) is given by.

$$\upsilon = \frac{V_{max}[S]}{K_m + [S]}$$

$$V_{max} = k_{cat}E_T \qquad (4.2)$$

where E_T is the total concentration of enzyme in the system (E_T = [E] + [ES]), $k_{cat} = k_2$, and $K_m = \frac{k_{-1} + k_2}{k_1}$.

The important kinetic parameters of the reaction, K_m and V_{max} may be determined from the measurable quantities: E_T, [S]and υ.

A plot of the rate *vs* substrate concentration for a reaction obeying the M-M mechanism is a rectangular hyperbola (Figure 4.8). At high substrate concentrations the rate approaches the limiting value of V_{max}; however, the limiting rate is never reached experimentally and the value of V_{max} can only be estimated. Inspection of the M-M rate equation 4.2, reveals that the K_m parameter is equal to the substrate concentration when the rate is equal to half V_{max}. Thus a direct plot of rate *vs* [S] also provides only an estimate of K_m.

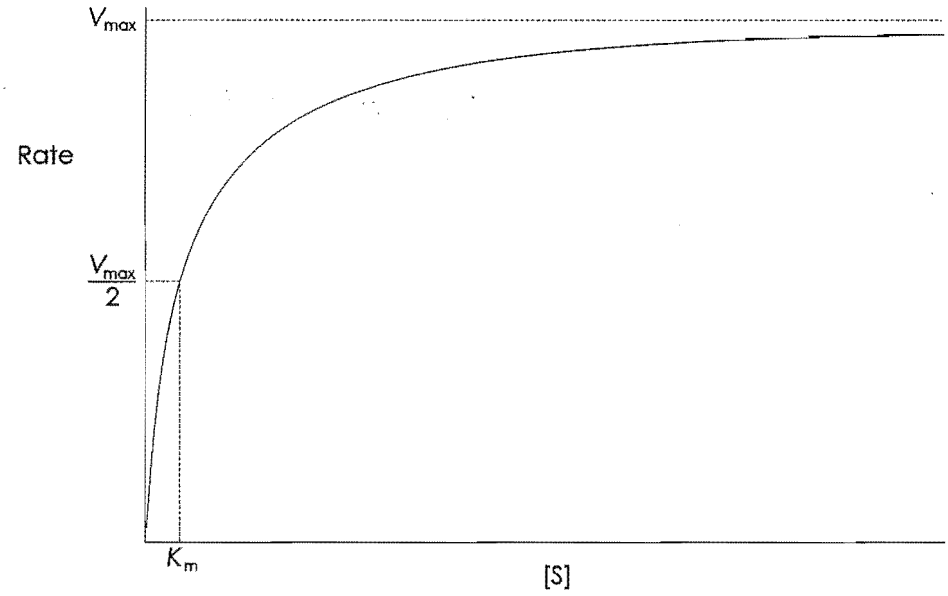

Figure 4.8: Graph of rate *vs* substrate concentration for a reaction obeying the M-M model.

More accurate kinetic parameters are obtained by transforming the data and plotting it in a linear fashion. Two commonly used transformations result in the Lineweaver-Burk plot and the direct linear plot (Appendix B).

4.3.1.3 Method and Results

The experimental protocol for determining K_m and V_{max} for *alpha*-amylase involved measuring the initial rate of reaction at various substrate concentrations, as detailed in Chapter 7. The enzyme was barley-malt *alpha*-amylase.

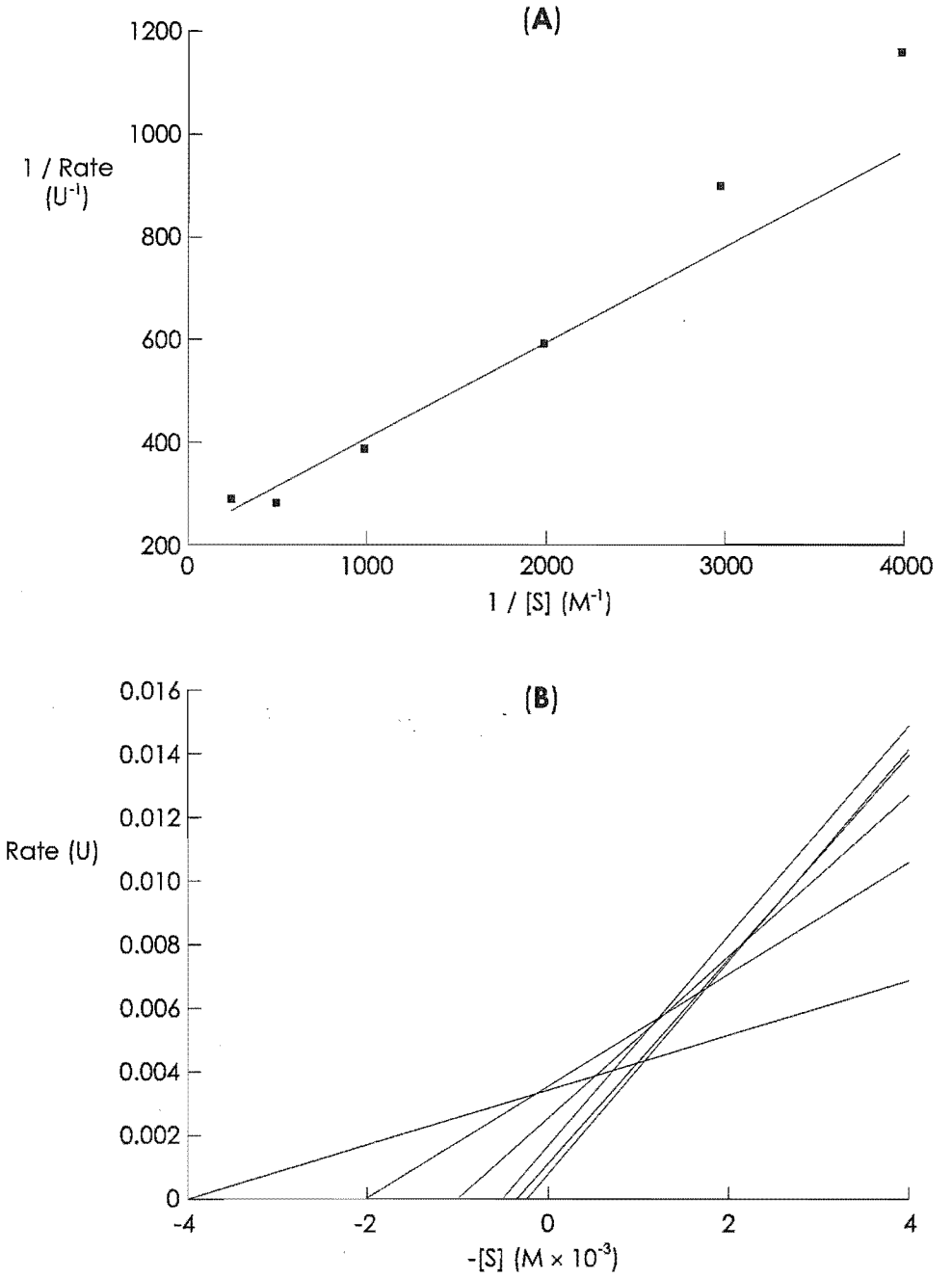

Figure 4.9: (**A**) Lineweaver-Burk (double-reciprocal) plot generated by ENZFITTER. (**B**) Direct linear plot constructed using Microsoft EXCEL.

A kinetics computer programme (ENZFITTER) measured the fit of the raw kinetic data to the M-M equation, and extracted values for K_m and V_{max} along with the associated, statistically determined, standard errors (SE). It also generated a linear Lineweaver-Burk plot with a weighted line-of-best-fit (Figure 4.9

A),* which provides a visual presentation of the goodness-of-fit between the experimental data and the model.

For comparison, the kinetic parameters were also determined using a direct linear plot of the raw data (Figure 4.9 B).

The results of these two methods (Table 4.5) gave comparable results: K_m = $1.2 \times 10^{-3} - 1.6 \times 10^{-3}$ M; $V_{max} = 1.11 \times 10^{-7} - 1.23 \times 10^{-7}$. These compare with results reported by MacGregor *et al.*[18] who have reported K_m values of 0.35×10^{-3} M and 0.8×10^{-3} M for the action of type 1 and type 2 barley-*alpha*-amylase isozymes on BPNPG7.

Table 4.5: Kinetic parameters of barley-malt *alpha*-amylase.

Method	K_m (mM)	S.E (mM)	V_{max} (Ms^{-1})	S.E (Ms^{-1})
Direct linear plot	1.20		1.11×10^{-7}	
Double reciprocal plot	1.62	0.04	1.23×10^{-7}	1.31×10^{-9}

4.3.2 Kinetics of Inhibited *Alpha*-Amylase

Having established K_m and V_{max} for the barley-malt-*alpha*-amylase system, we set about investigating the mode of inhibition of ascorbic acid and product **3.1**.

4.3.2.1 Modes of Inhibition

Inhibitors are generally described as irreversible or reversible.[1,15-17] Irreversible inhibitors effectively destroy the catalytic ability of the enzyme thus preventing the catalysed reaction from occurring at any appreciable rate. Reversible inhibitors often regulate enzyme activity. They bind to the enzyme through hydrogen bonding, hydrophobic interactions, or other weak attractive forces, and their activity can be weakened by dilution of the inhibitor, by increased substrate concentration, or by dialysis.[15,16]

Inhibitors can be further classified into four main categories: competitive, uncompetitive, non-competitive and mixed inhibitors (Figure 4.10).

---

* The best-fit-line for the Lineweaver-Burk plot is weighted so as to lower the importance of the larger 1/S and 1/υ values, which are inherently less accurate than the smaller values (see appendix A).

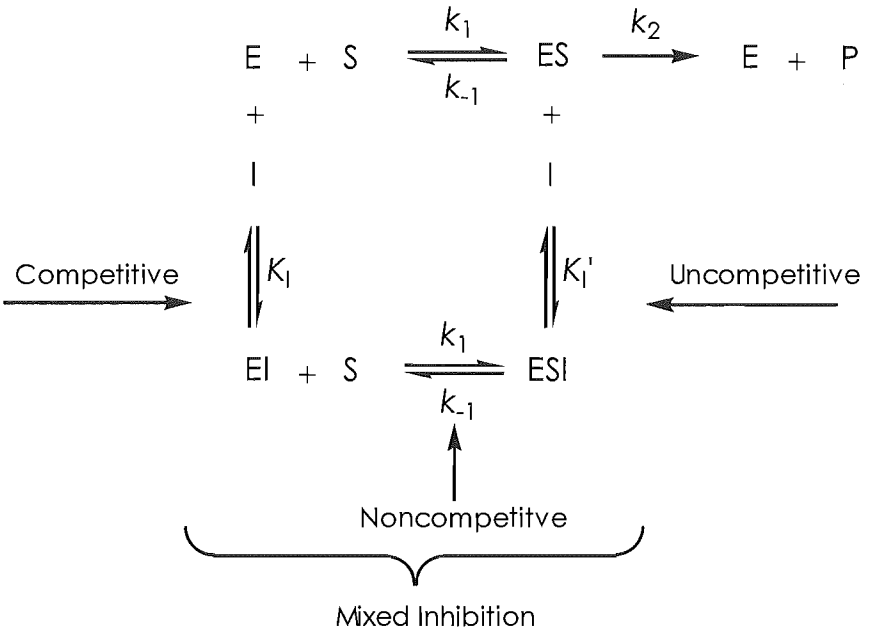

Figure 4.10: Simple schematic mechanistic model of the modes of inhibition. Competitive inhibitors bind to the free enzyme while uncompetitve inhibitors bind to the enzyme-substrate complex. Non-competitive inhibitors bind to the enzyme is such as way as to not affect the binding of the substrate, and mixed inhibitors exhibit a combination of these characteristics.

(i) Competitive Inhibitors

Competitive inhibition occurs when the substrate and inhibitor bind the same form of the enzyme such that when one is bound the other cannot. The successful formation of an enzyme-substrate (ES) complex results in conversion of substrate to product, but the formation of an enzyme-inhibitor (EI) complex leads to a dead-end reaction.

(ii) Uncompetitive Inhibitors

Uncompetitive inhibitors have no effect on the rate of ES complex formation; however, they do affect the rate of product formation once the ES complex is formed. This can be thought of in terms of the inhibitor binding the ES complex to form an Inhibitor-enzyme-substrate (ESI) complex, without binding the free enzyme. The probability of an inhibitor exhibiting such selective binding is very small.[16]

(iii) Non-competitive Inhibitors

Non-competitive inhibitors bind to both E and ES in a site other than the active site. This binding does not affect the rate of ES (or ESI)complex formation, however, it does slow the efficiency of product formation.

(iv) Mixed Inhibitors

An inhibitor that displays a mixture of inhibition characteristics is termed a mixed inhibitor. These inhibitors affect both the rate of product formation and the apparent affinity of the enzyme for substrate. The simplest example of such an inhibitor is one that binds both the free enzyme and the enzyme-substrate complex, and interferes with the formation of both the ES complex and the product.

4.3.2.2 GRAPHICAL DETERMIN ATION OF THE MODE OF INHIBITION

In the case where an inhibitor reacts with E or ES in a simple one-to-one fashion as in Figure 4.10, the rate-laws for each of the four modes of inhibition discussed above are linear with respect to the concentration of inhibitor (see Appendix A for a derivation of these rate-laws). In these cases, the reaction still obeys the M-M model; that is, a plot of rate *vs* substrate concentration is a rectangular hyperbola from which an *apparent* K_m and V_{max} can be determined.

If a series of experiments is performed in which the concentration of inhibitor is varied, then values for K_m, V_{max} and K_I (or K_I') *in the presence of inhibitor*, (as in Figure 4.10), can be determined. As with the uninhibited case, to accurately assess these kinetic parameters, it is most useful to transform the data and plot it in a linear form. Useful transformations include the Lineweaver-Burk, Dixon and modified Dixon plots,[16,19] examples of which are shown, for each of the four types of inhibitors in Appendix B.

In combination, these graphs are useful diagnostic tools for determining the mode of inhibition. The Dixon and modified Dixon plots provide an estimate of the EI dissociation constant K_I and K_I' respectively; an absolute measure of the degree of inhibition.

4.3.2.3 METHOD AND RESULTS

The kinetic parameters K_I/K_I', K_m and V_{max} in the presence of inhibitor were determined by measuring the initial reaction rate at varying substrate and inhibitor concentrations while keeping the enzyme concentration constant (see Chapter 7).

The mode of inhibition was determined using ENZFITTER. The raw data (that is, rate *vs* substrate concentration for a sequence of inhibitor concentrations) was fitted to the M-M equation and analysed for goodness of fit for the four modes of inhibition. The results for ascorbic acid using this analysis are shown in Table 4.6 and Table 4.7.

The kinetic parameters calculated by ENZFITTER are shown for each inhibitor concentration in Table 4.6; K_m and V_{max} are calculated along with an associated standard error (SE) for each, and a measure of the overall goodness-of-fit is given by the statistical parameter r^2. This parameter gives a measure of the strength of correlation between the experimental and predicted data; a value of 1 indicates perfect correlation, and 0, a complete absence of correlation. Assuming that the data does obey the M-M model, then a 95% confidence interval for the calculated parameters is given by ±2SE.

While at low ascorbic-acid concentrations our data fits the M-M model well (Table 4.6), as the concentration of inhibitor increases the fit is poor, as indicated by the large errors associated with V_{max} and K_m.

The values of K_I, K_m and V_{max} calculated by ENZFITTER assuming competitive, non-competitive, and uncompetitive modes of inhibition are shown in Table 4.7. The absence of values for the mixed mode of inhibition is due to an extremely poor fit of the data to this model. Based on these values, the mode of inhibition of *alpha*-amylase by ascorbic acid is most characteristic of a competitive inhibitor, with a calculated K_I value of 4.34×10^{-5} M. However, care must be taken interpreting these results as the calculations are based on the goodness of fit to the M-M model, which is shown in Table 4.6 to be not strongly held for the more concentrated solutions of inhibitor.

For comparison with the ENZFITTER data a Dixon plot was also constructed. This was consistent with that expected for a competitive inhibitor and gave a K_I value of 4.55×10^{-6} M.

The Lineweaver-Burk plot generated by ENZFITTER, and the Dixon plot constructed using Microsoft EXCEL, is shown in Figure 4.11.

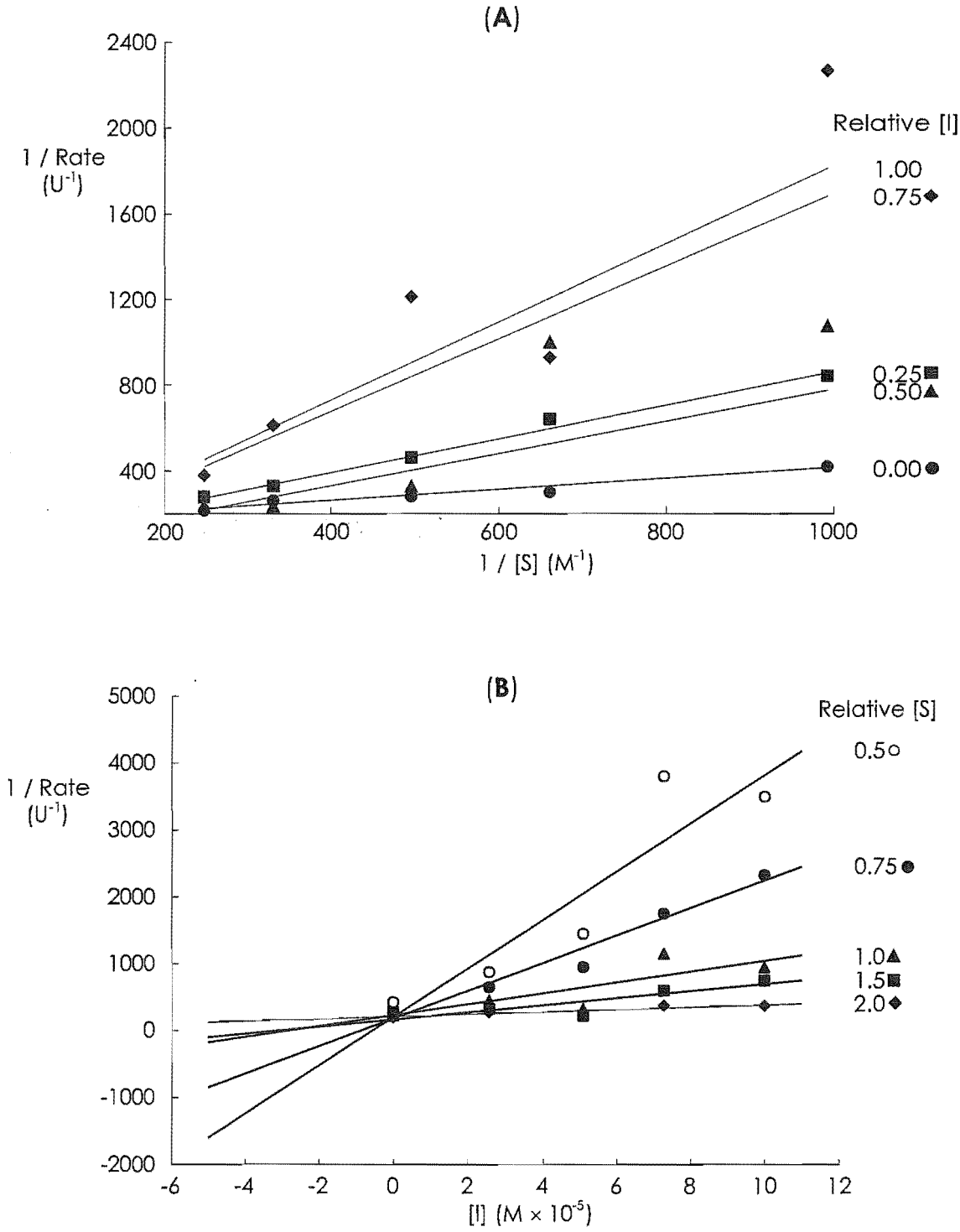

Figure 4.11: (**A**) Lineweaver-Burk double reciprocal plot, (**B**) Dixon plot of inhibition by ascorbic acid.

Table 4.6: Goodness of fit to the M-M equation for inhibition by ascorbic acid.

[INHIBITOR]	K_m (M)	SE (mM)	V_{max} (Ms^{-1})	SE (Ms^{-1})	r^2
0	1.62×10^{-3}	4.36×10^{-4}	1.23×10^{-7}	1.36×10^{-8}	0.944
2.56×10^{-5}	1.07×10^{-2}	3.15×10^{-3}	2.67×10^{-8}	2.65×10^{-7}	0.993
5.11×10^{-5}	3.20×10^{-2}	1.52×10^{-1}	8.27×10^{-7}	3.57×10^{-6}	0.823
7.26×10^{-5}	9.72×10^{3}	1.97×10^{7}	1.13×10^{1}	2.27×10^{2}	0.904
10.0×10^{-5}	8.37×10^{7}	2.93×10^{13}	9.00×10^{2}	3.14×10^{8}	0.825

Table 4.7: Analysis of the mode of inhibition for ascorbic acid.

MODE	K_m (M)	SE (mM)	V_{max} (Ms^{-1})	SE (Ms^{-1})	K_I/K_I' (M)	SE (M)	r^2
C	3.62×10^{-3}	2.47×10^{-3}	1.84×10^{-7}	7.20×10^{-8}	4.34×10^{-5}	1.70×10^{-5}	0.78
non-C	8.38×10^{-3}	6.87×10^{-3}	3.14×10^{-7}	1.91×10^{-7}	8.32×10^{-6}	2.33×10^{-5}	0.76
unC	2.31×10^{-2}	5.09×10^{-2}	6.80×10^{-7}	1.33×10^{-6}	1.01×10^{-5}	2.31×10^{-5}	0.69

The mode of inhibition for product **3.1** was also studied in this way. The results obtained using ENZFITTER are shown in Table 4.8 and Table 4.9

Table 4.8: Goodness of fit to the M-M equation for inhibition by compound **3.1**.

[INHIBITOR]	K_m (M)	SE (M)	V_{max} (Ms^{-1})	SE (Ms^{-1})	r^2
0	1.53×10^{-3}	7.0×10^{-4}	1.08×10^{-7}	1.80×10^{-8}	0.819
1.64×1^{-5}	2.84×10^{-3}	1.66×10^{-3}	1.13×10^{-7}	3.25×10^{-8}	0.829
3.27×10^{-5}	9.0×10^{6}	3.03×10^{11}	1.70×10^{2}	5.69×10^{6}	0.942
4.91×10^{-5}	2.11×10^{4}	1.34×10^{7}	3.10×10^{4}	1.96×10^{2}	0.69
6.54×10^{-5}	1.43×10^{2}	3.49×10^{4}	2.30×10^{-4}	5.43×10^{-2}	0.27

Table 4.9: Analysis of the mode of inhibition of compound **3.1**.

MODE	K_m	SE	V_{max}	SE	K_I/K_I'	SE	r^2
C	2.08×10^{-3}	2.04×10^{-3}	6.56×10^{-3}	2.74×10^{-3}	1.78×10^{-5}	1.13×10^{-5}	0.66
non-C	3.71×10^{-3}	3.12×10^{-3}	8.66×10^{-3}	4.10×10^{-3}	4.41×10^{-5}	1.28×10^{-5}	0.65
unC	4.92×10^{-3}	5.54×10^{-3}	1.01×10^{-2}	7.14×10^{-3}	1.71×10^{-5}	1.31×10^{-5}	0.62
mixed	2.63×10^{3}	1.57×10^{2}	3.29×10^{3}	1.97×10^{2}	K_I: 4.31×10^{-5} K_I': 6.96×10^{-8}	K_I: 8.16×10^{-6} K_I': 1.64×10^{-5}	0.60

Like ascorbic acid, compound **3.1**, also shows a good fit to the M-M equation at low inhibitor concentrations, but deviates strongly at higher concentrations. The mode of inhibition exhibited by compound **3.1** is most characteristic of the mixed model with $K_I = 4.31 \times 10^{-5}$ M and $K_I' = 6.9 \times 10^{-8}$ M; however, for this compound the fit to the M-M model is not as good as for ascorbic acid, and little significance can be attached to this result.

4.4 Conclusions

The work presented in this chapter has described the inhibitory activity of ascorbic-acid derivatives prepared, as detailed in chapter 3. Assays of all compounds prepared were performed using the Megazyme *alpha*-amylase kit.

The SAR studies for ascorbic acid and its derivatives have revealed the necessity for the ene-diol moiety for potent activity. The inhibitory activity of the

ring-open ene-diol analogue, DHFA, and the reduced activity of dehydroascorbic acid and the saturated **3.13** derivative, provide strong support for this hypothesis. In addition, inhibitory activity was relatively unaffected by modification of the diol chain, including epimerisation at C5.

The IC_{50} values calculated for ascorbic acid, **3.12**, and **3.14** show high degrees of potency; for ascorbic acid the value is 2.85×10^{-5} M.

Kinetic analysis has revealed that the inhibited reaction does not obey the M-M model at high inhibitor concentrations. Never-the-less the mode of inhibition of ascorbic acid is most characteristic of a competitive model with $K_I = 4.3 \times 10^{-5}$ M. In comparison, acarbose has a reported K_I of 10×10^{-6} M.[20] These results suggest that ascorbic acid may bind non-specifically in the active site of *alpha*-amylase interrupting productive binding of the substrate.

Product **3.1** obeyed the M-M model even more poorly than ascorbic acid at high concentrations, so little can be taken from the result that its mode of inhibition was most characteristic of a mixed-inhibitor model

4.5 Future Work

The potency of substrate-analogue inhibitors for *alpha*-amylase, such as acarbose (section 2.3.3.1), suggests that attachment of glucose residues onto the ascorbic-acid structure may lead to an inhibitor with increased potency relative to the unmodified compound. The glucose molecules may provide more sites for binding interactions between the enzyme and the inhibitor.

Our SAR results suggest that the attachment of the glucose residues onto the diol chain of ascorbic acid would be most beneficial, as modification of this part of the ascorbic-acid molecule does not interfere with the ene-diol functionality which is essential for ascorbic acid's activity. Given that *alpha*-amylase functions by hydrolysing α-1,4-glucosidic linkages, it is proposed that attachment of the glucose residues to ascorbic acid through an ether linkage at either the C4 or the C1 positions of the glucose ring would most resemble the natural substrate of *alpha*-amylase (Figure 4.12). The catalytic subsite of most *alpha*-amylase species is located in the centre of the active site surrounded by

other residue binding subsites. Therefore either of the postulated compounds shown in Figure 4.12 should display increased binding to the active site.

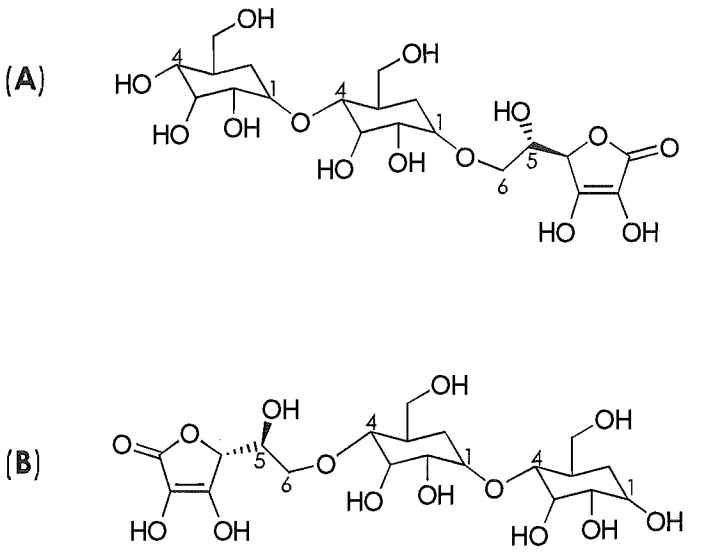

Figure 4.12: Potential potent ascorbic-acid-based inhibitors of *alpha*-amylases. (**A**) Linkage through the C1 anomeric carbon of the glucose residue. (**B**) Linkage through the C4 carbon of the Glucose residue.

4.6 References

(1) Cornish-Bowden, A. *Fundamental Enzyme Kinetics. Revised Edition*; Portland Press: Portland, 1995.

(2) Schomburg, D.; Salzmann, M., Eds. *Enzyme Handbook*; Springer-Verlag: Berlin, 1990.

(3) Boyer, P. D., Ed. *The Enzymes*, 3rd ed.; Academic Press: New York, 1971; Vol. 5.

(4) Searcy, R. L.; Wilding, P.; Berk, J. E. *Clin. Chim. Acta* **1967**, *15*, 189-197.

(5) Somogyi, M. *Clin. Chem.* **1960**, *6*, 23-35.

(6) Close, J. R.; Street, H. V. *Clin. Chim. Acta* **1958**, *3*, 476-479.

(7) *Approved Methods of the American Association of Cereal Chemists*; American Association of Cereal Chemists: St Paul, 1976.

(8) Babson, A. L.; Tenney, S. A.; Megraw, R. E. *Clinical Chemistry* **1970**, *16*, 39-43.

(9) Ceska, M.; Birath, K.; Brown, B. *Clin. Chim. Acta* **1969**, *26*, 437-444.

(10) Pierre, K. J.; Ker-Kong, T.; Rauscher, E.; Wahlefeld, A. W.; Foo, Y.; Rosalki, S. B. In *Methods of Enzymatic Analysis*, 3rd ed.; Bergmeyer, H. U.; Bergmeyer, J.; Graβl, M., Eds.; Verlag Chemie: Weinheim, 1984; Vol. IV, pp. 145-177.

(11) McCleary, B. V.; Sheehan, H. *Journal of Cereal Science* **1987**, 6, 237-251.

(12) Blair, H. E. USA Patent 4649108

(13) Palla, J. C.; Verrier, J. *Ann. Technol. agric.* **1974**, 23, 151-159.

(14) Davies, M. B.; Austin, J.; Partridge, D. A. *Vitamin C. Its Chemistry and Biochemistry*; The Royal Society of Chemistry: Letchworth, 1995.

(15) Voet, D.; Voet, J. G. *Biochemistry*; John Wiley and Sons: New York, 1990.

(16) Cornish-Bowden, A.; Wharton, C. W. *Enzyme Kinetics*; IRL Press: Oxford, 1988.

(17) Keleti, T. *Basic Enzyme Kinetics*; Akadémiai Kiadó: Budapest, 1986.

(18) MacGregor, A. W.; Morgan, J. E.; MacGregor, E. A. *Carbohydrate Research* **1992**, 227, 301-313.

(19) Henderson, P. J. F. In *Enzyme Assays A Practical Approach*; Eisenthal, R.; Danson, M. J., Eds.; IRL Press at OUP: Oxford, 1992; N.

(20) Mosi, R.; Sham, H.; Uitdehaag, J. C. M.; Ruiterkamp, R.; Dijkstra, B. W.; Withers, S. G. *Biochemistry* **1998**, *37*, 17192-17198.

5 Steroid 5α-R eductase

5.1 The Function of Steroid 5α-Reductase

Steroid 5α-reductase (SR) is a membrane-bound enzyme that is found predominantly in the skin, liver, and prostate tissues.[1-3] Its function is to catalyse the reduction of testosterone (T) to the androgen dihydrotestosterone (DHT) using nicotinamide adenine dinucleotide phosphate (NADPH). Both T and DHT bind a common receptor protein, but DHT has an increased affinity for the receptor and thus is a more potent hormone.

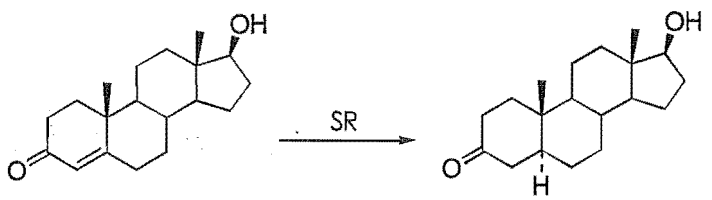

Testosterone (T) Dihydrotestosterone (DHT)

Figure 5.1: Testosterone (T) and Dihydrotestosterone (DHT).

The biological functions of DHT and T have been extensively investigated.[1,3] During embryonic development in male foetuses, T has been shown to be responsible for the differentiation of the wolfian ducts into seminal vesicles and epididymis, while DHT is required for the masculinisation of the external genitals. At the onset of puberty, T induces the maturation of the male external genitalia while DHT is necessary for full male body-hair growth patterns and subsequent male pattern baldness.

The various roles of T and DHT have been determined to some extent *via* the study of individuals who are SR deficient and who are thus unable to produce DHT. Whilst having male internal genitals, these people display ambiguous external female genitalia when born and are usually raised as girls. At puberty they undergo masculinisation including enlargement of the penis, descent of the testes increased muscle mass and deepening of the voice. However their prostates remain undeveloped and their body hair patterns stay predominantly female. Interestingly, these patients are also seldom reported to exhibit male pattern baldness or acne.

The isolation and characterisation of a cDNA, encoding human prostatic SR type 1, has revealed the presence of this gene in people suffering SR deficiency.[3] This information, coupled with the knowledge that SR expressed by this gene was poorly inhibited by finasteride, (a known potent inhibitor of human prostatic SR), lead to the conclusion that more than one isozyme of SR existed. This was confirmed by the subsequent isolation of a second isozyme (type 2), which is inhibited by finasteride.

For the SR type-1 and type-2 isozymes, the homology is approximately 50%. They differ in respect to their biochemical and pharmacological properties and also the region of the body in which they are predominantly expressed.[1,3] Type 1 is mostly associated with non-genital skin while the type-2 isozyme is generally located in the prostate and genital fibroblasts. Populations deficient in SR have been shown to be lacking an active type-2 isozyme, which has lead to the proposal that type-2 SR is responsible for prostate development and the growth of male body-hair patterns. The full role of type-1 SR is unclear, but it is thought to be associated with skin condition due to its prominent location in this organ.

Due to the importance of DHT for proper masculine development, the conversion of T into DHT is an essential process. However, elevated levels of DHT have been associated with various pharmacological disorders of the prostate and skin.[1,2] Benign prostatic hyperplasia (BPH) is a common non-cancerous enlargement of the prostate that leads to various urological disorders in ageing men. Treatment usually includes various pharmacological interventions and/or surgery involving a transurethral resection of the prostate.[2] Another more serious complaint is the development of prostatic cancers. The link between androgens such as DHT and prostatic carcinomas is well documented[1] and treatment usually involves tumour ablation by chemotherapy or castration. Less serious disorders such as acne, male pattern baldness and female hirsutism are also thought to be promoted by elevated levels of DHT.

Due to the suspected role of DHT in these conditions, it has been proposed that inhibition of SR would result in decreased levels of DHT and aid in the treatment of these ailments. It has also been suggested that selective inhibition of the different isozymes of SR may lead to greater accuracy in treating disorders thought to be specific to each type.

As SR has yet to be isolated and characterised, numerous SAR studies have been undertaken to identify key structural features of SR inhibitors responsible for potency and isozyme selectivity. SAR studies provide not only possible new drugs, but also information about the enzyme itself, which ultimately leads to better inhibitor design. The following is a brief review of the current findings of these investigations. Where possible activities are reported for human SR enzymes rather than for animal models. Many studies have shown differences in inhibition activities across species, which may be due to low enzyme homology.[1] This strongly suggests that care must be taken when choosing *in vivo* models for ascertaining activity.

5.2 Inhibitors of Steroid 5α-Reductase

The SR-catalysed reduction of T to DHT has been postulated to occur *via* an enolate transition-state as shown in Figure 5.2. The reaction is thought to proceed by the stereospecific transfer of the C-4 pro-S hydride from (NADPH) to the 5α position of T.[1,2]

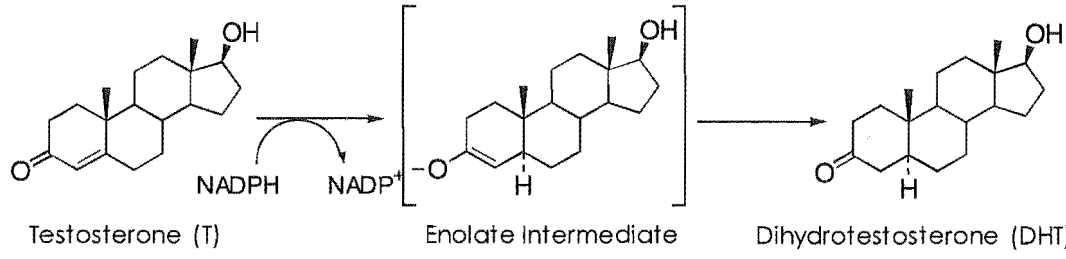

Figure 5.2: Enolate intermediate proposed for the reduction of T to DHT.

The oxyanion of the enolate intermediate is thought to be stabilised by the coordination of T near an electrophilic residue in the active site of SR. The enolate intermediate is protonated non-enzymatically to give DHT *via* an essentially irreversible process. The kinetic mechanism is believed to occur as shown in Figure 5.3.[4] The substrate is bound to the pre-formed enzyme-NADPH complex to give a ternary complex. Following the catalysed reaction, DHT is released from the binary enzyme-$NADP^+$ complex, which subsequently dissociates to give the free enzyme. Competitive inhibitors are thought to bind the enzyme-NADPH binary structure, while uncompetitive inhibitors interact with the enzyme-$NADP^+$ complex.

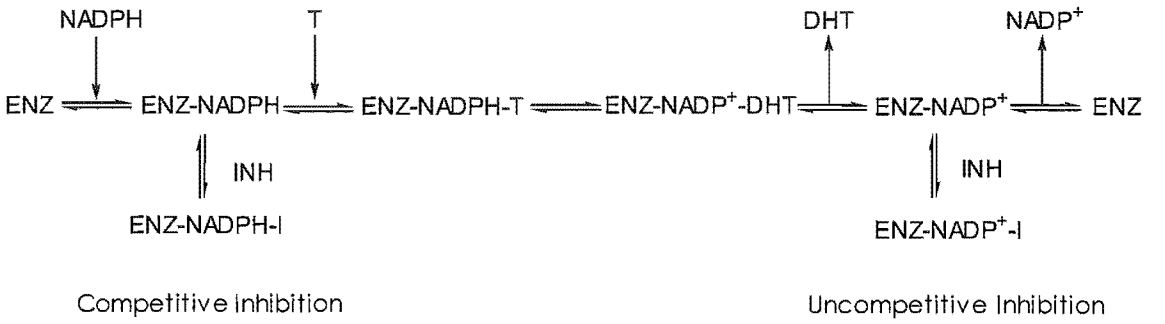

Figure 5.3: Proposed kinetic mechanism of SR.

5.2.1 Steroid-Based Inhibitors

In many instances, potent enzyme inhibitors are structurally similar to the natural substrate of an enzyme.[5] This is assumed to be due to similar binding affinities of the enzyme for both compounds. The initial designs of steroid 5α-reductase (SR) inhibitors included a structural element similar to that of the natural substrate (Figure 5.4) and a mimic of the putative enolate intermediate utilising various functionalities.

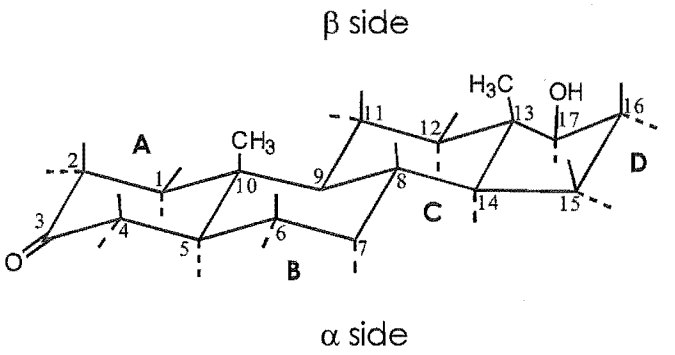

Figure 5.4: Basic steroid structure and numbering system.

5.2.1.1 4-Azasteroids

The first steroidal SR inhibitors developed, by Merck, were the 4-azasteroid class compounds; the basic structural skeleton resembling the natural substrate, and the enolate mimic provided by the amide functionality in the A-ring. Extensive SAR studies have revealed many factors that contribute to the potency of these inhibitors and their isozyme selectivity.[1,2] This work resulted in the development of the potent type-2 inhibitor finasteride (Type 1: IC_{50} = 500 nM; type

2: IC_{50} = 4.2 nM), which is currently marketed world-wide as a treatment for BPH, and more recently, male pattern baldness (Figure 5.5).

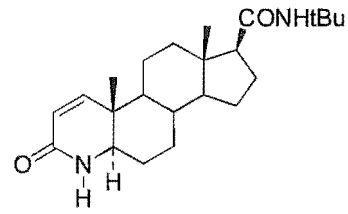

5.1

Figure 5.5: Finasteride.

Modification of the A-ring generally results in a decrease in inhibitory activity (Figure 5.6). Unsaturation at $\Delta^{1,2}$ and $\Delta^{5,6}$ reduces potency, as does substitution at the 4 position. Interestingly, it has been shown that $\Delta^{1,2}$ unsaturation is necessary for *in vivo* inhibition by finasteride. The effect of substituents on the A-ring of the 4-aza class of inhibitor has also been studied. It was proposed that the introduction of a halogen would lower the pK_a of the enolate mimic and enhance potency. However, the addition of halogen, methoxy, hydroxy or alkyl groups have no affect on activity.

The optimum ring size in this steroidal inhibitor has also been investigated. Increasing the A-ring to a 7-membered system reduces potency, however, changes in the size of the B and D-rings shows little influence on activity.

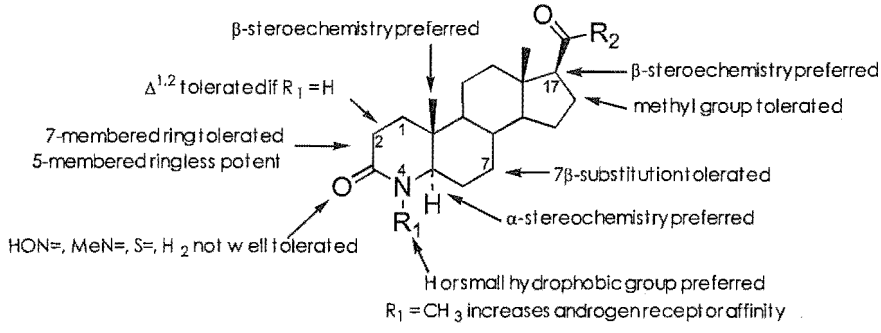

Figure 5.6: Summary of the results from SAR studies on the 4-azasteroid inhibitors of SR.

The type of substituent at the β–C17 position is most important for potency and selectivity, with amides based on small lipophilic amines preferred. The introduction of simple esters or ketones at C17 gives reasonably potent type-2 inhibitors; however, increasing the lipophilic nature of these groups also increases the potency of 4-aza inhibitors toward the type-1 isozyme (Table 5.1).

Table 5.1: The effect of different β–C17 substituents on the inhibitory activity of the 4-azasteroid compounds.

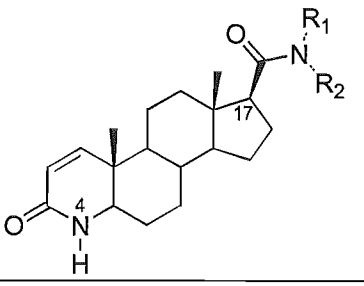

			IC_{50} (nM)	
No.	**R_1**	**R_2**	**Human SR 1**	**Human SR 2**
5.2	Ph	H	20	< 0.1
5.3	Ph	CH_3	350	0.2
5.4	Ph	Ph	>1000	25.2
5.5	1-indolinyl		120.2	0.4
5.6	2-$CF_3C_6H_4$	H	5.6	< 0.1
5.7	3-$C_6H_5C_6H_4$	H	14.0	<0.1
5.8	1-napthyl	H	8.1	0.2
5.9	2,5-CF_3-C_6H_3	H	2.4	0.5

SAR studies also led to the development of the potent dual inhibitor 4-MA which contains a fully saturated A-ring relative to finasteride. Activity in this compound is increased by N-alkylation, with a methyl group most preferred. However, commercial development of 4-MA has not been undertaken due its toxicity.[2]

Table 5.2: Activity of 4-MA relative to finasteride.

		IC_{50} (nM)	
Compound	**Structure**	**Human SR 1**	**Human SR 2**
4-MA **5.10**	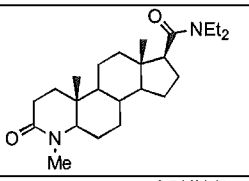	1.7	1.9
Finasteride **5.1**	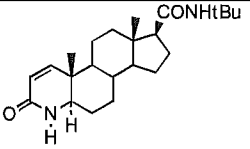	410	9.4

Analogues of the 4-azasteroid inhibitors containing an enone-enolate mimic prepared by Mann *et al.*[6] generally exhibit reduced activity relative to the lactam containing compounds, with only the 4-cyano-enone compound displaying significant inhibitory activity. However, a recently reported 4-triflouromethyl-substituted enone *has* shown increased potency over finasteride (Table 5.3 (a) and (b)).[7]

Table 5.3(a): Summary of results from SAR studies of 4-substituted-3-oxo-4-androstene inhibitors of SR.

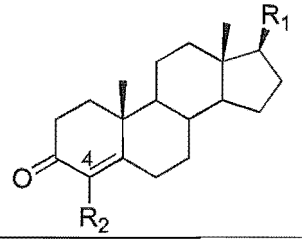

			IC_{50} (nM)	
No.	**R_1**	**R_2**	**Human SR 1**	**Human SR 2**
5.11	$CONH^tBu$	CN	-	2.9
5.12	$CONH^tBu$	SH	709	437
5.13	$CONH^tBu$	Cl	> 1000	192
5.14	$CONH^tBu$	Br	981	387

Table 5.3(b): Summary of results from SAR studies of 4-substituted-3-oxo-androstene inhibitors of SR.

			SR K_i values (nM)	
No.	**R_1**	**R_2**	**[^{3}H]-DHT**	**NADPH**
5.15	$CONH^tBu$	CF_3	20.9	20.2
5.16	CH_3CO	CF_3	>> 1000	>> 1000
5.17	O,O	CF_3	95.2	28.8
5.18	finasteride		88.2	54.7

5.2.1.2 6-AZASTEROIDS

Table 5.4: Summary of results from SAR studies of 6-azasteroid inhibitors of Human SR.

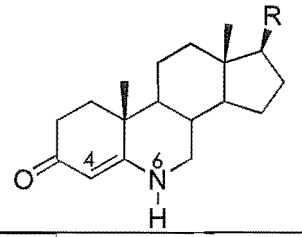

No.	**R**	**SR 1 K_i (nM)**	**SR 2 IC_{50} (nM)**
5.19	OMe	150	3.2
5.20	O-2-adamantyl	6.9	0.04
5.21	NEt_2	750	1.5
5.22	NH-1-adamantyl	11	0.07
5.23	NH^tBu	820	0.88
5.24	$N(iPr)_2$	190	0.36
5.25	$NHCHPh_2$	30	0.09
5.26	iBu	9	0.08
5.1	finasteride	150	0.18

The 6-azasteroid inhibitors are another example of amino-containing compounds developed to mimic the enolate intermediate.[1,2,8-10] The ketoenamine moiety provides structural and electronic features similar to those of the enzyme reaction intermediate. Activity is dominated by the choice of β–C17 substituent, and like the 4-azasteroid inhibitors, lipophilic groups are favoured (Table 5.4). These compounds display dual inhibition against SR and with

appropriate β–C17 substitution display potent, selective inhibition of type-2 SR. N6 substitution with small alkyl groups increases type-1 potency, as does substitution at C4 with small lipophilic groups. Large substituents in either of these positions reduce the inhibition against both isozymes significantly.

5.2.1.3 Nor-10-Azasteroids

One of the most recent series of steroid-based SR inhibitor developed is the nor-10-azasteroids.[11] As with other steroidal SR inhibitors, activity against both isozymes is enhanced by the presence of a lipophilic β–C17 substituent. The position of the double bond in the A-ring is critical to activity. Unsaturation at $\Delta^{1,2}$ relative to $\Delta^{4,5}$ decreases potency, whilst complete saturation of the A-ring removes all inhibitory activity. Potency is also increased if unsaturation of the C-ring is at the $\Delta^{8,9}$ position. Selective type-1 inhibition is achieved in the presence of a keto or hydroxy group at C17.

Table 5.5: SAR of 19-nor-10-azasteroids against human SR.

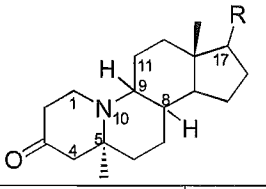

No.	R	Unsaturation	IC_{50} (nM)[a]	Selectivity SR 2 : SR 1
5.27	=O	$\Delta^{4,5}$	1265	1:15
5.28	=O	$\Delta^{1,2}$	18843	-
5.29	=O		>>100000	-
5.30	β-CONH^{t}Bu	$\Delta^{4,5}$, $\Delta^{9(11)}$	21.5	1:1
5.31	β-CONH^{t}Bu	$\Delta^{4,5}$, $\Delta^{8(9)}$	2.9	1:1

a Inhibition against SR type-2 human prostate homogenate

5.2.1.4 Carboxylate Steroids

A carboxylic-acid series of inhibitors, developed by Smith-Kline Beecham, mimic the putative enolate intermediate by use of a charged carboxylate group.[1,2,12] These inhibitors are postulated to preferentially bind the enzyme-$NADP^+$ complex due to favourable electrostatic interactions between the negatively-charged carboxylate and the positively-charged binary complex. They are potent inhibitors of type-2 SR.

The first of these inhibitors developed were the steroidal acrylates, which contain a carboxylate at the C3 position and unsaturation at $\Delta^{3,4}$. Development

then led to compounds incorporating dienes with unsaturation at $\Delta^{3,4}$ and $\Delta^{5,6}$ and aryl acids (Figure 5.7).

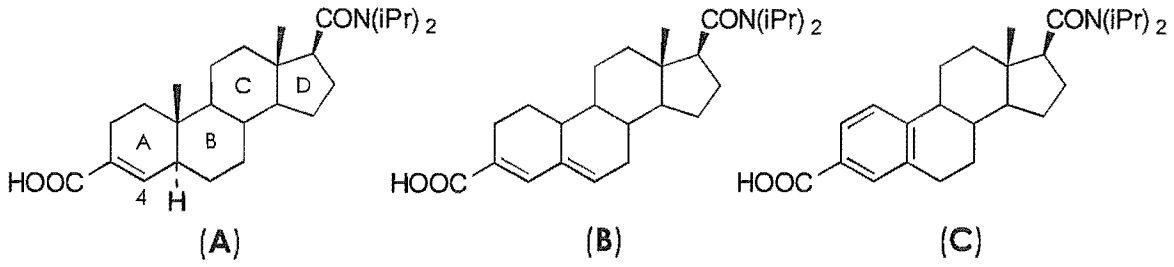

Figure 5.7: (**A**) $\Delta^{3,4}$ unsubstituted acids, (**B**) diene acids, and (**C**) aryl acids.

The position of A-ring unsaturation in these inhibitors has no influence on potency; however, complete saturation of the A-ring significantly reduces activity. Incorporation of an electronegative substituent onto the A-ring of the aryl acids was expected to decrease the electron density and lower the pK_a of the carboxylate. The use of fluoro and cyano groups for this purpose was proposed to also provide a hydrogen-bonding site.[12] However, introduction of this type of functionality results in no increased activity and substituents at C4 were actually found to decrease potency.

Extension of the carboxylate moiety by one carbon to increase conformational flexibility shows no adverse effects on the potency of inhibitors containing this group (Table 5.6). However, extension by two carbons or the presence of an exocyclic double bond reduces the potency significantly.

The greatest influence on potency for these inhibitors is the choice of substituent at C17. Like the 4-azasteroid inhibitors, lipophilic groups such as carboxamides are favoured.

Inhibitors have also been prepared with a negatively-charged species provided by phosphinic, phosphonic, and sulfonic substituents at the C3 position (Table 5.6). All show good potency against SR with the diene inhibitors showing slightly increased potency over the aryl compounds. Inhibitors containing phosphinic and sulfonic groups at C3 show no tolerance for chain extension.

Recently a diene steroidal analogue was reported that contained a phenyl acetylene group at the C3 position.[13] This compound was reported to have good activity against SR despite the fact that it possesses none of the basic structural

features considered necessary for inhibitory action (K_I of rat SR = 45.8 nM versus finasteride = 54.7 nM).

Table 5.6: SAR studies of the aryl acid inhibitors on Human prostate SR.

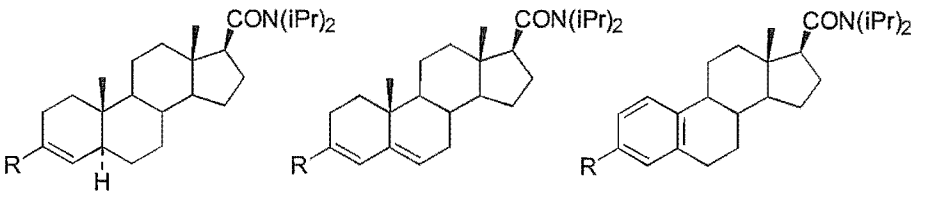

A B C

	A		B		C	
R	**No.**	**$K_{I,app}$ (nM)**	**No.**	**$K_{I,app}$ (nM)**	**No.**	**$K_{I,app}$ (nM)**
COOH	**5.32**	30	**5.33**	7 – 18	**5.34**	20
CH_2COOH	**5.35**	85	**5.36**	450	**5.37**	20
$(CH_2)_2COOH$		-		-	**5.38**	290
CHCOOH	**5.39**	> 5000		-		-
NO_2	**5.40**	50	**5.41**	500	**5.42**	> 10000
PO_3H_2		-	**5.43**	25	**5.44**	50
$CH_2PO_3H_2$		-		-	**5.45**	740
PHO_2H		-	**5.46**	7	**5.47**	13
SO_3H		-		-	**5.48**	20 - 40
CH_2SO_3H		-		-	**5.49**	> 5000

5.2.1.5 Summary

In general, steroid-based inhibitors are shown to exhibit preferential potency against the type-2 isozyme of SR over the type-1 enzyme. The potency is mostly determined by the substituent at β–C17, with lipophilic amides favoured. The choice of functionality for the enolate mimic does not seem to have much influence on the inhibitor's activity.

5.2.2 Non-Steroidal Inhibitors

As an alternative to steroid-based inhibitors many non-steroidal inhibitors have been developed. Initial efforts involved compound screening to reveal possible lead compounds and also the testing of tricyclic analogues of active steroid-based inhibitors. More recent trends to improve isozyme selectivity and to prepare dual inhibitors involve the connection of structural features known to be necessary for selective isozyme inhibition.

5.2.2.1 ONO 3805

Compound screening has revealed many different classes of non-steroidal SR inhibitors including retanoic acid, linolenic acid, and gossypol, which, though structurally dissimilar to the steroidal substrate, exhibit good inhibitory activity against SR (Figure 5.8).

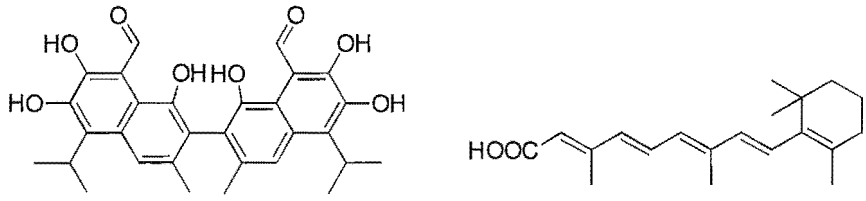

Gossypol Retanoic acid

Figure 5.8: Non-steroidal inhibitors of SR.

Compound screening also led to the discovery of the non-steroidal SR inhibitor ONO 3805.[1,2] A good inhibitor against the type-2 enzyme, ONO 3805 has also been a good lead compound for the development of novel potent dual inhibitors (Figure 5.9).

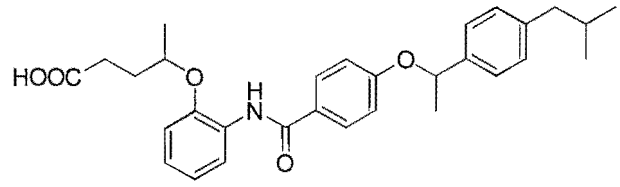

Figure 5.9: ONO 3805.

Initial SAR studies revealed that the amide linkage to the central phenyl spacer and the ether-linked butyric acid are necessary for activity. Replacement of the hydroxyaniline moiety to incorporate a structurally analogous acylindole group significantly improves the inhibitory action.[14] As can be seen from Table 5.7 the S-enantiomer of the methyl benzyl group is essential for increased potency; thus, the conformations of these inhibitors are important for their activity. Reversal of the central ether linkage also gives comparable results.

Given the increased activity of inhibitors containing an indole functionality, this moiety has been incorporated into several new inhibitors (Figure 5.10) capable of acting as dual inhibitors against SR and α_1-adrenoreceptor (another receptor implicated in the onset of BPH).[15-17]

Table 5.7: Summary of results from SAR of ONO-3085-analogue inhibitors on human SR.

		IC_{50} (nM)	
No.	**Structure**	**Human SR 1**	**Human SR 2**
5.50	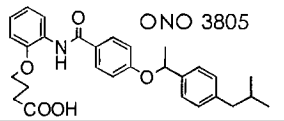	-	256
5.51	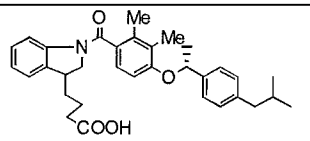	113	481
5.52	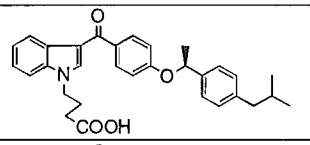	40	4
5.53	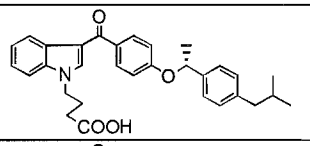	574	69
5.54	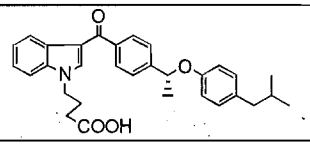	8	10

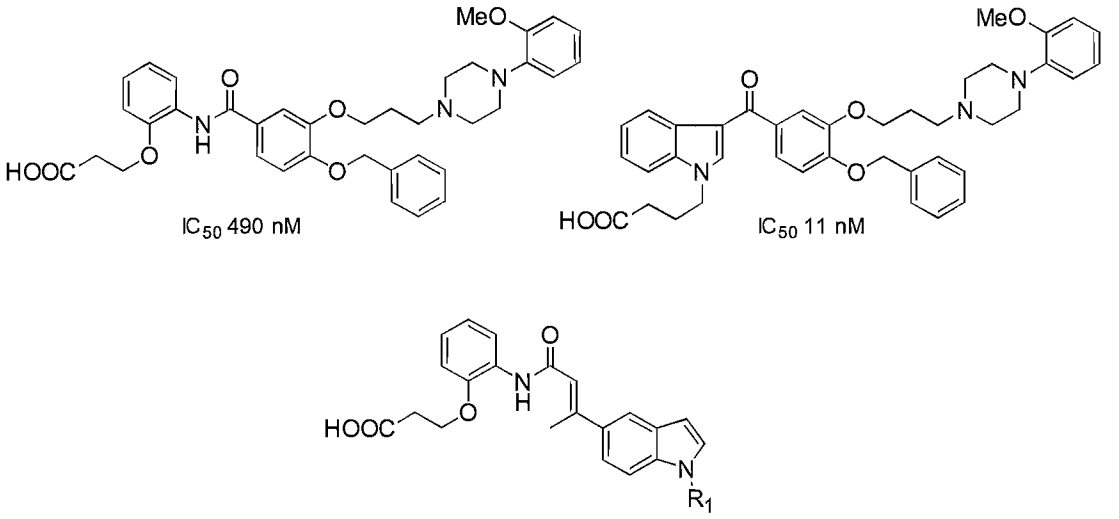

Figure 5.10: Inhibitors developed incorporating an indole functionality exhibit improved potency.

5.2.2.2 Benzoquinolinones

One of the most widely-studied classes of non-steroidal inhibitor is the benzoquinolinones.[1,2,18,19] These compounds are structurally analogous to the 4-azasteroid class of inhibitor previously mentioned (Figure 5.11). Unlike the 4-azasteroids however, benzoquinolinones show selectivity for the type-1 isozyme of SR only.

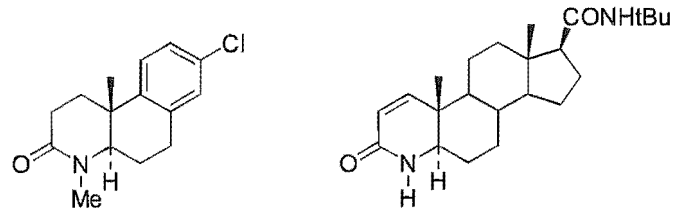

5.55 **5.1**

Figure 5.11: Comparison of the structures of finasteride (**5.1**) and the potent benzoquinolinone inhibitor LY191704 (**5.55**).

SAR studies (Figure 5.12) have shown certain requirements for potency in the benzoquinolinone type inhibitors.[18] Activity is increased by inclusion of a C8 substituent that has either electron withdrawing or electron donating ability; a chloride group gives the greatest potency. For molecules which posses a C10 angular methyl substituent, a trans ring junction is preferred over a cis conformation for potency. The cis conformation results in a deviation from the planar system thought to be important for activity. For molecules that contain no angular substituent both cis and trans conformations provide similar potency.[19] The presence of an N-methyl group also increases potency; however, substituents larger than a methyl group decrease the activity of the inhibitor. This trend is also observed for the 4-azasteroid inhibitors.

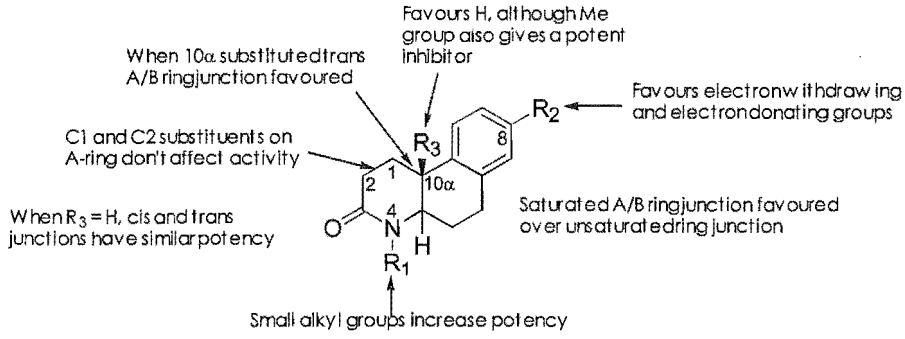

Figure 5.12: Summary of results from SAR studies for the benzoquinolinone inhibitors of SR.

Another observed trend in these studies, which is similar to the 4-azasteroid inhibitors, is the dependence of A-ring size on potency. A contraction of the A-ring to a 5-membered structure shows no significant difference in potency relative to the parent benzoquinolinone, but expansion to a 7-membered A-ring, results in decreased activity against the type-1 isozyme.[20] Thus, the order of potency for lactam A-rings is 6-membered > 5-membered >> 7-membered.

A recent study by Lilly[4] has shown that the inclusion of large hydrophobic groups at the C8 position increases the potency of non-steroidal benzoquinolinone inhibitors for the type-2 SR isozyme while maintaining the type-1 activity (Table 5.8). This result forms the basis of some of the work described in this thesis (Chapter 6).

Table 5.8: Summary of results from SAR studies for C8-substituted-benzoquinolinone inhibitors of SR.

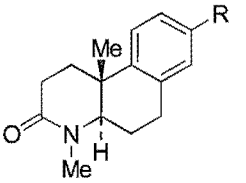

		IC_{50} (nM)	
No.	**R**	**Human SR 1[a]**	**Human SR 2[b]**
5.55	Cl	8	10000
5.56	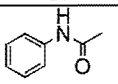	> 10000	520
5.57		59	> 10000
5.58		1000	> 10000
5.59	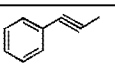	21	52
5.60		6	1400
5.61	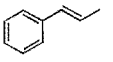	23	180
5.62	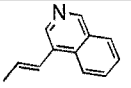	63	1340
5.63	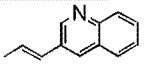	3.4	320
5.64	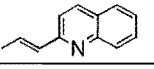	32	550

[a] human scalp; [b] human prostate

5.2.2.3 Phenanthridin-3-ones

The phenanthridinones are tricyclic analogues of the 6-azasteroid class of inhibitor.[21] Although selective for type-1 SR, these tricyclic inhibitors show similar structural requirements to the parental steroid compound with respect to potency; it increases with the presence of methyl substituents at C4, and/or a small alkyl substituent at C6 (Table 5.9).

Table 5.9: Summary of results from SAR studies for phenanthridinone inhibitors of SR.

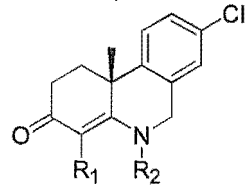

No.	R_1	R_2	Human SR 1 K_I (μM)
5.65	H	CH_3	>>10
5.66	CH_3	CH_3	1.1
5.67	CH_3	H	0.92

5.2.2.4 Diene Acids

Due to the potency exhibited by the tricyclic benzoquinolinone inhibitors a series of tetrahydrophenanthrene-2-acetic and phosphinic acids has also been prepared as tricyclic analogues of the potent diene acid inhibitor, epristeride (Figure 5.13). [22]

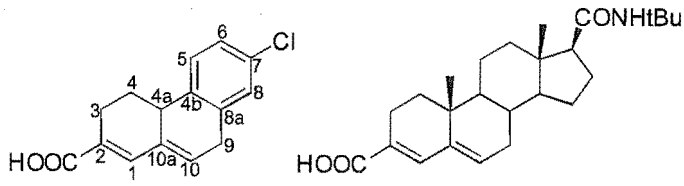

5.68

$K_{I,app}$ type 1 = 1200 nM, type 2 = 260 nM

epristeride

$K_{I,app}$ type 1 = 410 nM, type 2 = 0.2 nM

Figure 5.13: Comparison of epristeride with a tricyclic diene acid analogue.

Table 5.10: Summary of results from SAR studies for tricyclic-diene-acid inhibitors of SR.

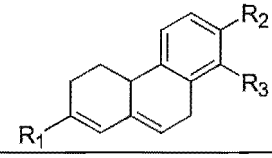

				$K_{I,app}$ (nM)	
No.	**R1**	**R2**	**R3**	**Human SR 1**	**Human SR 2**
5.68	COOH	Cl	H	1200	260
5.69	COOH	OMe	H	NI[a]	>2500[b]
5.70	COOH	H	OMe	1900	1600
5.71	PHOOH	Cl	H	1900	1600
5.72	PHOOH	H	OMe	1900	1600

[a] no inhibition at 2.5 μM; [b] 30% inhibition at 2.5 μM

The diene acids show preferential inhibition of the type-2 SR isozyme; however, these tricyclic analogues exhibit a decrease in potency relative to the

steroidal diene acids. Like the benzoquinolinone tricyclic inhibitors the diene acid inhibitors show increased inhibitory activity when they contain a C7 chloro substituent. The presence of a methoxyl substituent at either C7 or C8 results in a decrease in both type-2 selectivity and potency. The phosphinic acid compounds are modest inhibitors of SR (Table 5.10).

5.2.2.5 Aryl Acids

Tricyclic aryl acids have been prepared based on the steroidal-aryl-acid compounds.[23] They show potent type-1 inhibitory activity relative to the parent steroidal compounds (Figure 5.14) **5.73,** which are selective for type-2 SR. Their potency is influenced by the choice of C7 substituent: a bromo substituent gives significantly greater type-1 activity than either the chloro ($K_{I,app}$ type 1 = 320 nM, type 2 = 2500 nM) or unsubstituted compound ($K_{I,app}$ type 1 = 315 nM, type 2 = >10000 nM).

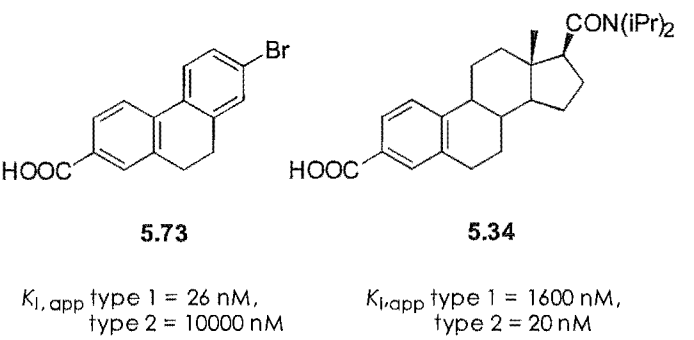

5.73 **5.34**

$K_{I,app}$ type 1 = 26 nM, type 2 = 10000 nM

$K_{I,app}$ type 1 = 1600 nM, type 2 = 20 nM

Figure 5.14: Structural comparison of steroidal and non-steroidal aryl acid SR inhibitors.

5.2.2.6 Benzophenones and Indole Carboxylic Acids

The inhibitory activity of the indole acids and benzophenone acids (Figure 5.15) was discovered whilst screening for non-steroidal aryl carboxylic acid, which retains the A-ring features necessary for activity in the steroidal aryl-acid inhibitors.[24] Both classes of compound are potent type-2 SR inhibitors.

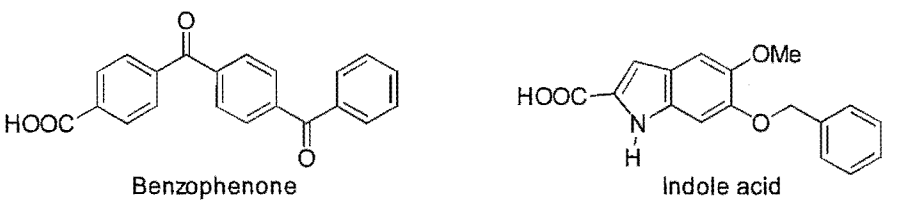

Benzophenone Indole acid

Figure 5.15: Benzophenone- and indole-acid inhibitors of SR.

SAR studies have shown that for the benzophenone carboxylic acid series, C-ring substitution or saturation is well tolerated. The carbonyl linker between the C and B rings may be exchanged without loss of activity and a direct link, between the two rings, is also tolerated. However, replacing the carbonyl group between rings A and B results in reduced activity (Table 5.11).

Table 5.11: Summary of results from SAR studies for benzophenone-carboxylic-acid inhibitors of type-2 SR.

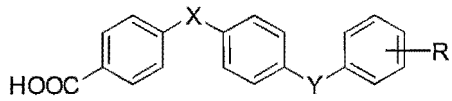

No.	X	Y	R	Type-2 SR $K_{i,app}$ (nM)
5.74	C=O	O	H	5
5.75	C=O	CH_2	4-Me	15
5.76	C=O	C=O	4-Me	10
5.77	C=O	C=O	H	40
5.78	C=O	C=O	4-Cl	35
5.79	C=O	C=O	Hexahydro	30
5.80	CH_2	O	H	35
5.81	-	$COCH_2$	H	60

For the indole-acid compounds, the position of the substituent on the B-ring is important for potency, and the C5 and C6 positions are more highly favoured for good activity, then the C4 position. Interestingly for C5-substituted derivatives, N-methylation is not favoured; however, for C5,C6-disubstituted compounds, N-methylation gives increased potency.

As the carboxylic-acid group provides an enolate mimic in both classes of inhibitor, this functionality is also necessary for activity.

Table 5.12: Summary of results from SAR studies for indole-carboxylic-acid inhibitors of SR.

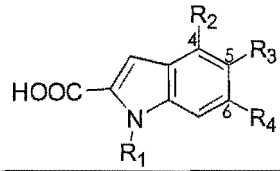

No.	R1	R2	R3	R4	Type 1(nM)	Type 2 (nM)
5.82	H	H	OCH_2Ph	H	> 2500	40
5.83	Me	H	OCH_2Ph	H	> 2500	310
5.84	H	H	OMe	OCH_2Ph	460	20-30
5.85	Me	H	OMe	OCH_2Ph	500	10
5.86	H	OCH_2Ph	H	H	> 2500	550
5.87	H	H	H	H	NI	230
5.88	Me	H	H	H	NI	NI

Two series of inhibitors have also been developed incorporating the biphenyl-acid structure of the benzophenone-type inhibitors. The first, based on

the tricyclic aryl acids, includes a phenyl-acid substituent at the C8 position of the parent compound. As seen in Table 5.13, inhibitors containing the phenyl-acid group show improved type-2 activity over the bromo-substituted compounds whilst still maintaining the type-1 potency.[25]

Table 5.13: Summary of results from SAR studies for C8-substituted non-steroidal-aryl-acids inhibitors of SR.

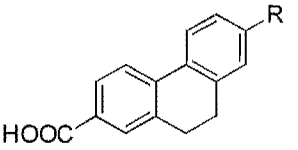

No.	R	Type-1 SR % inhibition	Type-2 SR % inhibition
5.73	Br	K_{iapp} 26 nM	50% (10 μM)
5.89	COOH	20% (2.5 μM)	50% (10 μM)
5.90	H	K_{iapp} 315 nM	20% (10 μM)
5.91	Ph	45% (2.5 μM)	K_{iapp} 2.2 μM
5.92	4-HOOCPh	80% (2.5 μM)	K_{iapp} 2.2 μM

The second type of inhibitor developed with the biphenyl template includes a substituted-indole functionality as a mimic of the steroidal C and D rings. The substituents chosen for the indole ring were those that gave optimal activities in the ONO 3805 series described previously. As can be seen from Table 5.14, these compounds show selective activity against type-1 SR.

Table 5.14: Summary of results from SAR studies for N-substituted indoylbenzoic-acid inhibitors of SR.

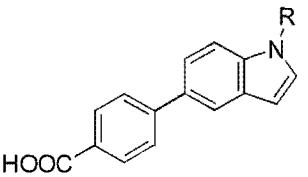

No.	R	Human SR type 2 % inhibition (10μM)	Human SR type 1 % inhibition (10μM)
5.93	Benzyl	60	67
5.94	Benzhydryl	40	81
5.95	1-Butyl	24	72
5.96	4-Heptyl	10	75
5.97	Cyclohexanemethyl	50	81
5.98	Cyclohexyl	36	-

5.2.2.7 Benzo[c]quinolizin-3-ones

Two tricyclic analogues based on the 19-nor-10-azasteroid inhibitors have been developed.[26] These two non-steroidal inhibitors differ only in the position of unsaturation in the A-ring (Figure 5.16). One is a proposed substrate-like transition-state mimic (**5.99**), and the other, a product-like mimic (**5.100**). Both compounds

were selective for type-1 SR inhibitors and their potency dependent on the position of unsaturation.

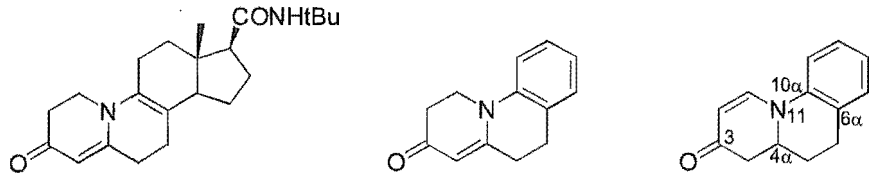

5.31 **5.99** **5.100**

Substrate-like mimic Product-like mimic

Figure 5.16: Tricyclic analogues of the 19-nor-10-azasteroid inhibitors.

5.2.2.8 SUMMARY

Unlike the steroidal inhibitors, the non-steroidal compounds that have been identified exhibit selectivity for both type-1 and type-2 SR. Inhibitors incorporating a charged carboxylate enolate mimic tend to display type-2 selectivity, as is shown by the tricyclic diene acids, the benzophenone and indole carboxylic acids. On the other hand, the neutral mimics incorporating amide or enamine groups, such as the benzoquinolinone and phenathridinones, show selectivity for type-1 SR. The majority of non-steroidal inhibitors discussed give increased activity when a lipophilic group is incorporated into their structure in a location that might be considered analogous to that of the steroidal D-ring.

Recent work by Ahmed *et al.*[27,28] has revealed that the most important feature of a SR inhibitor is the presence of an enolate mimic. The NADPH molecule has been shown to be positioned close to C5 in the enzyme-cofactor complex and therefore, the area about C4 and C5 is sterically hindered. This finding may account for decreased activity for inhibitors containing large substituents, in these locations.

The area surrounding the binding position of the C17 substituent has been shown to be very large, and it is postulated that this location is the entry and exit point for substrate molecules. The C17 binding area is also thought to lack H-bonding residues, and it is assumed that binding of substituents in this position occurs through polar interactions. These findings are based on conformational analysis of a selection of potent type-1 and type-2 SR inhibitors superimposed

upon a calculated low energy conformation of the proposed enolate intermediate.

5.2.2.9 Our Work on SR Inhibitors

Our interest in SR inhibitors is in the area of non-steroidal inhibitors, which have been developed from steroid-based compounds. In particular the benzoquinolinone (section 5.2.2.2) and tricyclic-aryl-acid compounds (section 5.2.2.5) that are potent type-1 inhibitors.

The work presented in the following chapter is based on three areas on investigation;

1) Improving the activity and selectivity of two known tricyclic inhibitors by incorporating hydrophobic substituents shown to improve the activity of related compounds.

2) An investigation of bicyclic analogues of the 4-azasteroid and benzoquinolinone compounds for use as inhibitors of SR.

3) An investigation of the activity of a novel enolate mimic; a thiolactam.

5.3 References

(1) Abell, A. D.; Henderson, B. R. *Current Medicinal Chemistry* **1995**, *2*, 583-597.

(2) Kenny, B.; Ballard, S.; Blagg, J.; Fox, D. *J. Med. Chem.* **1997**, *40*, 1293-1315.

(3) Andersson, S.; Berman, D. M.; Jenkins, E. P.; Russell, D. W. *Nature* **1991**, *354*, 159-161.

(4) Smith, E. C. R.; McQuaid, L. A.; Goode, R. L.; McNulty, A. M.; Neubauer, B. L.; Rocco, V. P.; Audia, J. E. *Bioorg. Med. Chem. Lett.* **1998**, *8*, 395-398.

(5) Bugg, T. *An Introduction to Enzyme and Coenzyme Chemistry*; Blackwell Science: Oxford, 1997.

(6) Haase-Held, M.; Hatzis, M.; Mann, J. *J. Chem. Soc. Perkin. Trans.* **1993**, *1*, 2907-2911.

(7) Fei, X.-S.; Tian, W.-S.; Chen, Q.-Y. *Bioorg. Med. Chem. Lett.* **1997**, *7*, 3113-3118.

(8) Frye, S. V.; Haffner, C. D.; Maloney, P. R.; Mook, R. A., Jr.; Dorsey, G. F.; Hiner, R. N.; Batchelor, K. W.; Bramson, H. N.; Stuart, J. D.; Schweiker, S. L.; van Arnold, J.; Bickett, D. M.; Moss, M. L.; Tian, G.; Unwalla, R. J.; Lee, F. W.;

Tippin, T. K.; James, M. k; Grizzle, M. K.; Long, J. E.; Schuster, S. V. *J. Med. Chem.* **1993**, *36*, 4313-4315.

(9) Frye, S. V.; Haffner, C. D.; Maloney, P. R.; Mook, R. A., Jr.; Dorsey, G. F., Jr.; Hiner, R. N.; Cribbs, C. M.; Wheeler, T. N.; Ray, J. A.; Andrews, R. C.; Batchelor, K. W.; Bramson, H. N.; Stuart, J. D.; Schweiker, S. L.; van Arnold, J.; Croom, S.; Bickett, D. M.; Moss, M. L.; Tian, G.; Unwalla, R. J.; Lee, F. W.; Tippin, T. K.; James, M. K.; Grizzle, M. K.; Long, J. E.; Schuster, S. V. *J. Med. Chem.* **1994**, *37*, 2352-2360.

(10) Frye, S. V.; Haffner, C. D.; Maloney, P. R.; Hiner, R. N.; Dorsey, G. F.; Noe, R. A.; Unwalla, R. J.; Batchelor, K. W.; Bramson, H. N.; Stuart, J. D.; Schweiker, S. L.; van Arnold, J.; Bickett, D. M.; Moss, M. L.; Tian, G.; Lee, F. W.; Tippin, T. K.; James, M. K.; Grizzle, M. K.; Long, J. E.; Croom, D. K. *J. Med. Chem.* **1995**, *38*, 2621-2627.

(11) Guarna, A.; Belle, C.; Machetti, F.; Occhiato, E. G.; Payne, A. H.; Cassiani, C.; Comerci, A.; Danza, G.; De Bellis, A.; Dini, S.; Marrucci, A.; Serio, M. *J. Med. Chem.* **1997**, *40*, 1112-1129.

(12) Holt, D. A.; Levy, M. A.; Ladd, D. L.; Oh, H.-J.; Erb, J. M.; Heaslip, J. I.; Brandt, M.; Metcalf, B. W. *J. Med. Chem.* **1990**, *33*, 937-942.

(13) Tian, W.; Zhu, Z.; Liao, Q.; Wu, Y. *Bioorg. Med. Chem. Lett.* **1998**, *8*, 1949-1952.

(14) Blagg, J.; Ballard, S. A.; Cooper, K.; Finn, P. W.; Johnson, P. S.; MacIntyre, F.; Maw, G. N.; Spargo, P. L. *Bioorg. Med. Chem. Lett.* **1996**, *6*, 1517-1522.

(15) Yoshida, K.; Horidoshi, Y.; Eta, M.; Chikazawa, J.; Ogishima, M.; Fukuda, Y.; Sato, H. *Bioorg. Med. Chem. Lett.* **1998**, *8*, 2967-2972.

(16) Kumazawa, T.; Takami, H.; Kishibayashi, N.; Ishii, A.; Nagahara, Y.; Hirayama, N.; Obase, H. *J. Med. Chem.* **1995**, *38*, 2887-2892.

(17) Soto, H.; Kitagawa, O.; Aida, Y.; Chikazawa, J.; Kurimoto, T.; Takei, M.; Fukuta, Y.; Yoshida, K. *Bioorg. Med. Chem. Lett.* **1999**, *9*, 1553-1558.

(18) Jones, C. D.; Audia, J. E.; Lawhorn, D. E.; McQuaid, L. A.; Neubauer, B. L.; Pike, A. J.; Pennington, P. A.; Stamm, N. B.; Toomey, R. E.; Hirsch, K. S. *J. Med. Chem.* **1993**, *36*, 421-423.

(19) Abell, A. D.; Yen, H.-K.; Yamashita, D. S.; Brandt, M.; Mohammed, H.; Levy, M. A.; Holt, D. A.; Erhard, K. F. *Bioorg. Med. Chem. Lett.* **1994**, *4*, 1365-1368.

(20) Abell, A. D.; Phillips, A. J.; Budhia, S.; McNulty, A. M.; Neubauer, B. L. *Aust. J. Chem.* **1998**, *51*, 389-396.

(21) Mook, R. A., Jr.; Lackey, K.; Bennett, C. *Tetrahedron Letters* **1995**, 36, 3969-3972.

(22) Abell, A. D.; Brandt, M.; Levy, M. A.; Holt, D. A. *Bioorg. Med. Chem. Lett.* **1994**, *4*, 2327-2330.

(23) Abell, A. D.; Brandt, M.; Levy, M. A.; Holt, D. A. *Bioorg. Med. Chem. Lett.* **1996**, *6*, 481-484.

(24) Holt, D. A.; Yamashita, D. S.; Konialian-Beck, A. L.; Luengo, J. I.; Abell, A. D.; Bergsma, D. J.; Brandt, M.; Levy, M. A. *J. Med. Chem.* **1995**, *38*, 13-15.

(25) Abell, A. D.; Brandt, M.; Levy, M. A.; Holt, D. A. *J. Chem. Soc. Perkin. Trans.* **1997**, *1*, 1663-1667.

(26) Guarna, A.; Occhiato, E. G.; Scarpi, D.; Tsai, R.; Danza, G.; Comeci, A.; Mancina, R.; Serio, M. *Bioorg. Med. Chem. Lett.* **1998**, *8*, 2871-2876.

(27) Ahmed, S.; Denison, S. *Bioorg. Med. Chem. Lett.* **1998**, *8*, 2615-2620.

(28) Ahmed, S.; Denison, S. *Bioorg. Med. Chem. Lett.* **1998**, *8*, 409-414.

6 Steroid 5α-R eductase Inhibitors

This chapter describes the synthesis and attempted synthesis of a series of potential SR inhibitors.

6.1 Tricyclic Inhibitors

A recent study by C. R. Smith *et al.*[1] reported the synthesis of tricyclic non-steroidal benzoquinolinone-type inhibitors of SR, incorporating various hydrophobic substituents at C8 of the parent compound (Table 5.8). The phenyl-acetylene-substituted compound, **5.59**, proved to be the best dual isozyme inhibitor (IC_{50} type 1 = 21 nM, type 2 = 52 nM), with the most potent isozyme-selective compound being the cis-styryl-substituted compound **5.60** (IC_{50}: type 1 = 6 nM, type 2 IC_{50} = 1400 nM).

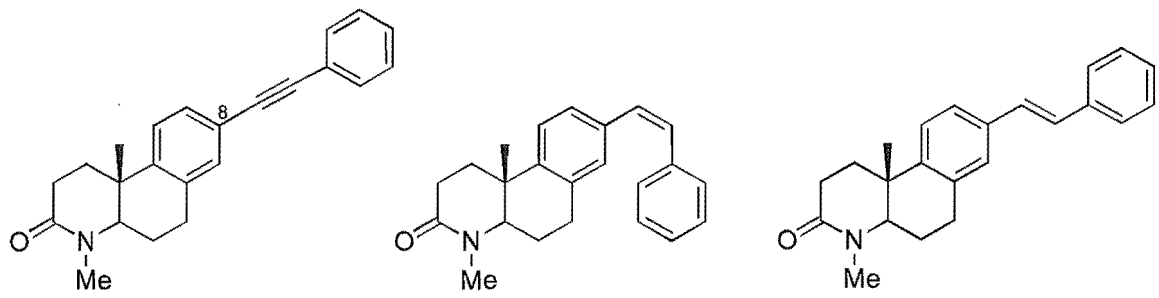

5.59 **5.60** **5.61**

Figure 6.1: Acetylene- and styryl-substituted benzoquinolinones.

We were interested by the potent type 1 selective inhibition, of the cis-styryl-substituted benzoquinolinone compound, **5.60**, relative to its trans isomer, **5.61**(IC_{50}: type 1 = 23 nM, type 2 = 180 nM, Figure 6.1). This result presented an opportunity to exploit the selective inhibition of each isomer and develop an isozyme-switchable inhibitor.

We postulate that the incorporation of a photoisomerisable-phenylazo substituent at the C8 position of a benzoquinolinone-type compound would effectively give access to both the cis and trans isomers within a single molecule. The sterically-favoured trans isomer potentially provides a dual inhibitor against type-1 and type-2 SR, while the cis conformation provides a potent, selective,

type-1 agent. The incorporation of a phenylazo group also provides a structural mimic to the hydrophobic styryl moiety, shown to give good activity.[1]

Given that the cis and trans isomers display such different activity and selectivity, we were interested in the concept of a single molecule that could be made to exhibit two different activities and selectivities through an easily applied photoisomerisation procedure. The phenylazo group effectively acts as a 'switch' by which the desired activity can be obtained. This type of switchability is a potentially useful tool, with possible applications in the design of other enzyme inhibitors.[2]

6.1.1 The Azo Substituent

We chose to incorporate the phenylazo substituent into the most basic benzoquinolinone structure to allow easy comparison against other inhibitors of the same class (Figure 6.2). Substitution of the azo moiety at the C8 position would enable direct comparison with the styrl-substituted benzoquinolinone inhibitors prepared by Smith *et al.*[1]

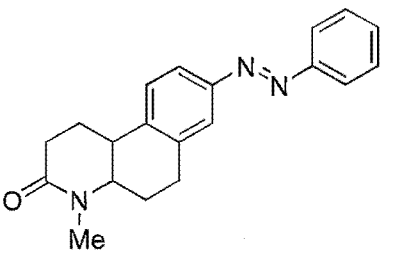

6.1

Figure 6.2: Target phenylazo compound.

The synthesis of an azo functionality can be achieved by a number of methods.[3,4] Common reactions involve oxidation of hydrazines or primary amines, or diazo coupling. Alternatively, condensation of a primary aromatic amine with nitrosobenzene will result in an azo compound. Except for the diazo coupling reaction, in which both nitrogen atoms are supplied by a diazo salt, these methods require the presence of a nitrogen-containing group at the C8 position of the benzoquinolinone skeleton to afford the desired target compound **6.1**.

The synthetic approach we selected for azo formation was a condensation reaction between nitrosobenzene and the appropriately substituted amino benzoquinolinone.

6.1.1.1 Retrosynthetic Analysis

Figure 6.3 shows a retrosynthetic analysis for the attempted routes to our target compound **6.1**. Synthesis of the C8-amino-substituted benzoquinolinone **6.2** was considered approachable from two directions. Route **A** involved preparation of the basic benzoquinolinone **6.3**, which could be nitrated, then reduced to afford the amine **6.2**. Alternatively, route **B** involved synthesis of the benzoquinolinone using an appropriately substituted starting material such as compound **6.4**.

As compound **6.4** is not commercially available, possible routes to this reagent were also considered (Figure 6.3). We proposed that nitration of β-tetralone followed by reduction could possibly afford compound **6.4**, or a Friedel-Crafts cyclisation using 4-amino phenylacetic acid (**6.5**) might give the desired compound.

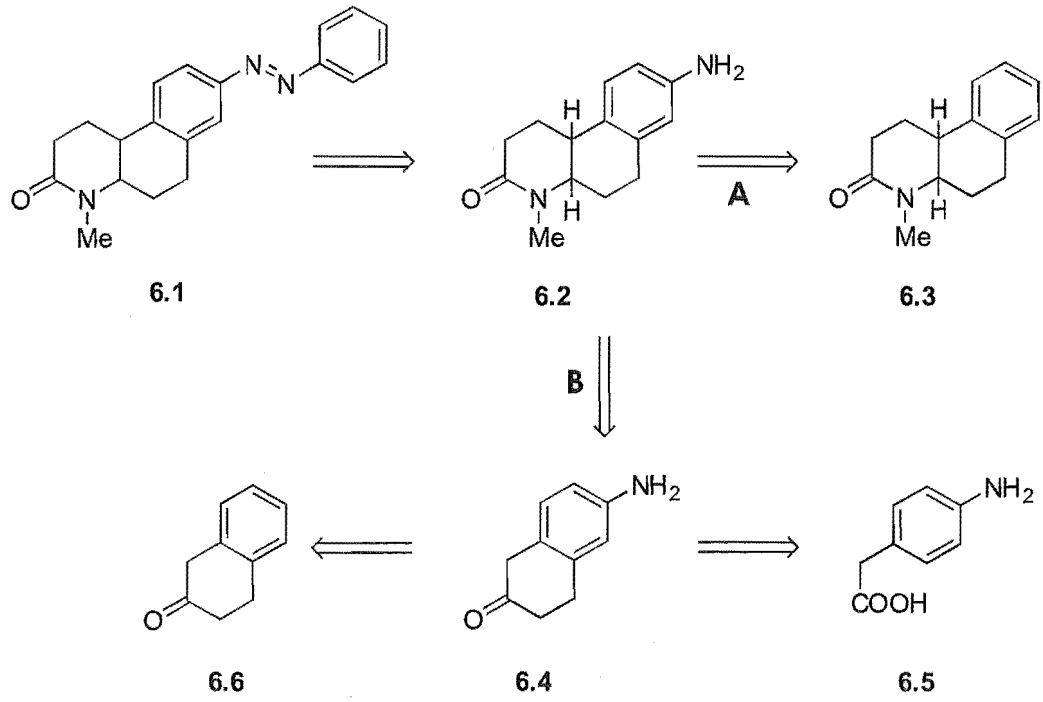

6.1 **6.2** **6.3** **6.4** **6.5** **6.6**

Figure 6.3: Synthetic approach to target compounds.

As a literature preparation of compound **6.3** was available, we decided to first attempt the synthesis of **6.2** using route **A**.

Synthesis of 4-Methyl-1,2,3,4,4a,5,6,10b-Octahydrobenzo[*f*]quinolin-3-one (6.3).

The benzoquinolinone **6.3** was synthesised as described by Jones *et al.*[5] (Scheme 6.1). β-Tetralone (**6.6**) and pyrrolidine were refluxed together in toluene for 4 hours. Removal of the solvent gave the enamine **6.7** in a 88% yield. Characterisation of the product by proton NMR revealed two four-proton resonances at δ 1.93 and 3.28 due to the pyrrolidine group, and a one-proton singlet at δ 5.14 ascribed to the olefinic proton of the enamine.

Reaction of **6.7** with acrylamide gave compound **6.8** in a 62% yield after recrystallisation. The proton-NMR spectrum of **6.8** relative to **6.7**, revealed an additional four-proton multiplet resonance at δ 2.69 due to the C1 and C2 protons. Loss of the pyrrolidine and olefinic resonances was also observed. Aza annulation reactions of this type are reported to give isomeric products,[6] but no attempt was made to isolate or quantify any minor products formed.

Reaction of **6.8** with NaH and iodomethane gave **6.9** in a 67% yield after recrystallisation. Methylation was confirmed by the presence of a singlet resonance at δ 3.14 in the proton-NMR spectrum.

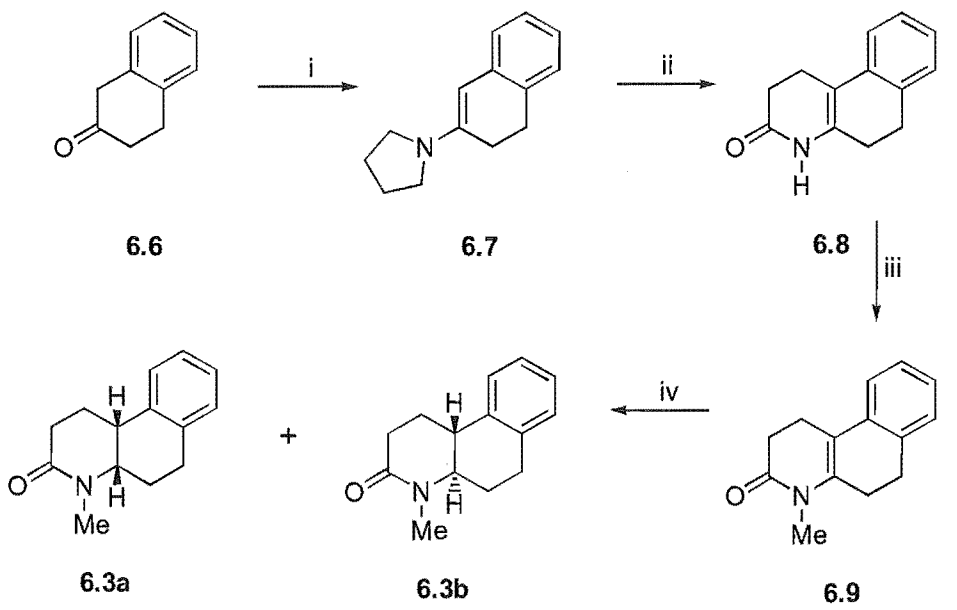

Scheme 6.1: (i) pyrrolidine, toluene reflux 4 hours; (ii) acrylamide, *p*-TSA heat 100°C 1 hour; (iii) NaH, glyme, MeI reflux 5 hours; (iv) triethylsilane, trifluroacetic acid, dichloromethane, stir 5 days.

Compound **6.9** was reacted with triethylsilane and TFA and stirred for five days. Workup gave **6.3** as a mixture of four stereoisomers: the (±) cis and (±) trans

compounds. The cis and trans products were separated by radial chromatography to give yields of 13% and 42% respectively.

The proton spectrum for each isomer contained two additional one-proton multiplets corresponding to reduction of the ring junction. Each isomer was identified by the characteristic chemical shift of the C4a and C10b hydrogens (Figure 6.4); the resonances due to the cis isomer (δ 3.55 and 3.15), shifted downfield relative to the trans (δ 3.14 and 2.72).[7] The mass spectrum contained the expected parent ion for each product.

Previous SAR studies on the benzoquinolinone inhibitors (section 5.2.2.2) have shown that the (±) **6.3** cis enantiomers give comparable inhibition results, as do the (±) trans enantiomers.[8] Because of this, and the inherent difficulty in separating (±) enantiomers, no attempt was made to separate the racemic cis or trans products. However, the trans geometry is slightly favoured over the cis for inhibitory activity against SR, as the increased planarity of the molecule more closely resembles that of the SR substrate.[5] The racemic trans isomer **6.3b** was therefore used in subsequent reactions.

We next turned our attention to the nitration of the benzoquinolinone **6.3b** and subsequent reactions in an attempt to synthesise the target compound **6.1**. It has been reported that nitration of **6.3** occurs predominantly at the C9 position rather than at C8.[9] However, we were interested to see if we could detect any of the desired C8-nitro compound.

Synthesis of 4-methyl-9-Phenylazo-1,2,3,4,4a,5,6,10b-Trans-octahydrobenzo[*f*]quinolin-3-one (6.12).

The nitration of **6.3b** to form **6.10** was carried out using a literature method[9] (Scheme 6.2). Compound **6.3b** was dissolved in a mixture of concentrated H_2SO_4 and acetic acid and cooled in an ice bath. HNO_3 was added slowly over 20 minutes and the resulting mixture was stirred for 2 hours. Workup gave the C9-substituted compound **6.10** as a yellow precipitate in a 41% yield.

A proton-NMR spectrum revealed a downfield shift in the aromatic resonances of **6.10** relative to **6.3**, from an unresolved multiplet at δ 7.14 to resonances at δ 8.15, 8.03 and 7.28, which is attributed to the presence of the nitro group. Analysis by mass spectrometry confirmed nitration had occurred by the detection of a molecular ion with a mass of 260 g/mol.

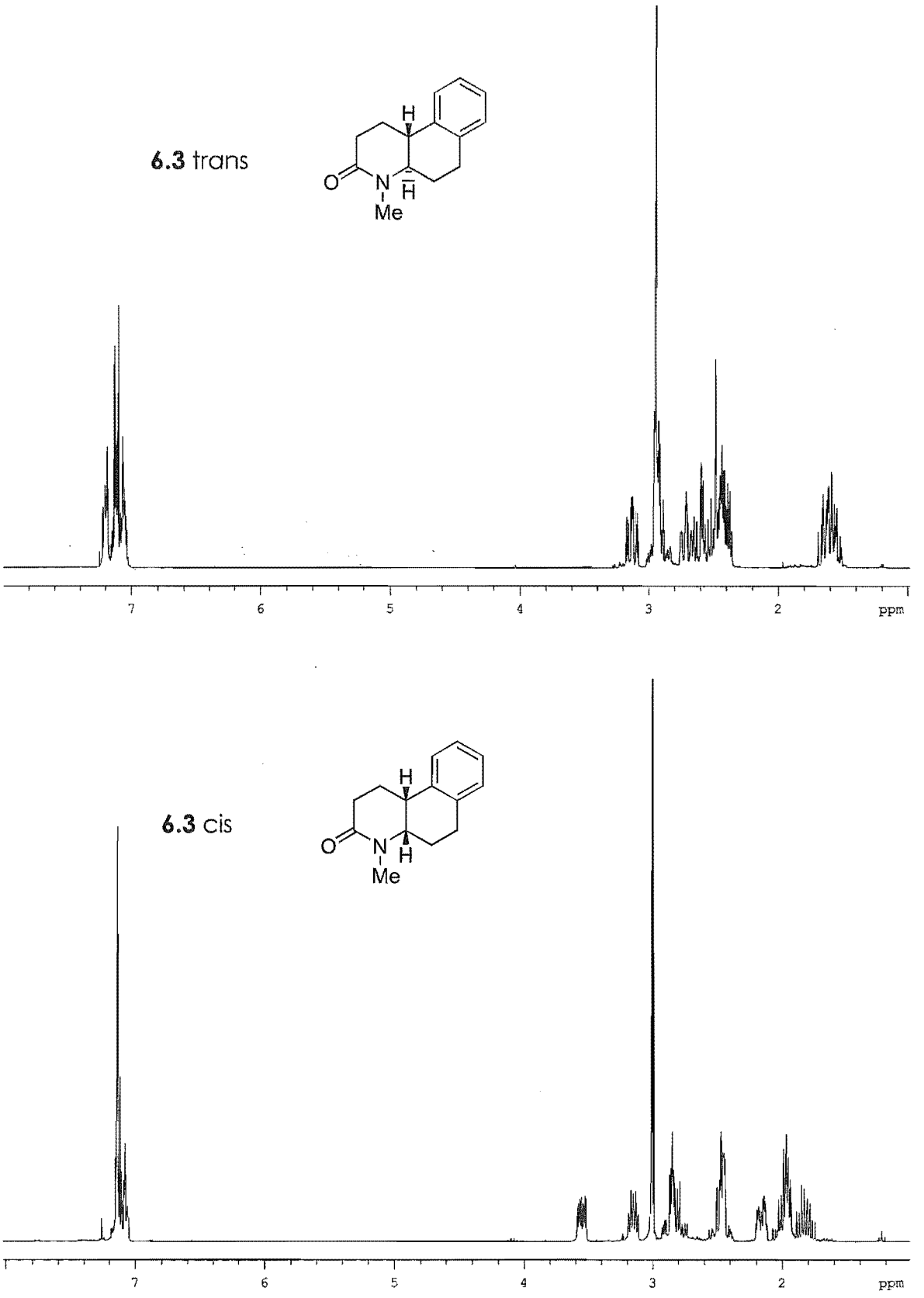

Figure 6.4: Proton-NMR spectra of the racemic cis and trans isomers of compound **6.3**.

The lack of a C8-nitro product may be due to the activating effects of the substituents on the C-ring in conjunction with inductive effects of the A-ring nitrogen, providing a more stabilised environment for the formation of the C9-substituted product.

Reduction of **6.10** to form **6.11** was achieved in a 39% yield as shown in Scheme 6.2. Compound **6.10** was dissolved in acetic acid and hydrogenated for three days. Workup and purification gave **6.11**.

Characterisation by proton-NMR spectroscopy revealed an upfield shift in the aromatic-proton resonances of **6.11** to δ 6.93, 6.62 and 6.56 relative to the chemical shifts of product **6.10**, indicating reduction had occurred.

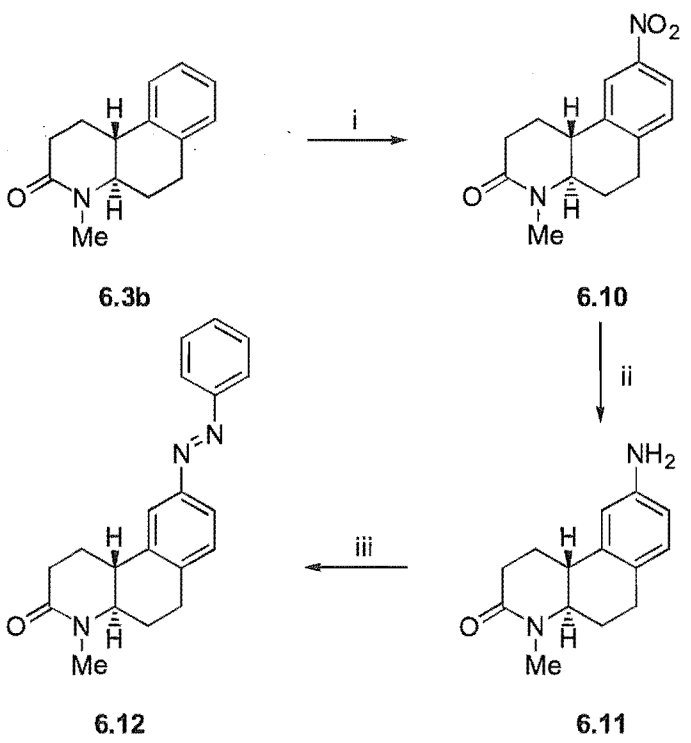

Scheme 6.2: (i) HNO_3, conc H_2SO_4 : acetic acid (1:1), stirred 2 hours; (ii) PtO_2, acetic acid, H_2, balloon, stirred 3 days; (iii) nitrosobenzene, acetic acid, stirred overnight.

Formation of the phenylazo group was achieved using a general procedure reported by Luckner *et al.*[10] The amine **6.11** and nitrosobenzene were stirred in acetic acid overnight as shown in Scheme 6.2. Workup and purification by column chromatography gave compound **6.12** as a yellow oil in a 88% yield. Characterisation by proton-NMR spectroscopy revealed resonances at δ 7.90 (three-proton), 7.77 (one-proton), 7.50 (three-proton) and 7.28 (one-proton)

corresponding to the incorporation of a trans-phenylazo group. Low-intensity resonances were also observed further upfield, (δ 7.36 – 6.69) corresponding to the cis isomer.[11] From the integral heights of the trans and cis isomers the fraction of cis present was determined to be 12%.

Irradiation of a sample of **6.12** in $CDCl_3$ for one hour at 330 – 370 nm, and subsequent NMR analysis, resulted in a mixture with 77% of the cis product, while further irradiation at wavelengths >400 nm for one hour gave a mixture with 85% of the trans product. These results are consistent with reported photostationary-equilibrium[2] ratios for azo isomers following irradiation.[12] No by-products due to photoisomerisation were detected in the NMR spectra.

As the major product of **6.3** nitration was the C9-substituted compound **6.10**, we were unable to synthesise our target compound **6.1** by route **A** and therefore turned our attention to route **B** (Figure 6.3). This involved the synthesis of the precursor **6.4**.

This synthesis was initially attempted using 4-amino phenylacetic acid as the starting material in a Friedel-Crafts cyclisation reaction to form the appropriately substituted tetralone (Figure 6.5).

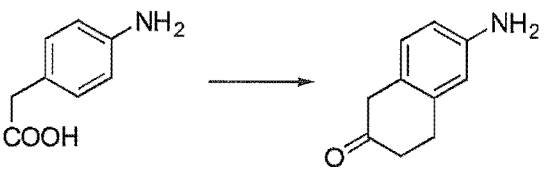

6.5 **6.4**

Figure 6.5: Desired Friedel-Crafts cyclisation.

Although Friedel-Crafts reactions involving aromatic molecules containing an activating substituent might be expected to form the desired tetralone, amines are *not* known to facilitate these reactions. This is due to their ability to coordinate the catalyst, thus removing it from the reaction mixture. Compounds containing an amine group are only known to undergo Friedel-Crafts alkylation reactions when the reagent is an olefin and the catalyst an aluminium anilide.[3,13] An additional problem with this type of cyclisation reaction is the requirement to form an acid chloride selectively at the carboxyl group, to allow chain extension by the introduction of an ethylene group, while leaving the amine unchanged.

We considered using 4-nitro phenylacetic acid as a starting material, but, Friedel-Crafts reactions, in which the aromatic ring contains deactivating substituents, such as NO_2, do not proceed well. Attempts by Burckhalter *et al.* to form a nitro containing tetralone using a Friedel-Crafts reaction had proved unsuccessful.[14]

We decided that protecting the amino group of 4-aminophenylacetic acid, to reduce its reactivity, before carrying out the cyclisation reaction, might be a viable approach. Amine protection has been extensively studied due to its applications in peptide synthesis.[15,16] We required a protecting group that would be stable under the reaction conditions, easily removed, and cause no interference with the reactions being carried out. With this in mind, we tried three different protections: benzyloxycarbonyl (Cbz), 9-fluorenylmethoxycarbonyl (Fmoc) and a phenylazo substituent (Figure 6.6).

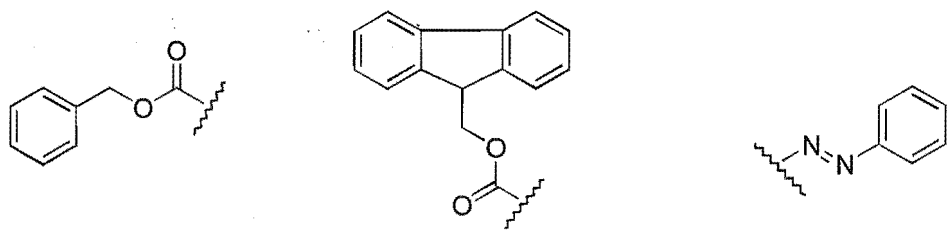

Figure 6.6: Protecting groups for 4-aminophenylacetic acid.

Synthesis and Reaction of 4-(Aminobenzocarbamate)-Phenylacetic Acid (6.13).

4-Aminophenylacetic acid (**6.5**) and benzylchloroformate were stirred together in an aqueous solution of $NaHCO_3$. Workup gave compound **6.13** as a white solid in a 90% yield. Characterisation by proton NMR revealed resonances at δ 7.37, 6.73 and 5.20 due to the carbamate group.

Compound **6.13** was then reacted with oxalyl chloride and DMF in acetonitrile at –20°C for 3 hours. Removal of the solvent by vacuum distillation gave a yellow oil that was stored overnight under vacuum. A proton-NMR spectrum of the oil gave a similar pattern of resonances to those of product **6.13.**

The next procedure required that the oil be dissolved in dichloromethane and reacted with $AlCl_3$ and ethylene gas at –76°C. However, the oil was only partially soluble in the solvent and reaction and workup resulted in a mixture of

products that were not identified. It is thought that the acid-labile Cbz group was hydrolysed from **6.13** during reaction to form the acid chloride.

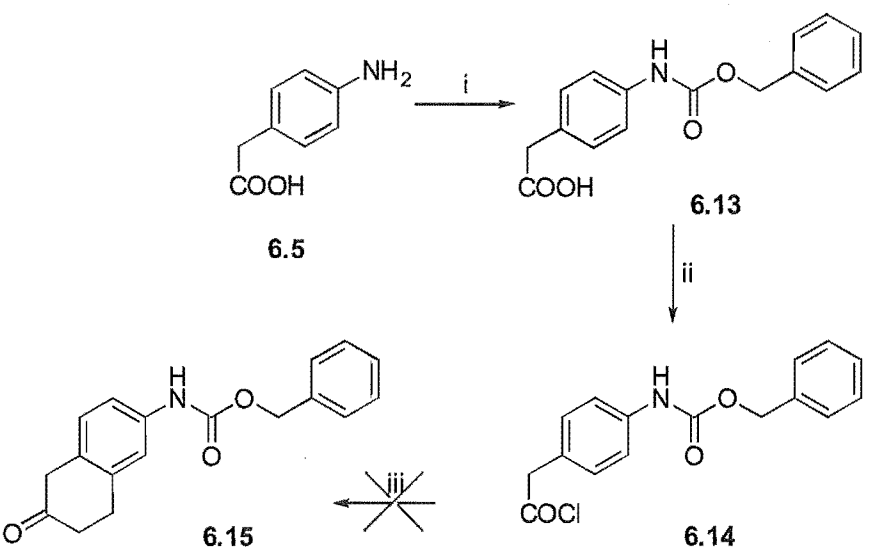

Scheme 6.3: (i) benzylchloroformate, $NaHCO_3$, water, stirred overnight; (ii) oxalyl chloride, DMF, acetonitrile, -20°C stirred 3 hours; (iii) $AlCl_3$, dichloromethane, ethylene –76°C , stirred overnight.

Synthesis and Reaction of 4-(Amino-(9-Fluromethylcarbamate)-Phenylacetic Acid (6.9)

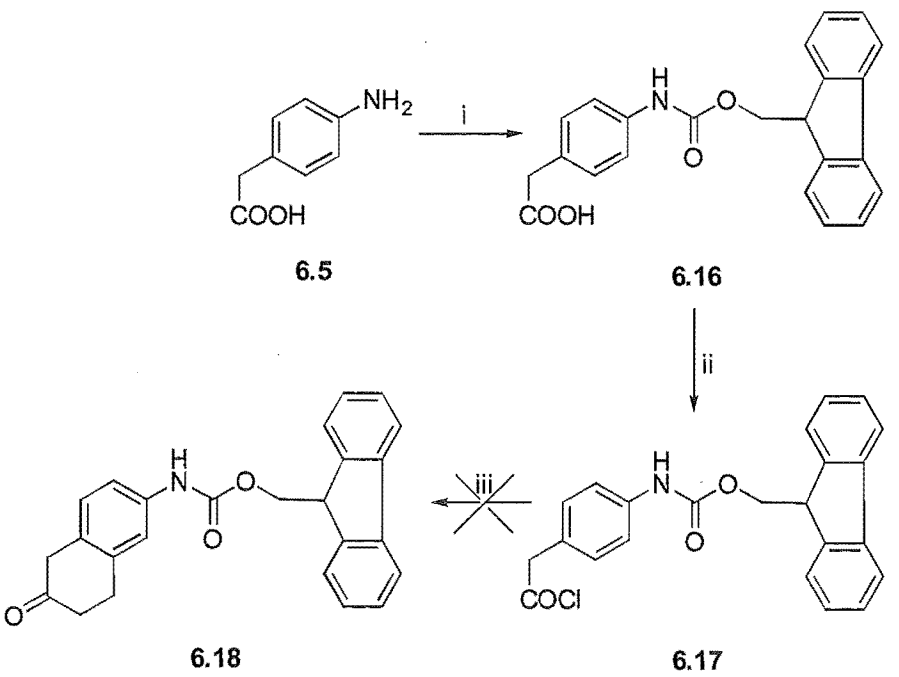

Scheme 6.4: (i) 9-fluoromethylchlorocarbamate, 10% Na_2CO_3, dioxane, stirred overnight; (ii) oxalyl chloride, DMF, toluene stirred overnight; (iii) $AlCl_3$, dichloromethane, ethylene –76°C , stirred overnight.

The Fmoc-protected 4-aminophenylacetic acid **6.16** was prepared by reacting 9-fluoromethylchlorocarbamate and 4-aminophenylacetic acid (**6.5**) with 10% aqueous Na_2CO_3 in dioxane overnight (Scheme 6.4). Reaction and subsequent workup gave **6.16** as a solid in a 73% yield. Characterisation by proton NMR revealed additional aromatic resonances between δ 7.54 – 6.91, a two-proton doublet at 4.23, and one-proton multiplet at 4.02 due to the Fmoc group.

Compound **6.16** was then reacted with oxalyl chloride and DMF in toluene overnight. Removal of the solvent by vacuum distillation gave **6.17**, a yellow solid, which was used immediately. Proton-NMR analysis of the acid chloride showed resonances similar to those seen in product **6.16**.

Compound **6.17** was dissolved in dichloromethane and added dropwise to a stirred mixture of $AlCl_3$ in dichloromethane at –76°C. Ethylene gas was bubbled though the mixture for an hour, before warming to room temperature and stirring overnight. Workup gave a yellow solid, however, proton-NMR analysis failed to show any new resonances corresponding to the desired cyclised product. This is thought to be due to both the deactivating effect of the protecting group and the ortho-, para-directing effects of this substituent (given the desired position of attachment was meta to the amine).

Synthesis and Reaction of Phenylazo Acetic Acid (6.19)

4-Aminophenylacetic acid (**6.5**) and nitrosobenzene were stirred together in acetic acid overnight (Scheme 6.5). Workup and purification by column chromatography gave compound **6.19** as an orange solid in a 83% yield. Proton-NMR spectroscopy revealed additional aromatic resonances at δ 7.90 (four-proton) and 7.39 (five-proton) corresponding to the phenylazo group.

Compound **6.19** was reacted with oxalyl chloride and DMF in acetonitrile for 3 hours. Removal of the solvent gave **6.20** as a dark-coloured residue that was used without purification. Compound **6.20** was reacted with $AlCl_3$ and ethylene in dichloromethane at –76°C (Scheme 6.5). Workup of the reaction mixture resulted in the formation of a brown insoluble precipitate that was not characterised. A red oil was also isolated from the reaction mixture, but analysis by proton-NMR

spectroscopy revealed none of the expected resonances for the desired cyclic product **6.21**.

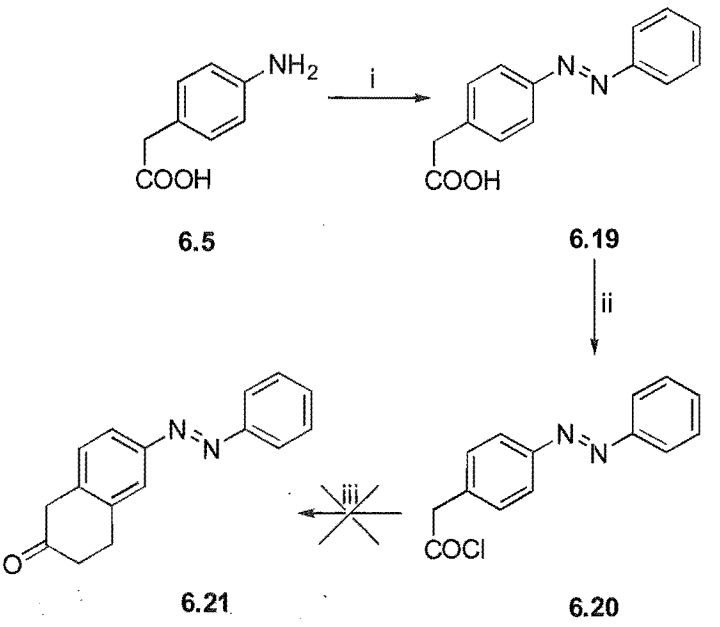

Scheme 6.5: (i) nitrosobenzene, acetic acid, stirred overnight; (ii) oxalylchloride, acetonitrile stirred 3 hours; (iii) $AlCl_3$, dichloromethane, ethylene –76°C , stirred overnight.

Synthesis of 7-Nitrotetralone (6.22) and 6-Nitrotetralone (6.23)

Given the difficulty in forming **6.4** *via* a Friedel–Crafts cyclisation, we attempted to directly nitrate β-tetralone.

The nitration of β-tetralone can conceivably occur in any of the positions, C5 – C8, due to the ortho-/para-directing effects of the alkyl substituents present on the aromatic ring.

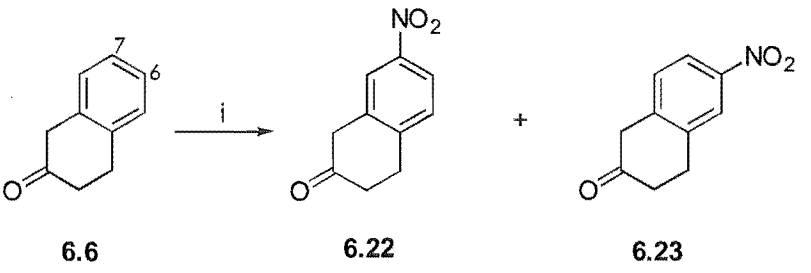

Scheme 6.6: (i) KNO_3, conc H_2SO_4, stirred 2 hours.

The conditions we employed for nitration of β-tetralone are shown in Scheme 6.6. β-Tetralone and KNO_3 were stirred together in concentrated

aqueous H_2SO_4 for 2 hours. Workup gave a mixture of **6.22** and **6.23** as a reddish oil with a total yield of 63%. The product was not purified further.

From the proton-NMR integrals the ratio of **6.23** to **6.22** was determined to be ~1:5. The spectrum of **6.22** had three new single-proton aromatic resonances relative to β-tetralone: a multiplet at δ 8.10, a singlet at 8.03 and a doublet at δ 7.42; the more downfield resonances (δ 8.10 and 8.03) indicative of aromatic protons directly adjacent to the nitro substituent. Compound **6.22** was established as the major isomer using an nOe experiment, which showed an interaction between the singlet proton resonance at δ 8.03 and the C1 protons at δ 3.69. This indicated that the resonance at δ 8.03 was the C8 proton and therefore, nitration in the major product had occurred at C7.

These NMR spectra were consistent with those of Pollack *et al.*[17] who reported that nitration of β-tetralone, using concentrated nitric acid, results in two products; C7 nitration in a 40% yield and C6 nitration in a 26% yield.

Synthesis and Reaction of 7-Nitro-2-(1-pyrrolidinyl)-3,4-Dihydronapthalene (6.24)

Although the nitration of β-tetralone did not yield large quantities of the desired C8-substitued isomer, the yield of product **6.22** was appreciable (52%). We therefore proposed that a route to compound **6.12**, using **6.22** (Scheme 6.7), might improve the final yield relative to the nitration of compound **6.3** as detailed above (Scheme 6.2).

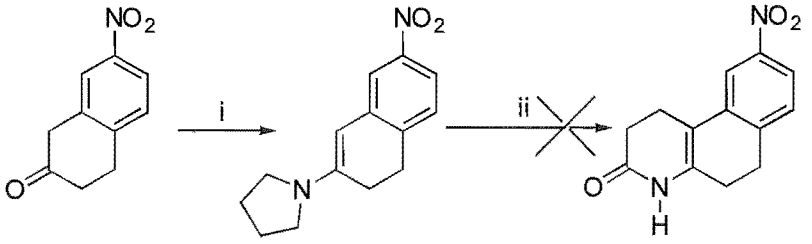

6.22 **6.24** **6.25**

Scheme 6.7: (i) pyrrolidine, toluene, reflux overnight; (ii) acrylamide, *p*-TSA, heat.

The impure **6.22** and pyrrolidine were refluxed in toluene (Scheme 6.7). Analysis of the crude mixture by proton-NMR spectroscopy revealed the presence of the enamine **6.24** in a mixture of unidentified products as indicated by two four-

proton resonances at δ 1.97 and 3.36 due to the pyrrolidine group, and a one-proton singlet at δ 5.20 due to the olefinic proton of the enamine.

Attempts to completely purify the compound using flash chromatography (20% ethyl acetate/petroleum ether) were unsuccessful. Therefore, the cleanest fraction was used in the subsequent reaction with acrylamide (Scheme 6.7) but failed to give the desired tricyclic product. This non-reaction can possibly be attributed to the deactivating effect of the nitro substituent, which reduces the nucleophilicity of the enamine, and prevents attack by the β-carbon centre of the enamine on the acrylamide.

Our attempts to prepare the C8-phenylazo substituted benzoquinolinone **6.1** by either of the routes outlined in Figure 6.3 were unsuccessful. Direct nitration of the benzoquinolinone compound gave predominantly the C9-substituted compound **6.10** in limited yield. We were, however, able to prepare the 9-phenylazo-benzoquinolinone compound **6.12** from this precursor. Synthesis using 4-amino phenylacetic acid also proved problematic. However, given our disappointing results for aza annulation of the 7-nitrotetralone **6.22**, successful cyclisation by a Friedel-Crafts reaction to give **6.4** may not have resulted in the desired tricyclic precursor of our target product **6.2**.

6.1.2 The Styryl Substituent

Abell *et al.*[18] reported a study on the synthesis of dual SR isozyme inhibitors incorporating features of the type-1-selective aryl acid tricyclic compounds, such as **5.73**, and the potent type-2 biphenyl-acid inhibitors, such as **5.81**, thought to be important for their activity and potency (Figure 6.7).

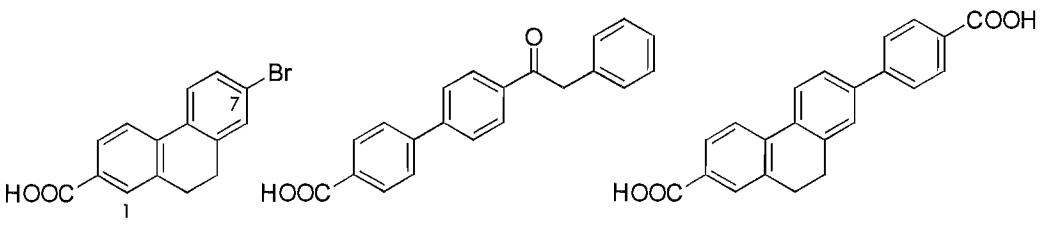

5.73 **5.81** **5.92**

Figure 6.7: Compound **5.92** incorporates structural features of both **5.73** and **5.81**.

Results of this study suggested that incorporation of hydrophobic groups onto the C7 position of aryl-acid inhibitors, improves their selectivity towards the type-2 isozyme, without significantly reducing the potency for the type-1 enzyme (Table 5.13).

Based on the positive effects of styryl substitution on the tricyclic benzoquinolinone inhibitors (Figure 6.1), we decided to investigate the possibility of improving the potency of aryl-acid tricyclic inhibitors against type-2 SR, by incorporating a styryl substituent at C7 (Figure 6.8). The results from the study by Abell *et al.* suggested that the potency of the parent tricyclic aryl-acid inhibitor toward type-1 SR should not be adversely affected, and a potent, dual inhibitor with increased activity towards type-2 SR might be expected from this modification.

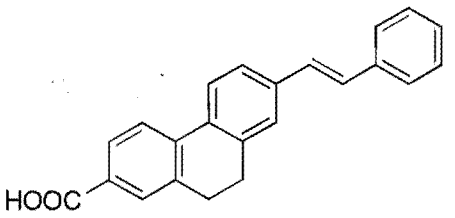

6.26

Figure 6.8: Target compound **6.26**.

The chemistry described by Smith *et al.*[1] for the preparation of the styryl-substituted benzoquinolinone derivatives utilised a palladium-catalysed coupling of styrene to the appropriately halo-substituted tricyclic compound. We chose to utilise this chemistry for the preparation of the styryl-substituted tricyclic aryl-acid inhibitor **6.26**, as is shown in Scheme 6.8.

Synthesis of 7-Styryl-9,10-Dihydrophenanthrene-2-Carboxylic Acid (6.26)

Styrene, compound **6.27**, $Pd(Ac)_2$, $(o\text{-tol})_3P$, Et_3N and MeCN, were reacted together in a sealed tube at 100°C for 24 hours. Workup afforded a white powder, a solution of which, gave purple luminescence in daylight, indicating the presence of a highly conjugated system. Hydrolysis of the methyl ester to give **6.26** was achieved by refluxing **6.28** in methanolic KOH.

Characterisation by NMR spectroscopy revealed appropriate additional resonances for the formation of the styryl substituent. Mass spectrometry gave a

molecular ion with a mass of 340, which is consistent with the incorporation of a styryl group.

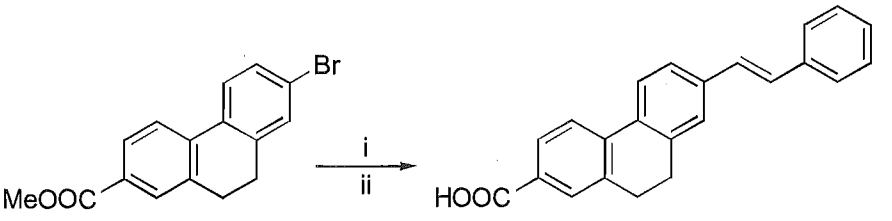

6.27 **6.26**

Scheme 6.8:(i) styrene, $Pd(OAc)_2$, $(o\text{-}tol)_3P$, Et_3N, acetonitrile, 100°C 24 hours; (ii) K_2CO_3, methanol: water (10:1), refluxed 18 hours.

6.2 Bicyclic Inhibitors

The carboxylic acid series of non-steroidal inhibitors (section 5.2.2.5), which are based on the potent steroidal type-2 inhibitor epristeride (**5.33**), includes tricyclic analogues such as **5.73** in which the steroid D-ring has been removed, and more recently, biphenyl structures such as **5.81** in which the B-ring is also deleted. While the tricyclic aryl acids have been shown to be potent type-1 inhibitors, the bicyclic compounds, like the parent steroid structures, are more active against type-2 SR (Figure 6.9).

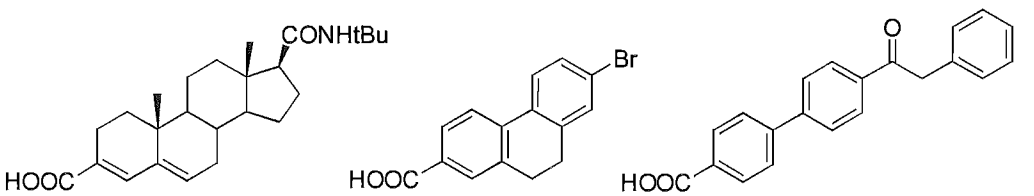

epristeride — $K_{I,app}$ type 2 = 0.2 nM

5.73 — $K_{I,app}$ type 1 = 26 nM

5.81 — $K_{I,app}$ type 2 = 60 nM

Figure 6.9: Steroid, tricyclic and biphenyl SR inhibitors incorporating a carboxylic acid enolate mimic.

Similarly, the tricyclic benzoquinolinone compounds, which are analogues of the potent 4-aza-steroiodal inhibitors, have also been shown to be potent SR inhibitors. However, related 4-aza compounds, in which the B-ring has also been deleted (**6.29**), have not been investigated with regard to their inhibitory activity against SR (Figure 6.10).

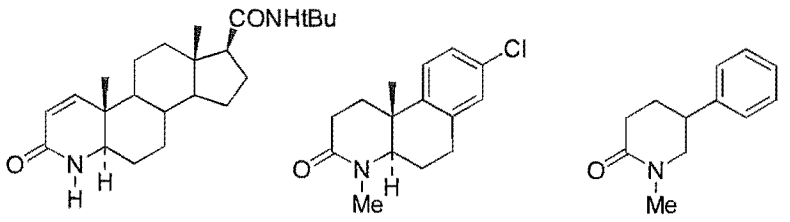

Figure 6.10: 4-aza series of SR inhibitors

While the preparation of potential inhibitors such as **6.29** is useful for comparison against the steroidal and tricyclic compounds of the 4-aza series of inhibitors, these bicyclic lactam-based inhibitors might also be considered to represent analogues of the potent type-2 benzophenone inhibitors exemplified by **5.81** (Figure 6.11). This analogy allows a comparison to be made of the efficacy and effectiveness of the neutral lactam enolate mimic of compound **6.29**, versus the charged carboxyl species utilised in the benzophenone class of inhibitor.

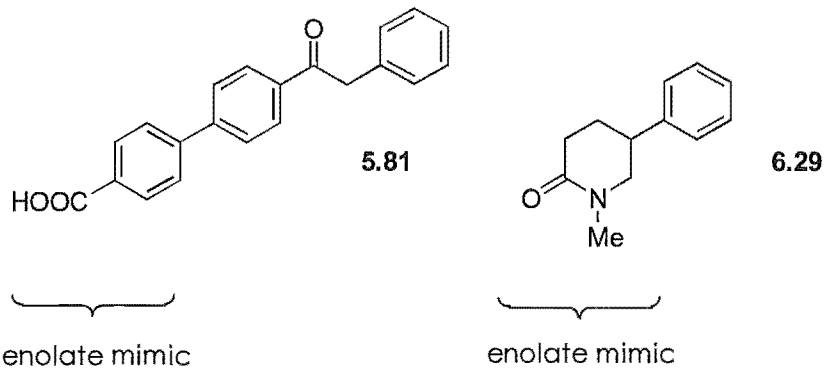

Figure 6.11: 4-aza and 3-carboxylate biphenyl inhibitors.

6.2.1 Target Molecules

We decided to prepare the basic piperidone compound **6.29** and derivatives containing substituents that have been shown to enhance inhibitor potency in the benzoquinolinone tricyclic series of inhibitors (section 5.2.2.2). Our target molecules are shown in Figure 6.12.

The piperidone **6.30**, the 1-methyl-piperidone **6.29** and the 5-(4-chlorophenyl)-1-methyl-2-piperidone **6.31** allow direct comparison of activity and selectivity against the tricyclic benzoquinolinone inhibitors. Due to the reported potency of tricyclic inhibitors containing hydrophobic groups, it was envisioned

that the incorporation of a similar substituent into compound **6.29** would result in potent SR inhibitors. Therefore, we decided to also prepare compound **6.33** incorporating a styryl moiety, and compound **6.32**, containing a photoisomerisable phenylazo group, using synthetic methods previously described in section 6.1. The styryl moiety, in which the predominant isomer is trans, provides a control for the phenylazo-substituted compound against which both cis and trans isomers may be compared. Preparation of **6.32** and **6.33** also allows a measure of any effects, which may result due to the nitrogen double bond, compared with the carbon double bond.

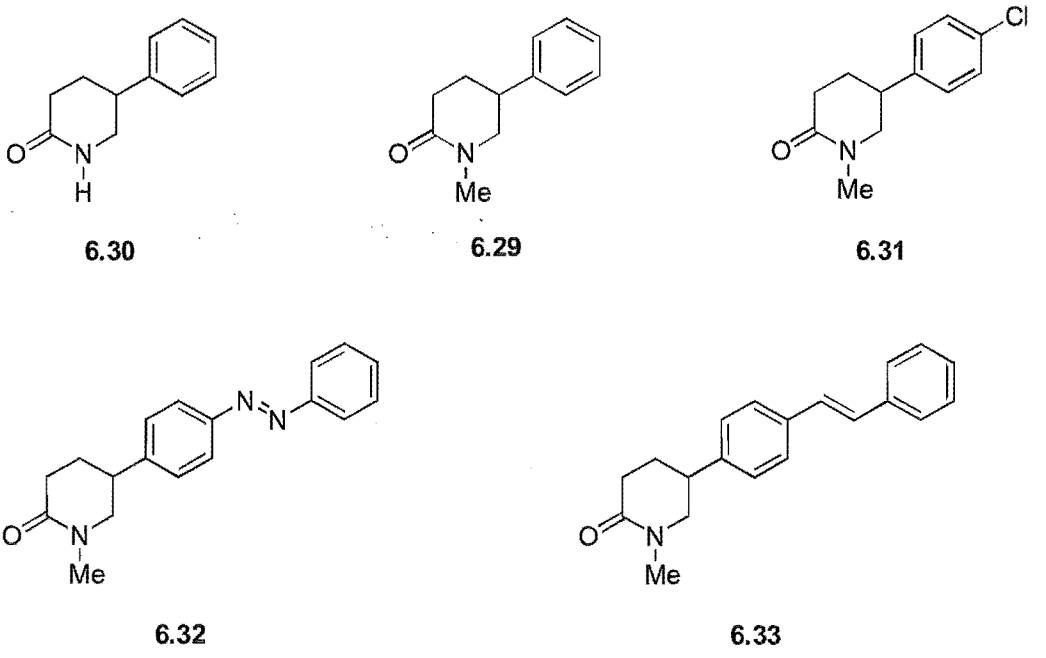

6.30 **6.29** **6.31**

6.32 **6.33**

Figure 6.12: Target bicyclic lactam compounds.

Preparation of the target compound **6.32**, using previously described methods (section 6.1.1), required a *p*-amino substituent on the phenyl ring of the basic piperidone structure. We considered two approaches to achieve this. The first involved the use of p-nitrobenzyl cyanide as the starting material. Alternatively, the unsubstituted methyl piperidone could be nitrated and subsequently reduced to the amine (Figure 6.13).

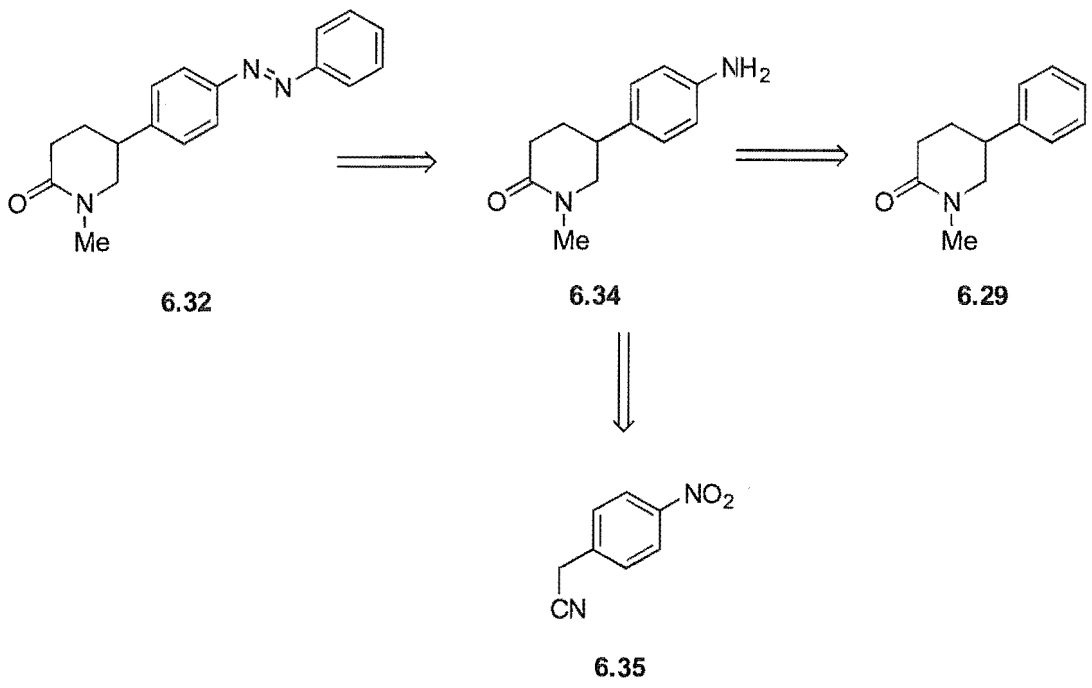

6.32 6.34 6.29

6.35

Figure 6.13: Synthetic approaches to phenylazo piperidone **6.32**.

Synthesis of the styryl-substituted compound **6.33** using previously discussed methods (section 6.1.2), required a *p*-bromo-substituted piperidone. Two alternative routes to this compound were considered. The first involved use of the *p*-bromobenzyl-cyanide starting material, while the second utilised a Sandmyer-type reaction (Figure 6.14).

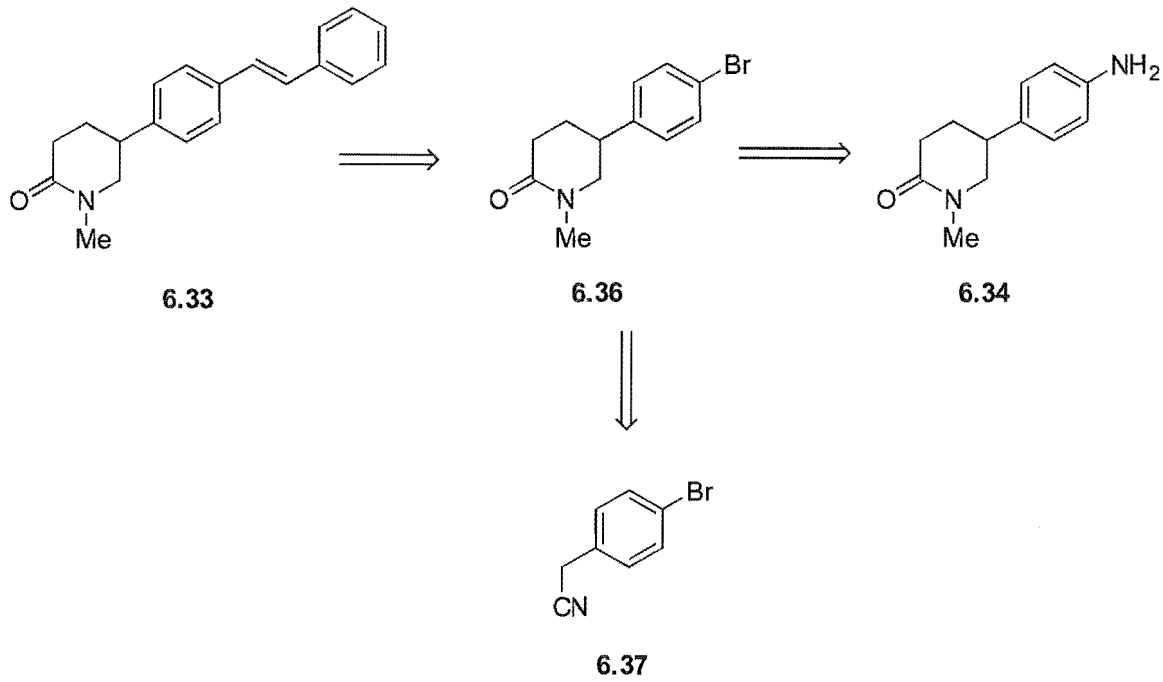

6.33 6.36 6.34

6.37

Figure 6.14: Synthetic approaches to styrl piperidones 6.33.

6.2.2 PIPERIDONES

All the target compounds were successfully prepared for this series of bicyclic inhibitors.

Synthesis of 5-Phenyl-1-Methyl-2-Piperidone (6.29)

The preparation of the basic bicyclic lactam compound **6.29** was by a known literature procedure[19,20] (Scheme 6.9). To a stirred mixture of benzyl cyanide, hydroquinone, and Triton B at 140°C was added methyl acrylate. Workup and purification by vacuum distillation gave compound **6.39a** in a 17% yield.

Characterisation by proton-NMR spectroscopy revealed two two-proton resonances at δ 2.21 and 2.49 due to the acrylate, and a change in the coupling pattern of the C4 proton, relative to **6.38a**, from a singlet to a multiplet. An infrared spectrum contained an absorption band at 1735 cm^{-1} corresponding to the carbonyl group, and a band at 2259 cm^{-1} due to the cyano group. Mass spectrometry revealed the expected molecular ion, further confirming that coupling had occurred.

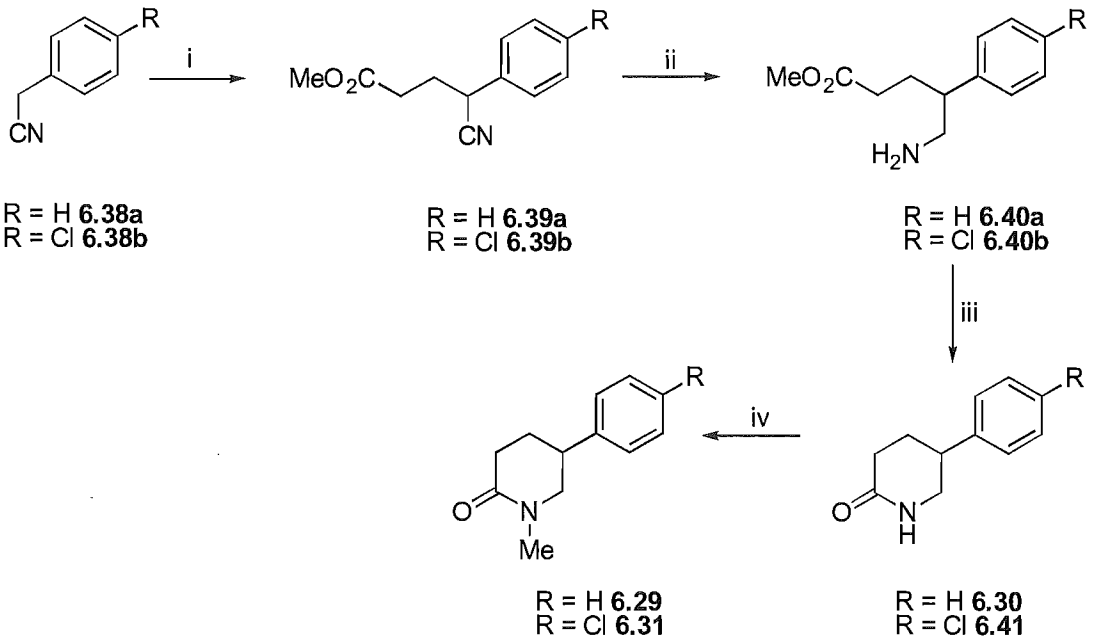

R = H **6.38a**
R = Cl **6.38b**

R = H **6.39a**
R = Cl **6.39b**

R = H **6.40a**
R = Cl **6.40b**

R = H **6.29**
R = Cl **6.31**

R = H **6.30**
R = Cl **6.41**

Scheme 6.9:(i) methyl acrylate, Triton B, hydroquinone; (ii) PtO_2, glacial acetic acid, H_2, 40 psi, 3 days; (iii) xylene or toluene, reflux, 20 hours; (iv) NaH, glyme, MeI, reflux 5 hours.

6.39a was then dissolved in acetic acid and hydrogenated at 40 psi for 3 days. Workup and solvent evaporation gave compound **6.40a**. Reflux of **6.40a** in toluene, followed by solvent evaporation gave the cyclised product **6.30** in a 61% yield. Characterisation by proton-NMR showed an absence of the methoxy resonance and the appearance of a broad singlet at δ 6.18 attributed to the amide.

Methylation of **6.30** was achieved by deprotonation with NaH followed by addition of iodomethane to give **6.29** in a 87% yield. The proton-NMR spectrum contained a resonance at δ 2.97 indicating methylation had occurred.

An equivalent series of reactions were carried out to form the 5-(4-chlorophenyl)-1-methyl-2-piperidone compound **6.31**.

Synthesis of 5-(4-Chlorophenyl)-1-Methyl-2-Piperidone (6.31)

To a mixture of *p*-chlorobenzyl cyanide (**6.38b**), hydroquinone and Triton B at 140°C was added methyl acrylate. Workup and purification by vacuum distillation gave compound **6.39b** in a 24% yield. Characterisation by proton-NMR spectroscopy revealed a three-proton singlet at δ 3.70, two two-proton resonances at δ 2.20 and 2.51 due to the acrylate, and a change in the coupling pattern of the C4 proton from a singlet to a multiplet. Mass spectrometry revealed the expected parent ion confirming that coupling had occurred.

6.39b was dissolved in acetic acid and hydrogenated at 40 psi for 1 day. Filtration to remove the PtO_2 catalyst and solvent evaporation gave compound **6.40b**. Reflux of **6.40b** in xylene afforded a white precipitate that was collected by filtration to give the cyclised product **6.41** in a 46% yield. Characterisation by proton-NMR spectroscopy revealed two new resonances at δ 3.49 and 3.35, relative to **6.39b**, corresponding to the reduction of the cyano group, a loss of the methoxy resonance, and the appearance of a broad singlet at δ 6.09 attributed to the amide.

Methylation of **6.41** was achieved by reaction with NaH and MeI to give **6.31** in a 59% yield. The proton-NMR spectrum contained a resonance at δ 2.98 indicating methylation had occurred.

Synthesis of 5-(4-Aminophenyl)-Piperidone (6.44)

Reaction of nitrobenzyl cyanide (**6.35**) with methyl acrylate at reflux gave the desired nitrophenyl butyrate **6.42** as a red oil in a 13% yield, following repeat extractions with cold ether and vacuum distillation to remove the unreacted cyanide starting material. A proton-NMR spectrum of **6.42** contained a three-proton singlet at δ 3.71, two two-proton multiplets at δ 2.55 and 2.24 due to the coupled acrylate, and a change in the coupling pattern of the C4 proton from a singlet to a multiplet.

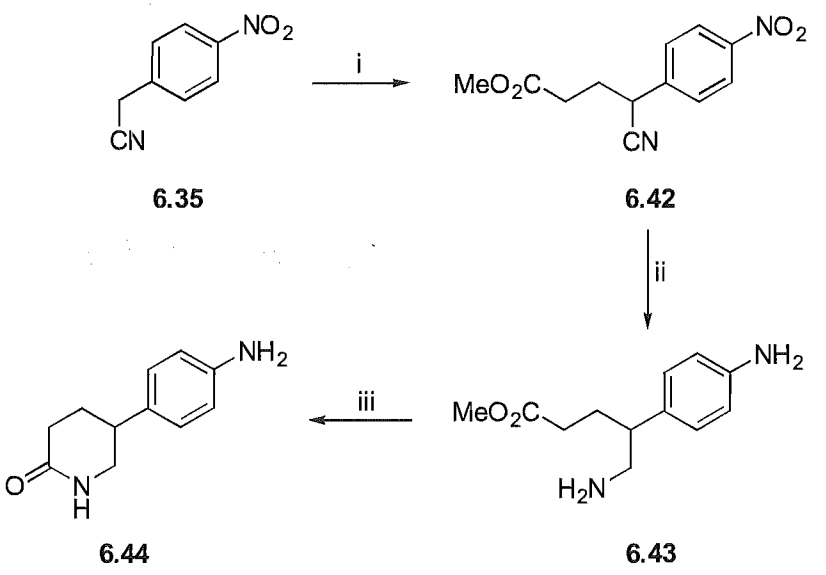

Scheme 6.10:(i) methyl acrylate, Triton B, hydroquinone; (ii) PtO_2, glacial acetic acid, H_2, 40 psi, 3 days; (iii) toluene, reflux, 20 hours.

Compound **6.42** was then dissolved in acetic acid and hydrogenated at 40 psi for 3 days. Workup gave compound **6.43**, which unfortunately underwent polymerisation to give a gel like substance that was quite insoluble in most solvents. However, a small sample was able to be dissolved in excess toluene and reacted at reflux overnight. Analysis by NMR spectroscopy revealed resonances indicative of the cyclised product **6.44**, but, this product was unable to be successfully purified.

Synthesis of 5-(p-Phenylazobenzyl)-1-Methyl-2-Piperidone (6.32)

Due to the difficulty we experienced in obtaining a clean sample of compound **6.44**, the alternative synthetic route to 5-(4-aminophenyl)-1-methyl-2-

piperidone (Figure 6.13) involving direct nitration of 5-phenyl-4-methyl–2-piperidone (**6.29**) was attempted.

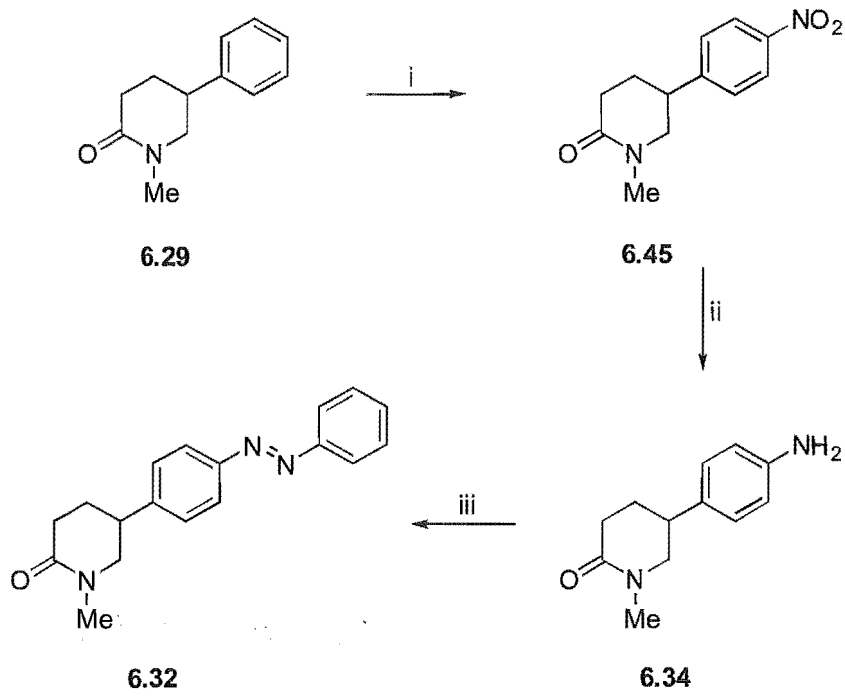

Scheme 6.11:(i) KNO_3, conc H_2SO_4, stirred 2 hours; (ii) PtO_2, glacial acetic acid, H_2, 3 days; (iii) nitrosobenzene, acetic acid, stirred overnight.

Compound **6.29** and KNO_3 dissolved in concentrated aqueous H_2SO_4 were stirred for 2 hours. Workup and purification by column chromatography gave **6.45** as a yellow oil in a 49% yield. Characterisation by proton-NMR spectroscopy revealed two two-proton doublets at δ 8.21 and 7.43. This resonance pattern is characteristic of symmetric para-substitution on the phenyl ring. Analysis by mass spectrometry revealed a molecular ion of mass 234 g/mol corresponding to the presence of a nitro group.

Hydrogenation of **6.45** giving the amino product **6.34** was achieved using PtO_2 and 40 psi of H_2. Workup and purification by radial chromatography gave **6.34** as an oil in a 51% yield. Reduction of the nitro substituent was indicated by an upfield shift of the aromatic-proton resonances, to δ 7.02 and 6.66, relative to compound **6.45**.

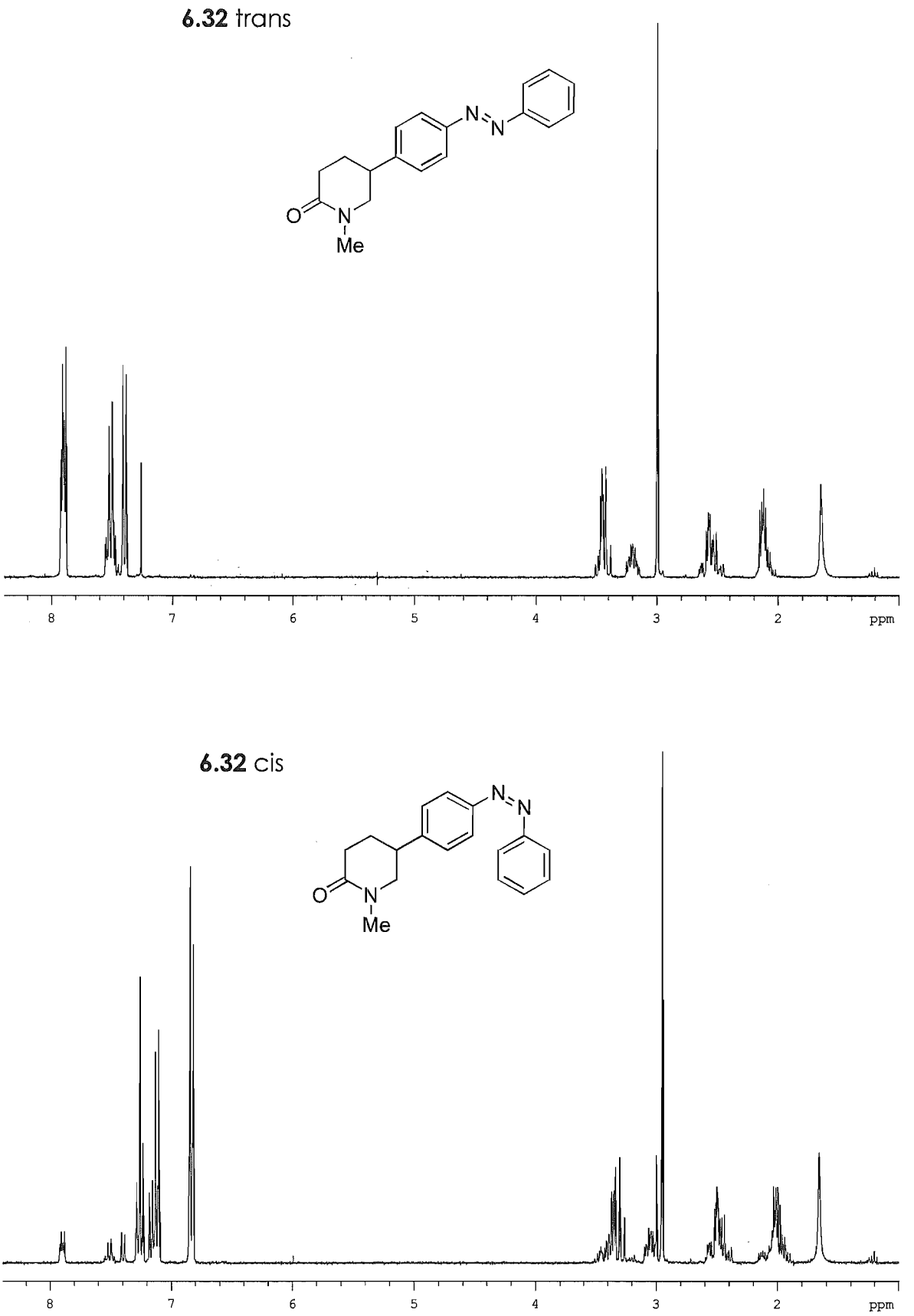

Figure 6.15: Product 6.32 (trans) before irradiation and product 6.32 (cis) following irradiation at 330 – 370 nm for 1 hour.

Compound **6.34** and nitrosobenzene were then dissolved in acetic acid and the solution stirred at room temperature overnight. Workup and purification by column chromatography gave **6.32** as an orange solid in a 62% yield. Proton-NMR analysis reveal two isomers in the ration of 1: 5.7 as determined by inspection of the respective integrals. The main isomer had resonances at δ 7.89, 7.50 and 7.37, due to the phenylazo group, that corresponded with a trans geometry.[11] Mass spectrometry revealed the expected parent ion.

Irradiation of **6.32** in $CDCl_3$ for one hour at 330 – 370 nm resulted in a mixture with 87% of the cis product, as determined by proton-NMR analysis (Figure 6.15). Further irradiation at wavelengths > 400 nm for one hour resulted in a reversion such that a mixture containing 83% trans was obtained. These results are consistent with reported photostationary-equilibrium ratios for azo isomers following irradiation.[12] No by-products due to photoisomerisation were detected in the NMR spectra.

Synthesis of 5-(Stilbenyl)-1-Methyl-2-Piperidone (6.33)

The preparation of amino piperidone **6.34** provided a useful starting material for the synthesis of the styryl-substituted methyl piperidone **6.33** *via* a Sandmyer reaction (Figure 6.14)

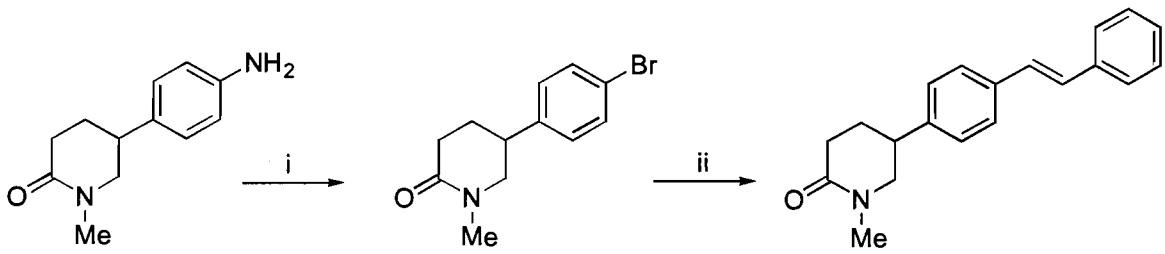

6.34 **6.36** **6.33**

Scheme 6.12:(i) $CuBr_2$, *t*-butylnitrite, acetonitrile, stirred 3 hours; (ii) styrene, $Pd(OAc)_2$, $(o\text{-tol})_3P$, Et_3N, acetonitrile, 100°C 24 hours.

The bromo piperidone **6.36** was prepared using a general method described by Doyle *et al.*[21] (Scheme 6.12). Compound **6.34** was stirred in acetonitrile, together with $CuBr_2$ and *t*-butylnitrite then quenched with 2 M HCl. Workup and purification by radial chromatography gave **6.36** as an oil in a 13% yield.

Characterisation by proton-NMR spectroscopy revealed a downfield shift in the aromatic resonances, relative to **6.34**, from δ 7.02 and 6.66 to 7.46 and 7.12 respectively. The detection of molecular ions with mass 269 and 267 in the mass spectrum confirmed the presence of a bromo substituent.

Given the relative ease with which compound **6.36** was prepared from **6.34**, no attempt was made to prepared the bromo piperidone compound using *p*-bromobenzyl cyanide.

Styrene, 5-(4-bromophenyl)-1methyl-2-piperidone (**6.36**), $Pd(Ac)_2$, $(o\text{-}tol)_3P$, Et_3N and MeCN, were reacted together in a sealed tube at 100°C for 24 hours. Workup and purification using plc gave **6.33** as a white solid in a 68% yield. Characterisation by NMR spectroscopy showed resonances due to a styryl substituent, and the detection of a molecular ion with a mass of 291 was also consistent with the attachment of a styryl moiety.

6.3 Enolate Mimics

In all the inhibitors of SR surveyed, one feature is considered essential to ensure inhibitory activity: a functionality that acts as a mimic for the proposed enolate intermediate formed during the reduction of T to DHT (see section 5.2). A variety of different functionalities have been used to achieve this, including lactams, acrylates, dienes and aryl acids, enones, ketoenamines and enols (see section 5.2.1 for a discussion). A necessary property of all these functionalities is the ability to bind an electrophilic residue in the active site postulated to stabilise the negatively-charged enolate intermediate.

One possible enolate mimic that is, as yet, unreported is a thiolactam. We postulated that this functionality would mimic the proposed enolate *via* a resonance structure that is similar those proposed for lactams (Figure 6.16). The large sulfur atom may provide enhanced binding to the proposed electrophilic residue in the active site and thus increase the potency of inhibitors that contain this group.

Figure 6.16: Postulated mechanisms of thiolactam enolate mimic.

Apart from any medical benefits that might be gained by the preparation of these mimics, they also provide SAR information, which gives insight into the active site of the enzyme. To this end we decided to prepare compounds **6.46**, **6.47**, **6.48** and **6.49** (Figure 6.17). The simple structure of compound **6.47** provides a control against which the activity of the other derivatives can be compared.

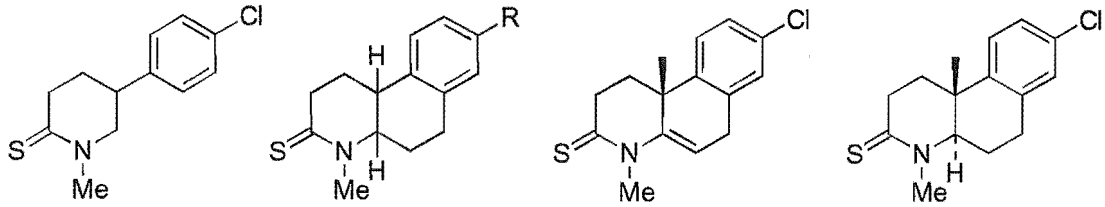

6.46 **6.47** **6.48** **6.49**

Figure 6.17: Target thiolactams.

The conversion of a lactam functionality into a thiolactam is readily achieved by reaction with Lawesson's reagent.[22] A positive result in terms of inhibition activity and isozyme selectivity of the thiolactam enolate mimic, means that any previously reported lactam-based inhibitor, whether steroidal or non-steroid-based, can theoretically be converted into the corresponding thiolactam. This simple procedure is therefore, a potentially powerful source of novel SR inhibitors.

6.3.1 Thiolactams

Preparation of all the target thiolactam derivatives was achieved, however, the ease with which the transformation to a thiolactam occurred seemed to have some dependence on the starting compound.

Synthesis of Thiolactams

The preparation of compounds **6.46**, **6.47**, **6.48** and **6.49** was *via* a general method described by Lawesson *et al.*[22] as detailed below.

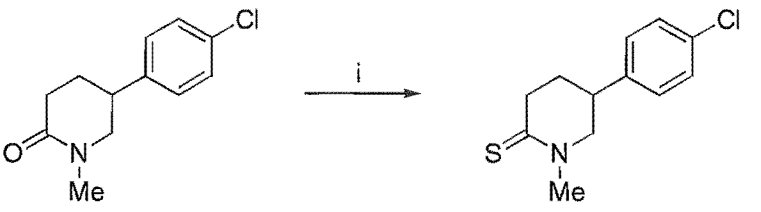

6.31 **6.46**

Scheme 6.13:(i) Lawesson's reagent, THF, stir 15 minutes.

Lactam **6.31**, dissolved in dry THF was stirred with Lawessons reagent for 15 minutes. Filtration and removal of the solvent gave compound **6.46** in a 87% yield after recrystallisation. Characterisation by NMR revealed a downfield shift for most resonances relative to **6.31**. Most notable was a C1 shift of the NMe singlet to δ 3.49 from 2.98. Analysis by mass spectrometry resulted in the detection of the expected parent ion.

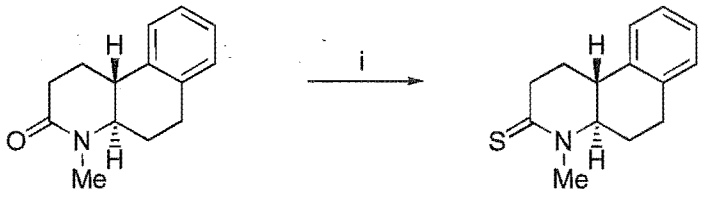

6.3 **6.47**

Scheme 6.14:(i) Lawesson's reagent, THF, stir 30 minutes.

Lactam **6.3,** dissolved in dry THF was stirred with Lawesson's reagent for 30 minutes. Workup and purification using radial chromatography gave compound **6.47** in a 45% yield. Characterisation by NMR showed a downfield shift for most resonances relative to **6.3**. Most notable was a downfield shift from δ 2.95 to 3.54 for the NMe singlet resonance. Mass spectrometry confirmed the transformation to the thiol group with the detection of the expected parent ion.

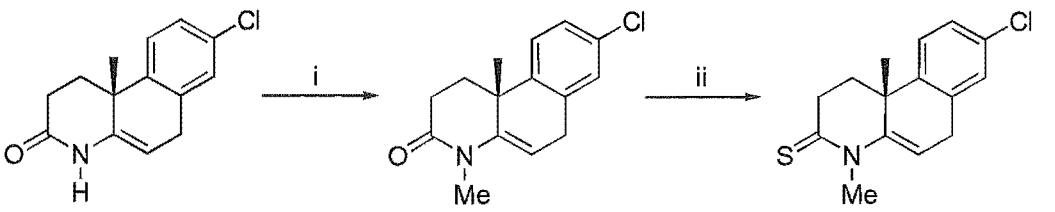

6.50 **6.51** **6.48**

Scheme 6.15:(i) NaH, glyme, MeI, reflux 5 hours; (ii) Lawessons reagent, THF, reflux 6 hours.

Reaction of compound **6.50** With NaH and iodomethane gave the methylated compound **6.51** in a 82% yield. Characterisation by proton-NMR spectroscopy revealed an addition resonance, relative to **6.50**, at δ 3.19, corresponding to the incorporation of a methyl group.

Lactam **6.51**, dissolved in dry THF was stirred with Lawessons reagent for 6 hours at reflux. Workup and purification using radial chromotogaphy gave **6.48** in a 58% yield. Characterisation by NMR showed the characteristic downfield shift for most resonances relative to the starting product. Most notable were: the resonances for the C5 proton moving from δ 5.29 to 5.70, the C2-proton resonances moving from δ 2.70 to 3.23 and the NMe singlet resonance moving downfield to δ 3.81 from 3.19.

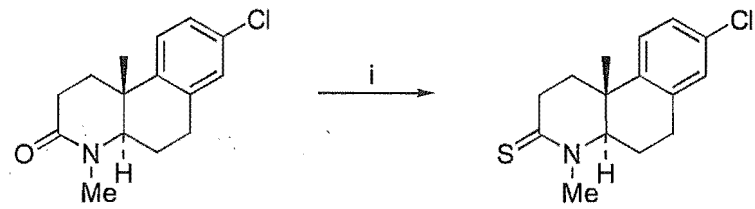

6.52 **6.49**

Scheme 6.16:(i) Lawessons reagent, THF, stir 60°C overnight.

Compound **6.52**, dissolved in dry THF was stirred with Lawesson's reagent overnight at 60°C. Workup and purification using radial chromatography gave compound **6.49** in a 54% yield. Characterisation by proton-NMR spectroscopy revealed a downfield shift for the C4a resonance, relative to **6.52**, from 3.49 to 3.72 and a shift for the NMe singlet resonance downfield to δ 3.57 from 3.03.

6.4 SUMMARY

Twelve potential SR inhibitors have been synthesised. Compound **6.12** contains a photoisomerisable phenylazo group that is envisioned to provide dual-isozyme-selective properties to the known base benzoquinolinone-type inhibitor. Although the position of azo substitution at C9 will not allow direct comparison with the styryl-substituted inhibitors prepared by Smith *et al.*(see section 6.1), the activity of this compound will hopefully provide information regarding the suitability of substitution in this location. Given the postulated large binding area in the SR enzyme for substituents bound in this location of the substrate, this

compound is expected to possess good activity. In compound **6.26** the incorporation of a styryl moiety is hoped to improve the potency and selectivity of the aryl-acid class of tricyclic inhibitor.

The piperidone compounds have been prepared as bicyclic analogues of both the steroidal and tricyclic 4-aza series of SR inhibitors. Incorporation of appropriate substituents onto the bicyclic structure, enables direct comparison of activity with known potent 4-aza inhibitors. It is envisioned that the piperidone compounds might display similar activity and selectivity as observed in the benzophenone bicyclic compounds such as **5.81**.

The preparation of four thiolactam derivatives allows investigation of a new, potential enolate mimic. As the four derivatives prepared are based on the 4-aza series of inhibitor, differences in activity due to the structural differences of the compounds will also provide information about the preferred substrate of the enzyme.

6.5 Structure Activity Relationships

6.5.1 SR Assays

The compounds prepared were analysed for activity against the SR type-1 and type-2 isozymes at Lilly Pharmaceuticals.

6.5.1.1 Type-1 Assay

The type-1 analysis utilised an assay which measured the conversion of ^{3}H-labelled T into ^{3}H-labelled DHT by type-1 SR isolated from human scalp in a method previously described.[5] The test compounds were dissolved in methanol to 10, 100, 1000, and 10000 nM concentrations. Labeled T (80 nM, 8.07 x 10-3 μCi specific activity 92.41 Ci/mmol) and unlabelled T (0.92 μM) were combined with the test compounds to give a total substrate concentration of 1.0 μM in a volume of 200 μL.

The assay was initiated by the addition of 0.015 – 0.025 mg of type 1 SR homogenate to the substrate and the mixture was then incubated for 1 hour at 37°C. Substrates and metabolites were quantified by HPLC separation and in-line flow radioactivity detection of the labelled androgens.

The activity of the assay was characterised using a known type-1 inhibitor, which gave an IC_{50} result of 4.5 nM.

6.5.1.2 Type-2 Assay

This assay utilised SR isolated from human prostate tissues in a concentration of 11.34 mg per reaction. The concentration of testosterone added was 50 nM (specific activity 40.3 Ci/mmol). The reaction was incubated at 25°C for 1 hour. The inhibitors were prepared and tested as described for the type-1 assay. The assay was calibrated using a known type-2 inhibitor, which gave an IC_{50} value of 10 nM. A type-1 specific inhibitor was also analysed for activity against the enzyme preparation and showed no detectable inhibition at 1 μM concentration.

6.5.2 Results

Compounds **6.26**, **6.29**, **6.31**, **6.32**, **6.33**, **6.46**, **6.47**, **6.48** and **6.49** were analysed for activity against type-1 and type-2 SR preparations. The results for this analysis are shown in Table 6.1 and are reported as IC_{50} values in either nM concentrations or as a percentage inhibition at a constant concentration.

Table 6.1: Activity of the prepared tricyclic, bicyclic and thiolactam compounds against type-1 and type-2 SR.

Compound	Structure	Type-1 IC_{50} (nM)	Type-2
6.26	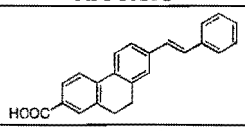	152 +/- 30	340 +/- 127 nM
6.29	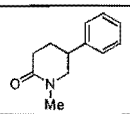	2477 +/- 1200	13.5% @ 40 μM
6.31	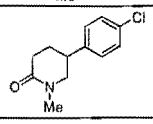	1690 +/- 320	12350 +/- 4300
6.32	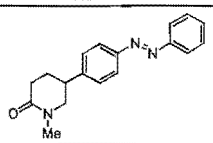	302 +/- 150	579 +/- 410 nM
6.33	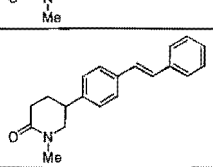	107 +/- 80	617 +/- 170 nM
6.46	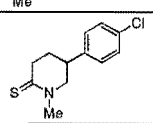	3360 +/-1170	14% @ 40 μM

6.47	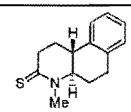	1450 +/-320	19.9% @ 40 μM
6.48	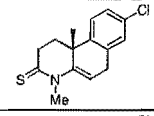	377 +/-370	13.2% @ 40 μM
6.49	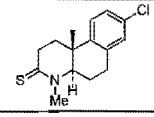	183 +/-70	21.6% @ 40 μM

6.5.2.1 TRICYCLIC COMPOUNDS

Analysis of compound **6.26** revealed good potency against type-1 SR with an IC_{50} value of 152 nM. This shows increased potency relative to the phenyl-substituted compound **5.91**, which gave 45% inhibition of type-1 SR at 2500 nM. The potency of **6.26**, however, was not as good as that given by the bromo substituted aryl acid **5.73** (type-1 $K_{I,\ app}$ 26 nM).[18] The type-2 analysis of compound **6.26** showed an IC_{50} value of 340 nM. This value indicates that **6.26** is also a respectable type-2 inhibitor and has significantly improved potency relative to the bromo-substituted inhibitor **5.73** which has very poor type-2 activity of IC_{50} =10000 nM. The potency of **6.26** however is not as great as that found in the styryl-substituted tricyclic lactam-based inhibitors **5.60** (IC_{50} type-1 = 6 nM, type-2 = 1400 nM) and **5.61** (IC_{50} type-1 = 23 nM, type-2 180 nM).[1]

These combined results suggest that the inclusion of a styryl substituent, in the appropriate position of the lactam-based and aryl acid-type tricyclic inhibitors, results in no significant change to type-1 potency, but gives significant improvement in the inhibition of type-2 SR. This type of substituent can therefore be considered important for the design of dual SR inhibitors.

6.5.2.2 BICYCLIC COMPOUNDS

An inspection of the results in Table 6.1 shows that the piperidone compounds prepared, are in general poorer type-1 SR inhibitors, relative to their tricyclic analogues, which show selective, potent inhibition of the type-1 isozyme (see Table 6.2).[5] Potency for this series of bicyclic compounds is increased with a lipophilic para substituent on the phenyl ring. The styryl substituted **6.33** showing greatest potency with a type-1 IC_{50} = 107 nM relative to IC_{50} values of 302 nM and

1690 nM for compounds **6.32** and **6.31** respectively. The unsubstituted compound **6.29** gave the least potency against type-1 SR with and IC_{50} of 2477 nM.

The type-2 analysis of the bicyclic compounds has revealed a general trend in which the bicyclic derivatives have less potency against the type-2 enzyme, relative to results found for type-1 activity. However compounds **6.32** and **6.33** which contain the phenylazo and styryl substituents respectively, still possess reasonable activity with type-2 IC_{50} values of 579 nM and 617 nM respectively. This is in keeping with the tricyclic derivatives **5.60** and **5.61**, which display good inhibition of type-2 SR, relative to tricyclic inhibitors lacking the styryl substituent. This result also points to the usefulness of the styryl group for improving type-2 selectivity.

Overall these results suggest that the B-ring of the tricyclic derivatives is important for inhibitor potency. This is possibly due to the increased planarity of the tricyclic structure relative to the bicyclic compounds, which have free rotation about the piperidone-phenyl bond.

Table 6.2: Comparison of the type-1 and type-2 SR activities of the prepared thiolactam compounds relative to the lactam analogues.

Structure	Compound	Type-1 IC_{50} (nM)	Type-2 IC_{50} (nM)
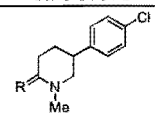	R = S **6.46**	3360	14% @ 40 μM
	R = O **6.31**	1690	12350 +/- 4300
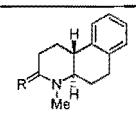	R = S **6.47**	1450	19.9% @ 40 μM
	R = O **6.3**	560	
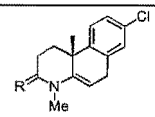	R = S **6.48**	377	13.2% @ 40 μM
	R = O **6.50**	120	
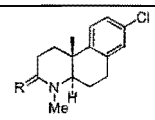	R = S **6.49**	183	21.6% @ 40 μM
	R = O **6.52**	17	

6.5.2.3 Enolate Mimics

Table 6.1 shows the thiolactam compounds **6.46**, **6.47**, **6.48** and **6.49** have reasonable potency against type-1 SR. However, their potency relative to the lactam inhibitors (**6.31**, **6.3**, **6.50** and **6.52**) is significantly reduced as can be seen in Table 6.2.[5] Given that the major difference between the two sets of inhibitors is

the relative sizes of the oxygen and sulfur atoms, these results suggest the enolate-binding pocket of SR is of a limited size.

The potency of the thiolactam compounds against the type-2 isozyme is poor. This is not unexpected given the general lack of type-2 inhibition displayed by the lactam containing compounds.

6.6 Conclusions

The work presented in this chapter has detailed the synthesis and analysis of various SR inhibitors.

This SAR study has shown the importance of a styryl-type substituent for improving the type-2 isozyme-selectivity of the inhibitors. This selectivity is achieved in most instances without significantly affecting the potency of the inhibitors against the type-1 enzyme.

Our investigations into the effectiveness of bicyclic derivatives have shown that the potency of these inhibitors is reduced relative to their tricyclic analogues. This result points to the importance of the B-ring for the inhibitory activity of this class of inhibitor,

The novel enolate-mimic investigated, the thiolactam, displays less potency than the analogous lactam mimic. This suggests that the SR enolate binding pocket is of limited size. The thiolactam functionality also appears to have no influence on the selectivity of the inhibitor for the type-1 or type-2 isozyme.

6.7 References

(1) Smith, E. C. R.; McQuaid, L. A.; Goode, R. L.; McNulty, A. M.; Neubauer, B. L.; Rocco, V. P.; Audia, J. E. *Bioorg. Med. Chem. Lett.* **1998**, *8*, 395-398.

(2) Morrison, H., Ed. *Biological Applications of Photochemical Switches. Bioorganic Photochemical Series*; John Wiley and Sons: New York, 1993; Vol. 2.

(3) Banks, B. E. C.; Banthorpe, D. V.; Butler, A. R.; Challis, B. C.; Chuchani, G.; Daudel, R.; Gibson, M. S.; Lemal, D. M.; Martin, R. B.; Smith, J. W.; Sollenberger, P. Y.; White, E. H.; Wolman, Y.; Woodcock, D. J.; Zabicky, J. *The Chemistry of the Amino Group*; John Wiley and Sons: New York, 1968.

(4) Zollinger, H. *Diazo Chemistry I. Aromatic and Heteroaromatic Compounds*; VCH: Weinheim, 1994.

(5) Jones, C. D.; Audia, J. E.; Lawhorn, D. E.; McQuaid, L. A.; Neubauer, B. L.; Pike, A. J.; Pennington, P. A.; Stamm, N. B.; Toomey, R. E.; Hirsch, K. S. *J. Med. Chem.* **1993**, *36*, 421-423.

(6) Cannon, J. G.; Chang, Y.-an; Amoo, V. E.; Walker, K. A. *Synthesis Communications* **1986**, 494-496.

(7) ADA. ; Private communication.

(8) Abell, A. D.; Yen, H.-K.; Yamashita, D. S.; Brandt, M.; Mohammed, H.; Levy, M. A.; Holt, D. A.; Erhard, K. F. *Bioorg. Med. Chem. Lett.* **1994**, *4*, 1365-1368.

(9) Lilly. USA Patent EP 0 532 190 A2, 1993.

(10) Luckner, U.; Chmielewski, J. *Bioorg. Med. Chem. Lett.* **1994**, *4*, 2145-2146.

(11) Ege, S. N.; Sharp, R. R. *J. Chem. Soc. B* **1971**, 2014-2020.

(12) Vollmer, M. S.; Clark, T. D.; Steinem, C.; Ghadiri, M. R. *Angew. Chem. Int. Ed.* **1999**, *38*, 1598-1601.

(13) Roberts, R. M.; Khalaf, A. A. *Friedel-Crafts Alkylation Chemistry. A Century of Discovery*; Marcel Dekker Inc.: New York, 1984.

(14) Burckhalter, J. H.; Campbell, R. *J. Org. Chem.* **1961**, *26*, 4232-4235.

(15) Davies, S. G., Ed. *Amino Acid and Peptide Synthesis*; Oxford Science Publications: Oxford, 1992.

(16) Bodanszky, M.; Bodanszky, A. *The Practise of Peptide Synthesis*; Springer-Verlag: Berlin, 1984.

(17) Nevy, J. B.; Hawkinson, D. C.; Blotny, B.; Yao, X.; Pollack, R. M. *J. Am. Chem. Soc.* **1997**, *119*, 12722-12726.

(18) Abell, A. D.; Brandt, M.; Levy, M. A.; Holt, D. A. *J. Chem. Soc. Perkin. Trans.* **1997**, *1*, 1663-1667.

(19) Shen, T.; Witzel, B. E. U.S.A. Patent 808,660, 1969.

(20) Julia, M.; Siffert, O.; Bagot, J. *Journal Bulletin De La Societe Chimique De France* **1968**, *3*, 1000-1005.

(21) Doyle, M. P.; Siegfried, B.; Dellaria, J. F., Jr. *J. Org. Chem.* **1977**, *42*, 2426-2430.

(22) Yde, B.; Yousif, N. M.; Pedersen, U.; Thomsen, I.; Lawesson, S. O. *Tetrahedron* **1984**, *40*, 2047-2052.

7 EXPERIMENTAL

7.1 *ALPHA*-AMYLASE ASSAY PROTOCOL

7.1.1 GENERAL EQUIPMENT AND TECHNIQUES

The "Megazyme" *alpha*-amylase kit used to assay the prepared derivatives was purchased from Deltagen, Australia.

The *alpha*-amylase enzymes assayed were obtained from Sigma. The inhibitors and reagents used to prepare them are detailed in section 7.2.1.

Assay solutions were prepared using Eppendorf micropipettes. Unless otherwise stated, all aqueous solutions were prepared using triply distilled water. The pH of solutions was measured using an in-house digital testmeter.

The absorbance of the samples was measured at 410 nm using a Pharmacia spectrophotometer.

The assay reagents were prepared and used as described below.

7.1.1.1 ASSAY KIT

The "Megazyme" *alpha*-amylase kit contained two vials of substrate, one vial of concentrated enzyme extract buffer, one vial of concentrated stopping-reagent and one vial of control malt flour.

(i) Substrate

Each substrate vial contained

- Blocked *p*-nitrophenol maltoheptaoside (BPNPG7, 54.5 mg)
- Glucoamylase (100 U at pH 5.2)
- α-Glucosidase (100 U at pH 5.2)

The entire contents of the vial were dissolved in distilled water (10 mL), and the solution was divided into 1 mL aliquots and stored at –24°C. The substrate is indefinitely stable at –24°C, and stable for up to seven days when refrigerated.[1] The concentration of the substrate in solution was 4.03 $x10^{-3}$ M and is referred to as either the standard or 1X concentration of substrate.

(ii) Extraction Buffer

The concentrated extraction buffer contained,

- 1 M sodium malate
- 1 M sodium chloride
- 40 mM calcium chloride
- 0.1% sodium azide

The entire contents (50 mL) were diluted to 1 L with distilled water and the solution was stored at 6°C. The pH was measured to be 5.2

(iii) Stopping Reagent

The concentrated stopping reagent was 20% (w/v) Trizma base. The entire contents (25 mL) was diluted to 500 mL with distilled water and stored at room temperature.

7.1.1.2 INHIBITORS

Each inhibitor tested was prepared as a 0.1-mM solution in deoxygenated water. The water was degassed by bubbling N_2 through for 5 minutes. In the case where the inhibitor was insoluble in water, either a suspension was made or the sample was dissolved in distilled ethanol. Solutions were made just prior to use; either a 0.50-mL or 0.25-mL volume.

7.1.1.3 ENZYMES

Five different *alpha*-amylase enzymes were used in the assay. Solutions of these enzymes were prepared such that the absorbance at 410 nm of each at the end of the 10 minutes assay, without inhibitor, was between 0.6 and 0.8.

(i) Type VIII-A Barley Malt (2.1 U / mg solid)

Barley malt (2.3 mg) was dissolved in enzyme extract buffer (20 mL) and stored on ice until required. New solutions were prepared every 3 hours. For the purposes of description, this concentration of enzyme is referred to as the standard or 1x concentration.

(ii) Type X-A Fungal Crude from Aspergillus Oryzae (40.0 U / mg solid)

Fungal *alpha*-amylase (1.0 mg) was dissolved in enzyme extract buffer (1 mL). This solution was used as the enzyme concentrate from which later dilutions were prepared. This stock solution was stored at -24°C. An aliquot of the stock solution (5 μL) was diluted with enzyme extract buffer to a volume of 1 mL. An aliquot of this new solution (250 μL) was further diluted with buffer to 1 mL and stored on ice until required. New solutions were prepared every 3 hours.

(iii) Type II-A Bacillus Species (1,820 U / mg solid)

Bacillus-species *alpha*-amylase (1.0 mg) was dissolved in enzyme extract buffer (1 mL). This solution was used as the enzyme concentrate from which later dilutions were prepared. This stock solution was stored at -24°C. An aliquot of the stock solution (20 μL) was diluted with enzyme extract buffer to a volume of 1 mL. An aliquot of this new solution (20 μL) was further diluted with buffer to 1 mL and stored on ice until required. New solutions were prepared every 3 hours.

(iv) Type I-A DFP Treated from Porcine Pancreas (790 U / mg protein)

Porcine-pancreas *alpha*-amylase (33.33 μL) was mixed with enzyme extract buffer (1 mL). This solution was used as the enzyme concentrate from which later solutions were prepared. This stock solution was stored at 6°C. An aliquot of the stock solution (50 μL) was diluted with enzyme extract buffer to a volume of 1 mL. An aliquot of this new solution (30 μL) was further diluted with buffer to 1 mL and stored on ice until required. New solutions were prepared every 3 hours.

(v) Type XIII-A Crude from Human Saliva (72.0 U / mg solid)

Human-saliva *alpha*-amylase (1.0 mg) was dissolved into enzyme extract buffer (1 mL). This solution was used as the enzyme concentrate from which later solutions were prepared. The stock solution was stored at –24°C. An aliquot of the stock solution (20 mL) was diluted with enzyme extract buffer to a volume of 1 mL and stored on ice until required. New solutions were prepared every 3 hours.

7.1.2 METHOD

The following methods were used to collect data for determination of inhibition activities and kinetic analysis.

7.1.2.1 Inhibition Assays

The inhibition results were obtained using the following assay procedures. Unless otherwise stated all measurements were collected in triplicate.

(i) The Blank

Into a plastic cuvette was placed 50 μL of water. The cuvette was allowed to equilibrate to 40°C for 2 minutes in a water bath. The assay substrate (50 μL), also equilibrated to 40°C, was then added and after exactly 10 minutes, stopping reagent (750 μL) was added to the cuvette. The cuvette was removed from the water bath and used as a blank for all subsequent readings. The absorbance reading of this solution at 410 nm was set to zero.

(ii) The Controls

Prior to running any assays, a control was used to determine the absorbance of the substrate in the absence of any inhibitors. A control was also run with each inhibitor assayed, in order to monitor any decrease in the activity of the enzyme over time.

Into each plastic 1 mL cuvette was placed an aliquot of water* (5 μL) and an aliquot of *alpha*-amylase enzyme solution (45 μL). The mixture was allowed to equilibrate at room temperature for 20 minutes. The cuvettes were then placed into a 40°C water bath and allowed to reach equilibrium over 2 minutes. The substrate (50 μL) also equilibrated to 40°C was then added to the cuvette. After exactly 10 minutes, stopping reagent (750 μL) was added to the cuvette, which was then removed from the water bath. The absorbance at 410 nm of each control was measured relative to the blank.

(iii) The Inhibitors

Into each plastic 1-mL cuvette was placed an aliquot of inhibitor solution (5 μL) and an aliquot of *alpha*-amylase enzyme solution (45 μL). The mixture was allowed to equilibrate at room temperature for 20 minutes. The cuvettes were then placed into a 40°C water bath and allowed to reach equilibrium over 2 minutes. The substrate (50 μL), also equilibrated to 40°C, was then added to the

cuvette. After exactly 10 minutes, stopping reagent (750 μL) was added to the cuvette, which was then removed from the water bath. The absorbance of each inhibitor at 410 nm was measured.

(iv) Calculation of Inhibitor Activity and Errors

The inhibitory activity of the prepared derivatives was determined by calculating the average absorbance for each inhibited sample as a percentage of the average of the controls. These values were then converted to a percentage inhibition of the enzyme. The reported values are the average of at least three measurements.

The absolute error associated with these values was determined to be approximately 10% by taking the 95% confidence interval for the mean of each set of measurements as a percentage of the average uninhibited absorbance.

7.1.2.2 Linearity of the Assay

Linearity of the assay over time was measured at six different enzyme and six different substrate concentrations. The different enzyme concentrations were measured against the standard substrate concentration and the different substrate concentrations were measured against the standard enzyme concentration (see section 4.3.1.1 for results).

Into a plastic 1-mL Eppendorf tube was placed an aliquot of water (50 μL) and an aliquot of enzyme solution (450 μL), (2x, 3/2x, 1x, 3/4x, 1/2x and 1/4x original concentration). The mixture was allowed to equilibrate at room temperature for 20 minutes. The Eppendorf was then placed into a 40°C water bath and allowed to reach equilibrium over 2 minutes. The substrate (500 μL; 2x, 1x, 1/2x, 1/4x, 1/6x and 1/8x original concentration), also equilibrated to 40°C, was then added to the Eppendorf and the mixture shaken. At 1-, 2-, 3-,....., 10-minute intervals after initiation, an aliquot (100 μL) was removed from the bulk mixture and added to 750 μL of stopping reagent in a cuvette. The absorbance at 410 nm of each aliquot was then measured.

---

* When a control was required for an inhibitor prepared in ethanol, a 5 μL aliquot of ethanol was added to the cuvette instead of water.

The linearity of the assay over time was also measured in the presence of inhibitor. Into ten plastic 1-mL cuvettes was placed an aliquot of 0.1-mM inhibitor solution (5 μL) and enzyme solution (45 μL). The mixtures were allowed to equilibrate to room temperature for 20 minutes. The cuvettes were then placed into a 40°C water bath and allowed to reach equilibrium over 2 minutes. To each cuvette, an aliquot of substrate (50 μL) also equilibrated to 40°C, was added. Each of the ten cuvettes was reacted for a different length of time, ranging from 1 minute, to 10 minutes. After the allocated time, the reaction was quenched by the addition of stopping reagent (750 μL) to the cuvette. The absorbance at 410 nm of each sample was measured relative to the blank.

7.1.2.3 Inhibitor Incubation : Substrate Versus Enzyme

The following experimental protocol was used to compare the incubation of the inhibitor with the *enzyme* versus incubation of the inhibitor with the *substrate*.

(i) Inhibitor Plus Substrate

Into three 1-mL cuvettes was placed an aliquot of 0.1-mM ascorbic-acid solution (5 μL) and substrate solution (50 μL). The mixtures were equilibrated to room temperature for 20 minutes, then placed into a 40°C water bath and allowed to reach equilibrium over 2 minutes. To each cuvette, an aliquot of enzyme solution (45 μL) also equilibrated to 40°C, was added. Each of the cuvettes was reacted for 10 minutes, then quenched by the addition of stopping reagent (750 μL). The absorbance of each sample at 410 nm was then measured.

(ii) Inhibitor Plus Enzyme

The inhibitor was incubated with enzyme and reacted as previously described in section 7.1.2.1.

Table 7.1: Results of inhibitor incubation experiments.

Experimental protocol	Average absorbance at 410 nm
Incubation of the inhibitor with the substrate	0.073
Incubation of the inhibitor with the enzyme	0.062
Control experiment containing no inhibitor	1.011

7.1.2.4 Acetal Hydrolysis

The following procedure was carried out to determine if acetal hydrolysis occurred in inhibitors under the reaction conditions of the assays.

Product **3.1** and product **3.12** were dissolved in D_2O and $CDCl_3$ respectively and immediately analysed by proton-NMR spectroscopy (for proton-NMR data see section 7.2.2.1). The samples were then subjected to the same temperature and time conditions as occur in the Megazyme assay: They were equilibrated at room temperature for 20 minutes, then placed in a 40°C water bath for 12 minutes and subsequently re-analysed by proton NMR spectroscopy.

7.1.2.5 Uninhibited-Enzyme Kinetic Assays

The following reagents and protocols were used to gather data for kinetic analysis.

(i) Substrate

Substrate solutions were prepared, based on the standard (1x) concentration recommended by the suppliers as described in section 7.1.1.1(i). Concentrations of 2x, 1.7x, 1.5x, 1.4x, 0.75x, 0.7x, 0.5x, 0.25x were made by suitable dilution with distilled water.

(ii) Enzyme

The enzyme used for the kinetic analysis was barley-malt *alpha*-amylase. The concentration of the enzyme solution was such that the absorbance at 410 nm after the 10 minutes assay, with no inhibitor and standard substrate concentration, was between 0.6 and 0.8. Solutions were prepared as described in section 7.1.1.3.

(iii) Inhibitors

The inhibitors used for kinetic analysis were ascorbic acid and product **3.1**. The concentrations of the inhibitor solutions were prepared such that the highest and lowest values would give absorbance readings of between 0.0 and 1.0 over all substrate concentrations at 410 nm. For each inhibitor, four solutions were prepared within the concentration ranges shown below.

- Ascorbic acid = 5.12×10^{-4} M – 2.00×10^{-3} M
- Product **3.1** = 3.27×10^{-4} M – 1.31×10^{-3} M

(iv) Blanks and Controls

Assay blanks and controls were determined using the same protocols as described previously for the inhibition assays (section 7.1.2.1).

7.1.2.6 Inhibited-Enzyme Kinetic Assays

Solutions of each inhibitor were prepared at four different concentrations and assayed against a standard enzyme solution at various concentrations of substrate. The concentrations reported below refer to the concentration in the assay mixture.

Each assay was performed using the standard procedures previously described in section 7.1.2.1.

(i) Ascorbic acid

Enzyme concentration: equal to the standard enzyme solutions as described in section 7.1.1.3.

Inhibitor concentrations: = **1x** (2.0 x10^{-3} M), **0.72x** (1.453 x 10^{-3} M), **0.5x** (01.022 x 10^{-3} M), **0.25x** (5.11 x 10^{-4} M).

Substrate concentrations: = **2x** (4.031 x 10^{-3} M), **1.5x** (3.023 x 10^{-3} M), **1x** (2.016 x 10^{-3} M), **0.75x** (1.512 x 10^{-3} M), **0.5x** (1.008 x 10^{-3} M).

(ii) Product 3.1

Enzyme concentration: = equal to the standard enzyme solutions as described in section 7.1.1.3.

Inhibitor concentrations: **1x** (1.309 x 10^{-3} M), **0.75x** (9.815 x 10^{-4} M), **0.5x** (6.544 x 10^{-4} M), **0.25x** (3.272 x 10^{-4} M).

Substrate concentrations: **2x** (4.0311 x 10^{-3} M), **1.7x** (3.4264 x 10^{-3} M), **1.4x** (2.822 x 10^{-3} M), **1x** (2.016 x 10^{-3} M), **0.7x** (1.411 x 10^{-3} M).

7.2 Synthesis

7.2.1 General Equipment and Techniques

7.2.1.1 Reagents and Equipment

All reaction vessels were either flame-dried or oven-dried overnight (> 110°C), assembled and then cooled to room temperature under a dry N_2 atmosphere. All solvents were distilled using known literature procedures.[2,3] Dry solvents were distilled and collected just prior to use.

L-ascorbic acid was obtained from PSM Holdings Ltd., D-isoascorbic acid and dihydroxyfumaric acid were purchased from Sigma, dehydroascorbic acid was kindly gifted by S. Fayle. 10b-methyl-8-chloro1,2,6-trihydrobenzo[*f*]quinolin-3-one, 10b-methyl-8-chloro-4-methyl-1,2,4a,5,6-pentabenzo[*f*]quinolinone and 9,10-dihydrophenanthrene-2-carboxylic acid were kindly gifted by Eli Lilly.

Reaction temperatures reported refer to oil bath temperature.

Melting points were recorded on an electrothermal melting-point apparatus and are uncorrected.

The rotary vein vacuum pump had a measured pressure of 2 mmHg.

Hydrogenation procedures were carried out using a Parr Instruments Company Inc. pressure reaction apparatus model 4513 with 40 psi H_2 at room temperature.

Vacuum distillations were performed using a Buchi GKR 50 Kugeral distillation apparatus connected to a vacuum pump.

All radial chromatography was performed on a Harrison Research Inc. Chromatotron model 7924. Radial chromatography plates of 1 and 2 mm thickness were prepared using silica gel 60 PF_{254} containing gypsum as described in the instruction manual.[4]

All column chromatography was performed using Silica 60 200-400 mesh flash silica. Thin layer chromatography (tlc) and preparative thin layer chromatography (plc) was run on aluminium-backed Silica gel 60 F_{245} sheets. Unless otherwise stated eluting solvents are appropriate mixtures of ethyl acetate and petroleum ether (boiling fraction 50 – 70°C) or ethyl acetate and methanol.

Irradiation of compounds for photoisomerisation experiments was performed using a 200-watt mercury high-pressure arc lamp. The required wavelengths were selected using appropriate filters.

7.2.1.2 Nuclear Magnetic Resonance Spectroscopy

All proton spectra, nOe, and 2D experiments (HMQC, HMBC) were recorded on a Varian Unity 300 instrument (300 MHz). Carbon spectra were recorded on either a Varian Unity 300 or a Varian XL 300 (75 MHz). The solvent used was either $CDCl_3$ containing tetramethylsilane (TMS) as an internal standard, D_2O referenced at 4.7 ppm, or CD_3COCD_3 referenced to 2.17 ppm. Chemical shifts are reported as parts per million (ppm) downfield from the TMS resonance (δ

0.0) or referenced to the D_2O or CD_3COCD_3 resonances for proton spectra. For carbon spectra resonances are referenced relative to the $CDCl_3$ resonance (δ 77.0) or the CD_3COCD_3 resonances (δ 29.2, 204.1). Resonances in the proton spectra are described as singlet (s), broad singlet (bs), doublet (d), triplet (t), quartet (q) doublet of doublets (dd) doublet of triplets (dt) or multiplet (m). Resonances are assigned as H#, where # represents the numbering of the carbon atoms to which the protons that contribute to the resonances are attached, in the compound concerned.

7.2.1.3 Mass Spectrometry

Mass spectra were recorded on either a Kratos MS80RFA mass spectrometer, for samples analysed by electron impact (EI-MS) or fast atom bombardment (FAB-MS), or a Micromass LCT mass spectrometer, for samples analysed using an electrospray (ES-MS) technique. EI-MS was performed typically at 70eV with 4kV accelerating voltage. FAB-MS analysis utilised a nitrobenzyl alcohol matrix with xenon as the carrier gas. The ion gun used was a Iontech ZN11NE. Found masses are reported, along with a calculated mass, accurate to four decimal places.

7.2.1.4 Infra-red Spectrom etry

Infrared spectra were recorded on a Shimadzu FTIR 8201PC spectrophotometer. Compounds were prepared as nujol mulls on KBr discs. Bands are reported using the wavenumber scale in cm^{-1}.

7.2.1.5 X-ray Crystallogra phy

Crystallography intensity data were collected with a Siemens P4s four-circle diffractometer using monochromatised Mo Kα radiation. Cell parameters were determined by least-squares refinement of at least 25 accurately centred reflections ($2\theta > 24°$). Throughout the data collections the intensities of three standard reflections were monitored at regular intervals, which showed no significant crystal decomposition. The structures were solved by direct methods using SHELXS90,[5] and refined using SHELXL93,[6] on F^2 using all data. The functions minimised were $(\Sigma\omega(F_o^2 - F_c^2)$ with $\omega = [\sigma^2(F_o^2) + aP^2 + bP]^{-1}$ where $P = [\max(F_o^2 + 2F_c)]/3$. The hydrogens were included in calculated positions and assigned isotropic displacement parameters 1.3 times the isotropic equivalent of their

carrier atoms. In all cases the final Fourier synthesis did not show any significant residual electron density in chemically-sensible locations.

7.2.2 Experimental for Chapter 3

7.2.2.1 Ascorbic-Acid Derivatives

Where indicated, ascorbic-acid derivatives were prepared according to literature procedures.

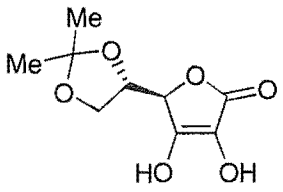

(i) 5,6-Isopropylidene-L-Ascorbic Acid (3.1)[7]

Ascorbic acid (10 g, 0.06 mol), acetone (40 mL) and acetyl chloride (1 mL, 0.02 mol) were stirred at room temperature for 3 hours, then refrigerated for 8 hours. The precipitate that formed was isolated by vacuum filtration and washed with a small amount of cold acetone, then air-dried. Recrystallisation from acetone-petroleum ether gave **3.1** as a white solid (10.3 g, 84%): mp 209-211°C (lit mp[7] 195 - 200°C); ^{1}H NMR (D_2O) δ 4.85 (d, *J* = 2.5 Hz, 1H, H4), 4.52 (m, 1H, H5), 4.23 (m, 1H, H6a), 4.10 (dd, *J* = 4.0 Hz, 9.5 Hz, 1H H6b), 1.30 (s, 6H, 2 x Me); ^{13}C NMR (D_2O) δ 26.09, 26.91, 67.20, 75.06, 77.99, 112.94, 134.15, 145.12, 174.14; IR: υ_{max} 1665, 1753 cm^{-1}; EI-MS: *m/z* 216 [M$^+$], HRMS $C_9H_{12}O_6$ requires 216.06339, found 216.06355.

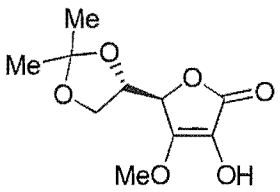

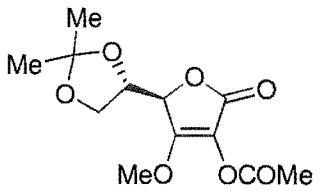

(ii) 3-O-Methyl-5,6-Isopropylidene-L-Ascorbic Acid (3.2)[8], 2-Acetyl-3-O-Methyl-5,6-Isopropylidene-L-Ascorbic Acid (3.3)

Dry $NaHCO_3$ (0.25 g, 2.97 mmol) was added to a solution of compound **3.1** (0.5 g, 2.34 mmol) in DMSO (10 mL) and the mixture vigorously stirred for 20 minutes. Iodomethane (0.2 mL, 2.16 mmol) was added drop-wise to the mixture

over 30 minutes and then the mixture was heated to 50°C and stirred overnight. The mixture was cooled to room temperature, diluted with water (20 mL), neutralised with 2M aqueous HCl (universal indicator paper) and then extracted with ethyl acetate (3 x 20 mL). The organic layers were combined, dried over Na_2SO_4 and the solvent was evaporated under reduced pressure to give a yellow oil which was purified by radial chromatography (30% ethyl acetate/petroleum ether) to give **3.2** (0.1 g, 19%) ^{1}H NMR ($CDCl_3$) δ 4.54 (d, *J* = 3.9 Hz, 1H, H4), 4.25 (m, 1H, H5), 4.18 (s, 3H, 3-OMe), 4.13 (dd, *J* = 8.3 Hz, 6.3 Hz, 1H, H6a), 4.04 (dd, *J* = 8.3 Hz, 6.3 Hz, 1H, H6b), 1.39 (s, 3H, Me), 1.36 (s, 3H, Me).

Compound **3.3** was isolated during the purification of product **3.2**, the preparation of which is reported above. Removal of the eluting solvent under reduced pressure gave **3.3** as a white solid (0.05 g, 8%), mp 89-90°C: ^{1}H NMR ($CDCl_3$) δ 4.67 (d, *J* = 3.0 Hz, 1H, H4), 4.36 (m, 1H, H5), 4.16 (dd, *J* = 8.8 Hz, 6.8 Hz, 1H, H6a), 4.08 (m, 4H, H6b & 3-OMe), 2.29 (s, 3H, COMe), 1.40 (s, 3H, Me), 1.36 (s, 3H, Me); ^{13}C NMR ($CDCl_3$) δ 20.20, 25.50, 25.72, 59.27, 65.13, 73.50, 75.08, 110.63, 114.59, 160.76, 168.01; IR: υ_{max} 1695, 1769, 1780 cm^{-1}; EI-MS: *m/z* 272 [M$^+$], HRMS $C_{12}H_{16}O_7$ requires 272.08960, found 272.08960.

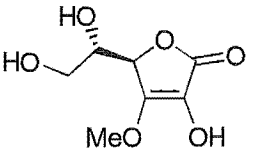

(iii) 3-O-Methyl-L-Ascorbic Acid (3.4)

2 M HCl (1 mL) was added to product **3.2** (0.1 g, 0.43 mmol) dissolved in methanol (1.5 mL) and the mixture stirred at 50°C overnight. The mixture was cooled to room temperature and the solvent evaporated under reduced pressure. Purification by radial chromatography (30% ethyl acetate/petroleum ether) gave product **3.4** as an oil in a 56% yield: ^{1}H NMR ($CDCl_3$) δ 4.82 (d, *J* = 1.9 Hz, 1H, H4), 4.08 (s, 3H, 3-Ome), 3.91 (m, 1H, H5), 3.62 (d, *J* = 6.8 Hz, 2H, H6), EI-MS: *m/z* 190 [M$^+$], HRMS, $C_{10}H_{14}O_6$ requires 190.04774, found 190.04767.

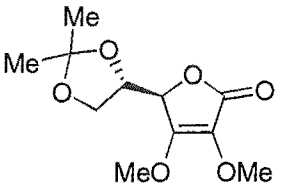

(iv) 2,3-Di-O-Methyl-5,6-Isopropylidene-L-Ascorbic Acid (3.5)

To a stirred solution of **3.1** (0.10 g, 0.46 mmol) and K_2CO_3 (0.19 g, 1.4 mmol) in acetone (1 mL, 0.023 mol) was added dimethyl sulfate (0.2 mL, 2.2 mmol) dropwise over 15 minutes. The mixture was then heated and refluxed overnight. The resulting yellow solution was cooled to room temperature and the excess K_2CO_3 was removed by vacuum filtration. The solid residue was washed with cold acetone until the yellow colour was removed and the combined acetone solutions were concentrated under vacuum. The residue was refrigerated and **3.5** crystallised out of solution as white needles, which were vacuum filtered, washed with a small amount of cold ether and air-dried (0.33 g, 29 %): mp 93-96°C (lit mp[7] 90-94°C); ^{1}H NMR ($CDCl_3$) δ 4.51 (d, *J* = 3.5 HZ, 1H, H4), 4.28 (dt, *J* = 3.0 Hz, 6.5 Hz, 1H, H5), 4.15 (s, 3H, 3-OMe), 4.13 (dd, *J* = 6.5 Hz, 8.5 Hz, 1H, H6a), 4.03 (dd, *J* = 6.5 Hz, 8.5 Hz, 1H, H6b), 3.86 (s, 3H, 2-OMe), 1.39 (s, 3H, Me), 1.36 (s, 3H, Me); ^{13}C NMR ($CDCl_3$) δ 25.54, 25.80, 59.45, 60.32, 65.22, 73.83, 74.44, 110.36, 123.20, 156.67, 168.90; IR: υ_{max} 1679, 1760, 2853, 2928 cm^{-1}; EI-MS: *m/z* 244 [M^+], HRMS $C_{11}H_{16}O_6$ requires 244.09469 found 244.09421.

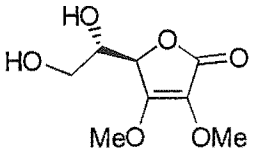

(v) 2,3-Di-O-Methyl-L-Ascorbic Acid (3.6)

Compound **3.5** (0.5 g, 2.05 mmol) was dissolved in dry methanol (8 mL). To this solution was added 2 M aqueous HCl (5 mL) and the mixture was heated to 50°C and stirred for 4 hours. The mixture was cooled to room temperature and the solvent evaporated under reduced pressure. The resulting yellow solid was dried under vacuum to give **3.6**, which was recrystallised from ether (0.3 g, 70%): mp 56-57°C (lit mp[9] 63°C); ^{1}H NMR ($CDCl_3$) δ 4.68 (d, *J* = 2.5 Hz, 1H, H4), 4.17 (s, 3H, 3-OMe), 3.93 (m, 1H, H5), 3.85 (s, 3H, 2-OMe), 3.80 (m, 2H, H6); ^{13}C NMR ($CDCl_3$) δ

59.49, 60.54, 63.23, 69.92, 75.80, 122.90, 157.97, 169.84; IR: υ_{max} 1678, 1769 cm^{-1}; EI-MS: *m/z* 204 [M^+], HRMS $C_8H_{12}O_6$ requires 204.06339, found 204.06319.

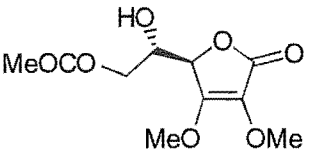

(vi) 2,3-Di-O-Methyl-6-Acetyl-L-Ascorbic Acid (3.7)

The above procedure for preparation of compound **3.6** was repeated using compound **3.5** (1.0 g, 4.1mmol), methanol (15 ml) and 2M aqueous HCl (8 ml). After refluxing the mixture for 4 hours at 50°C, the solution was cooled and the product extracted with ethyl acetate (3 x 20 mL). The organic layers were combined, washed with brine and dried over Na_2SO_4. The solvent was evaporated under reduced pressure to give a pale yellow oil that was dried under vacuum to give **3.7** as a solid which was recrystallised from ether as colourless prisms (0.74g, 74%): mp 95-99°C; ^1H NMR ($CDCl_3$) δ 4.66 (d, *J* = 2.5 Hz, 1H, H4), 4.34 (dd, *J* = 7.0 Hz, 12.0 Hz, 1H, H6a), 4.22 (dd, *J* = 5.0 Hz, 12.0 Hz, 1H, H6b), 4.16 (s, 3H, 3-OMe), 4.09 (m, 1H, H5), 3.85 (s, 3H, 2-OMe), 2.11 (s, 3H, Me); ^{13}C NMR ($CDCl_3$) δ 20.81, 59.55, 60.47, 64.83, 68.01, 75.09, 123.15, 156.95, 169.13, 171.01; IR: υ_{max} 1672, 1735, 1747 cm^{-1}; EI-MS: *m/z* 246 [M^+], HRMS $C_{10}H_{14}O_7$ requires 246.07395, found 246.07362

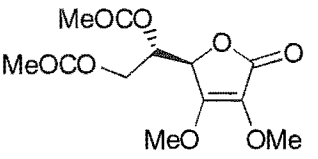

(vii) 2,3-Di-O-Methyl-5,6-Diacetyl-L-Ascorbic Acid (3.8)

Compound **3.6** (0.2 g, 1.14 mmol) was dissolved in pyridine (2 mL), acetic anhydride (1 mL, 0.014 mol) added drop-wise and the mixture stirred for 2 hours. The solvent was removed under reduced pressure and the resulting oil was dried under vacuum overnight. The resulting solid was recrystallised from ether to give **3.8** as platelets (0.08 g, 24%): mp 68-70°C; ^1H NMR ($CDCl_3$) δ 5.35 (m, 1H, H5), 4.78 (d *J* = 2.0 Hz, 1H, H4), 4.36 (dd, *J* = 5.5 Hz, 11.5 Hz, 1H, H6a), 4.26 (dd, *J* = 7.0 Hz, 11.5 Hz, 1H, H6b), 4.10 (s, 3H, 3-OMe), 3.84 (s, 3H, 2-OMe), 2.07 (s, 6H, 2 x Me); ^{13}C NMR

($CDCl_3$) δ 20.36, 20.55, 59.41, 60.33, 61.95, 67.59, 73.29, 123.16, 155.72, 168.36, 169.38, 170.22; IR: υ_{max} 1690, 1744, 1774, 2341, 2360 cm^{-1}; EI-MS: *m/z* (228,11), (186, 100).

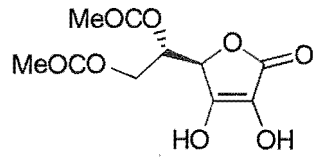

(viii) 5,6-Diacetyl-L-Ascorbic Acid (3.9)[10]

Ascorbic acid (0.88 g, 5.0 mmol) and acetic anhydride (1.2 mL, 0.02 mol) were mixed together with 2 drops of concentrated aqueous H_2SO_4. The temperature of the mixture increased to approximately 40°C and was stirred for 2 hours with gentle heating. The resulting amber-coloured syrup was evaporated under reduced pressure, seeded with ascorbic-acid crystals and left standing for 3 days. Product **3.9** formed as needle-shaped crystals, which were washed with cold ether to remove the syrup, air-dried and recrystallised from nitromethane (0.24 g 18%): mp 144-146°C (lit mp[10] 154°C): ^1H NMR (CD_3COCD_3) δ 5.43 (m, 1H, H5), 4.99 (d, *J* = 2.93 Hz, 1H, H4), 4.37 (dd, *J* = 4.88 Hz, 11.72 Hz, 1H, H6a), 4.23 (dd, *J* = 7.32 Hz, 11.27 Hz, 1H, H6b), 2.00 (s, 3H, Me), 1.97 (s, 3H, Me); ^{13}C NMR (CD_3COCD_3)) δ 19.81, 19.92, 62.22, 67.89, 73.70, 87.90, 102.99; IR: υ_{max} 1670, 1707, 1742 cm^{-1}.

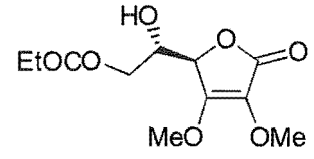

(ix) 2,3-Di-O-Methyl-6-Propionyl-L-Ascorbic Acid (3.10)

Compound **3.6** (0.5 g, 2.45 mmol) and a catalytic amount of *p*-toluenesulfonic acid (pTSA) were dissolved in ethyl propionate (10 mL, 0.14 mol). The mixture was heated to 70°C and stirred for 16 hours. The solution was then cooled to room temperature, washed with a saturated $NaHCO_3$ solution and dried over Na_2SO_4. The solvent was removed under reduced pressure to give a yellow oil that was dried under vacuum overnight. Purification by radial chromatography (30% ethyl acetate/ petroleum ether) gave **3.10** as a yellow oil; (0.08 g, 12%) ^1H

NMR ($CDCl_3$) δ 4.65 (d, *J* = 2.0 Hz, 1H, H4), 4.35 (dd, *J* = 12.2 Hz, 6.3 Hz, 1H, H6a), 4.24 (dd, *J* = 10.7 Hz, 4.8 Hz, 1H, H6b), 4.16 (s, 3H, 3-OMe), 4.08 (m, 1H, H5), 3.84 (s, 3H, 2-OMe), 2.38 (q, *J* = 6.8 Hz, 15.0 Hz, 2H, **CH_2**Me), 1.15 (t, *J* = 7.5 Hz, 3H, CH_2**Me**); ^{13}C NMR ($CDCl_3$) δ 8.97, 27.38, 59.51, 60.43, 64.71, 68.05, 75.05, 123.12, 156.88, 169.06, 174.45; IR: υ_{max} 1678, 1765 cm^{-1}; EI-MS: *m/z* 260 [M^+], HRMS $C_{11}H_{16}O_7$ requires 260.08960, found 260.08782

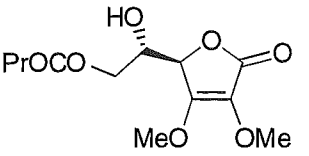

(x) 2,3-Di-O-Methyl-6-Butyryl-L-Ascorbic Acid (3.11)

Compound **3.6** (0.5 g, 2.45 mmol) was dissolved in ethyl butyrate (10 mL, 0.12 mol) and a catalytic amount of *p*TSA added. The mixture was heated and stirred for 16 hours at 70°C. The solution was then cooled to room temperature, washed with a saturated $NaHCO_3$ solution and dried over Na_2SO_4. The solvent was removed under reduced pressure to give a yellow oil that was dried under vacuum overnight. Purification by radial chromatography (30% ethyl acetate/ petroleum ether) gave **3.11** as a yellow oil (0.05g, 7%) ^1H NMR ($CDCl_3$) δ 4.65 (d, *J* = 2.5 Hz, 1H, H4), 4.35 (dd, *J* = 11.7 Hz, 6.8 Hz, 1H, H6a), 4.23 (dd, *J* = 11.7 Hz, 4.8 Hz, 1H, H6b), 4.16 (s, 3H, 3-OMe), 4.09 (m, 1H, H5), 3.85 (s, 3H, 2-OMe), 2.34 (t, *J* = 7.3 Hz, 2H, **CH_2**CH_2Me), 1.67 (q, *J* = 15.0 Hz, 8.0 Hz, 2H, CH_2**CH_2**Me), 0.96 (t, *J* = 7.3 Hz, 3H, CH_2CH_2**Me**); ^{13}C NMR ($CDCl_3$) δ 13.61, 18.32, 35.93, 59.51, 60.43, 64.57, 68.02, 75.06, 123.11, 156.93, 169.13, 173.64; EI-MS: *m/z* 274 [M^+], $C_{12}H_{18}O_7$ requires 274.10525, found 274.10519

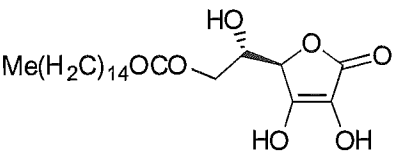

(xi) 6-Palmitate-L-Ascorbic Acid (3.12)[11]

Palmitic acid (4.15 g, 0.016 mol) was added to a solution of ascorbic acid (2.11 g, 0.012 mol) in H_2SO_4 (10 mL). The mixture was heated and stirred for 2 hours

at 25-30°C until it became homogenous. The resulting yellow syrup was left to stand for 2 days at room temperature during which time the colour intensified. The syrup was then poured onto crushed ice, stirred, then extracted with ether, washed gently with brine and dried over Na_2SO_4. The solvent was evaporated under reduced pressure to give a white solid, which was washed extensively with petroleum ether to remove unreacted palmitic acid and the remaining **3.12** was air dried (2.8 g, 42%): mp 112-116°C (lit mp[11] 115-116°C); ^{1}H NMR ($CDCl_3$/DMSO) δ 4.66 (d, *J* = 2.5 Hz, 1H, H4), 4.28 (dd, *J* = 6.8 Hz, 11.2 Hz, 1H, H6a), 4.20 (dd, *J* = 5.8 Hz, 11.2 Hz, 1H, H6b), 4.08 (m, 1H, H5), 2.33 (t, *J* = 7.5 Hz, 2H, CO**CH$_2$**), 1.61 (m, 2H, COCH$_2$**CH$_2$**), 1.25 (s, 26H, **(CH$_2$)$_{13}$**), 0.87 (t, *J* = 6.5 Hz, 3H, Me).

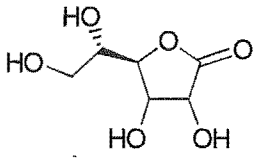

(xii) L-Gulono-1,4-Lactone (3.13)[12]

A solution of ascorbic acid (5 g, 0.03 mol) in water (40 mL) was hydrogenated over 10% Pd/C (0.5 g) in a Parr Hydrogenator at room temperature and 40 psi of hydrogen for 72 hours. The resultant solution was then filtered through celite to remove the Pd/C and the water evaporated under vacuum to give a white solid. **3.13** was recrystallised from methanol-ethyl acetate as colourless prisms (1.29 g, 25%): mp 182-185°C (lit mp[12] 180-181°C); ^{1}H NMR (D_2O) δ 4.64 (d, *J* = 4.4 Hz, 1H, H4), 4.43 (m, 2H, H2 & H3), 3.97 (m, 1H, H5), 3.7 (dd, *J* = 12.2 Hz, 3.4 Hz, 1H, H6a), 3.59 (dd, *J* = 12.2 Hz, 5.8 Hz, 1H, H6b); ^{13}C NMR (D_2O) δ 63.62, 71.70, 72.21, 72.93, 83.47, 180.07; IR: υ_{max} 1782 cm^{-1}; EI-MS: *m/z* (147, 6), (118, 9), (85, 26), (73, 100)

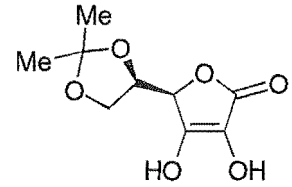

(xiii) 5,6-Isopropylidene-D-Isoascorbic Acid (3.14)[13]

D-isoascorbic acid (10.0 g, 0.06 mol) and dimethoxypropane (10 mL, 0.13 mol) were suspended, with stirring, in boiling acetone (100 mL). To this mixture $SnCl_3$ (0.02 g, 0.35 mmol) was added and the suspension dissolved to give a clear solution. The mixture was reacted for 15 minutes, quenched by the addition of pyridine (50 μL) and then cooled to room temperature. The solvent was evaporated under reduced pressure to give a white, waxy solid, which was washed with dichloromethane to give **3.14** as a white solid which was vacuum filtered then washed with dry ether (8.12 g, 64%) mp 135-137°C; ^{1}H NMR (D_2O) δ 4.88 (d, *J* = 3.0 Hz, 1H, H4), 4.53 (m, 1H, H5), 4.04 (dd, *J* = 9.3 Hz, 7.3 Hz, 1H, H6a), 3.89 (dd, *J* = 9.3 Hz, 5.3 Hz, 1H, H6b), 1.34 (s, 3H, Me), 1.27 (s, 3H, Me); ^{13}C NMR (D_2O) δ 25.790, 26.924, 65.208, 76.452, 77.586, 112.814, 142.149, 158.372, 174.886; EI-MS: *m/z* 216 [M^+], $C_9H_{12}O_6$ requires 216.06339, found 216.06349.

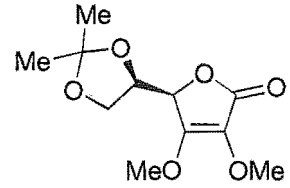

(xiv) 2,3-Di-O-Methyl-5,6-Isopropylidene-D-Isoascorbic Acid (3.15)

To a stirred solution of compound **3.14** (0.5 g, 2.31 mmol) in acetone (30 mL) was added K_2CO_3 (1.0 g, 7.25 mmol) to give a very viscous mixture. Dimethyl sulfate (1.5 mL, 0.016 mol) was added drop-wise and the mixture was refluxed gently overnight. The resulting yellow solution was cooled to room temperature and the excess K_2CO_3 removed by vacuum filtration. The solid residue was washed with cold acetone until all yellow colour was removed and the resulting solution evaporated under vacuum to give an oil. Purification by radial chromatography (40% ethyl acetate/ petroleum ether) gave **3.15** as a brown oil;

(0.388 g, 68%)^{1}H NMR ($CDCl_3$) δ 4.67 (d, *J* = 5.0 Hz, 1H, H4), 4.28 (m, 1H, H5), 4.15 (s, 3H, 3-OMe), 4.02 (dd, *J* = 8.8 Hz, 6.8 Hz, 1H, H6a), 3.91 (dd, *J* = 8.8 Hz, 5.9 Hz, 1H, H6b), 3.85 (s, 3H, 2-OMe), 1.45 (s, 3H, Me), 1.37 (s, 3H, Me); EI-MS: *m/z* 244 [M^+], HRMS $C_{11}H_{16}O_6$ requires 244.09469, found 244.09454.

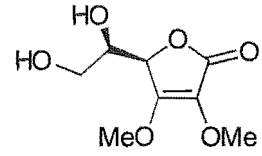

(xv) 2,3-Di-O-Methyl-D-Isoascorbic Acid (3.16)

Compound **3.16** is a colourless oil that resulted from slow hydrolysis of the acetonide group off product **3.15**: ^{1}H NMR (D_2O) δ 4.85 (d, *J* = 3.0 Hz, 1H, H4), 4.07 (s, 3H, 3-OMe), 4.03 (m, 1H, H5), 3.67 (s, 3H, 2-OMe), 3.50 (d *J* = 6.3 Hz, 2H, H6)

(xvi) Attempted Synthesis of C2 and C3 Methoxy Derivatives Using Diazomethane[7]

Ascorbic acid (0.5 g, 2.8 mmol) was dissolved in a 1:1:1 solution of ether, methanol and water (15 mL). To this swirled solution was added dropwise an ethereal solution of diazomethane (10 mmol). The mixture was left for 4 days to allow the excess diazomethane to evaporate and then the solvent was removed under reduced pressure to give a yellow oil.

(xvii) Attempted Synthesis of 2-O-Methyl-5,6-Isopropylidene-L-Ascorbic Acid

To deoxygenated water (7 mL) at 60°C was added compound **3.1** (0.49 g, 2.29 mmol) and 10M aqueous NaOH (dropwise) until pH 10 was reached (universal indicator paper). To this stirred solution was added dimethyl sulfate (0.3 mL, 0.032 mol) dropwise whilst maintaining the pH and temperature, and the mixture was stirred for 1 hour. After cooling to room temperature, the solution was acidified with 10% aqueous H_2SO_4 until pH 3 was reached, and extracted with ethyl acetate. The organic layer was dried over Na_2SO_4 and evaporated under reduced pressure to give a yellow oil.

(xviii) Attempted Synthesis of 2,3-Di-O-Methyl-6-Benzoyl-L-Ascorbic Acid

Compound **3.6** (0.056 g, 0.27 mmol) was dissolved in ethyl butyrate (5 mL, 0.12 mol) and a catalytic amount of pTSA added. The mixture was heated and

stirred overnight at 50°C. The solution was then cooled to room temperature, washed with a saturated $NaHCO_3$ solution and dried over Na_2SO_4. The solvent was removed under reduced pressure to give a yellow oil that was dried under vacuum overnight.

7.2.3 Experimental for Chapter 6

Where indicated, derivatives were prepared according to literature procedures.

7.2.3.1 General Procedures

The following are general procedures employed in the synthesis of some SR inhibitors

(i) (A) N-methylation

2 molar-equivalents of sodium hydride were washed three times with dry pet ether and then dried under nitrogen. Dry glyme and 1 molar-equivalent of lactam-containing compound were added to the sodium hydride and the mixture stirred at reflux under nitrogen for 2 hours. The mixture was cooled to room temperature and iodomethane (6 molar-equivalents) was added carefully to the solution, which was then stirred at reflux for 3 hours. The mixture was cooled to room temperature and water added cautiously to destroy any excess sodium hydride. Solvents were removed under vacuum and the resulting residue was extracted with ethyl acetate. The organic layer was washed with water (3x) and brine before being dried over $MgSO_4$. The solvent was removed under vacuum and if required, the resulting oil was purified by radial chromatography to give the N-methylated product.

(ii) (B) Nitration

The aromatic compound (1 molar-equivalent) was added to concentrated aqueous H_2SO_4 (40 mL) previously cooled in a ice bath. To this stirred solution, KNO_3 (1 molar-equivalent) was added portion-wise over 20 minutes. The mixture was then stirred at 0°C for 1 hour, warmed to room temperature and stirred for a further 1 hour, before being poured onto ice (30 mL) and left to stand until the ice had melted. The aqueous solution was extracted with ethyl acetate (3x), the

extracts combined and then washed with water. The organic layer was washed with saturated bicarbonate solution and brine before being dried over Na_2SO_4. The solvent was evaporated under reduced pressure to give the nitrated product.

(iii) (C) Palladium Coupling[14]

Bromo starting-material (1 molar-equivalent), $Pd(OAc)_2$ (0.1 molar-equivalent), $(o\text{-}tol)_3P$ (0.5 molar-equivalent), triethylamine (1.25 molar-equivalent), styrene (1.25 molar-equivalent), and dry acetonitrile were combined together under a nitrogen atmosphere in a sealed tube and heated at 100°C overnight. The tube was then cooled to room temperature and the contents diluted with 10% aqueous HCl (10.0 mL). The aqueous mixture was extracted with ethyl acetate, washed with water and dried over $NaSO_4$. The solvent was removed under vacuum and the resulting residue purified via radial chromatography.

(iv) (D) Friedel-Crafts Cyclisation Reaction

To a mechanically stirred solution of dichloromethane and $AlCl_3$ (2 molar-equivalents) cooled to -76°C, was added dropwise, the acid chloride (1-molar equivalent) dissolved in dichloromethane. Ethylene gas was then bubbled through the stirred solution for 1 hour at -76°C and then for a further hour while the mixture warmed to room temperature. It was then stirred overnight. The mixture was cooled in an ice salt bath and water (70 mL) was added dropwise to quench the reaction. Mechanical stirring was continued until all solids had dissolved. The organic layer was separated, washed with water, 10% aqueous HCl and saturated $NaHCO_3$ solution before being dried over Na_2SO_4. Evaporation of the solvent gave the product.

7.2.3.2 Tricyclic Derivative s

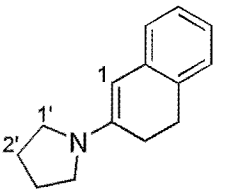

(i) 2-(1-Pyrrolidinyl)-3,4-Dihydronapthalene (6.7)[15]

To a solution of dry toluene (100 mL) and pyrrolidine (9.10 mL, 0.11 mol) was added β-tetralone (2.20 mL, 0.06 mol). The mixture was refluxed for 4 hours under a Dean-Stark condenser containing 4Å molecular sieves. The solution was then cooled to room temperature and the solvent was evaporated under vacuum. The resulting residue was dried overnight under vacuum to give a brown solid that was not purified further (9.6 g, 88%): mp 80 – 81°C; ^{1}H NMR ($CDCl_3$) δ 7.04 – 6.81 (m, 4H, H5 – H8), 5.14 (s, 1H, H1), 3.28 (m, 4H, H1'), 2.84 (m, 2H, H4), 2.49 (m, 2H, H3), 1.93 (m, 4H, H2')

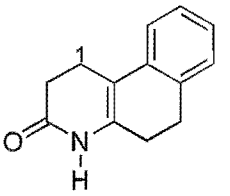

(ii) 1,2,3,4,5,6-Hexahydrobenzo[*f*]quinolin-3-one (6.8)[15]

A flask containing acrylamide (6.86 g, 0.10 mol) was submerged into an oil bath at 85°C and allowed to equilibrate. Product **6.7** (9.60 g, 0.05 mol) and *p*TSA (0.10 g) were quickly added to the molten liquid and the mixture was heated to 100°C for 1 hours. The mixture was further heated at 140°C for 30 minutes to polymerise excess acrylamide, and then cooled to room temperature. The syrup was added to water, (100 mL) and the resulting precipitate was filtered overnight. Purification of the residue by chromatography (50% ethyl acetate/petroleum ether), gave the desired product **6.8,** which was recrystallised from dichloromethane/petroleum ether (5.90 g, 62%): mp 172 - 173°C; ^{1}H NMR ($CDCl_3$) δ 7.53 (bs, 1H, NH), 7.17 (m, 4H, H7 – H10), 2.91 (m, 2H, H6), 2.69(m, 4H, H1 & H2),

2.37(m, 2H, H5); IR: υ_{max} 1664 cm^{-1}; EI-MS: *m/z* 199 [M^+], HRMS, $C_{13}H_{13}NO$ requires 199.09971, found 199.09970.

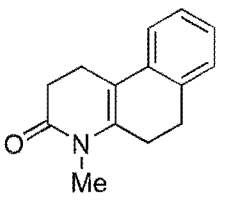

(iii) 4-Methyl-1,2,3,4,5,6-Hexahydrobenzo[*f*]quinolin-3-one (6.9)[15]

This product was prepared as is described in general procedure A. Sodium hydride (0.024 g, 1.0 mmol), dry glyme (7.5 mL) and product **6.8** (0.103 g, 0.5 mmol) were refluxed under nitrogen for 2 hours. Iodomethane (0.2 mL, 3.02 mmol) was added and the mixture stirred at reflux for 3 hours. The mixture was worked up to give compound **6.9** as a brown solid that was recrystallised from dichloromethane/petroleum ether (0.07 g, 67%): mp 98 - 100°C; ^{1}H NMR ($CDCl_3$) δ 7.14 (m, 4H, H7 – H10), 3.14 (s, 3H, NMe), 2.90 (m, 2H, H6), 2.64 (m, 4H, H2 & H1), 2.50 (m, 2H, H5).

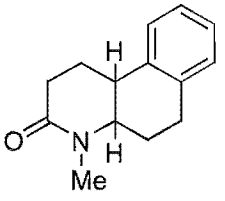

(iv) Cis and Trans-4-Methyl-1,2,3,4,4a,5,6,10b-Octahydrobenzo[*f*]quinolin-3-one (6.3a & 6.3b)[15]

To a solution of product **6.9** (0.38 g, 1.8 mmol) in dichloromethane (7 mL) was added triethylsilane (0.86 mL, 5.4 mmol). The solution was cooled below 0°C and trifluroacetic acid (2.28 mL, 0.03 mol) added dropwise. The mixture was warmed to room temperature and stirred under nitrogen for five days. Volatiles were removed under vacuum and the resulting residue was extracted with dichloromethane, washed with sodium bicarbonate solution and dried over Na_2SO_4. Purification by radial chromatography (gradient elution 10 – 100% ethyl acetate/petroleum ether) gave the trans isomer, followed by the cis compound.

TRANS:(0.16 g, 42%): mp 118 -122°C; ^{1}H NMR ($CDCl_3$) δ 7.14 (m, 4H, H7 - H10), 3.14 (m, 1H, H4a), 2.95 (s, 3H, NMe), 2.93 (m, 2H, H2), 2.72 (m, 1H, H10b), 2.66 – 2.37 (m, 4H, H5 & H6), 1.617 (m, 2H, H1); ^{13}C NMR ($CDCl_3$) δ 23.39, 27.49, 27.87, 29.98, 32.00, 40.79, 60.46, 124.31, 125.65, 126.23, 128.10, 134.86, 136.53, 169.87; IR: υ_{max} 1637 cm^{-1}; EI-MS: *m/z* 215 [M^+], HRMS $C_{14}H_{17}NO$ requires 215.13101, found 215.13164.

CIS:(0.05 g, 13%): mp 129 -131°C; ^{1}H NMR ($CDCl_3$) δ 7.10 (m, 4H, H7 - H10), 3.55 (m, 1H, H4a), 3.15 (m, 1H, H10b), 3.01 (s, 3H, NMe), 2.86 (m, 2H, H6), 2.47 (m, 2H, H2), 2.16 (m, 1H, H1a), 1.99 (m, 2H, H5), 1.85 (m, 1H, H1b); ^{13}C NMR ($CDCl_3$) δ 23.72, 27.83, 28.11, 31.47, 33.32, 37.59, 58.72, 125.92, 126.14, 128.37, 128.73, 134.61, 137.67, 169.19; IR: υ_{max} 1643, 2341, 2361 cm^{-1}; EI-MS: *m/z* 215 [M^+], HRMS $C_{14}H_{17}NO$ requires 215.13101, found 215.13160.

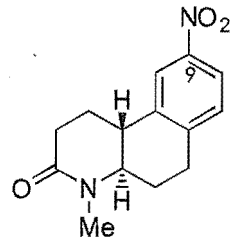

(v) 4-Methyl-9-Nitro-1,2,3,4,4a,5,6,10b-Trans-Octahydrobenzo[f]quinolin-3-one (6.10)[16]

Product **6.3b** (19.7 mg, 0.1 mmol) was dissolved in a solution of H_2SO_4/acetic acid (1:1 v/v, 0.8 mL) which had been cooled below 0°C. Fuming nitric acid (5.5 μL, 0.14 mmol) was added carefully to the cooled solution so that the temperature remained below 10°C. The mixture was stirred for 2 hours at 0°C and then poured into water (10 mL) where product **6.10** formed as a yellow precipitate which was collected by filtration (9.7 mg, 41%): ^{1}H NMR ($CDCl_3$) δ 8.15 (s, 1H, H10), 8.03 (m, 1H, H8), 7.28 (d, *J* = 8.79 Hz, 1H, H7), 3.25 (dt, *J* = 3.418 Hz, 11.23 Hz, 1H, H4b), 3.30 – 2.50 (m, 11H, NMe, H4a, H10b, H2, H6 & H5), 1.78 (m, 2H, H1); ^{13}C NMR ($CDCL_3$) δ 23.68, 27.43, 28.39, 30.54, 32.07, 41.09, 60.22, 120.26, 121.80, 129.44, 138.77, 143.28; EI-MS: *m/z* 260 [M^+], HRMS $C_{14}H_{16}N_2O_3$ requires 260.11609, found 260.11618.

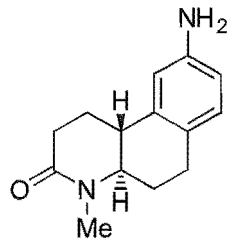

(vi) 4-Methyl-9-Amino-1,2,3,4,4a,5,5,10b-Trans-Octahydrobenzo[*f*]quinolin-3-one (6.11)

To product **6.10** (9.0 mg, 34.6 μmol) dissolved in glacial acetic acid (1 mL), was added PtO_2 (1.0 mg). The mixture was stirred under a H_2 balloon, at room temperature for 3 days then filtered through celite to remove the catalyst. The solvent was removed under reduced pressure and the resulting residue purified by plc (30% methanol/ ethyl acetate) to give product **6.11** as an oil (3.1 mg, 39%): ^1H NMR ($CDCl_3$) δ 6.93 (d, *J* = 7.814 Hz, 1H, H7), 6.62 (s, 1H, H10), 6.56 (d, *J* = 8.302 Hz, 1H, H8), 3.64 – 2.42 (m, 11H, NMe, H4a, H10b, H2, H6, H5), 1.68 (m, 2H, H1); ^{13}C NMR ($CDCl_3$) δ 23.91, 27.55, 28.19, 30.52, 32.48, 41.31, 61.17, 111.57, 114.04, 129.42, 158.91.

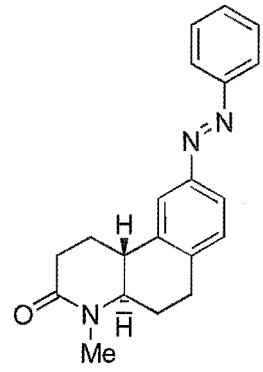

(vii) 4-Methyl-9-Phenylazo-1,2,3,4,4a,5,6,10b-Trans-Octahydrobenzo[f]quinolin-3-one (6.12)

Nitrosobenzene (1.4 mg, 13.5 μmol) dissolved in acetic acid (1 mL) was added to product **6.11** (3.1 mg, 13.5 μmol) and stirred at room temperature for 20 hours. The reaction was quenched by addition of water (0.5 mL) and a yellow precipitate formed. The mixture was extracted with ethyl acetate, washed with saturated bicarbonate and brine then dried over Na_2SO_4. The solvent was

removed under reduced pressure and the resulting yellow residue was purified by column chromatography (5% methanol/ethyl acetate) to give product **6.12** as a yellow oil (3.8 mg, 88%): ^{1}H NMR ($CDCl_3$) δ 7.90 (m, 3H, aromatic), 7.77 (m, 1H, aromatic), 7.50 (m, 3H, aromatic), 7.28 (m, 1H, aromatic), 3.31 (m, 1H, H4a), 3.14 – 2.50 (m, 10H, NMe, H10b, H2, H5 & H6), 1.69 (m, 2H, H1); ES-MS m/z 320 $[M+1]^+$, HRMS $C_{20}H_{22}N_3O$ requires 320.1757, found 320.1763.

CIS: ^{1}H NMR ($CDCl_3$) d 7.36 (m, 2H, aromatic), 7.16 (m, 1H, aromatic), 6.99 (m, 1H, aromatic), 6.84 (m, 3H, aromatic), 6.69 (m, 1H, aromatic), 3.15(m, 1H, H4a), 3.05-2.17 (m, 10H, NMe, H2, H5 & H6), 1.68 (m, 2H, H1)

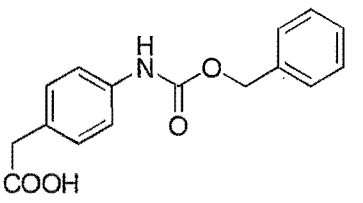

(viii) 4-(Aminobenzocarbamate)-Phenylacetic Acid (6.13)

To a mechanically stirred suspension of 4-aminophenylacetic acid (1.0 g, 6.62 mmol) in water (25 mL) was added $NaHCO_3$ (1.39 g, 0.02 mol). Benzylchloroformate (3.22 mL, 7.95 mmol, 50% in toluene) was added to the solution dropwise and the mixture stirred overnight at room temperature. The mixture was extracted twice with ether and acidified with concentrated HCl to give a white precipitate, which was extracted with ethyl acetate. The organic layers were combined, dried over $MgSO_4$ and the solvent removed under vacuum to give **6.13** as a white solid (1.69 g, 90%): mp 150-151°C; ^{1}H NMR ($CDCl_3$) δ 7.37 (m, 7H, aromatic) 7.22 (m, 2H, aromatic), 6.73 (bs, 1H, NH), 5.20 (s, 2H, **CH_2**Ph), 3.61 (s, 2H, **CH_2**COOH).

To a stirred solution of Acetonitrile (10 mL), DMF (0.16 mL, 2.11 mmol) and oxalyl chloride (61.0 μL, 0.70 mmol) cooled to -20°C, was added product **6.13** (0.2 g, 0.70 mmol) dissolved in acetonitrile (3 mL). The mixture was stirred for 3 hours and then the solvent removed by evaporation to give a yellow oil which was not purified further. ^{1}H NMR (CDCl3) δ 7.29 – 7.09 (m, 7H, aromatic), 5.08 (s, 2H, **CH_2**Ph), 3.47 (s, 2H, **CH_2**COCl).

Attempted synthesis of the cyclic compound **6.15** was carried out as described in general procedure D.

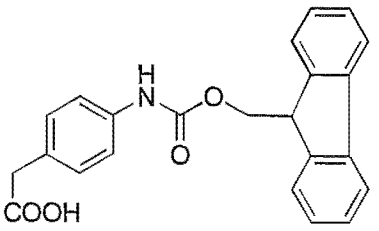

(ix) 4-(Amino-9-Fluromethylcarbamate)-Phenylacetic Acid (6.16)

Dioxane (7 mL) was added to an ice-cooled solution of 4-aminophenylacetic acid (0.20 g, 1.3 mmol), dissolved in 10% aqueous Na_2CO_3 (3.5 mL), and the mixture allowed to equilibrate. To this solution was added 9-fluoromethylchlorocarbamate (0.34 g, 1.3 mmol) portion-wise over 30 minutes. The resulting mixture was stirred in an ice bath for 4 hours then warmed to room temperature and stirred overnight. The mixture, which had formed a white precipitate, was poured into water (50 mL) and the precipitate extracted with ether. The ether was evaporated under reduced pressure to give product **6.16** as a white solid (0.36 g, 73%): mp 210 - 214°C; ^{1}H NMR ($CDCl_3$) δ 7.54 – 6.91 (m, 12H, aromatic), 4.23 (d, *J* = 6.84 Hz, 2H, Fmoc CH_2), 4.02 (m, 1H, Fmoc CH), 3.25 (s, 2H, **CH_2**COOH), FAB-MS: *m/z* 374 [M + 1]$^+$, HRMS $C_{23}H_{20}NO_4$ requires 374.13923, found 374.13981.

To product **6.16** (0.1 g, 0.28 mmol), dissolved in toluene (4 mL), was added 1 drop of DMF and oxalyl chloride (27 μL, 3.10 mmol). The mixture was stirred at room temperature overnight and the solvent evaporated to give a yellow residue ^{1}H NMR ($CDCl_3$) δ 7.78 – 7.16 (m, 12H, aromatic), 4.52 (d, *J* = 6.35 Hz, 1H, Fmoc CH_2), 4.26 (m, 1H, Fmoc C_H), 3.58 (s, 2H, **CH_2**COCl).

Attempted synthesis of the cyclic compound **6.18** was carried out as described in general procedure D.

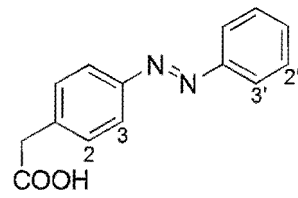

(x) 4-(Phenylazo)-Phenylacetic Acid (6.19)

Nitrosobenzene (0.15 g, 1.41 mmol), dissolved in acetic acid (5 mL), was added to 4-aminophenylacetic acid (0.21 g, 1.41 mmol) and stirred at room temperature for 20 hours. The reaction was quenched by addition of water (1 mL) and a brown precipitate formed. The mixture was extracted with ethyl acetate, the organic solvents combined, washed with saturated bicarbonate solution and brine then dried over Na_2SO_4. The solvent was removed under reduced pressure and the resulting brown residue was purified by column chromatography (50% dichloromethane/petroleum ether) to give product **6.19** as an orange solid (0.05 g, 83%): mp 118 - 120°C; ^{1}H NMR ($CDCl_3$) δ 7.90 (m, 4H, H3 & H3'), 7.39(m, 5H, H2, H2' & H1'), 3.75 (s, 2H, **CH_2**COOH).

To product **6.19** (0.5 g, 2.1 mmol), suspended in acetonitrile (20 mL), was added oxalyl chloride (3 mL, 0.03 mol) dropwise until a clear solution was obtained. The reaction mixture was stirred for 3 hours then the solvent was removed under reduced pressure to give a dark coloured residue that was immediately used in the cyclisation reaction described in general procedure D.

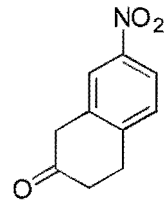

(xi) 7-Nitrotetralone (6.22) and 6-Nitrotetralone (6.23)

A mixture of products **6.22** and **6.23** was prepared as is described in general procedure B. β-Tetralone (0.90 mL, 6.81 mmol), concentrated aqueous H_2SO_4 (40 mL) and KNO_3 (0.7 g, 6.9 mmol) were reacted together and worked up to give products **6.22** and **6.23** as a red/brown oil which was used in a subsequent reaction without further purification (0.83g 63%): **6.22** (53%) ^{1}H NMR ($CDCl_3$) δ 8.10

(m, 1H, H6), 8.03 (s, 1H, H8), 7.42 (d, J = 7.81, 1H, H5), 3.69 (s, 2H, H1), 3.18 (t, J = 6.84 Hz, 2H, H3), 2.60 (m, 2H, H4).

6.23 (10%) ^{1}H NMR ($CDCl_3$) δ 8.13 (s, 1H, H5), 8.10 (m, 1H, H7), 7.30 (d, J = 8.30 Hz, 1H, H8), 3.69 (s, 2H, H1), 3.18 (m, 2H, H3), 2.60 (m, 2H, H4)

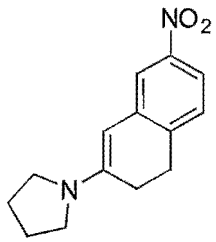

(xii) 7-Nitro-2-(1-Pyrrolidinyl)-3,4-Dihydronapthalene (6.24)

To a stirred solution of product **6.22** (0.3 g, 1.6 mmol) in dry toluene (20 mL) was added pyrrolidine (0.26 mL, 3.1 mmol). The mixture was refluxed overnight under a Dean-Stark condenser containing 4Å molecular sieves. The solution was then cooled to room temperature and the solvent evaporated under vacuum to give a red/brown residue that was partially purified by flash chromatography (20% ethyl acetate/petroleum ether) to give **6.24**; ^{1}H NMR ($CDCl_3$) δ 7.91 (dd, J = 2.44 Hz, 8.79 Hz, 1H, H6), 7.86 (s, 1H, H8), 6.79 (d, J = 8.79 Hz, 1H, H5), 5.20 (s, 1H, H1), 3.36 (m, 4H, H1'), 2.87 (m, 2H, H4), 2.50 (m, 2H, H3), 1.97 (m, 4H, H2').

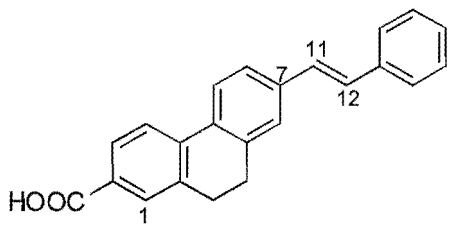

(xiii) 7-Styryl-9,10-Dihydrophenanthrene-2-Carboxylic Acid (6.26)

Product **6.26** was prepared as described in general procedure C. Product **6.27** (49.2 mg, 0.16 mmol), $Pd(OAc)_2$ (8.0 mg, 3.0 μmol), $(o\text{-}tol)_3P$ (2.5 mg, 7.9 μmol), triethylamine (20 μL, 0.2 mmol), styrene (22.0 μL, 0.2 mmol) and acetonitrile (1 mL) were reacted together for 24 hours, and worked up to give **6.28** which was recrystallised from methanol (25 mg, 68%): mp 132-133°C; ^{1}H NMR ($CDCl_3$) δ 7.97 (m, 1H, H3), 7.92 (d, J = 1.47 Hz, 1H, H1), 7.79 (m, 2H, H4 & H5), 7.55 (d, J = 1.47 Hz, 1H, H8), 7.48 (dd, J = 1.95 Hz, 8.30 Hz, 1H, H6), 7.42 – 7.25 (m, 5H, H13 – H17), 7.15

(dd, J = 16.60 Hz, 22.46 Hz, 2H, H11 & H12), 3.93 (s, 3H, Me), 2.93 (m, 4H, H8 & H9); ^{13}C NMR ($CDCl_3$) δ 28.85, 28.91, 52.05, 118.61, 123.50, 124.70, 125.42, 126.23, 126.55, 127.76, 128.12, 128.31, 128.71, 129.12, 129.32, 137.22, 137.49, 138.24, 167.09; EI-MS: m/z 340 [M^+], HRMS, $C_{24}H_{20}O_2$ requires 340.14633, found 340.14649.

Product **6.28** (8.6 mg, 0.025 mmol) and K_2CO_3 (6.9 mg, 0.05 mmol) were refluxed for 18 hours in methanol/water (3 mL, 10:1 v/v). The solvent was removed under reduced pressure and the residue extracted with ethyl acetate and dried over Na_2SO_4. The resulting solid was purified by radial chromatography (5% ethyl acetate/ petroleum ether) to give **6.26** ^1H NMR ($CDCl_3$) δ 7.74 (m, 2H, H1 & H3), 7.61 – 7.44 (m, 3H, H4, H5 & H6), 7.35 – 7.07 (m, 6H, H8 & H13 – H17), 6.95 (d, J = 5.37 Hz, 2H, H11 & H12), 2.73 (m, 4H, H9 & H10).

7.2.3.3 Bicyclic Derivatives

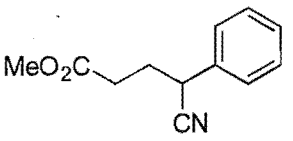

(i) Methyl 4-Cyano-4-(Phenyl)-Butyrate (6.39a)[17,18]

To a stirred mixture of benzyl cyanide (**6.38a**) (4.9 mL, 0.04 mol) and hydroquinone (5.3 mg, 4.8 μmol) was added Triton B (0.59 mL, 1.29 mmol). The mixture was heated to 140°C and methyl acrylate (1.9 mL, 0.02 mol) added dropwise over 30 minutes. The mixture was further heated to 160°C and stirred for 1 hour, then cooled to room temperature and neutralised (pH paper) with glacial acetic acid (15 drops). The mixture was extracted from ether and water, the organic layer dried over $MgSO_4$ and the solvent removed by evaporation. The resulting dark yellow oil was purified by vacuum distillation (3 mmHg) to give product **6.39a** (the fraction which distilled between 170 and 180°C; 1.44 g, 17%): ^1H NMR ($CDCl_3$) δ 7.35 (m, 5H, aromatic), 3.97 (m, 1H, H4), 3.67 (s, 3H, Me), 2.49 (m, 2H, H3), 2.21 (dd, J = 7.33 Hz, 15.14 Hz, 2H, H2); ^{13}C NMR ($CDCl_3$) δ 30.66, 30.71, 36.22, 51.76, 120.13, 127.21, 128.25, 129.12, 134.89, 172.38; IR: υ_{max} 1735, 2259 cm^{-1}; EI-MS: m/z 203 [M^+], HRMS, $C_{12}H_{13}NO_2$ requires 203.09463, found 203.09476.

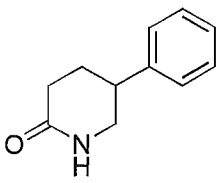

(ii) 5-Phenyl-Piperidone (6.30)[17,18]

To Product **6.39a** (1.0 g, 4.9 mmol) dissolved in glacial acetic acid (10 mL) was added PtO_2 (0.01g). The mixture was agitated at room temperature, and 40 psi of H_2 for 3 days. The mixture was then filtered through celite to remove the catalyst and the solvent was removed under reduced pressure to give product **6.40a** as an oil which was used without further purification: Product **6.40a** (0.90 g 4.3 mmol) was dissolved in dry toluene (25 mL) and refluxed for 20 hours. The solvent was then evaporated under reduced pressure to give a brown oil which crystallised to give product **6.30** (0.47 g 61%): mp 125-127°C; ^{1}H NMR ($CDCl_3$) δ 7.31 (m, 5H, aromatic), 6.18 (bs, 1H, NH), 3.50 (m, 1H, H4a), 3.38 (m, 1H, H4b), 3.07 (m, 1H, H5), 2.52 (m, 2H, H1), 2.08 (m, 2H, H6); ^{13}C NMR ($CDCl_3$) δ 27.66, 31.15, 39.41, 48.45, 126.89, 127.02, 128.64, 141.70, 172.14; IR: υ_{max} 1659 cm^{-1}; EI-MS: *m/z* 175 [M$^+$], HRMS, $C_{11}H_{13}NO$ requires 175.09971, found 175.09986.

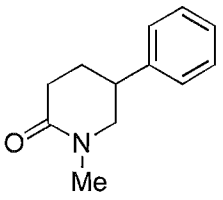

(iii) 5-Phenyl-1-Methyl-2-Piperidone (6.29)[17,18]

Product **6.29** was prepared as is described in general procedure B. Sodium hydride (0.24 g, 4.91 mmol), product **6.30** (0.43 g, 2.46 mmol) and distilled glyme (10 mL) were refluxed under nitrogen for 2 hours. Iodomethane (0.9 mL, 0.02 mol) was added and the mixture stirred at reflux for 3 hours. The mixture was worked up to give product **6.29** as an oil (0.4 g, 87%): ^{1}H NMR ($CDCl_3$) δ 7.30 (m, 5H, aromatic), 3.38 (m, 2H, H4), 3.11 (m, 1H,H5), 2.97 (s, 3H, NMe), 2.54 (m, 2H, H1), 2.06 (m, 2H, H6).

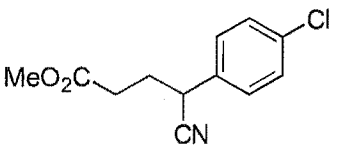

(iv) Methyl 4-Cyano-4-(4-Chlorophenyl)-Butyrate (6.39b)

To a stirred mixture of p-chlorobenzyl cyanide (**6.38b**) (22.76 g, 0.15 mol) and hydroquinone (20.0 mg, 0.18 mmol) was added Triton B (5.5 mL, 12.0 mmol). The mixture was heated to 140°C and methyl acrylate (3.3 g, 38.0 mmol) added dropwise over 30 minutes. The mixture was further heated to 160°C and stirred for 1 hour, then cooled to room temperature and neutralised (pH paper) with glacial acetic acid (15 drops). The mixture was then extracted from ether and water, the organic layer dried over $MgSO_4$ and the solvent removed by evaporation. The resulting oil was purified by vacuum distillation (3 mmHg; bp 170 – 173°C) followed by flash chromatography (30% ethyl acetate/petroleum ether) to give product **6.39b** (2.26 g, 24%): ^{1}H NMR ($CDCl_3$) δ 7.38 (m, 2H, H9 & H10), 7.29 (m, 2H, H8 & H11), 3.98 (m, 1H, H4), 3.70 (s, 3H, Me), 2.51 (m, 2H, H3), 2.20 (m, 2H, H2); IR: υ_{max} 1736, 2259 cm^{-1}; EI-MS: *m/z* 203 [M$^+$], HRMS, $C_{12}H_{12}NO_2Cl$ requires 237.05566, found 237.05570.

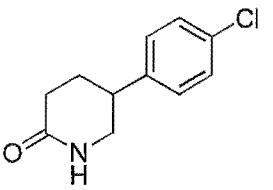

(v) 5-(4-Chlorophenyl)-Piperidone (6.41)

To product **6.39b** (1.94 g, 8.2 mmol) dissolved in glacial acetic acid (10 mL) was added PtO_2 (0.17g). The mixture was agitated at room temperature, 40psi H_2 for 1 day. The mixture was then filtered through celite to remove the catalyst and the solvent was removed under reduced pressure to give product **6.40b** as an oil that was used without further purification: Product **6.40b** (0.90 g 4.3 mmol) was dissolved in dry xylene (16.5 mL) and refluxed for 20 hours. The solid that formed was collected by filtration and washed with xylene to give **6.41** (0.79 g 46%): mp 160 - 163°C; ^{1}H NMR ($CDCl_3$) δ 7.32 (m, 2H, H9 & H10), 7.19 (m, 2H, H8 & H11), 6.09 (bs, 1H, NH), 3.49 (m, 1H, H4a), 3.35 (m, 1H, H4b), 3.05 (m, 1H, H5), 2.51 (m, 2H, H1),

2.06 (m, 2H, H6); ^{13}C NMR ($CDCl_3$) δ 27.66, 31.02, 38.87, 48.33, 128.27, 128.82, 132.80, 140.14, 171.92; IR: υ_{max} 1659 cm^{-1}; EI-MS: *m/z* 209 [M^+], HRMS, $C_{11}H_{12}NOCl$ requires 209.06074, found 209.06066.

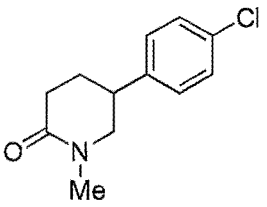

(vi) 5-(4-Chlorophenyl)-1-Methyl-2-Piperidone (6.31)

Sodium hydride (0.15 g, 1.6 mmol), product **6.41** (0.15 g, 0.7 mmol) and toluene (4 mL) were refluxed under nitrogen for 2 hours. Iodomethane (0.68 g, 4.8 mmol) was added and the mixture stirred at reflux for 3 hours. The mixture was worked up as described and the resulting solid recrystallised from ether/ petroleum ether to give product **6.31** as needles (95.0 mg, 59%): ^1H NMR ($CDCl_3$) δ 7.30 (m, 2H, H9 & H10), 7.18 (m, 2H, H8 & H11) 3.37 (m, 2H, H4), 3.10 (m, 1H,H5), 2.98 (s, 3H, NMe), 2.52 (m, 2H, H1), 2.01 (m, 2H, H6); 13C NMR ($CDCl_3$) d 28.01, 31.68, 34.61, 39.60, 56.07, 128.26, 128.83, 132.83, 140.12, 169.25; IR: υ_{max} 1631 cm^{-1}; EI-MS: *m/z* 223 [M^+], HRMS, $C_{12}H_{14}NOCl$ requires 223.07639, found 223.0745.

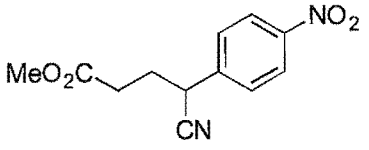

(vii) Methyl 4-Cyano-4-(4-Nitrophenyl)-Butyrate (6.42)

To a stirred solution of 4-nitrobenzylcyanide (**6.35**) (6.96 g, 0.04 mol) and hydroquinone (5.1 mg, 4.8 mmol) in dioxane (10 mL) was added Triton B (0.59 mL, 1.30 mmol). The mixture was heated to 120°C and methyl acrylate (3.84 mL, 0.043 mol) added dropwise over 30 minutes. The mixture was then heated to 160°C and stirred for 2 hours, then cooled to room temperature and neutralised (pH paper) with glacial acetic acid (10 drops). The addition of ice-cold ether caused precipitation of unreacted nitrobenzyl cyanide, which was separated by filtration. The ether-extract was further purified by vacuum distillation (3 mmHg); the product distilling at 180 – 200°C (1.3 g, 13%): ^1H NMR ($CDCl_3$) δ 8.26 (m, 2H, H2' &

H3'), 7.56 (m, 2H, H1' & H4'), 4.18 (m, 1H, H4), 3.71 (s, 3H, Me), 2.55 (m, 2H, H3), 2.24 (m, 2H, H2).

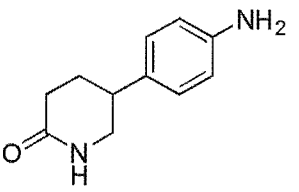

(viii) 5-(4-aminophenyl)-Piperidone (6.44)

To Product **6.42** (1.3 g, 5.2 mmol), dissolved in glacial acetic acid (15 mL), was added PtO_2 (0.01g). The mixture was agitated at room temperature, 40 psi H_2 for 3 days then filtered through celite to remove the catalyst. The solvent was removed under reduced pressure to give product **6.43** as an oil which rapidly polymerised to an insoluble gel. A sample (~0.1 g) was dissolved in excess toluene (500 mL) and refluxed overnight. Evaporation of the solvent gave the crude **6.44** as an oil. 1H NMR (CDCl3) d 7.03 (d, J = 8.30 Hz, 2H, aromatic), 6.66 (d, J = 8.30 Hz, 2H, aromatic), 3.43 (m, 1H, H4a), 3.34 (m, 1H, H4b), 2.88 (m, 1H, H5), 2.48 (m, 2H, H1), 1.96 (m, 2H, H6).

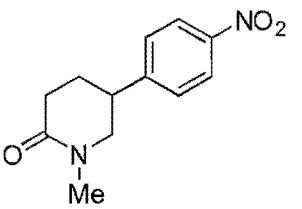

(ix) 5-(4-Nitrophenyl)-1-Methyl-2-Piperidone (6.45)

Product **6.45** was prepared as is described in general procedure B. Product **6.29** (0.23 g, 1.20 mmol), concentrated aqueous H_2SO_4 (15 mL) and KNO_3 (0.12 g, 1.20 mmol) were reacted and worked up to give a yellow residue. Purification by column chromatography (5% methanol/ethyl acetate) gave product **6.45** as a yellow oil (0.14 g, 49%): ^1H NMR ($CDCl_3$) δ 8.21 (d, J = 8.30 Hz, 2H, aromatic), 7.43 (d, J = 8.79 Hz, 2H, aromatic), 3.44 (m, 2H, H4), 3.26 (m, 1H, H5), 2.99 (s, 3H, NMe), 2.54 (m, 2H, H1), 2.10 (m, 2H, H6); EI-MS: m/z 234 [M^+], HRMS $C_{12}H_{14}NO_3$ requires 234.10044, found 234.10100.

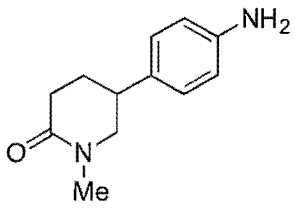

(x) 5-(4-Aminophenyl)-1-Methyl-2-Piperidone (6.34)

To Product **6.45** (0.14 g, 0.58 mmol), dissolved in glacial acetic acid (15 mL), was added PtO_2 (0.01g). The mixture was agitated at room temperature, 40psi H_2 for 3 days then filtered through celite to remove the catalyst. The solvent was removed under reduced pressure and the resulting oil was purified by radial chromatography (5% methanol/ethyl acetate) to give Product **6.34** (0.061g, 51%): ^{1}H NMR ($CDCl_3$) δ 7.02 (m, 2H, aromatic), 6.66 (m, 2H, aromatic), 3.30 (m, 2H, H4), 2.95 (m, 4H, NMe & H5), 2.50 (m, 2H, H1), 2,03 (m, 2H, H6); ^{13}C NMR ($CDCl_3$) δ 28.24, 31.95, 34.64, 39.40, 56.681, 115.27, 127.74.

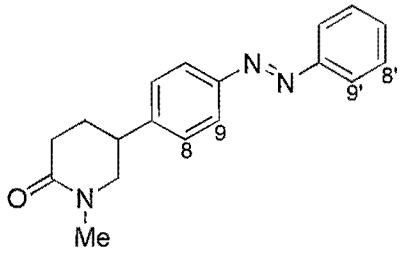

(xi) 5-(p-Phenylazobenzyl)-1-Methyl-2-Piperidone (6.32)

Nitrosobenzene (0.01 g, 98 μmol), dissolved in acetic acid (1 mL), was added to product **6.34** (0.018 g, 98 μmol) and stirred at room temperature for 20 hours. The reaction was quenched by addition of water (0.5 mL) and a yellow precipitate formed. The mixture was extracted with ethyl acetate, washed with saturated bicarbonate and brine, then dried over Na_2SO_4. The solvent was removed under reduced pressure and the resulting yellow residue purified by column chromatography (100% ethyl acetate) to give product **6.32** as orange crystals (0.016 g, 62%): mp 128 – 131°C; ^{1}H NMR ($CDCl_3$) δ 7.89 (m, 4H, H9, H9', H11 & H11'), 7.50 (m, 3H, H7', H8', H12'), 7.37 (d, J = 8.302 Hz, 2H, H8 & H12), 3.39 (m, 2H, H4), 3.16 (m, 1H, H5), 2.97 (s, 3H, NMe), 2.53 (m, 2H, H1), 2.07 (m, 2H, H6); ^{13}C NMR ($CDCl_3$) δ 27.97, 31.68, 34.61, 40.06, 55.93, 122.72, 123.10, 127.62, 129.01, 130.98,

144.68, 151.65, 152.45, 169.26; IR: υ_{max} 1637 cm^{-1}; EI-MS: *m/z* 293 [M^+], HRMS $C_{18}H_{19}N_3O$ requires 293.15281, found 293.15287.

CIS ^1H NMR ($CDCl_3$) δ 7.26 (m, 2H, H8 & H12), 7.14 (m, 3H, H7', H8' & H12'), 6.83 (d, J = 8.302 Hz, 4H H9, H9' H11 and H11'), 3.33 (m, 2H, H4), 305 (m, 1H, H5), 2.95 (s, 3H, NMe), 2.48 (m, 2H, H1), 2.00 (m, 2H, H6)

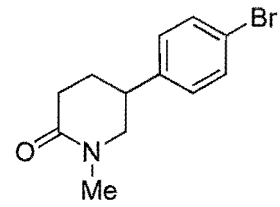

(xii) 5-(4-Bromophenyl)-1-Methyl-2-Piperidone (6.36)

$CuBr_2$ (0.66 g, 0.29 mmol) and *t*-Butylnitrite (0.044mL, 0.37 mmol) were suspended in dry acetonitrile (1.5 mL) and cooled in an ice bath. On addition of product **6.34** (0.05 g, 0.25 mmol), dissolved in dry acetonitrile (0.5 mL), the stirred suspension turned black and a gas was evolved. The mixture was stirred on an ice bath for 0.5 hours, warmed to room temperature, then stirred for a further 2 hours. The mixture was then poured into 20% HCl (5 mL) and extracted with ether. The organics were washed with 20% HCl, dried over $MgSO_4$ and the solvent removed under reduced pressure to give a yellow residue. Purification by radial chromatography (80% ethyl acetate/ petroleum ether) gave product **6.36** as an oil (8.3 mg, 13%):^1H NMR ($CDCl_3$) δ 7.46(d, *J* = 8.30 Hz, 2H, H2' & H4'), 7.12 (d, *J* = 8.79 Hz, 2H, H1' & H5'), 3.36 (m, 2H, H4), 3.04 (m, 1H, H5), 2.97 (s, 3H, NMe), 2.51 (m, 2H, H1), 2.02 (m, 2H, H6); EI-MS: *m/z* 269 [M^+, ^{81}Br], 267 [M^+ ^{79}Br], HRMS $C_{12}H14NOBr^{81}$ requires 269.02396, found 269.02358, $C_{12}H_{14}NOBr^{79}$ requires 267.02588, found 267.02538.

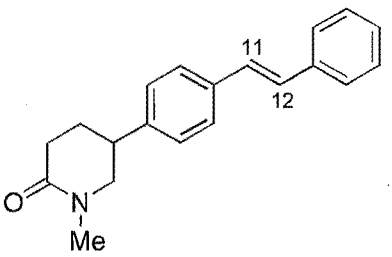

(xiii) 5-(4-Stilbenyl)-1-Methyl-2-Piperidone (6.33)

Product **6.33** was prepared as is described in general procedure C. Product **6.36** (8.3 mg, 31 μmol), $Pd(OAc)_2$ (7.0 mg, 3.1 μmol), $(o\text{-}tol)_3P$ (4.7 mg, 0.72 mmol), triethylamine (5.4 μL, 38.7 μmol), styrene (4.5 μL, 38.7 μmol) and acetonitrile (0.5mL) were reacted together for 24 hours and worked up to give product **6.33** as a white solid (6.1 mg, 68%): ^1H NMR ($CDCL_3$) δ 7.53 – 7.22 (m, 9H, aromatic), 7.09 (s, 2H, H11 & H12), 3.40 (m, 2H, H4), 3.10 (m, 1H, H5), 2.99 (s, 3H, NMe), 2.54 (m, 2H, H1), 2.07 (m, 2H, H6); ^{13}C NMR ($CDCL_3$) δ 28.01, 31.80, 34.73, 39.95, 56.23, 126.45, 126.79, 127.28, 127.68, 127.96, 128.23. 128.67, 128.75, 136.33, 137.13, 141.01; EI-MS: *m/z* 291 [M^+] HRMS $C_{20}H_{21}NO$ requires 291.16231, found 291.16293.

7.2.3.4 Thiolactam Derivatives

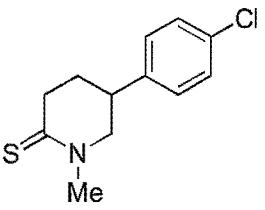

(i) 5-(4-Chlorophenyl)-1-Methyl-2-Thiopiperidone (6.46)

Product **6.31** (0.06 g, 0.25 mmol), Lawesson's reagent (0.3 g, 0.74 mmol) and THF (1.5 mL) were reacted for 15 minutes. The solution was then filtered, the solvent evaporated and the resulting residue recrystallised from ether/petroleum ether to give **6.46** as a pale solid.(0.52 g, 87%): mp143 - 146°C; ^1H NMR ($CDCl_3$) δ 7.32 (m, 2H, H9 & H10), 7.15 (m, 2H, H8 & H11), 3.64 (dd, J = 13.67 Hz, 5.37 Hz, 1H, H4a), 3.49 (s, 3H NMe), 3.46 – 2.95 (m, 4H, H4b, H5 & H1), 1.96 (m, 2H, H6) ^{13}C NMR ($CDCl_3$) δ 27.43, 39.51, 41.42, 58.98, 128.25, 129.00, 133.12, 139.57, 198.74; IR: υ_{max} 2937 cm^{-1}; EI-MS: *m/z* 239 [M^+], HRMS $C_{14}H_{17}NS$ requires 239.05355, found 239.05356.

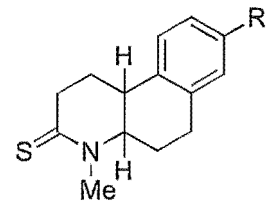

(ii) 4-Methyl-3-Thiol-1,2,3,4,4a,5,6,10b-Trans-Octahydrobenzo[*f*]quinolinone (6.47)

Product **6.3b** (0.02 g, 93 μmol) and Lawesson's reagent (0.11 g, 0.28 mmol), dissolved in THF (1 mL), were stirred together for 30 minutes at room temperature. The solution was then filtered, the solvent evaporated and the resulting residue purified by radial chromatography (20% ethyl acetate/ petroleum ether) to give **6.39** as a pale solid (9.8 mg, 45%): ^{1}H NMR ($CDCl_3$) δ 7.18 (m, 4H, H7 – H10), 3.54 (s, 3H, NMe), 3.38 (m, 2H, H4a & H2a), 3.18 – 2.86 (m, 4H, H2b, H6 & H10b), 2.59 (m, 1H, H5a), 2.45 (m, 1H, H1a), 1.76 (m, 2H, H1b & H5b); ^{13}C NMR ($CDCl_3$) δ 23.51, 28.00, 28.24, 39.66, 41.33, 42.28, 64.31, 124.59, 126.35, 126.93, 128.41, 134.89, 137.10; EI-MS: *m/z* 231 [M^+], HRMS $C_{14}H_{17}NS$ requires 231.10817, found 231.10865.

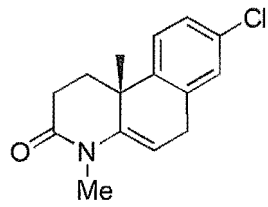

(iii) 10b-Methyl-8-Chloro-4-Methyl-1,2,6-Trihydrobenzo[*f*]quinolin-3-one (6.51)

This compound was prepared as described in general procedure A. Sodium hydride (0.01 g, 0.45 mmol), distilled glyme (7.5 mL) and 10b-methyl-8-chloro-1,2,6-trihydrobenzo[f]quinolin-3-one (0.05 g, 0.23 mmol) were stirred at reflux under nitrogen for 2 hours. Iodomethane (84 μL, 1.4 mmol) was added and the mixture refluxed for 3 hours. The mixture was worked up and product **6.51** was used without further purification (0.04 g, 82%): ^{1}H NMR ($CDCl_3$) δ 7.18 (m, 3H, H7, H9 & H10), 5.29 (m, 1H, H5), 3.48 (m, 2H, H6), 3.19 (s, 3H, NMe), 2.70 (m, 2H, H2), 2.29 (m, 1H, H1), 1.94 (m, 1H, H1), 1.30 (s, 3H, Me).

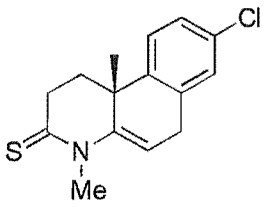

(iv) 10b-Methyl-8-Chloro-4-Methyl-3-Thiol-1,2,6-Trihydrobenzo[*f*]quinolinone (6.48)

Product **6.51** (15.7 mg, 0.06 mmol), and Lawesson's reagent (0.017 g, 0.042 mmol) dissolved in THF (2 mL), were reacted for 6 hours at reflux. The solution was then cooled, filtered, and the solvent removed under reduced pressure to give a residue that was purified by radial chromatography (30% ethyl acetate/ petroleum ether) to give **6.48** as a pale solid (9.7 mg, 58%); ^{1}H NMR ($CDCl_3$) δ 7.25 (m, 2H, H9 & H10), 7.16 (s, 1H, H7), 5.70(m, 1H, H5), 3.81 (s, 3H, NMe), 3.57 (m, 2H, H6), 3.23 (m, 2H, H2), 2.12 (m, 2H, H1), 1.34 (s, 3H Me)

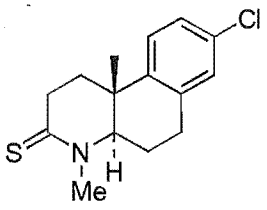

(v) 10b-Methyl-8-Chloro-4-Methyl-3-Thiol-1,2,4a,5,6-Pentabenzo[*f*]quinolinone (6.49)

6-Chloro-4-methyl-1,2,4a,5,6-pentabenzo[*f*]quinolinone (0.015 g, 0.06 mmol) and Lawesson's reagent (0.02g, 0.05 mmol) were stirred in THF (1 mL) at 60°C overnight. The solution was filtered and the solvent evaporated to give a residue that was purified by radial chromatography (30% ethyl acetate/ petroleum ether) to give **6.49** (8.5 mg, 54%); ^{1}H NMR ($CDCl_3$) δ 7.17 (m, 2H, H7 & H9), 7.08 (m, 1H, H10), 3.72 (m, 1H, H4a), 3.57 (s, 3H, NMe), 3.35 (m, 1H, H2), 3.02 (m, 3H, H2 & H6), 2.41 (m, 1H, H5), 2.18 (m, 1H, H5), 2.15 (m, 2H H1), 1.09 (s, 3H, Me)

Proton-NMR data for the starting material used to prepare compound **6.49** is as follows ^{1}H NMR ($CDCl_3$) δ 7.16 (m, 3H aromatic), 3.49 (dd, J = 3.42 Hz, 13.19 Hz, 1H, H4a), 3.03 (s, 3H, NMe), 2.99 (m, 2H, H2), 2.63 (m, 2H, H6), 2.34 (m, 2H, H5), 1.86 (m, 2H, H1)

7.2.3.5 Photoisomerisation Experiments

Photoisomerisation of products **6.19** and **6.32** was carried out using the following procedure.

The sample dissolved in $CDCl_3$ was prepared as for NMR analysis. A proton spectrum was taken of the sample, which was then irradiated with light from a filtered (330 – 370 nm) mercury lamp for 1 hour. Following initial irradiation, the sample was analysed by proton-NMR spectroscopy and then subjected to a further hour of irradiation from the mercury lamp at >400 nm wavelength. The sample was then again analysed by proton-NMR spectroscopy.

7.3 References

(1) Megazyme Alpha Amylase Assay Procedure (Ceralpha method), For the measurement of cereal and microbial alpha-amylases.

(2) Vogel, A. I. *Vogels Textbook of Practical Organic Chemistry*, 5th ed.; Longman Group: Singapore, 1998.

(3) Perrin, D. D.; Armarego, W. L. F.; Perrin, D. R. *Purification of Laboratory Chemicals*, 2nd ed.; Pergamon Press:, 1980.

(4) Harrison Research Inc. Chromatotron Users Manual.

(5) Sheldrick, G. M. *Acta. Crystallogr.,Sect. A* **1990**, *46*, 467.

(6) Sheldrick, G. M. SHELXL-93; University of Gottingen 1993.

(7) Jung, M. E.; Shaw, T. J. *J. Am. Chem. Soc.* **1980**, *102*, 6304-6311.

(8) Nihro, Y.; Miyataka, H.; Sudo, T.; Matsumoto, H.; Satoh, T. *J. Med. Chem.* **1991**, *34*, 2152-2157.

(9) Haworth, W. N.; Hirst, E. L.; Smith, F. *J. Chem.* **1934**, 1556-1560.

(10) Creighton, M.; Wenner, W.; Wuest, H. M. *J. Org. Chem.* **1948**, *13*, 613-615.

(11) Cousins, R. C.; Seib, P. A.; Hoseney, R. C.; Deyoe, C. W.; Liang, Y. T.; Lillard, D. W., Jr. *Journal of the American Oil Chemists' Society* **1977**, *54*, 308-312.

(12) Andrews, G. C.; Crawford, T. C.; Bacon, B. E. *J. Org. Chem.* **1981**, *46*, 2976-2977.

(13) Vekemans, J. A. J. M.; Boerekamp, J.; Godefroi, E. F.; Chittenden, G. J. F. *Recl. Trav. Chim. Pays-Bas* **1985**, *104*, 266-272.

(14) Ziegler, C. B., Jr.; Heck, R. F. *J. Org. Chem.* **1978**, *43*, 2941-2947.

(15) Jones, C. D.; Audia, J. E.; Lawhorn, D. E.; McQuaid, L. A.; Neubauer, B. L.; Pike, A. J.; Pennington, P. A.; Stamm, N. B.; Toomey, R. E.; Hirsch, K. S. *J. Med. Chem.* **1993**, 36, 421-423.

(16) Lilly. USA Patent EP 0 532 190 A2, 1993.

(17) Shen, T.; Witzel, B. E. U.S.A. Patent 808,660, 1969.

(18) Julia, M.; Siffert, O.; Bagot, J. *Journal Bulletin De La Societe Chimique De France* **1968**, *3*, 1000-1005.

APPENDIX A

A DERIVATION OF THE MICHAELIS–MENTEN EQUATION.[175,48]

The Michaelis-Menten (M-M) model for an enzyme system is shown below.

$$E + S \underset{k_{-1}}{\overset{k_1}{\rightleftharpoons}} ES \xrightarrow{k_2} E + P \qquad \text{(A1.1)}$$

The free enzyme (E) and substrate (S) bind reversibly to form the enzyme-substrate complex (ES) which then reacts to release the enzyme and products (P). The total enzyme in the system is given by

$$E_T = [E] + [ES] \qquad \text{(A1.2)}$$

To derive a rate equation for the M-M model, it is assumed that the substrate is in excess relative to the concentration of enzyme, so the enzyme is working at its highest catalytic rate. This then allows for the application of the steady-state approximation (that is, the concentration of the ES complex quickly reaches a level at which it remains throughout the reaction). The rate of formation of ES is given by

$$\frac{d[ES]}{dt} = k_1[E][S] - k_{-1}[ES] - k_2[ES] = 0 \qquad \text{(A1.3)}$$

Solving for [E] gives

$$[E] = \frac{K_m[ES]}{[S]} \qquad \text{(A1.4)}$$

where

$$K_m = \frac{k_{-1} + k_2}{k_1} \qquad \text{(A1.5)}$$

is the Michaelis constant. The equation for the total enzyme may then be expressed as

$$[ES] = \frac{E_T[S]}{K_m + [S]} \qquad \text{(A1.6)}$$

If the rate-determining step of the reaction is the conversion of ES to P, then the overall rate (υ) is given by

$$\upsilon = k_2[ES]$$

$$\upsilon = \frac{k_2 E_T[S]}{K_m + [S]} \qquad \text{(A1.7)}$$

Derivations of the Michaelis-Menten equation in the presence of inhibitors.[1,2]

Competitive Inhibitors

A model for competitive inhibition is given by the following reaction scheme.

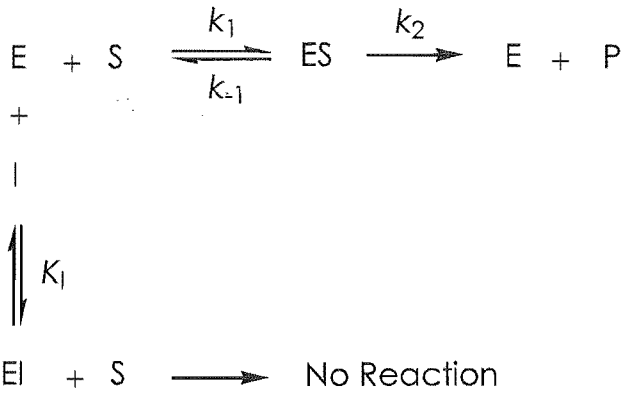

I is the inhibitor, EI is the enzyme-inhibitor complex and K_I is the dissociation constant for the EI complex. The EI complex is assumed to be in equilibrium with the free reagents so

$$[EI] = \frac{[E][I]}{K_I} \qquad \text{(A1.8)}$$

Assuming steady-state conditions for ES, the amount of free enzyme E is given by (A1.4) so (A1.8) becomes

$$[EI] = \frac{K_m[ES][I]}{K_I[S]} \qquad \text{(A1.9)}$$

The total enzyme E_T is now equal to [E] + [ES] + [EI], or:

$$E_T = \frac{[ES]}{[S]} + [ES] + \frac{K_m[ES][I]}{K_I[S]} \qquad \text{(A1.10)}$$

Thus,

$$[ES] = \frac{E_T[S]}{K_m(1 + \frac{[I]}{K_I}) + [S]} \qquad (A1.11)$$

The rate of the reaction then becomes

$$\upsilon = k_2[ES]$$

$$\upsilon = \frac{V_{max}[S]}{\alpha K_m + [S]} \qquad (A1.12)$$

where

$$V_{max} = k_2 E_T$$

$$\alpha = 1 + \frac{[I]}{K_I} \qquad (A1.13)$$

UNCOMPETITIVE INHIBITORS

A model for uncompetitive inhibition is given by the following reaction scheme.

$$E + S \underset{k_{-1}}{\overset{k_1}{\rightleftharpoons}} ES \xrightarrow{k_2} E + P$$

$$ES + I \rightleftharpoons ESI \quad (K_I')$$

$$ESI \longrightarrow \text{No Reaction}$$

ESI is the enzyme-substrate-inhibitor complex and K_I' is the dissociation constant for the ESI complex. The ESI complex is assumed to be in equilibrium with the ES complex thus

$$K_I' = \frac{[ES][I]}{[ESI]} \qquad (A1.14)$$

The total enzyme E_T is now given by

$$E_T = [E] + [ES] + [ESI] \qquad (A1.15)$$

Substituting [A1.4] and [A1.14] into [A1.15] gives

$$[ES] = \frac{E_T[S]}{K_m + (\frac{[I]}{K_I'} + 1)[S]} \qquad (A1.16)$$

so the rate of the reaction is now given by

$$\upsilon = \frac{V_{max}[S]}{K_m + \alpha'[S]} \qquad \text{(A1.16)}$$

where

$$\alpha' = \frac{[I]}{K_I'} + 1 \qquad \text{(A1.17)}$$

NON-COMPETITIVE INHIBITORS

A model for non-competitive inhibition is given by the reaction scheme:

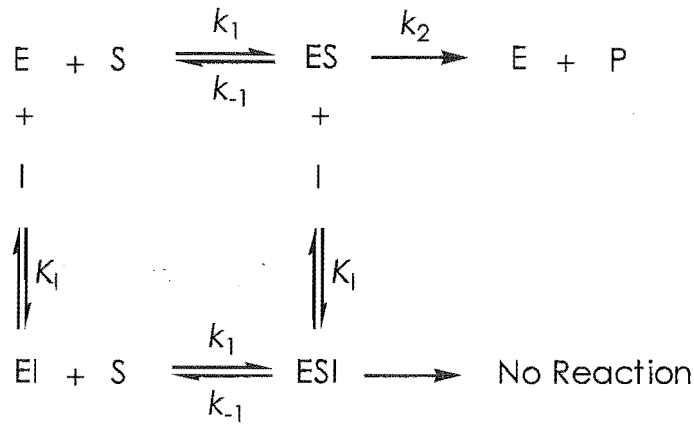

As the inhibitor I does not bind to the active site of the enzyme the dissociation constant K_I for the inhibitor binding the free enzyme E and the enzyme-substrate complex ES is the same thus

$$K_I = \frac{[ES][I]}{[ESI]} = \frac{[E][I]}{[EI]} \qquad \text{(A1.18)}$$

The total enzyme concentration is then given by

$$E_T = [E] + [ES] + [EI] + [ESI] \qquad \text{(A1.19)}$$

Substitution of (A1.4), (A1.9) and (A1.14) into (A1.19) gives

$$[ES] = \frac{E_T[S]}{\alpha(K_m + [S])} \qquad \text{(A1.20)}$$

so the rate of the reaction is given by

$$\upsilon = \frac{V_{max}[S]}{\alpha(K_m + [S])} \qquad \text{(A1.21)}$$

MIXED INHIBITORS

A model for mixed inhibition is similar to that of non-competitive model and is given by the following reaction scheme.

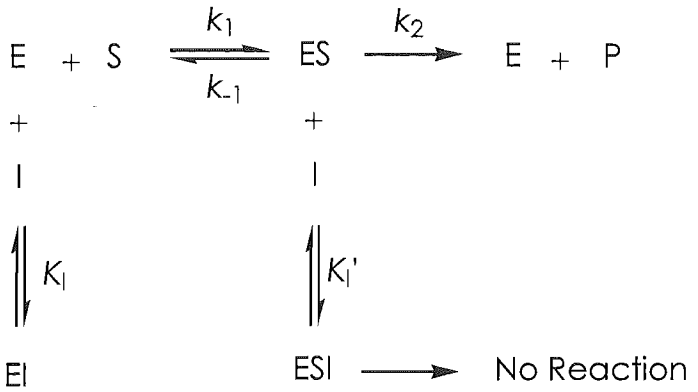

For mixed inhibition, the dissociation constant for the EI and ESI complexes are different. Therefore,

$$[ES] = \frac{E_T[S]}{K_m(1 + \frac{[I]}{K_I}) + [S](1 + \frac{[I]}{K_I'})} \qquad [A1.19]$$

and

$$\upsilon = \frac{V_{max}[S]}{K_m\alpha + [S]\alpha'} \qquad [A1.20]$$

Discussion of Kinetic Parameters

V_{max}

V_{max} is the maximum rate of the catalysed reaction when the enzyme is operating under substrate saturation conditions.

K_m

K_m (the *Michaelis constant*) has units of mol/L. Its value is equal to the concentration of substrate at which the enzyme achieves half its maximal rate, V_{max}. Therefore, K_m provides a measure of the catalytic efficiency of the enzyme; the smaller the value of K_m the more efficient the enzyme. K_m can also be considered in terms of the affinity of the enzyme for its substrate, where a smaller value indicates an increased affinity.

References

(1) Voet, D.; Voet, J. G. *Biochemistry*; John Wiley and Sons: New York, 1990.

(2) Mathews, C. K.; van Holde, K. E. *Biochemistry*; Benjamin/Cummings: Redwood City, 1990.

Appendix B

Transformations of the Michaelis-Menten Rate-equation

The following is a discussion of useful linear and direct-linear transformations of the M-M rate-equation in the absence and presence of inhibitors.

Linear Plots

Lineweaver-Burk (Double-Reciprocal plot)

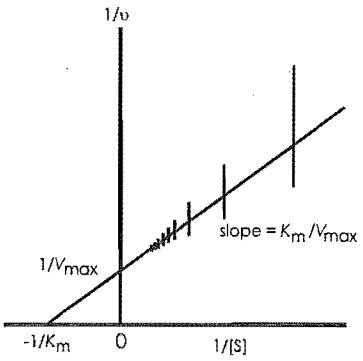

$$\frac{1}{\upsilon} = \frac{1}{V_{max}} + \frac{K_m}{V_{max}} \cdot \frac{1}{[S]}$$

Figure B.1: Double-reciprocal plot of the Michaelis –Menten rate-equation. Also shown is the trend in errors of the plotted data that arises due to a constant absolute-error in the rate measurements.

The Lineweaver-Burk or double-reciprocal plot (Figure B.1) is generated by plotting 1/[S] (on the abscissa) against 1/υ (on the ordinate). The straight line produced has a slope of K_m/V_{max}, a ordinate-intercept of $1/V_{max}$, and an abscissa-intercept of $-1/K_m$.

Although the values of V_{max} and K_m are simply related to the slope and ordinate-intercept of this plot, the large errors associated with the inversion of small values of [S] and, in particular υ (for which the errors are generally larger than for [S]) prevent an accurate estimate of the line-of-best-fit for the data points, and thus an unreliable measure of K_m and V_{max}.[1]

The Eadie-Hofstee and Hanes plots detailed below, although not entirely free from distortion, are less severely affected than the double-reciprocal plot.

EADIE-HOFSTEE PLOT

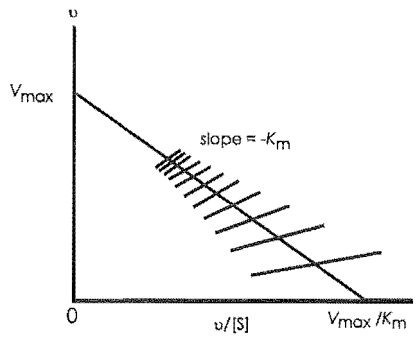

$$\upsilon = V_{max} - K_m \frac{\upsilon}{[S]})$$

Figure B.2: Eadie-Hofstee plot of the M-M rate-equation. Also shown is the trend in errors of the plotted data points resulting from a constant absolute-error in the rate measurements.

The Eadie-Hofstee plot is generated by plotting $\upsilon/[S]$ (on the abscissa) against υ (on the ordinate). The resulting line has a slope of $-K_m$, a ordinate-intercept of V_{max} and an abscissa-intercept of V_{max}/K_m. As can be seen in Figure B.2, υ occurs in both of the plotted variables axes, and the error associated with it results in an angular distortion to the error bars.

HANES PLOT

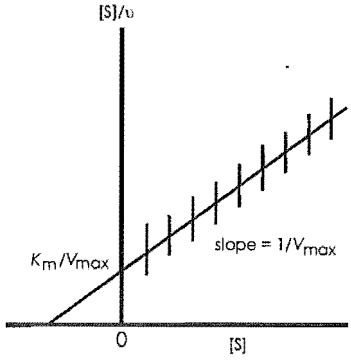

$$\frac{[S]}{\upsilon} = \frac{K_m}{V_{max}} + \frac{1}{V_{max}} \cdot [S]$$

Figure B.3: Hanes plot of the Michaelis- Menten rate-equation. Also shown is the trend in errors of the plotted data that arises due to a constant absolute-error the rate measurements.

This representation of the M-M rate-equation demonstrates that a plot of [S] (on the abscissa) against $[S]/\upsilon$ (on the ordinate) gives a straight line with a slope of $1/V_{max}$, a ordinate-intercept of K_m/V_{max} and an abscissa-intercept of $-K_m$. As can be seen from Figure B.3 the error associated with each data point, due to the rate measurements, varies less than for the double-reciprocal plot. Kinetic parameters generated from this plot are more reliable than those from a Lineweaver-Burk or Eadie-Hofstee plots.[2]

DIRECT-LINEAR PLOTS

Two forms of direct-linear plot are shown in Figure B.4. Each is generated by treating the observed values of υ and [S] as constants and K_m and V_{max} as variables. Joining the point at which each υ datum lies on ordinate, with the point at which the corresponding [S] datum lies on the abscissa, results in a family of lines. The abscissa and ordinate coordinates for the intersections between these lines are distributed about the true value of K_m and V_{max}. The best overall estimate of K_m and V_{max} of the system is given by the median of coordinates of all intersections.*[2]

The plot in Figure B.4 (**B**) has an advantage over that in (**A**) since it provides more clearly-defined intersection points, although the latter is an easier plot to construct.

The values of K_m and V_{max} estimated by the use of direct-linear plots are considered to be statistically similar to values generated by a least-squares fits of the observed data to the M-M rate-equations.[2]

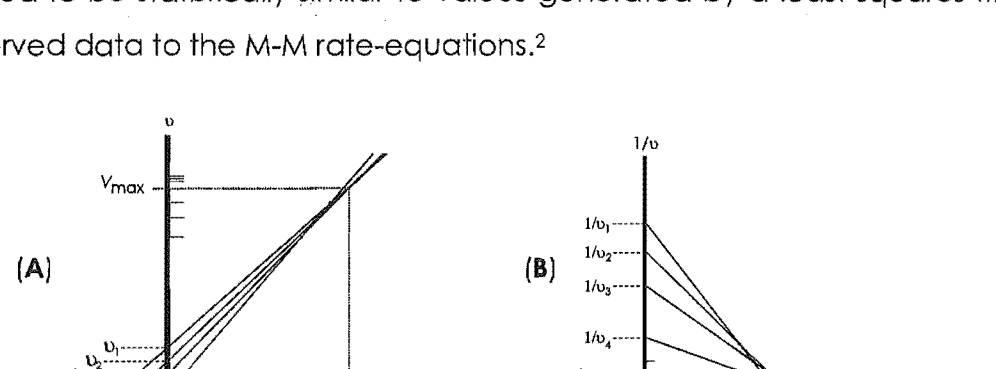

Figure B.4: Direct-linear plots . Lines are constructed by joining the points at which the measured data coordinates lie on the abscissa and ordinate. (**A**) υ data is marked on the ordinate and −[S] on the abscissa. (**B**) 1/υ is marked on the ordinate and [S]/υ on the abscissa.

* For an even number of intercepts the average of the two middle observations is used.

Plots of the Michaelis–Menten Rate-Equation in the Presence of Inhibitors

Derivation of the M-M rate-equation in the presence of competitive, uncompetitive, non-competitive and mixed inhibitors has been shown in appendix A. The following linear plots for each of the cases demonstrate the effect of each type of inhibitor on the kinetic parameters of K_m and V_{max}, and allow determination of the mode of inhibition and the inhibitor-enzyme dissociation constant K_I and/or K_I'.

In the following, for the double-reciprocal (Lineweaver-Burk) plots the terms α and α' refer to $1 + [I]/K_I$ and $1 + [I]/K_I'$ respectively, whereas for the Dixon plot, $\alpha = 1 - K_I/K_I'$, and for the modified Dixon plot, $\alpha = 1 - K_I'/K_I$.

Double-reciprocal plots

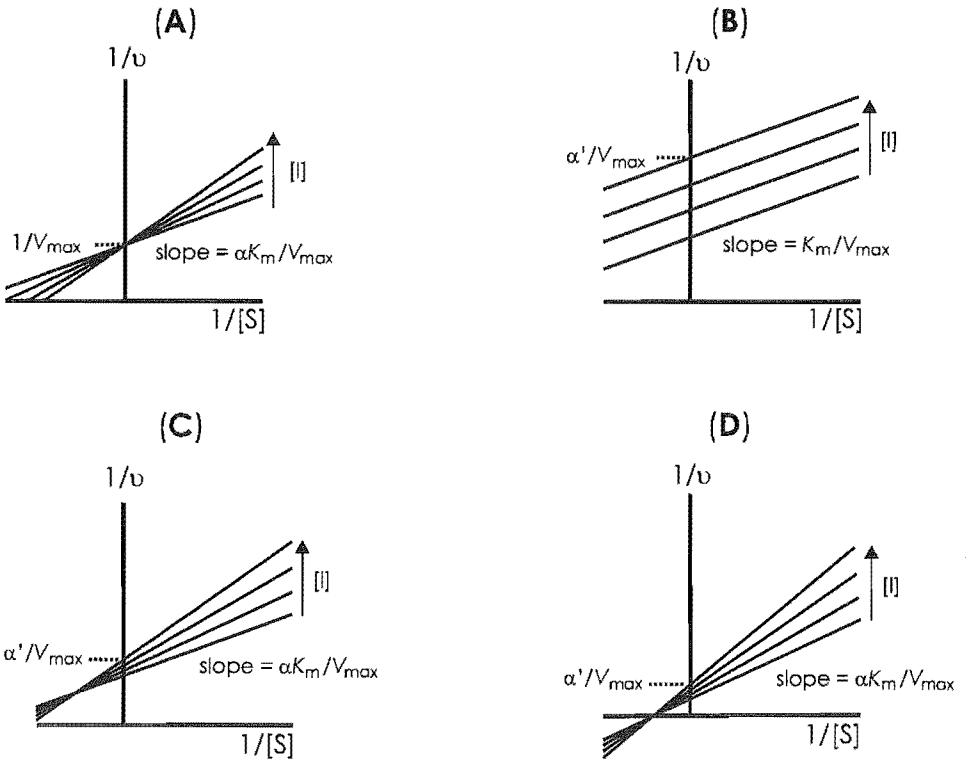

Figure B.5: Lineweaver-Burk plots in the presence of (**A**) a competitive inhibitor, (**B**) an uncompetitive inhibitor, (**C**) a mixed inhibitor, and (**D**) a non-competitive inhibitor.

The appearance of the double-reciprocal plots for a series of inhibitor concentrations is dependent on the mode of inhibition (Figure B.5).

Consider the M-M rate-equation for a competitive inhibitor:

$\frac{1}{\upsilon} = \frac{K_m\alpha}{V_{max}} \cdot \frac{1}{[S]} + \frac{1}{V_{max}}$ as the concentration of inhibitor increases, the term α gets larger so that the apparent K_m (αK_m) also increases. The resulting appearance in a double-reciprocal plot, is a line with a steeper gradient than that resulting from a system containing less inhibitor. The V_{max} for the system is unaffected by a competitive so that the intercept of these lines with the $1/\upsilon$ axis remains unchanged in this case (Figure B.5 (**A**)).

In the presence of an uncompetitive inhibitor, the M-M rate-equation is given by

$$\frac{1}{\upsilon} = \frac{K_m}{V_{max}} \cdot \frac{1}{[S]} + \frac{\alpha}{V_{max}}$$

In this system K_m is independent of the concentration of inhibitor, and thus so to is the slope of the line in the double-reciprocal plot. However, the inhibitor concentration does change the ordinate-intercept such that the apparent V_{max} increases with increasing [I] (Figure B.5 (**B**)).

For a mixed or non-competitive inhibitor, the M-M rate-equation may be expressed as

$$\frac{1}{\upsilon} = \frac{K_m\alpha}{V_{max}} \cdot \frac{1}{[S]} + \frac{\alpha'}{V_{max}}$$

In terms of this expression, the only difference between these two models is that for the latter $\alpha = \alpha'$. Thus, these two models behave equivalently with respect to a double-reciprocal plot; the apparent values for both the K_m and V_{max} increase with increasing concentrations of inhibitor (Figure B.5 (**C**) and (**D**)).

Dixon Plots

Dixon plots are obtained by plotting $1/\upsilon$ (on the ordinate)against [I] (on the abscissa). The appearance of these plots for a series of substrate concentrations is similar to that of the double reciprocal plots for a series of inhibitor concentrations, and as such also provide information regarding the mode of inhibition. In addition, for competitive, mixed or non-competitive inhibitors, a Dixon plot can be used to obtain a value of K_I. As illustrated in Figure B.6, this information is obtained, not from the slope or axis-intercepts of the plotted lines as with the double-

reciprocal plots, but from the coordinates of the points of intersection of the plotted lines.

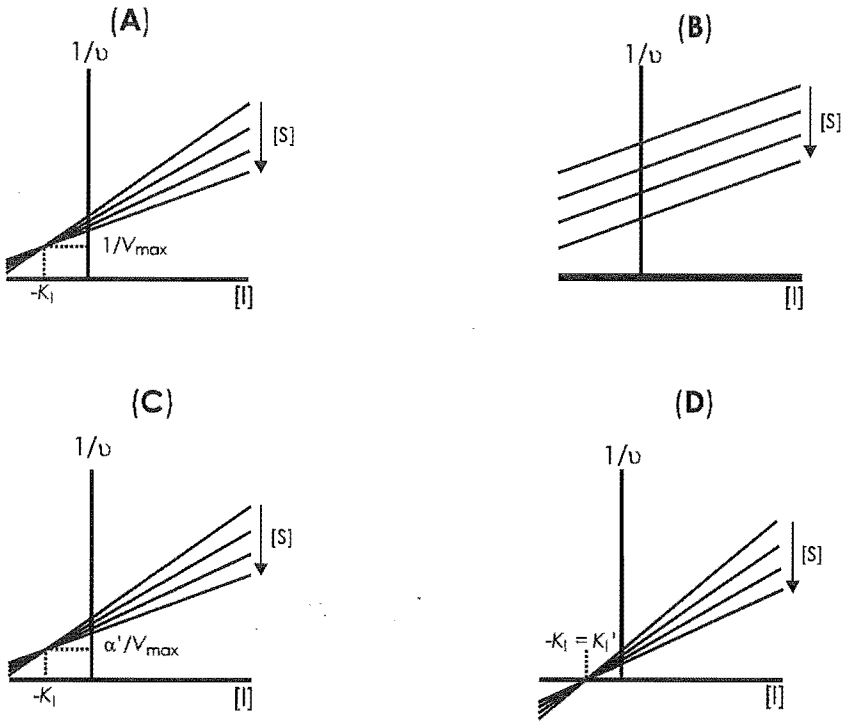

Figure B.6: Dixon plots in the presence of (**A**) a competitive inhibitor, (**B**) an uncompetitive inhibitor, (**C**) a mixed inhibitor, and (**D**) a non-competitive inhibitor.

Modified Dixon plots

Modified Dixon plots are generated by plotting [S]/υ (on the ordinate) against [I] (on the abscissa). The appearance of these plots for a series of substrate concentrations is similar to those of the Dixon plots. However the abscissa coordinate of the point at which the lines intercept in this case gives a measure of K_I' for a uncompetitive, non-competitive or mixed inhibitor. For a competitive inhibitor, the lines in a modified Dixon plot do not intercept.

References

(1) Cornish-Bowden, A. *Biochem. J.* **1974**, *137*, 143-144.

(2) Henderson, P. J. F. In *Enzyme Assays A Practical Approach*; Eisenthal, R.; Danson, M. J., Eds.; IRL Press at OUP: Oxford, 1992; N.

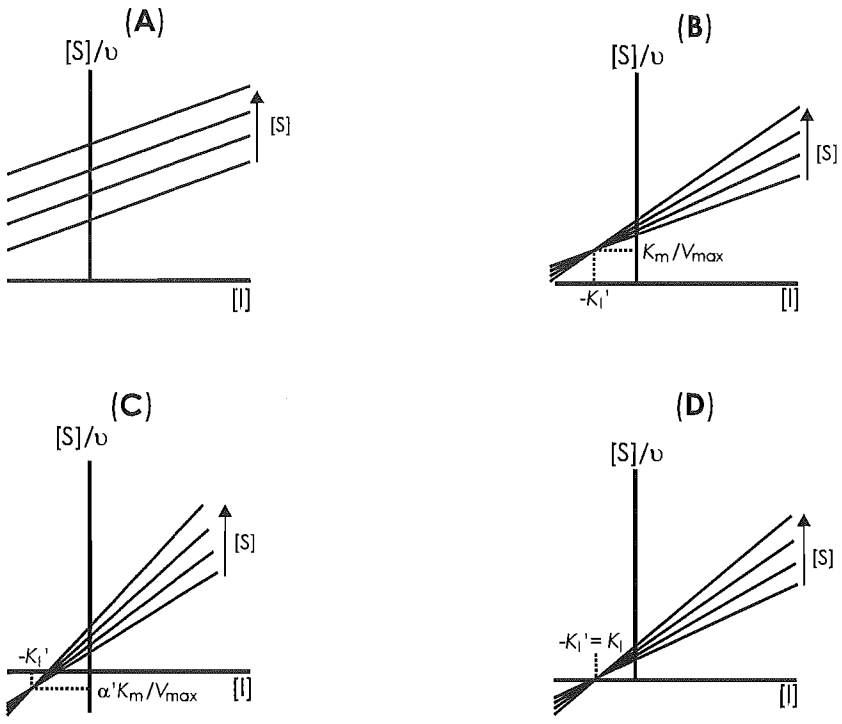

Figure B.7: Modified Dixon plots in the presence of (**A**) a competitive inhibitor, (**B**) an uncompetitive inhibitor, (**C**) a mixed inhibitor, and (**D**) a non-competitive inhibitor.

APPENDIX C

CRYSTALLOGRAPHIC TABLES

COMPOUND 3.7

Table C.1. Crystal data and structure refinement for 3.7.

Identification code	3.7	
Empirical formula	C10 H14 O7	
Formula weight	246.21	
Temperature	153(2) K	
Wavelength	0.71073 Å	
Crystal system	Monoclinic	
Space group	P(2)1	
Unit cell dimensions	a = 5.9860(10) Å	α= 90°.
	b = 11.425(4) Å	β=104.330(10)°.
	c = 8.618(2) Å	γ = 90°.
Volume	571.0(3) $Å^3$	
Z	2	
Density (calculated)	1.432 Mg/m^3	
Absorption coefficient	0.123 mm^{-1}	
F(000)	260	
Crystal size	1.00 x 0.60 x 0.30 mm^3	
Theta range for data collection	2.44 to 25.00°.	
Index ranges	-7<=h<=1, 0<=k<=13, -9<=l<=10	
Reflections collected	1180	
Independent reflections	1051 [R(int) = 0.0329]	
Completeness to theta = 25.00°	98.8 %	
Max. and min. transmission	0.9640 and 0.8869	
Refinement method	Full-matrix least-squares on F^2	
Data / restraints / parameters	1051 / 1 / 157	
Goodness-of-fit on F^2	1.268	
Final R indices [I>2sigma(I)]	R1 = 0.0733, wR2 = 0.2073	
R indices (all data)	R1 = 0.0942, wR2 = 0.2268	
Absolute structure parameter	4(4)	
Largest diff. peak and hole	0.543 and -0.478 $e.Å^{-3}$	

Table C.2. Atomic coordinates (x 10^4) and equivalent isotropic displacement parameters ($Å^2$x 10^3) for 3.7. U(eq) is defined as one third of the trace of the orthogonalized U^{ij} tensor.

	x	y	z	U(eq)
O(1)	7526(9)	5770(6)	3675(7)	33(1)
O(2)	10039(9)	7698(5)	2531(6)	30(1)
O(3)	13160(10)	6324(5)	725(7)	33(1)
O(4)	9277(10)	4577(4)	2278(7)	30(1)
O(5)	13968(9)	4263(5)	3782(6)	26(1)
O(6)	14632(10)	2024(5)	2541(7)	35(2)
O(7)	12725(14)	377(6)	1714(11)	58(2)
C(1)	8846(13)	5637(6)	2860(9)	23(2)
C(2)	10256(13)	6514(7)	2283(9)	24(2)
C(2')	10994(18)	8061(8)	4161(11)	43(2)
C(3)	11536(14)	5964(7)	1469(9)	27(2)
C(3')	14028(16)	7494(7)	1080(13)	39(2)
C(4)	11020(13)	4692(7)	1389(9)	22(2)
C(5)	13108(14)	3936(7)	2162(10)	25(2)
C(6)	12502(13)	2666(8)	2085(10)	28(2)
C(7)	14499(16)	855(8)	2302(10)	32(2)
C(8)	16805(17)	314(8)	2845(10)	36(2)

Table C.3. Bond lengths [Å] and angles [°] for 3.5.

O(1)-C(1)	1.190(10)
O(2)-C(2)	1.380(10)
O(2)-C(2')	1.441(10)
O(3)-C(3)	1.354(10)
O(3)-C(3')	1.439(10)
O(4)-C(1)	1.360(10)
O(4)-C(4)	1.444(9)
O(5)-C(5)	1.414(10)
O(6)-C(7)	1.350(11)
O(6)-C(6)	1.439(10)
O(7)-C(7)	1.190(12)
C(1)-C(2)	1.473(10)
C(2)-C(3)	1.320(11)
C(3)-C(4)	1.484(11)
C(4)-C(5)	1.529(11)
C(5)-C(6)	1.494(11)
C(7)-C(8)	1.478(13)
C(2)-O(2)-C(2')	113.8(6)
C(3)-O(3)-C(3')	116.4(6)
C(1)-O(4)-C(4)	110.1(5)
C(7)-O(6)-C(6)	116.6(7)
O(1)-C(1)-O(4)	123.1(6)
O(1)-C(1)-C(2)	129.2(7)
O(4)-C(1)-C(2)	107.7(7)
C(3)-C(2)-O(2)	129.6(7)
C(3)-C(2)-C(1)	108.2(7)
O(2)-C(2)-C(1)	122.0(7)
C(2)-C(3)-O(3)	133.4(8)
C(2)-C(3)-C(4)	110.4(7)
O(3)-C(3)-C(4)	116.2(7)
O(4)-C(4)-C(3)	103.5(6)
O(4)-C(4)-C(5)	109.7(6)
C(3)-C(4)-C(5)	113.2(6)
O(5)-C(5)-C(6)	109.0(6)
O(5)-C(5)-C(4)	109.9(6)

C(6)-C(5)-C(4)	111.5(6)
O(6)-C(6)-C(5)	107.1(6)
O(7)-C(7)-O(6)	122.1(9)
O(7)-C(7)-C(8)	127.4(9)
O(6)-C(7)-C(8)	110.5(8)

Symmetry transformations used to generate equivalent atoms:

Table C.4. Anisotropic displacement parameters ($Å^2 x\ 10^3$) for 3.5.

The anisotropic displacement factor exponent takes the form:

$-2\pi^2[\ h^2\ a^{*2}U^{11} + ...\ + 2\ h\ k\ a^*\ b^*\ U^{12}\ ]$

U^{11}	U^{22}	U^{33}	U^{23}	U^{13}	U^{12}
O(1)24(3)	28(3)	50(3)	-3(3)	15(3)	-2(3)
O(2)31(3)	15(3)	41(3)	-1(2)	5(3)	4(2)
O(3)40(3)	21(3)	38(3)	-1(2)	14(3)	-4(3)
O(4)34(3)	8(3)	51(3)	-1(2)	13(3)	-1(2)
O(5)30(3)	18(3)	28(3)	-3(2)	5(2)	-4(2)
O(639(3)	12(3)	53(4)	-4(3)	7(3)	4(3)
O(7)50(4)	15(3)	91(6)	-9(3)	-17(4)	-4(3)
C(1)21(4)	5(3)	42(5)	4(3)	5(3)	-5(3)
C(2)32(4)	10(4)	27(4)	2(3)	2(3)	-11(3)
C(2')55(6)	26(5)	45(5)	-10(4)	8(5)	0(4)
C(3)27(4)	26(5)	27(4)	3(3)	1(3)	3(3)
C(3')35(4)	17(4)	70(6)	8(4)	21(4)	-6(4)
C(4)26(4)	16(4)	23(4)	-1(3)	5(3)	-5(3)
C(5)24(4)	20(4)	33(4)	2(3)	11(3)	-2(3)
C(6)21(4)	15(4)	46(5)	-6(4)	5(3)	0(3)
C(7)42(5)	18(4)	36(4)	0(4)	11(4)	2(4)
C(8)59(6)	14(4)	36(4)	2(3)	12(4)	10(4)

Table C.5. Hydrogen coordinates (x 10^4) and isotropic displacement parameters ($Å^2$x 10^{-3}) for 3.5.

	x	y	z	U(eq)
H(5A)	15183	4654	3878	39
H(2'A)	11071	8918	4211	64
H(2'B)	12548	7736	4544	64
H(2'C)	10012	7777	4838	64
H(3'A)	15563	7555	877	59
H(3'B)	14127	7671	2208	59
H(3'C)	12984	8052	398	59
H(4A)	10380	4448	252	26
H(5B)	14339	4066	1580	30
H(6A)	11521	2488	2826	34
H(6B)	11648	2450	986	34
H(8A)	16679	-533	2662	54
H(8B)	17421	468	3990	54
H(8C)	17842	648	2243	54

Table C.6. Torsion angles [°] for 3.5.

C(4)-O(4)-C(1)-O(1)	-177.7(7)
C(4)-O(4)-C(1)-C(2)	2.8(8)
C(2')-O(2)-C(2)-C(3)	-111.3(9)
C(2')-O(2)-C(2)-C(1)	73.2(9)
O(1)-C(1)-C(2)-C(3)	177.5(8)
O(4)-C(1)-C(2)-C(3)	-3.0(8)
O(1)-C(1)-C(2)-O(2)	-6.2(12)
O(4)-C(1)-C(2)-O(2)	173.3(6)
O(2)-C(2)-C(3)-O(3)	6.1(14)
C(1)-C(2)-C(3)-O(3)	-177.9(7)
O(2)-C(2)-C(3)-C(4)	-174.0(7)
C(1)-C(2)-C(3)-C(4)	2.0(8)
C(3')-O(3)-C(3)-C(2)	12.9(12)
C(3')-O(3)-C(3)-C(4)	-167.0(7)
C(1)-O(4)-C(4)-C(3)	-1.6(7)
C(1)-O(4)-C(4)-C(5)	119.5(7)
C(2)-C(3)-C(4)-O(4)	-0.4(8)
O(3)-C(3)-C(4)-O(4)	179.6(6)
C(2)-C(3)-C(4)-C(5)	-119.1(7)
O(3)-C(3)-C(4)-C(5)	60.8(9)
O(4)-C(4)-C(5)-O(5)	-57.2(8)
C(3)-C(4)-C(5)-O(5)	58.0(8)
O(4)-C(4)-C(5)-C(6)	63.7(8)
C(3)-C(4)-C(5)-C(6)	178.9(7)
C(7)-O(6)-C(6)-C(5)	-169.5(7)
O(5)-C(5)-C(6)-O(6)	-69.8(8)
C(4)-C(5)-C(6)-O(6)	168.8(6)
C(6)-O(6)-C(7)-O(7)	1.5(14)
C(6)-O(6)-C(7)-C(8)	-179.2(7)

Symmetry transformations used to generate equivalent atoms:

COMPOUND 3.13

Table C.7. Crystal data and structure refinement for 3.13.

Identification code	3.13	
Empirical formula	C6 H10 O6	
Formula weight	178.14	
Temperature	293(2) K	
Wavelength	0.71073 Å	
Crystal system	Orthorombic	
Space group	P(2)1(2)1(2)1	
Unit cell dimensions	a = 6.5460(10) Å	α= 90°.
	b = 9.438(2) Å	β= 90°.
	c = 11.3970(10) Å	γ = 90°.
Volume	704.12(19) $Å^3$	
Z	4	
Density (calculated)	1.680 Mg/m^3	
Absorption coefficient	0.154 mm^{-1}	
F(000)	376	
Crystal size	0.76 x 0.68 x 0.40 mm^3	
Theta range for data collection	2.80 to 27.48°.	
Index ranges	-8<=h<=8, -12<=k<=0, -14<=l<=0	
Reflections collected	1773	
Independent reflections	1610 [R(int) = 0.0164]	
Completeness to theta = 27.48°	100.0 %	
Absorption correction		
Refinement method	Full-matrix least-squares on F^2	
Data / restraints / parameters	1610 / 0 / 109	
Goodness-of-fit on F^2	1.298	
Final R indices [I>2sigma(I)]	R1 = 0.0437, wR2 = 0.1479	
R indices (all data)	R1 = 0.0457, wR2 = 0.1492	
Absolute structure parameter	-0.3(15)	
Largest diff. peak and hole	0.596 and -0.544 $e.Å^{-3}$	

Table C.8 Atomic coordinates (x 10^4) and equivalent isotropic displacement parameters ($Å^2$x 10^3)for 3.13.

U(eq) is defined as one third of the trace of the orthogonalized U^{ij} tensor.

	x	y	z	U(eq)
O(5)	8505(3)	8632(2)	10080(1)	17(1)
O(1)	14036(3)	8685(2)	7125(2)	26(1)
O(2)	12956(3)	11496(2)	6297(2)	21(1)
O(4)	11659(2)	9063(2)	8494(1)	16(1)
O(6)	5127(2)	10668(2)	10021(2)	25(1)
O(3)	9142(3)	11005(2)	7087(2)	21(1)
C(3)	10615(3)	11369(2)	7945(2)	15(1)
C(1)	12963(4)	9500(2)	7645(2)	16(1)
C(5)	8377(3)	9794(2)	9275(2)	15(1)
C(2)	12757(3)	11092(2)	7476(2)	15(1)
C(6)	7212(4)	10999(3)	9851(2)	20(1)
C(4)	10510(3)	10287(2)	8949(2)	14(1)

Table C.9. Bond lengths [Å] and angles [°] for 3.13.

O(5)-C(5)	1.433(3)
O(1)-C(1)	1.198(3)
O(2)-C(2)	1.403(3)
O(4)-C(1)	1.354(3)
O(4)-C(4)	1.474(3)
O(6)-C(6)	1.413(3)
O(3)-C(3)	1.415(3)
C(3)-C(2)	1.523(3)
C(3)-C(4)	1.536(3)
C(1)-C(2)	1.522(3)
C(5)-C(4)	1.518(3)
C(5)-C(6)	1.519(3)
C(1)-O(4)-C(4)	109.55(17)
O(3)-C(3)-C(2)	110.04(18)
O(3)-C(3)-C(4)	108.86(18)
C(2)-C(3)-C(4)	100.88(17)
O(1)-C(1)-O(4)	121.8(2)
O(1)-C(1)-C(2)	128.6(2)
O(4)-C(1)-C(2)	109.6(2)
O(5)-C(5)-C(4)	109.70(17)
O(5)-C(5)-C(6)	108.97(19)
C(4)-C(5)-C(6)	109.78(18)
O(2)-C(2)-C(1)	112.42(19)
O(2)-C(2)-C(3)	112.04(19)
C(1)-C(2)-C(3)	101.92(19)
O(6)-C(6)-C(5)	112.3(2)
O(4)-C(4)-C(5)	108.38(17)
O(4)-C(4)-C(3)	103.65(17)
C(5)-C(4)-C(3)	115.26(18)

Symmetry transformations used to generate equivalent atoms:

Table C.10. Anisotropic displacement parameters ($Å^2 x\ 10^3$) for 3.13.

The anisotropic displacement factor exponent takes the form:

$-2\pi^2[\ h^2\ a^{*2}U^{11} + ...\ + 2\ h\ k\ a^*\ b^*\ U^{12}\ ]$

U^{11}	U^{22}	U^{33}	U^{23}	U^{13}	U^{12}
O(5)19(1)	17(1)	16(1)	1(1)	1(1)	-2(1)
O(1)24(1)	21(1)	31(1)	-4(1)	7(1)	7(1)
O(2)23(1)	23(1)	17(1)	4(1)	5(1)	4(1)
O(4)17(1)	12(1)	20(1)	2(1)	2(1)	2(1)
O(6)14(1)	29(1)	30(1)	9(1)	3(1)	2(1)
O(3)21(1)	25(1)	18(1)	1(1)	-5(1)	2(1)
C(3)19(1)	12(1)	14(1)	-1(1)	-1(1)	1(1)
C(1)15(1)	15(1)	19(1)	0(1)	-2(1)	1(1)
C(5)15(1)	16(1)	14(1)	1(1)	-1(1)	-1(1)
C(2)16(1)	13(1)	15(1)	1(1)	-1(1)	0(1)
C(6)16(1)	19(1)	24(1)	1(1)	2(1)	1(1)
C(4)13(1)	13(1)	16(1)	-1(1)	-1(1)	2(1)

Table C.11. Hydrogen coordinates (x 10^4) and isotropic displacement parameters ($Å^2$x 10^3) for 3.13.

	x	y	z	U(eq)
H(5A)	7963	8854	10702	26
H(2A)	13148	10791	5891	32
H(6A)	5029	9963	10437	37
H(3A)	9180	11583	6550	32
H(3B)	10449	12344	8224	18
H(5B)	7653	9491	8565	18
H(2B)	13768	11591	7957	17
H(6B)	7830	11211	10605	24
H(6C)	7319	11839	9365	24
H(4A)	11199	10668	9645	17

Table C.12. Torsion angles [°] for 3.13.

C(4)-O(4)-C(1)-O(1)	-178.5(2)
C(4)-O(4)-C(1)-C(2)	0.0(2)
O(1)-C(1)-C(2)-O(2)	35.1(4)
O(4)-C(1)-C(2)-O(2)	-143.2(2)
O(1)-C(1)-C(2)-C(3)	155.2(3)
O(4)-C(1)-C(2)-C(3)	-23.1(2)
O(3)-C(3)-C(2)-O(2)	40.6(2)
C(4)-C(3)-C(2)-O(2)	155.47(18)
O(3)-C(3)-C(2)-C(1)	-79.8(2)
C(4)-C(3)-C(2)-C(1)	35.1(2)
O(5)-C(5)-C(6)-O(6)	-68.3(2)
C(4)-C(5)-C(6)-O(6)	171.50(19)
C(1)-O(4)-C(4)-C(5)	146.04(18)
C(1)-O(4)-C(4)-C(3)	23.1(2)
O(5)-C(5)-C(4)-O(4)	55.1(2)
C(6)-C(5)-C(4)-O(4)	174.85(17)
O(5)-C(5)-C(4)-C(3)	170.71(18)
C(6)-C(5)-C(4)-C(3)	-69.6(3)
O(3)-C(3)-C(4)-O(4)	79.8(2)
C(2)-C(3)-C(4)-O(4)	-35.9(2)
O(3)-C(3)-C(4)-C(5)	-38.4(3)
C(2)-C(3)-C(4)-C(5)	-154.19(18)

Symmetry transformations used to generate equivalent atoms: